



This work is protected by copyright and other intellectual property rights and duplication or sale of all or part is not permitted, except that material may be duplicated by you for research, private study, criticism/review or educational purposes. Electronic or print copies are for your own personal, non-commercial use and shall not be passed to any other individual. No quotation may be published without proper acknowledgement. For any other use, or to quote extensively from the work, permission must be obtained from the copyright holder/s.

**The design and synthesis of drug carrier  
molecules to improve oral bioavailability  
via hPepT1**

**Gayle Wilson**

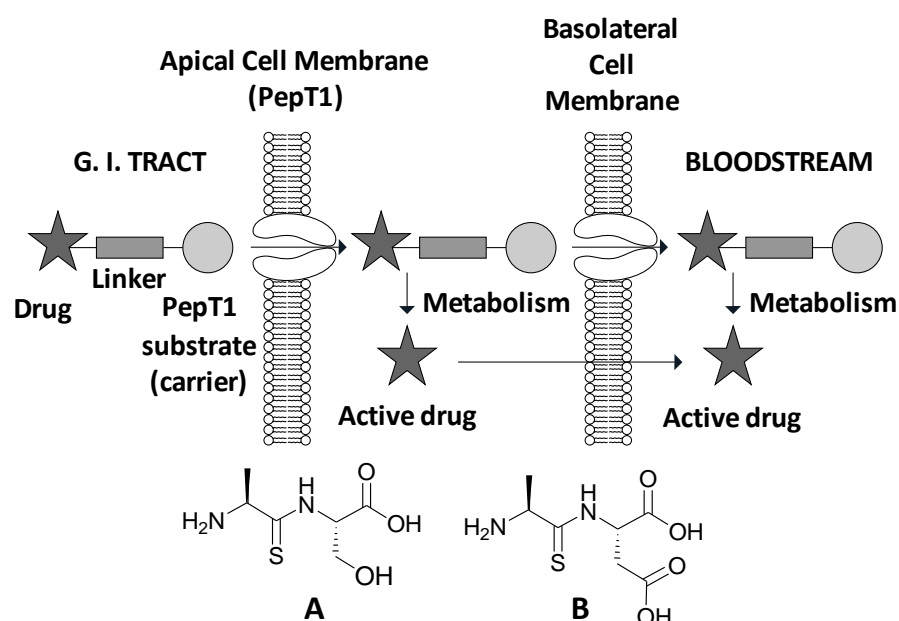
**PhD**

**March 2016**

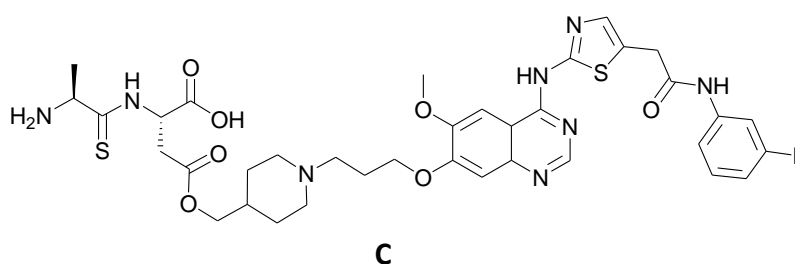
**Keele University**

## Abstract

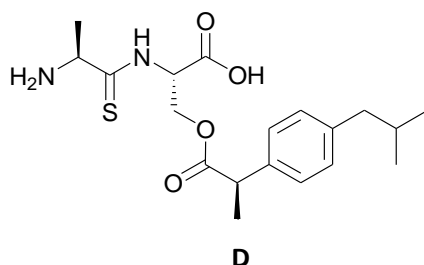
PepT1 (SLC15A1) is a low affinity high capacity, di- and tri-peptide transmembrane transporter primarily located in the brush border membrane in the small intestines. As well as transporting oligopeptides, PepT1 has been discovered to transport a wide range of xenobiotics including,  $\beta$ -lactams and ACE inhibitors. This broad substrate capacity makes PepT1 ideal as a vehicle for the targeted delivery of xenobiotic prodrugs. It has been shown that our hydrolysis resistant thiodipeptide PepT1 substrates (e.g. **A** and **B**) can be used as 'carriers' for the prodrug targeting of poorly bioavailable drugs towards PepT1 *via* the strategy illustrated below.



In this thesis, using this approach, the xenobiotics attached to our carriers will be expanded from commercially available drugs to new chemical entities which display undesirable physiochemical properties, such as the Aurora kinase inhibitor **C**.



The discovery that PepT1 is over-expressed in pancreatic adenocarcinoma cell lines, AsPc-1 and Capan-2,4 has also led to research being undertaken into targeted anti-cancer therapy *via* our thiodipeptide carriers. The use of PepT1 targeting in cancer therapy has the potential to reduce side effects due to the minimisation of off target delivery. Pancreatic cancer often has a poor prognosis, with only a 5% survival rate 5 years after diagnosis. Thiodipeptide **D** will be shown in this research to significantly reduce cell proliferation and vitality in AcPc1 cells. This is the first time that reduced cell proliferation by ibuprofen or an ibuprofen prodrug has been reported in this cell line. The use of our thiodipeptides to improve the oral bioavailability of an oncology drug through PepT1 targeting will also be explored.



The development of new hydrolysis resistant dipeptide carriers will also be explored as the presence of a sulfur atom in our present carriers has historically resulted in non-crystalline prodrugs being synthesised, which is not ideal for formulation.

## Contents

List of Figures.....	i
List of Tables.....	iii
List of Equations and Schemes.....	iv
Acknowledgements.....	v
Abbreviations .....	vi
Amino acid abbreviations.....	ix
<b>Chapter: 1 Drug delivery <i>via</i> the PepT1 Transporter .....</b>	<b>1</b>
1.1    Drug delivery <i>via</i> the oral route.....	3
1.2    Strategies to improve oral bioavailability .....	4
1.2.1    Prodrugs.....	4
1.2.2    Targeting transporters .....	5
1.3    PepT1 .....	7
1.3.1    Location and transport.....	7
1.3.2    Regulation .....	10
1.3.3    Discovery.....	12
1.3.4    Structure .....	13
1.3.5    PepT1 homologues.....	18
1.3.6    Identifying PepT1 substrate structural features.....	23
1.3.7    QSAR studies .....	29
<b>Chapter 2: Targeting drugs towards PepT1.....</b>	<b>31</b>
2.1    Targeting drugs towards PepT1. ....	33
2.1.1    Changing the drug to make it a substrate.....	33
2.1.2    Attaching a substrate carrier. ....	35
2.2    Using thiodipeptides as carriers.....	37
2.3    Synthesis of thiodipeptide carriers. ....	41
2.4    Synthesis of alternatively protected thiodipeptide carrier.....	44
2.5    PepT1 targeted prodrugs using commercially available drugs.....	47
2.5.1    Propofol.....	47

2.5.2	Ibuprofen .....	49
2.5.3	Aspirin. ....	50
2.6	AstraZeneca new chemical entities .....	57
2.6.1	Aurora kinase inhibitor .....	58
2.6.2	$\alpha 1\beta 5$ Integrin inhibitor.....	65
2.7	<i>In vitro</i> biological testing.....	73
2.7.1	Binding Affinity.....	74
2.7.2	Oocyte transport assay. ....	75
2.7.3	Caco-2 assays. ....	76
2.7.4	Biological results. ....	77
<b>Chapter 3: Alternative carriers.....</b>		<b>82</b>
3.1	Synthesis of carriers .....	84
3.2	<i>In vitro</i> biological testing.....	89
3.3	<i>In vivo</i> biological testing.....	92
3.3.1	Pharmacokinetic study.....	92
3.3.2	Taste assessment. ....	95
<b>Chapter 4: Utilising the PepT1 transporter for targeted drug deliver .....</b>		<b>97</b>
4.1	PepT1 in cancer .....	99
4.2	Ala(S)Ser-ibuprofen.....	100
4.2.1	<i>In vitro</i> testing .....	101
4.2.2	Conclusions .....	105
4.3	Gemcitabine prodrugs .....	106
4.3.1	Gemcitabine prodrug synthesis. ....	110
4.3.2	<i>In vitro</i> testing .....	113
4.3.3	Conclusions .....	118
<b>Chapter 5: Conclusions .....</b>		<b>120</b>

<b>Chapter 6: Experimental.....</b>	<b>133</b>
6.1 General methods .....	135
6.1.1 Oocyte binding affinity.....	135
6.1.2 Oocyte <i>trans</i> -stimulation assay.....	135
6.1.3 Caco-2 assay .....	136
6.1.4 AcPc1 assay .....	137
6.1.5 Pharmacokinetic study in rat .....	137
6.1.7 Synthetic materials .....	138
6.1.8 Characterisation.....	139
6.2 Synthesis of Benzyl type protected carriers (section 2.4).....	140
6.3 Synthesis of PepT1 targeted prodrugs using commercial drugs (section 2.5).....	151
6.3.1 Propofol prodrug (section 2.5.1).....	151
6.3.2. Ibuprofen prodrug (section 2.5.2).....	154
6.3.3 Aspirin prodrug (section 2.5.3). ....	156
6.4 Synthesis of polyethylene glycol based linkers (section 2.6.1).....	160
6.5 Synthesis of Aurora Kinase inhibitor prodrug (section 2.6.1).....	165
6.6 Synthesis of alternative carriers section (3.1).....	172
6.6.1. Serine component (section 2.3 and 3.1).....	172
6.6.2. Cycloleucine-serine carrier (section 3.1).....	176
6.6.3. Cyclopropane-serine carrier (section 3.1).....	183
6.6.4. Cyclobutane carrier (section 3.1).....	189
6.6.5. Homocycloleucine carrier (section 3.1). ....	195
6.7 Synthesis of gemcitabine prodrugs (section 4.3.1).....	201
<b>References.....</b>	<b>209</b>

## List of Figures

<b>Figure 1</b> Mechanisms of absorption across a cell membrane. ....	<b>3</b>
<b>Figure 2</b> The uptake transporters expressed in the intestinal enterocytes which are involved in drug transport. ....	<b>6</b>
<b>Figure 3</b> The mechanism of transport for a PepT1 substrate. ....	<b>8</b>
<b>Figure 4</b> Model to show how PepT1 mediates electrogenic substrate influx at varying pH. ....	<b>9</b>
<b>Figure 5</b> Lee's models of the substrate binding site of PepT1 <sup>67,69</sup> .....	<b>15</b>
<b>Figure 6</b> The secondary structure of human PepT1.....	<b>17</b>
<b>Figure 7</b> Meredith model of the arrangement of rPepT1-trunc's 12 transmembrane domains <sup>84</sup> ...	<b>19</b>
<b>Figure 8</b> Homology model of human PEPT1 overlaid with corresponding YdgR residues. ....	<b>20</b>
<b>Figure 7</b> The crystal structures of POT transporters which have given insight into the alternating access transport cycle of PepT1 <sup>90</sup> .....	<b>21</b>
<b>Figure 10</b> Topology model showing amino acid residues similarities between; PepT1, PepT <sub>so</sub> , PepT <sub>str</sub> , GkPOT and PepT <sub>so2</sub> .....	<b>22</b>
<b>Figure 11</b> Examples of the classes of drugs that are PepT1 substrates.....	<b>23</b>
<b>Figure 12</b> Peptomimetics used by Börner <sup>94</sup> which are substrates of PepT1, but do not possess a free terminal carboxylic acid group.....	<b>24</b>
<b>Figure 13</b> The constrained dipeptide analogues used by Bailey <sup>97</sup> to demonstrate high affinity binding when the free <i>N-terminus</i> is directed back in the plane. ....	<b>26</b>
<b>Figure 14</b> The conformational arrangement of the <i>N-terminus D-</i> or <i>L-</i> tripeptide conformational isomer used in Baileys experiment <sup>97</sup> .....	<b>26</b>
<b>Figure 15</b> Side chain positioning in <i>L-</i> and <i>D-</i> carboxy- <i>terminus</i> dipeptides.....	<b>28</b>
<b>Figure 16</b> The Bailey PepT1 substrate template, showing the four key binding sites <sup>104</sup> .....	<b>28</b>
<b>Figure 17</b> CoMISA standard deviation coefficient contour plots of a PepT1 substrate <sup>104</sup> .....	<b>30</b>
<b>Figure 18</b> Standardised dipeptide carriers investigated by Taub's group <sup>112-3</sup> .....	<b>35</b>
<b>Figure 19</b> The 4-(4-chlororphenyl)-4,5,6,7-terahydrothieno[3,2-C]pyridin-5-yl-phenylmethanone derivatives and their prodrug counterparts used by Taub. <sup>114</sup> .....	<b>36</b>



<b>Figure 20</b> Routes of aspirin ester hydrolysis.....	<b>52</b>
<b>Figure 21</b> Side chains identified through structure affinity optimisation of a non peptidic $\alpha 5\beta 1$ antagonist <sup>143-4</sup> .....	<b>66</b>
<b>Figure 22</b> Oocyte inhibition assay.....	<b>75</b>
<b>Figure 23</b> Oocyte <i>trans</i> -stimulation assay diagram .....	<b>75</b>
<b>Figure 24</b> A bar chart showing how transport is assessed using <i>trans</i> -stimulation data. ....	<b>76</b>
<b>Figure 25</b> A Caco-2 monolayer.....	<b>77</b>
<b>Figure 26</b> Immunoblot assay showing absence of PepT1 at the surface of AsPc1 PepT1 -/- cells.	<b>102</b>
<b>Figure 27</b> Rate of proliferation in cells exposed to Ala(S)Ser-ibuprofen (79).....	<b>102</b>
<b>Figure 28</b> Ala(S)Ser-ibuprofen (79) competitive inhibition study.....	<b>103</b>
<b>Figure 29</b> Ala(S)Ser-ibuprofen (79) MTT cell viability assay. ....	<b>104</b>
<b>Figure 30</b> Immunoblot assay showing COX-2 levels after AsPc1 and AsPc1 PepT1 -/- cells were exposed to Ala(S)Ser-ibuprofen (79) .....	<b>105</b>
<b>Figure 31</b> 4'- <i>N</i> -Ala(S)Asp-gemcitabine (194) MTT cell viability assay.....	<b>113</b>
<b>Figure 32</b> 5'- <i>O</i> -Ala(S)Asp-gemcitabine (193) MTT cell viability assay.....	<b>114</b>
<b>Figure 33</b> 3'- <i>O</i> -Ala(S)Asp-5'- <i>O</i> -Ala(S)Asp-gemcitabine (198) MTT cell viability assay .....	<b>114</b>
<b>Figure 34</b> Rate of proliferation in cells exposed to different concentrations of 3'- <i>O</i> -Ala(S)Asp-5'- <i>O</i> -Ala(S)Asp-gemcitabine (198) after 48 hours. ....	<b>115</b>
<b>Figure 35</b> Competitive inhibition study of 3'- <i>O</i> -Ala(S)Asp-5'- <i>O</i> -Ala(S)Asp-gemcitabine (198).....	<b>116</b>
<b>Figure 36</b> 3'- <i>O</i> -Ala(S)Asp-5'- <i>O</i> -Ala(S)Asp-gemcitabine (198) against gemcitabine (184) MTT cell viability assay.....	<b>116</b>
<b>Figure 37</b> Acetic acid glycol linkers attached to (73) .....	<b>122</b>

## List of Tables

<b>Table 1</b> Drug uptake transporters identified in the small intestine .....	<b>6</b>
<b>Table 2</b> Prodrugs which display improved bioavailability through PepT1 targeting. ....	<b>34</b>
<b>Table 3</b> Reaction conditions tried in the mono protection of H-Ser(OBn)-OH.....	<b>43</b>
<b>Table 4</b> Hydrolysis conditions attempted to remove the benzyl ester protecting groups in compounds (117) and (118). ....	<b>64</b>
<b>Table 5</b> Conditions used for the coupling of Boc-Ala(S)Ser-OtBu (56) to the integrin inhibitor (136) .....	<b>68</b>
<b>Table 6</b> Conditions used for the coupling of (112) to the integrin inhibitor (136) .....	<b>70</b>
<b>Table 7</b> Conditions employed for the secondary amine protection of the integrin inhibitor (136).	<b>72</b>
<b>Table 8</b> <i>In vitro</i> data for prodrugs (76), (79) and (108).....	<b>78</b>
<b>Table 9</b> <i>In vitro</i> data for thiodipeptide prodrugs synthesised by R. Pathak (unpublished). ....	<b>80</b>
<b>Table 10</b> Optimisation of the coupling conditions for Boc-cycloleucine-Ser(Bn)-OtBu (159) .....	<b>87</b>
<b>Table 11</b> Binding affinity and <i>trans</i> -stimulation efflux for dipeptides.....	<b>90</b>
<b>Table 12</b> Summary of the mean calculated pharmacokinetic parameters for the ibuprofen pharmacokinetic study .....	<b>93</b>
<b>Table 13</b> Caco-2 and AsPc1 data for 5'-amino acid ester prodrugs of gemcitabine.....	<b>108</b>

## List of Equations and Schemes

<b>Equation 1</b> Synthesis of (65) .....	<b>55</b>
<b>Scheme 1</b> The metabolism of the nabumetone hydroxyimine prodrug <i>in vivo</i> and the two nabumetone hydroxyimine-carrier prodrugs tested <i>in vitro</i> .....	<b>39</b>
<b>Scheme 2</b> Synthesis of the protected thiodipeptide carriers .....	<b>41</b>
<b>Scheme 3</b> Attempted synthesis of Ala(S)Asp-doxorubicin prodrug by Dr. R. Pathak.....	<b>44</b>
<b>Scheme 4</b> Synthesis of the benzyl protected thiodipeptide carriers.....	<b>47</b>
<b>Scheme 5</b> Synthesis of Ala(S)Asp-2,6-diisopropylphenol (76) .....	<b>49</b>
<b>Scheme 6</b> Synthesis of Ala(S)Ser-ibuprofen (79) .....	<b>50</b>
<b>Scheme 7</b> Theorised synthesis of thiodipeptide aspirin prodrug .....	<b>54</b>
<b>Scheme 8</b> Synthesis of modified salicylic prodrug.....	<b>56</b>
<b>Scheme 9</b> Synthesis of Aurora kinase inhibitor thiodipeptide prodrug (108). ....	<b>60</b>
<b>Scheme 10</b> Synthesis of glycol acid spacers .....	<b>61</b>
<b>Scheme 11</b> Intended synthesis of Ala(S)Asp glycol Aurora kinase prodrugs.....	<b>62</b>
<b>Scheme 12</b> Original proposed synthesis of Ala(S)Ser-Integrin prodrug .....	<b>67</b>
<b>Scheme 13</b> Revised synthesis of Ala(S)Asp-linker-Integrin prodrug.....	<b>69</b>
<b>Scheme 14</b> Attempted secondary amide protection of integrin inhibitor .....	<b>71</b>
<b>Scheme 15</b> Initial synthesis of cycloleucine-Ser-ibuprofen (162).....	<b>86</b>
<b>Scheme 16</b> Synthesis of H-cycloleucine-Ser(Bn)-OH (163), H-cycloleucine-Ser(OH)-OH (155) and H-cycloleucine-Ser(ibuprofen)-OH (162).....	<b>88</b>
<b>Scheme 17</b> Synthesis the free carrier, carrier with benzyl attachment and carrier with ibuprofen attachment for the cyclopropane, cyclobutane and homocycloleucine carriers .....	<b>89</b>
<b>Scheme 18</b> Synthesis of 4'-N-Ala(S)Asp-gemcitabine (194).....	<b>111</b>
<b>Scheme 19</b> Synthesis of 5'-O-Ala(S)Asp-gemcitabine (193) and 3'-O-Ala(S)Asp-5'-O-Ala(S)Asp-gemcitabine (198).....	<b>112</b>

## Acknowledgements

Firstly I would like to thank Prof. Pat Bailey for allowing me to join his research group. The support and encouragement you have given me over the years has ensured completion of this work was possible. I would also like to thank Dr. Tess Phillips. Once providing guidance and enthusiasm as a group member, I am ever grateful that you agreed to be my supervisor when Pat left for pastures new and of course for proof reading my thesis! In addition, my second Keele supervisor Dr. Russell Pearson most definitely needs to be thanked for providing encouragement and support, especially when it was thesis writing time.

This work would not have been possible without my industrial supervisor Dr. Kevin Foote. As well as being a great help when synthetic work was proving difficult, you were instrumental in organising the team of people from different departments that helped on the project. I would like to thank Kate Harris, also at AstraZeneca, who had the unlucky task of teaching a chemist how to perform Caco-2 studies. You have gone above and beyond to make things work despite the difficulties we encountered, for that I owe you a huge thanks. There have been large number of people at AstraZeneca who have had involvement in this project and my thanks go to all. Thanks also goes to Dr. David Meredith and his group at Oxford Brookes University, without their knowledge and expertise, oocyte analysis of my samples would not have been possible. My many thanks for taking the time to generate some much needed data! Thanks also have to go to Ana Santos Cravo and Prof. Randy Mersny at the University of Bath, a chance encounter at a conference led this project in an exciting but unexpected direction.

I would also like to thank group members past and present Ravi, Mark and Gareth for their patience and valuable discussions over the years. Thanks also go to everyone else at Keele for their assistance on a day to day basis.

Most of all I would like to thank my wonderful husband Dan. You supported me through the difficult periods and shared my joy. This thesis is dedicated to you.

## Abbreviations

<b>ABC</b>	ATP binding cassette
<b>Ac</b>	acetyl
<b>Aib</b>	$\alpha$ -aminoisobutyric
<b>ATP</b>	adenosine triphosphate
<b>AUC</b>	area under curve
<b>Bn</b>	benzyl
<b>Boc</b>	<i>N</i> - <i>tert</i> -butoxycarbonyl
<b>BSA</b>	bovine serum albumin
<b>BuChE</b>	butyrylcholinesterase
<b>Cbz</b>	carboxybenzyl
<b>CDA</b>	cytidine deaminase
<b>CDI</b>	carbonyldiimidazole
<b>C<sub>last</sub></b>	last measured serum concentration
<b>C<sub>max</sub></b>	maximum measured serum concentration
<b>CoMFA</b>	comparative molecular field analysis
<b>CoMSIA</b>	comparative molecular similarity indices analysis
<b>COMU</b>	(1-Cyano-2-ethoxy-oxoethylidenaminoxy)dimethylamino-morpholino-carbenium hexafluorophosphate
<b>COX-2</b>	Cyclooxygenase-2
<b>DCC</b>	<i>N,N'</i> -dicyclohexylcarbodiimide
<b>DCM</b>	dichloromethane
<b>DIAD</b>	diisopropyl azodicarboxylate
<b>DIPEA</b>	diisopropylethylamine
<b>DMAP</b>	4-(dimethylamino)pyridine
<b>DMF</b>	<i>N,N</i> -dimethylformamide

<b>DMSO</b>	dimethyl sulfoxide
<b>DNA</b>	deoxyribonucleic acid
<b>DPPA</b>	diphenylphosphoryl azide
<b>EDC</b>	1-(3-dimethylaminopropyl)-3-ethylcarbodiimide
<b>Fmoc</b>	9-fluorenylmethoxycarbonyl
<b>GlPT</b>	glycerol-3-phosphate antiporter
<b>HATU</b>	<i>O</i> -(7-azabenzotriazol-1-yl)- <i>N,N,N',N'</i> -tetramethyluronium hexafluorophosphate
<b>HBBS</b>	Hanks balanced salt solution
<b>HBTU</b>	<i>O</i> -(benzotriazol-1-yl)- <i>N,N,N',N'</i> -tetramethyluronium hexafluorophosphate
<b>HEPES</b>	(4-(2-hydroxyethyl)piperazine-1-ethanesulfonic acid
<b>HOBt</b>	1-hydroxybenzotriazole
<b>LCMS</b>	high pressure liquid chromatography
<b>IC<sub>50</sub></b>	half maximal inhibitory concentration
<b>I<sub>max</sub></b>	maximal inward current
<b>IR</b>	infra-red
<b>K<sub>i</sub></b>	binding affinity
<b>K<sub>m</sub></b>	Michaelis-Menten affinity constant
<b>LacY</b>	lactose permease
<b>LCMS</b>	liquid chromatography mass spectrometry
<b>LDA</b>	lithium diisopropylamide
<b>Log P</b>	partition co-efficient
<b>MEMSAT3</b>	membrane protein structure and topology, version 3
<b>MES</b>	2-( <i>N</i> -morpholino)ethanesulfonic acid
<b>MFS</b>	major facilitator superfamily
<b>MP</b>	melting point
<b>mRNA</b>	mitochondrial ribonucleic acid

<b>MS</b>	mass spectrometry
<b>NHS</b>	<i>N</i> -hydroxysuccinimide
<b>NMR</b>	nuclear magnetic resonance
<b>NSAID</b>	non-steroidal anti-inflammatory drug
<b>P<sub>app</sub></b>	apparent permeability
<b>PGE<sub>2</sub></b>	prostaglandin E2
<b>P-gp</b>	P-glycoprotein
<b>POT</b>	proton oligopeptide transporter
<b>QSAR</b>	quantitative structure affinity relationship
<b>R<sub>f</sub></b>	retention factor
<b>SLC</b>	solute carrier
<b>TBAF</b>	tetrabutylammonium fluoride
<b>TBTU</b>	<i>N,N,N',N'</i> -tetramethyl-O-(benzotriazole-1-yl)uronium tetrafluoroborate
<b><sup>t</sup>Bu</b>	<i>tert</i> -butyl
<b>TEA</b>	triethylamine
<b>TEER</b>	<i>trans</i> -epithelial electrical resistance
<b>TFA</b>	trifluoroacetic acid
<b>TFFH</b>	fluoro- <i>N,N,N',N'</i> -tetramethylformamidinium hexafluorophosphate
<b>THF</b>	tetrahydrofuran
<b>T<sub>last</sub></b>	time at which last concentration (C <sub>Max</sub> ) was recorded
<b>TLC</b>	thin layer chromatography
<b>T<sub>max</sub></b>	time at which maximum concentration (C <sub>Max</sub> ) was recorded
<b>UV</b>	ultraviolet
<b>V<sub>m</sub></b>	membrane potential
<b>V<sub>max</sub></b>	maximum initial rate of transport or product production

### Amino acid abbreviations

Name	Three Letter	One Letter
Alanine	Ala	A
Arginine	Arg	R
Asparagine	Asn	N
Aspartate	Asp	D
Cysteine	Cys	C
Glutamate	Glu	E
Glutamine	Gln	Q
Glycine	Gly	G
Histidine	His	H
Isoleucine	Ile	I
Leucine	Leu	L
Lysine	Lys	K
Methionine	Met	M
Ornithine	Orn	-
Phenylalanine	Phe	F
Proline	Pro	P
Sarcosine	Sar	-
Serine	Ser	S
Threonine	Thr	T
Tryptophan	Trp	W
Tyrosine	Tyr	Y
Valine	Val	V



# **Chapter 1**

## **Drug delivery *via* the PepT1 transporter**

## Chapter One Contents

1.1	Drug delivery <i>via</i> the oral route .....	3
1.2	Strategies to improve oral bioavailability .....	4
1.2.1	Prodrugs .....	4
1.2.2	Targeting transporters .....	5
1.3	PepT1 .....	7
1.3.1	Location and transport.....	7
1.3.2	Regulation .....	10
1.3.3	Discovery.....	12
1.3.4	Structure .....	13
1.3.5	PepT1 homologues.....	18
1.3.6	Identifying PepT1 substrate structural features. ....	23
1.3.7	QSAR studies .....	29

## 1.1 Drug delivery *via* the oral route

Oral administration is often the favoured route of drug delivery. The simplicity of swallowing a pill allows the patient to administer the dose at home without the need for training or special apparatus and increases the likelihood of patient compliance.<sup>1</sup> However, the development of drugs for the oral route can be particularly challenging. Any drug administered orally faces obstacles before it can pass into the bloodstream and become effective. How much of this dose is absorbed and becomes available at the site of action is often referred to as bioavailability. Drugs administered *intravenously* have a 100% bioavailability by this definition.

Oral bioavailability is determined by whether the drug is stable in the gastrointestinal tract, how water soluble it is, its dissolution rate, how well it is able to pass through gut wall mucosa of the gastrointestinal tract into the hepatic portal vein, whether it is an efflux transporter substrate and whether it is able to remain intact during first pass metabolism.<sup>1</sup> Absorption of the drug through the gut wall of the gastrointestinal tract is the primary determinant of bioavailability, as this determines what quantity of the initial dose will reach the bloodstream.

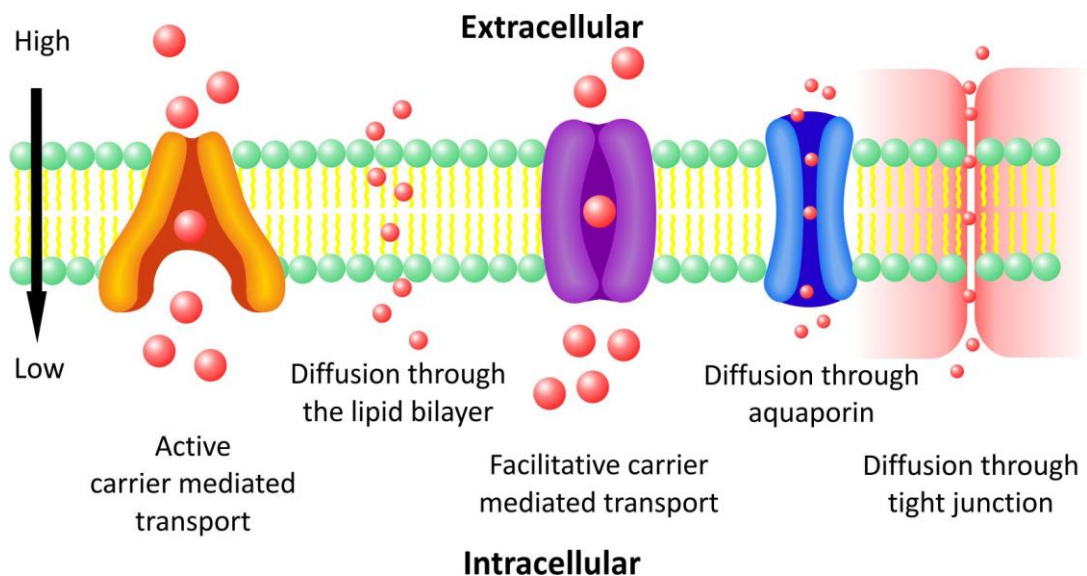


**Figure 1 Mechanisms of absorption across a cell membrane.**

Drugs which can passively diffuse through the cell are thought to generally follow Lipinski's 'rule of 5'.<sup>2</sup> These are; 1) a molecular weight less than 500 g mol<sup>-1</sup>, 2) no more than five hydrogen bond donors, 3) no more than ten hydrogen bond acceptors, 4) a LogP (partition co-efficient, a measure of lipophilicity) of less than five.

## 1.2 Strategies to improve oral bioavailability

During drug development compounds are optimised for maximum efficacy at a target, with the lead compounds having the best *in vitro* action. However, they may display a poor *in vivo* pharmacological effect due to their physiochemical properties. This may be low bioavailability, rapid metabolism and/or excretion. The strategies to overcome these issues can be grouped into three main categories; Formulation, bioactivity compromise in order to include good oral absorption features into the drug design and prodrug design.<sup>1</sup>

### 1.2.1 Prodrugs

A prodrug is a chemical precursor of a drug which undergoes enzymatic or chemical biotransformation in cells before eliciting a pharmacological effect.<sup>1</sup> As an example, acid groups add to the hydrophilicity of a molecule and are often ionised at physiological pH. This can impede the drug's ability to cross a cell's lipid bilayer. By changing the acid group to an ester group lipophilicity is increased and *in vivo* hydrolysis releases the original active drug.<sup>1</sup> By utilising the prodrug strategy to change the physiochemical properties of a drug, oral bioavailability can be improved. This may occur by: increased solubility and stability; the reduction of drug degradation through metabolism; allowing the drug to be passively absorbed and targeting the drug towards an active transporter.<sup>1</sup> Although the use of prodrugs can significantly improve oral bioavailability it is not without its drawbacks. Finding a suitable prodrug form can be time consuming and therefore expensive. By changing the structure of the molecule the pharmacokinetics and

pharmacodynamics may also be altered. Any by-products of the prodrugs breakdown into the active form must also be fully assessed.

### 1.2.2 Targeting transporters

More than 400 membrane transporters have been annotated in the human genome.<sup>3</sup> These can be classified into two superfamilies; ATP-binding cassette (ABC) and solute carrier (SLC). Many of these transporters are localised into important barrier tissues such as the luminal and/ or basolateral membranes of enterocytes, hepatocytes and renal tubular epithelial cells as well as the blood-brain, blood-testis and placental barriers.<sup>3</sup> Their role is to control the uptake and efflux of essential compounds such as amino acids, inorganic ions, nucleotides, sugars and xenobiotics. This may occur *via* either a facilitated or active mechanism.<sup>3</sup> Facilitated transport allows solutes to move through the cell membrane down their electrochemical gradient without energy expense. Active transport involves a substrate moving across the membrane at an energy cost to the cell. This energy can be obtained from adenosine triphosphate (ATP) hydrolysis, or by the co-transport of another molecule (i.e. a proton) down its chemiosmotic gradient.

The transporters involved in drug uptake in the small intestines are detailed in Figure 2 and Table 1. When targeting a drug towards a transporter, a drugs natural affinity can often be taken advantage of. For example, peptidomimetics such as penicillins often display affinity for and are transported by PepT1. When this is not the case, prodrugs can be used to mimic the structural requirements needed for transport. There are several excellent recent reviews of the use of active transporters as a route for drug delivery.<sup>4-6</sup> The use of PepT1 as a vehicle for drug delivery is a major area of research in our group.

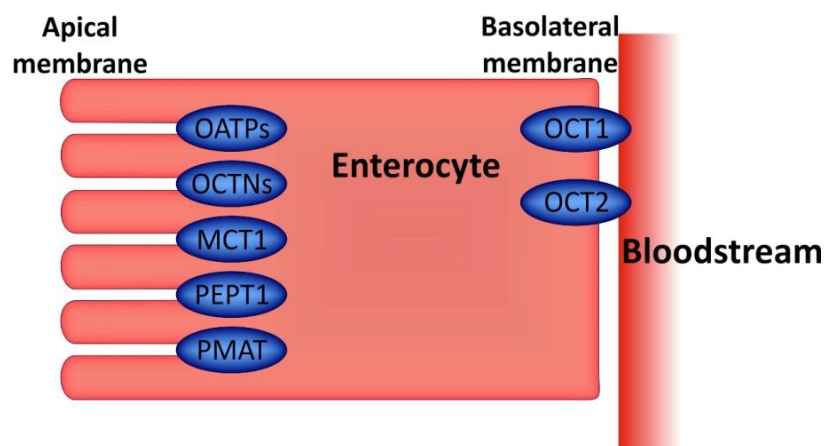


**Figure 2** The uptake transporters expressed in the intestinal enterocytes which are involved in drug transport.

**Table 1** Drug uptake transporters identified in the small intestine.<sup>3</sup>

Transporter	Substrate specificity	Example substrate
OATPs	Organic anions	Ciprofloxacin
OCTs	Low molecular weight organic cations	Metformin
OCTNs	Carnitine and organic cations	Pyrimidine
MCT1	Unbranched aliphatic and substituted monocarboxylates	Salicylic acid
PepT1	Di- and tri-peptides	Penicilins
PMAT	Organic cations	Dopamine

### 1.3 PepT1

#### 1.3.1 Location and transport

PepT1 is primarily expressed in the brush border of the absorptive enterocytes which line the small intestine. Its function is to transport the di- and tri-peptides, which are the result of the hydrolytic breakdown of dietary proteins, from the gastrointestinal tract into the blood stream.<sup>4</sup> As a result it is a high capacity transporter.<sup>7</sup> Within the gastrointestinal tract expression is at its highest in the duodenum and jejunum, with lower levels being present in brush border membrane of the ileum.<sup>7</sup> In comparison, the large intestine contains low levels of PepT1 unless small intestine trauma has occurred and no expression has been found in the stomach. PepT1 is also expressed, at low concentrations, in the liver, bile duct and nasal epithelium<sup>8</sup> as well as in the kidneys where it plays a role in the re-absorption of proteins from the glomerular filtrate.<sup>9</sup> PepT1 has also been found to be over expressed in gastric, pancreatic and prostate cancer cells,<sup>10</sup> this opens up the possibility of tumour specific drug delivery *via* the PepT1 transporter.

Transport occurs across the cell membrane as a result of electrogenic H<sup>+</sup>-coupled oligopeptide co-transport (Figure 3).<sup>11</sup> The symporting of a H<sup>+</sup> ion down its concentration gradient, by way of facilitated diffusion, creates an electrochemical potential difference. This drives the di- and tri- peptides to move across the membrane against their concentration gradient. This co-transport was first demonstrated by Ganapathy *et al.*,<sup>12,13</sup> whose further work went on to prove a mechanism that is now widely accepted.<sup>14-16</sup> The inward H<sup>+</sup> gradient is maintained by the apically located Na<sup>+</sup>/H<sup>+</sup> transporter NHE3<sup>17</sup> and is indirectly dependent on extracellular Na<sup>+</sup>.<sup>18</sup> With PepT1, generally only relatively weak binding of a substrate is seen. This is due to the necessary rapid release of substrates after transport. A high affinity substrate for PepT1 is classed as having a binding affinity less than 1 mM and a medium affinity substrate has a binding affinity less than 5mM whereas typical enzymatic binding is in the nM range.

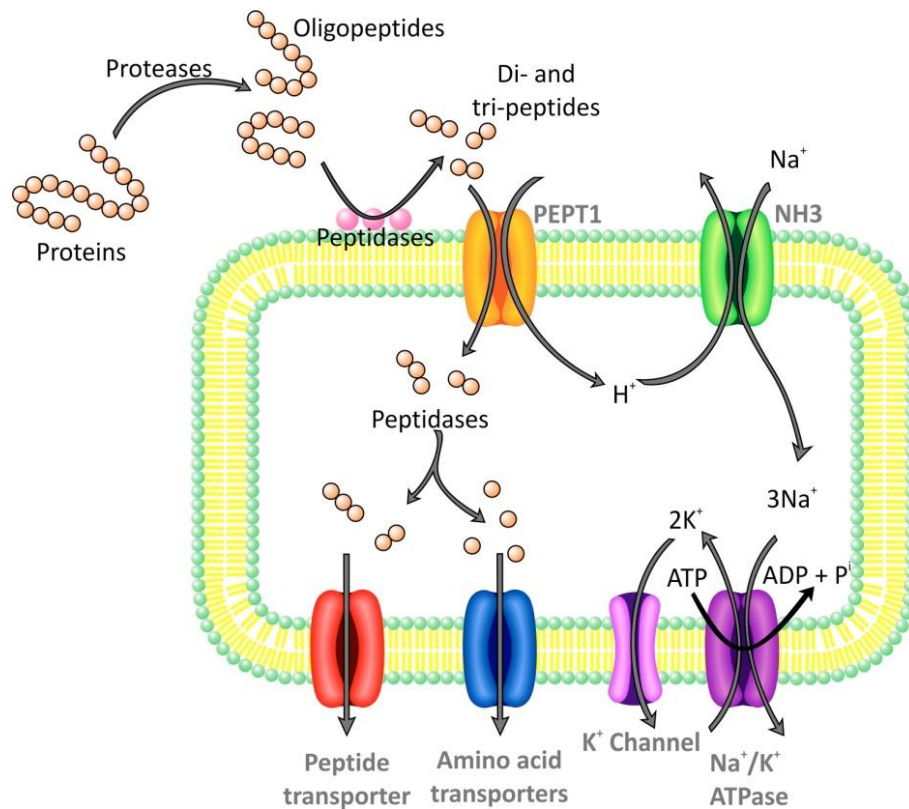


**Figure 3 The mechanism of transport for a PepT1 substrate.**

The indirect dependence of peptide transport on  $\text{Na}^+$  was first proposed by Ganapathy *et al.* in 1983.<sup>11</sup> Thwaites *et al.*<sup>19,20</sup> have since demonstrated this model using Caco-2 cell monolayers loaded with the dye 2',7'-bis(carboxyethyl)-5(6)-carboxyfluorescein (BCECF). It was shown that  $\text{H}^+$ /peptide co-transport resulted in intracellular increase in pH. This reduces the  $\text{H}^+$  electrochemical gradient and therefore inhibits further peptide uptake.  $\text{H}^+$  influx is minimised by the NHE3  $\text{Na}^+/\text{H}^+$  exchanger, which utilises the energy stored in the  $\text{Na}^+$  gradient to efflux  $\text{H}^+$  ions. This was demonstrated by Thwaites *et al.* who showed that inhibition of NHE3 reduced peptide transport.<sup>16</sup> The net result of the  $\text{H}^+$  cycling mechanism is a microclimate surrounding the microvilli of the brush boarder membrane of pH 6, which is not affected by the pH of the small intestine.<sup>21</sup>

There are several other transporters within the human body which display proton-coupled oligopeptide transport. These are the renal peptide transporter PepT2 and the peptide/histidine transporters PhT1 and PhT2, which alongside PepT1 are classified as the SLC15 family.



PepT1 is structurally most similar to PepT2 which is found mainly in the epithelial cells of the kidney tubule, where its role is to recover peptides from urine. Due to its location in areas that generally have low peptide concentrations, unlike PepT1, it is a low capacity transporter. PepT2 also displays a much higher affinity for di- and tri-peptides, as necessitated by its protein scavenging role.<sup>22</sup>

When transporting a substrate PepT1 is able to mediate electrogenic substrate influx, independent of net charge.<sup>23</sup> However, the rate and capacity of PepT1 to transport neutral and charged peptides is thought to be affected by extracellular pH. This was first proposed independently in 1996 by the Leibach<sup>23</sup> and Daniel<sup>24</sup> research groups, before being expanded by Irie in 2005.<sup>25</sup> The Daniel group<sup>24</sup> observed that neutral and charged substrates differently affected both the Michaelis-Menten affinity constant ( $K_m$ ) and the maximal inward current ( $I_{max}$ ) values as a function of membrane potential ( $V_m$ ) and external pH. Utilising rabbit mRNA expressing *Xenopus laevis* oocytes it was found that a decrease in external pH induced an increase in the rate of transport of anionic species, and to a lesser extent neutral species. In contrast an increase in external pH induced an increase in the rate of uptake of cationic species. The proton stoichiometry of transport was investigated by Temple *et al.*<sup>26</sup> and alluded to by Leibach.<sup>23</sup> Two protons are co-transported alongside anionic species, whereas neutral and cationic peptides are only transported with a singular proton, thus maintaining the membrane potential (Figure 4).

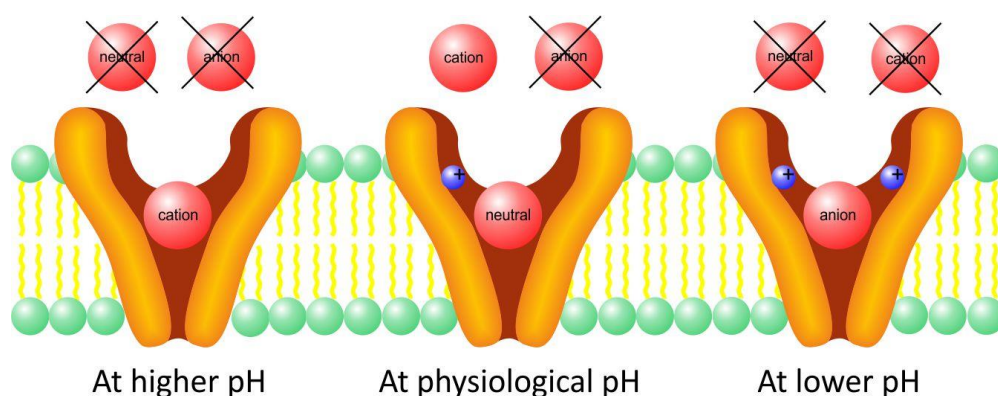


**Figure 4 Model to show how PepT1 mediates electrogenic substrate influx at varying pH.**

Once a substrate has been transported into the cell, any di- and tri peptides can be hydrolysed into their constituent amino acids by peptidases located within the cytosol. The resultant amino acids are transported out of the cell and into the blood stream *via* basolateral amino acid transporters.<sup>27</sup> Available information suggests that at least six amino acid transporters fulfil this role.<sup>28-30</sup> Not all peptides, such as Gly-Sar, are susceptible to hydrolysis which makes them ideal as controls in transport experiments. Dyer *et al.*<sup>31</sup> was the first to study peptide transport through the basolateral membrane. Using Caco-2 cells Berthelson *et al.*<sup>32</sup> showed that the uptake kinetics had a Michaelis-Menten like relationship which is indicative of carrier-mediated transport. There is disagreement as to whether PepT1 transport is proton dependant, with several papers being published suggesting this is not the case.<sup>33-35</sup> However, Thwates,<sup>19</sup> Dyer<sup>31</sup> and Berthelsen<sup>32</sup> all agree that transport is in fact proton dependant. Berthelsen offers the explanation that the differing views may be due to experimental set up, with the apical pH of 6.0 used by Irie,<sup>34</sup> Saito,<sup>35</sup> and Terada<sup>33</sup> resulting in a lower proton gradient across the basolateral membrane. All studies agree that the basolateral peptide transporter has a lower capacity than PepT1, but broad substrate specificity to include not only peptides but peptidomimetics. No specific transporter has been universally accepted as fulfilling the role of basolateral peptide transporter. Shepard *et al.*<sup>36</sup> has suggested a 112 kDa protein but little other characterisation at the molecular level has been carried out.

### 1.3.2 Regulation

When considering PepT1 as a vehicle for oral drug delivery attention must be paid to regulation of the protein in the small intestines. Any changes could significantly impact oral bioavailability which is particularly significant in prodrugs with small therapeutic windows. The regulation of PepT1 intestinal expression could emanate from pathological, pharmacological and physiological factors. These changes may be nonspecific such as nutritional status or a disease state which changes expression and/or membrane surface area. Specific inhibition of the transport mechanism may occur either by blocking the PepT1 protein or by altering any of

chemiosmotic gradients necessary for transport. Attention must also be paid to any substance that alters the expression of PepT1 this includes transcription and translation which affects the levels found in the enterocytes. There are several in depth reviews of the regulation of PepT1, primarily from an *in vitro* perspective.<sup>4,36,38</sup> Highlighted below are the aspects which potentially play a significant role in the oral bioavailability of PepT1 transported drugs.

Upregulation of PepT1 has been reported in bowel subjected to inflammation, starvation and a high protein diet. Ziegler *et al.*<sup>39</sup> reported that humans with Short Bowel Syndrome, small-bowel resection or a combination of small-bowel plus colonic resection, displayed a 5 fold increase in colonic PepT1 expression. This shows that the bowel is able to mitigate peptide absorption dysfunction after small intestine damage. Increased colonic PepT1 expression has also been reported in patients with chronic ulcerative colitis (chronic inflammation of the colon) and Crohn's disease (an inflammatory disease of the intestines).<sup>40</sup> The colon has a significantly higher bacterial population than the small intestines, resulting significantly higher concentrations of bacteria derived di- and tri-peptides. These small peptides are transported by PepT1 and have been shown to contribute to colonic inflammation.<sup>41,42</sup> If in these cases PepT1 can be inhibited or downregulated in the colon, then patients could potentially see an ease in some symptoms. Habold *et al.*<sup>43</sup> showed that in male Winsor rats subjected to prolonged fasting, upon the mobilisation of stored fats PepT1 expression significantly increased. Ma *et al.*<sup>44</sup> has since shown *in vivo* that this can occur in as little as 16 hours. The expression of intestinal PepT1 has also been found to increase in response to high dietary protein levels,<sup>45</sup> and has been shown to have a diurnal rhythm based on habitual feeding times.<sup>46</sup>

Hormonal expression has been found to both up regulate and inhibit PepT1 expression in the small intestine. Ashida *et al.*<sup>47</sup> showed decreased PepT1 expression in the small intestines of rats after hyperthyroidism was induced. The same group also demonstrated reduced PepT1 expression in Caco-2 cells upon treatment with the thyroid hormone 3,3',5-triiodo-L-thyronine.<sup>48</sup> Stimulation of PepT1 activity by insulin has also been found in Caco-2 cells. Thamotharan *et al.*<sup>49</sup>

showed that physiological concentrations of insulin stimulated Gly-Gln uptake 30-60 minutes after dosing. This is thought to occur as a result of insulin binding to a receptor in PepT1 as the stimulation was blocked with an inhibitor. Remarkably, increased expression of PepT1 is also noted in a sex dependant manner in rats induced with diabetes. In female rats an increase in mRNA lead to increased PepT1 expression. However, in male rats an increase in mRNA lead to a decrease in PepT1 expression. It was thought that this difference may be due to a sex dependent hormone such as oestrogen.<sup>50</sup>

Zinc, iron and copper ions have also been shown to have an inhibitory effect on the PepT1 transporter.<sup>51</sup> This suggests that supplements or medications containing these ions may alter the uptake of PepT1 transported drugs. This inhibition can most likely be attributed to the cations competitively inhibiting H<sup>+</sup> binding. Similarly, any drugs which affect the chemiosmotic gradient of a cell can affect PepT1 transport. This usually occurs *via* inhibition or stimulation of the sodium-proton antiporter. Known drugs which do this include calcium channel blockers such as nifedipine<sup>52</sup> and the diuretic amiloride.<sup>53</sup> Caffeine,<sup>54</sup> as well as several naturally occurring flavonoids<sup>55</sup> have also been shown to affect PepT1 transport *via* interaction with the sodium-proton antiporter. This may have significance for PepT1 drug substrates with narrow therapeutic windows and is a much underexplored area.

### 1.3.3 Discovery

In 1978 Kimura *et al.*<sup>56</sup> discovered that the abnormally high bioavailability of penicillin  $\beta$ -lactam antibiotics was due to a mechanism of absorption which was the same as dipeptides. This led not only to the discovery of PepT1, but also to its potential as a vehicle for targeted delivery. Up until this point it was only known that dipeptides were transported *via* a separate mechanism to amino acids, which were known to be actively transported. The discovery centred around  $\beta$ -lactams as they have a high bioavailability, even though are ionised at physiological pH and have low lipid solubility so therefore should not be absorbed.

Hou and Poole<sup>57</sup> were the first to note the physio-chemical similarities between amino acids and  $\beta$ -lactams (which have a peptide like core structure). This led to the theory that the absorption of both may occur *via* the same process. This speculation was further strengthened by Levine,<sup>58</sup> who discovered that drug absorption by active mechanisms is limited to compounds bearing a structural resemblance to the products of the gastrointestinal break down of food.

Utilising the everted gut sac technique, in which a rat intestine is used to study intestinal absorption, Dixon and Mizen<sup>59</sup> investigated the transport of several  $\beta$ -lactams. Although no relationship between the transport of amino acids and  $\beta$ -lactams was discovered, the transport of cyclacillin became saturated once a certain concentration was reached. It was also noted that the forward flux of cyclacillin was far greater than its backward flux. It had been recently discovered<sup>60</sup> that dipeptides were transported *via* a separate mechanism to amino acids. Dixon and Mizen<sup>59</sup> postured that it would be interesting to see if cyclacillin uptake was *via* the same mechanism as dipeptides. This work was in fact carried out by Kimura *et al.*<sup>56</sup> using *in situ* perfusion, leading to the discovery of PepT1.

#### 1.3.4 Structure

The knowledge that PepT1 could transport substrates other than natural dipeptides prompted research into the pharmacophoric pattern required for PepT1 substrates. This has been conducted utilising both biological and chemical characterisation, as no crystal structure has yet been generated. By understanding the physical structure of PepT1, its binding site and the conformational change involved in transport, greater understanding can be applied to the limits of size and spatial arrangement for PepT1 targeted drugs.

PepT1 is a member of both the proton-dependent oligopeptide transporter (POT) and major facilitator superfamily (MFS) and is encoded by the SLC15A1 gene. It was first functionally characterised and cloned from a rabbit small intestine in 1994 by Fei *et al.*<sup>61</sup> and later that year by Boll *et al.*<sup>62</sup> Human PepT1 (hPepT1) was subsequently cloned by Liang *et al.*<sup>63</sup> in 1995. It was

found to contain 708 amino acid residues and be a 81% match to rabbit PepT1, which contains 707 amino acid residues. In the first paper to be published on the structure of PepT1, utilising a hydropathy plot based on the Kyte-Doolittle algorithm, Fei<sup>61</sup> predicted the presence of 12 transmembrane spanning domains. This was subsequently confirmed by Covitz *et al.*<sup>64</sup> using EE epitope tagging. Covitz<sup>65</sup> also showed that the *C-terminus* of hPepT1 was intracellular and a large extracellular loop existed between transmembranes 9 and 10. The role of this large loop is still unknown, but it has been shown to contain several putative glycosylation sites.

The first attempt to elude the structure of PepT1 *via* computer modelling came with Vincent Lee's group.<sup>66-67</sup> Models of hPepT1 were generated based on minimising the facial interactions of paired transmembrane domains. This was based on a study by Fei *et al.*<sup>68</sup> that predicted that the  $\alpha$ -helical transmembrane domains are important for substrate/  $H^+$  binding. In their models both Bolger and Yeung arranged the transmembrane sequences of PepT1 helically, so that each had 7 faces and therefore 49 possible interactions. After minimising and modelling the 12 transmembrane domains, taking into consideration amphipathicity and hydrophobicity, they predicted the arrangement of the domains around a central channel. Bolger also modelled the presence of the PepT1 substrates Gly-Gln and Gly-Gly-Gly in the created channel. Through this work several amino acid residues that have a potential interaction with bound substrates were identified (Figure 5).

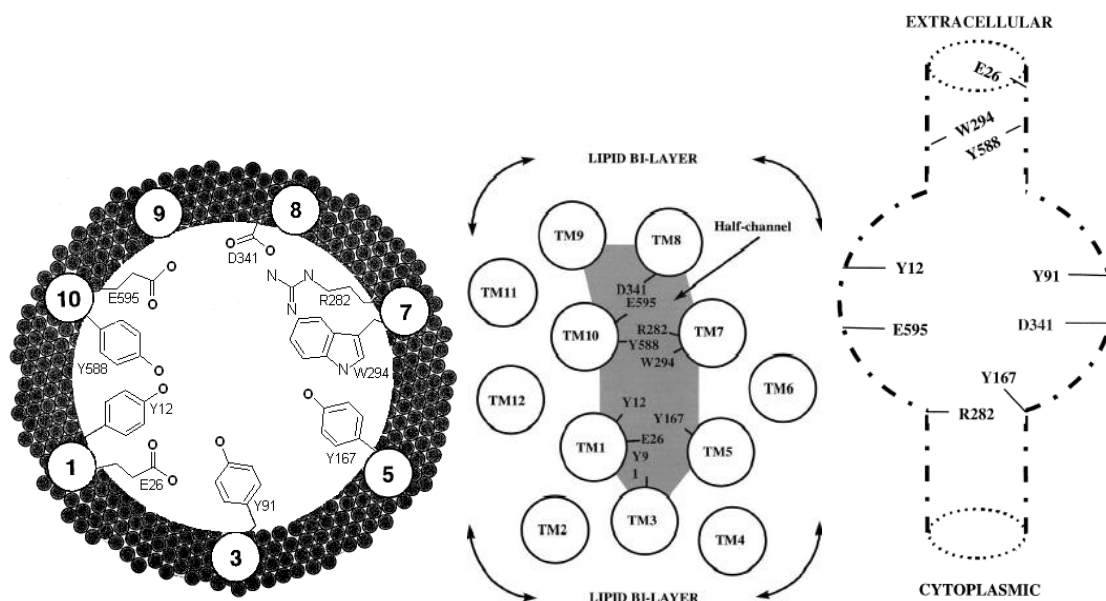


**Figure 5** Lee's models of the substrate binding site of PepT1. Left: A schematic view looking at the computationally modelled transmembrane domains buried in the phospholipid membrane.<sup>67</sup> Middle: A schematic view of the lipid-bilayer showing the arrangement of all 12 transmembrane domains.<sup>69</sup> Right: The vestibule model showing the amino acid residues identified as potentially interacting with a substrate.<sup>69</sup> Reproduced with the kind permission of the publishers, © Elsevier Ltd.

Lee's group<sup>69</sup> further refined their model in 1999, with the prediction of the presence of a vestibule in the centre of the modelled channel large enough to hold a dipeptide. To test the vestibule model, site directed mutations were made to the residues identified by Bolger as being potentially involved in substrate interaction. This work was primarily performed by the Lee and Meredith research groups and showed that if mutated all residues identified in the vestibule model, except E26 and Y588, have a detrimental effect on rabbit and/or human PepT1 function. Despite the mutation of Y588 having no effect on transport, when several other tyrosine residues were systematically mutated effects were seen in affinity and transport rate.<sup>70</sup> Interestingly, mutation of both R282 and D341 have been shown to alter the pH profile of PepT1 without affecting transporter function.<sup>71,37</sup> However, the double mutant R282D-D341R had no effect on pH profile suggesting that these residues are involved in a salt bridge.

Several studies have shown that histidyl residues participate in proton and substrate recognition,<sup>37</sup> but are not included in Lee's model. Of note is H57, located on transmembrane domain 2. When Fei *et al.*<sup>72</sup> mutated this residue they found the mutant PepT1 was no longer able to transport substrates. To find out if the residue was responsible for H<sup>+</sup> binding and therefore initiating co-transport, Chen *et al.*<sup>73</sup> mutated the aromatic residues tyrosine 56 and tyrosine 64 which are located near H57. They concluded that by interacting with H57 the aromatic tyrosine residues stabilize the charge on the H<sup>+</sup>, confirming that H57 is essential for the normal function of PepT1.

Other site directed mutagenesis work of note is the investigation of the residues in transmembranes 3,<sup>74</sup> 5<sup>75</sup> and 7<sup>76</sup> for involvement in the putative central channel of PepT1. Each of the amino acid residues in these transmembrane domains were systematically changed to a cysteine so that the effect of each residue could be assessed. Several residues were theorised to play an important structural role in transporter function (Figure 6) as negligible Gly-Sar uptake was seen in PepT1 which had these residues mutated. Two of the mutated transporters Y287C- and M292C-hPepT1 were not found to express at the plasma membrane, suggesting that these residues may be integral for transcription and/or translation. By assessing the solvent accessibility of the various residues the orientation of transmembrane domains 3, 5 and 7 could be eluded and all were predicted to lie diagonal to the plane of the membrane.

The site directed mutagenesis of PepT1 is an expanding area of research and plays a critical role in the identification of the function of areas and residues within the transmembrane domains and loops. This includes the residues responsible for substrate binding and recognition, as well as salt bridges and the conformational changes that are involved in transport. There are several comprehensive reviews on the work determining function of domains using site directed mutagenesis.<sup>77,78</sup>





### 1.3.5 PepT1 homologues

Further insight into the structure of PepT1 was obtained by comparison of the published crystal structures of LacY<sup>81</sup> and GlpT<sup>82</sup> which are homologous 12 membrane domain POT transporters. The similarity in the structures of LacY, a proton-coupled lactose permease transporter, and GlpT, a phosphate coupled glycerol-3-phosphate antiporter, was shown by Ambramson *et al.*<sup>83</sup> When both 3D structures were superimposed only the transmembrane domains 2 and 8 were displaced. This displacement may be due to the fact that unlike GlpT, LacY was crystallised while bound to a substrate.

As PepT1 is also a member of the major facilitator superfamily, Meredith and Price<sup>84</sup> decided to homology model rabbit PepT1 against the crystal structures of LacY and GlpT. As PepT1 contains a large extracellular loop that neither LacY or GlpT contains, this was removed and a modified form of the rabbit PepT1 overlaid on both structures. The modified PepT1 (rPepT1-trunc) was then run through the transmembrane prediction program MEMSAT3. In the model proposed by Meredith many of the transmembrane domains are not adjacent to their predecessor (Figure 7). This is contrast to Lee's model which was based on the assumption that there is 3D restriction of the transmembrane domains. Meredith's model also predicts that several of the transmembrane domains lie diagonal to the plane of the membrane.

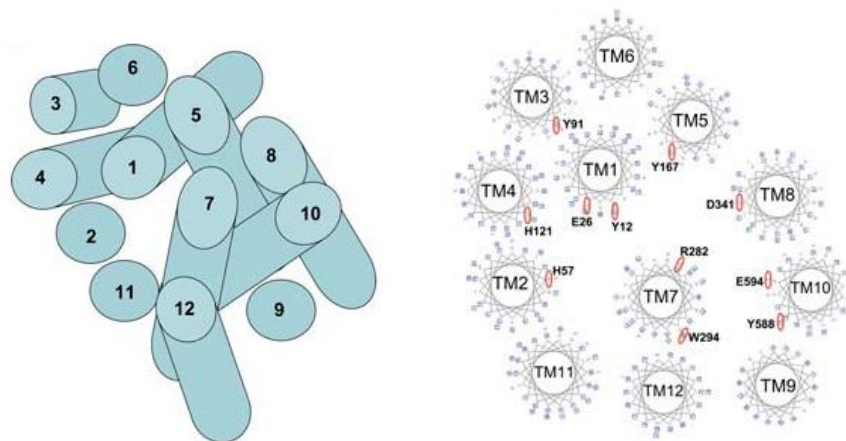


**Figure 7 Meredith model of the arrangement of rPepT1-trunc's 12 transmembrane domains.**

**Left: A cartoon showing several of the domains lying diagonal to the plane. Right: A helical wheel plan of r-PepT1-trunc. Reproduced with the kind permission of the publishers and authors, © Springer Science and Business Media, LLC (2007)<sup>84</sup>**

The first topology model of a POT transporter with a similar substrate recognition pattern to PepT1 was published by Weitz *et al.*<sup>85</sup> in 2007. YdgR, a POT transporter found in *E. coli*, was found to transport both di- and tri-peptides and aminocephalosporins with similar affinities to that of PepT1. By representing a substrate recognition pattern which corresponds to mammalian PEPT1, the architecture of the substrate binding domain should be the same. However, YdgR does not contain a histidine residue in the area of H57, which is thought to be essential for the normal function of PepT1. H121 is also absent in YdgR, although there is a histidine residue located nearby. This suggests that the identification of the residues in YdgR which are responsible for transport activity would aid in understanding the mechanisms of PepT1. YdgR also lacks a large extracellular loop between the transmembrane domains 9 and 10, suggesting this region of PepT1 is unlikely to be essential for the transport process.

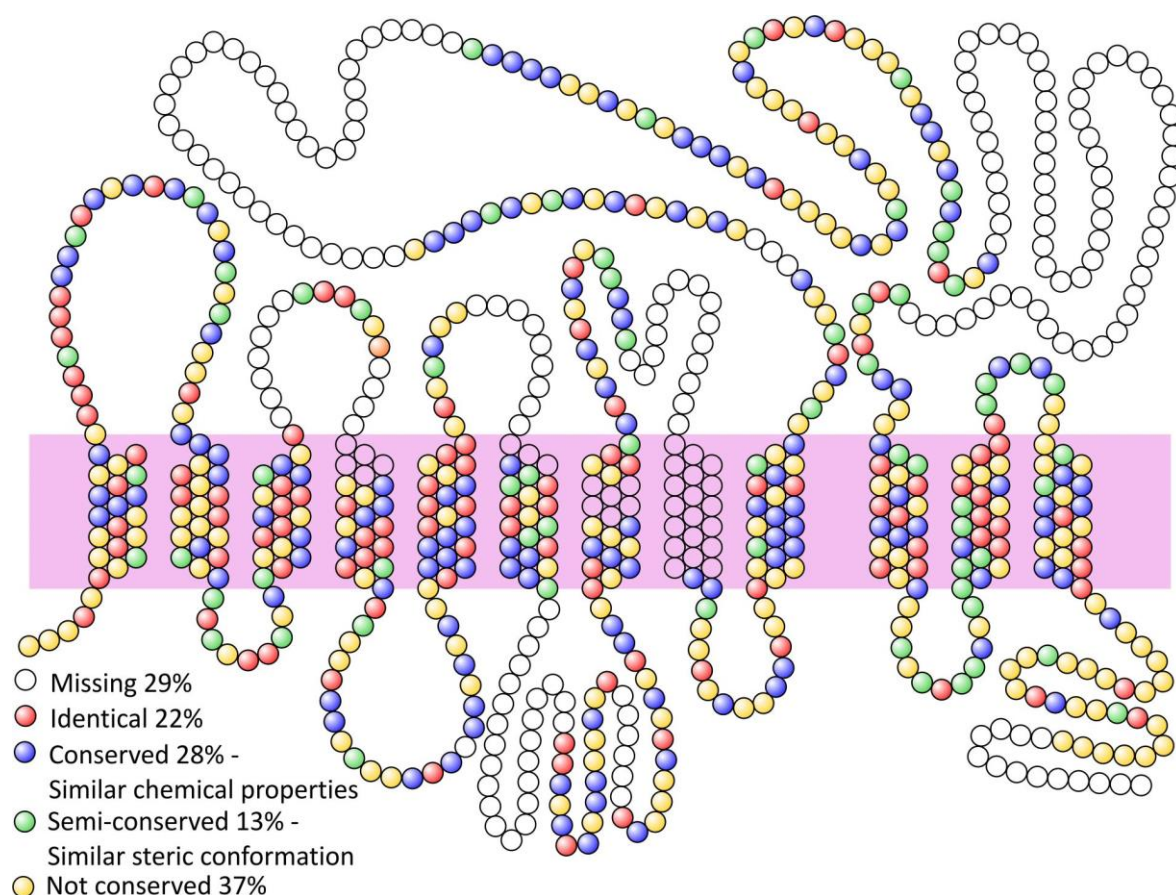


**Figure 8 Homology model of human PEPT1 overlaid with corresponding YdgR residues.**

The recently published crystal structures of four different prokaryotic POT transporters, has given insight into the alternating access transport cycle of PepT1. The first to be crystallised was PepT<sub>so</sub><sup>86</sup> which is found in *Shewanella oneidensis*, an anaerobic bacterium, and has a 30% identity with to Pep1. Newstead<sup>87</sup> concluded that there was a central ligand binding site equidistant to the intracellular and extracellular sites which, when bound to a ligand, presented a novel occluded conformation. In contrast PepT<sub>st</sub><sup>87</sup> found in *Streptococcus oneidensis*, was crystallised in an inward facing conformation. Two pairs of salt bridges R53-E312 and R33-E312 were found to facilitate the close packing of gate helices at the extracellular end of the extracellular cavity, which are proposed to facilitate closure of the extracellular gate. The intracellular gate is thought to be controlled by a salt bridge between K126 and E400. It is proposed that the binding of a substrate and proton with the central ligand site disrupts this salt bridge and therefore facilitates the release of the intracellular gate. E400 corresponds to E594 in



human PepT1 and has been suggested by Meredith's research group as being involved in transport. The third and fourth POT homologues GkPOT,<sup>88</sup> from *Geobacillus kaustophilus*, and PepT<sub>so2</sub>,<sup>89</sup> found in *Shewanella oneidensis*, were crystallised in the inward open state with a peptide in the peptide binding site. This only leaves the crystal structure of a substrate bound POT transporter in the outward open conformation to be captured for the sequence to be completed.

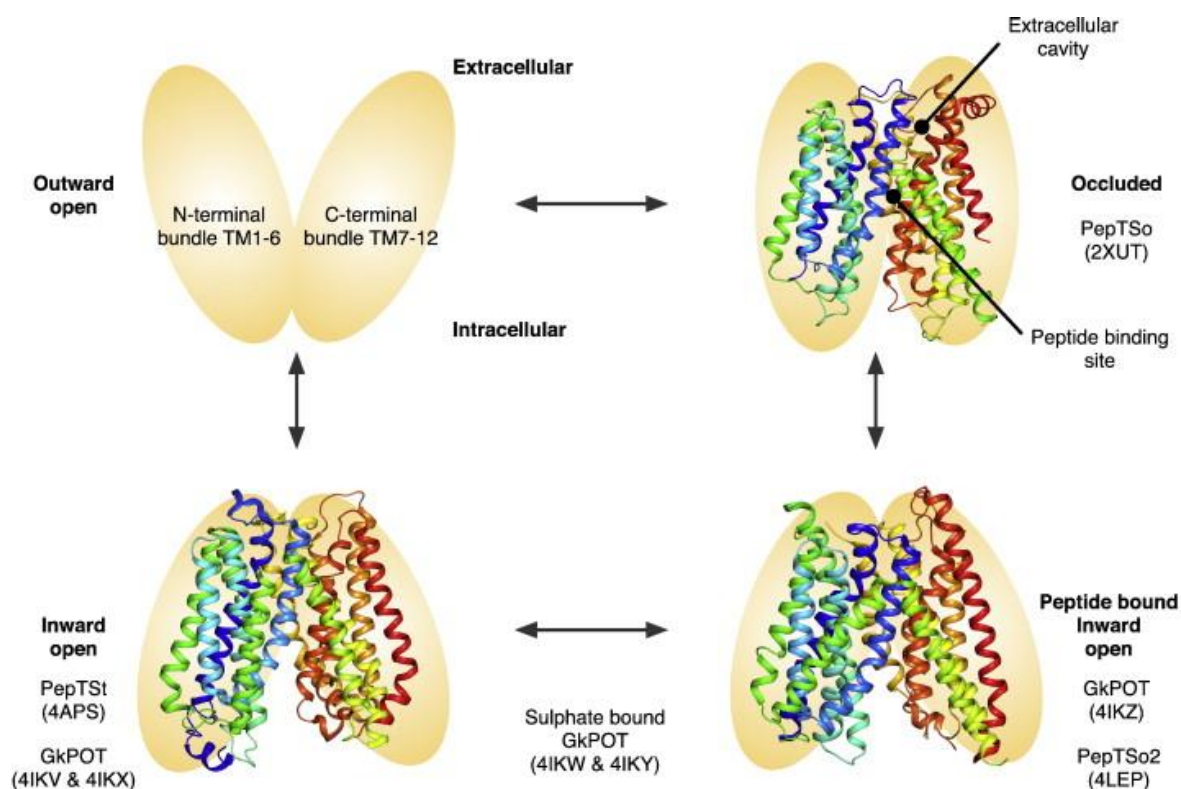


**Figure 9** The crystal structures of POT transporters which have given insight into the alternating access transport cycle of PepT1. Blue denotes *N-terminus* and red the *C-terminus*.<sup>90</sup> Reproduced under the creative commons attribution licence.

PepT1 is able to accommodate a wide range of ligands whilst maintaining specificity for peptides two or three residues in length within the central ligand binding site. To better understand the mechanisms behind this, Lyons *et al.*<sup>91</sup> determined the crystal structure of PepT<sub>st</sub> in complex with physiologically relevant di- and tri- peptides. *L*-Ala-*L*-Phe was found to sit laterally in the binding site, with the amino *terminus* forming a hydrogen bond with N328 and interaction

occurring with E400. Coordination of the dipeptides carboxy *terminus* with N156 forms a ligand-coordinated bridge between the C- and N-terminal bundles of PepT<sub>st</sub>. Two elongated cavities in the ligand binding site were observed. The first being 16 x 7 x 11 Å at the N-terminal end of the ligand and the second a hydrophobic pocket 10 x 10 x 3 Å accommodating the phenyl side chain. The position of the phenyl side chain brings it into close proximity to the side chain of Y68, causing  $\pi$ - $\pi$  stacking interactions. This suggests that Y68 is involved in determining substrate specificity and corresponds to Y64 in human PepT1, which has been identified as being essential for transport. In contrast, *L*-Ala-*L*-Ala-*L*-Ala was found to sit vertically in the ligand binding site. However, poor electron density of the crystal structure means it cannot be established whether the *C-terminus* is orientated towards the cytoplasmic or periplasmic space.

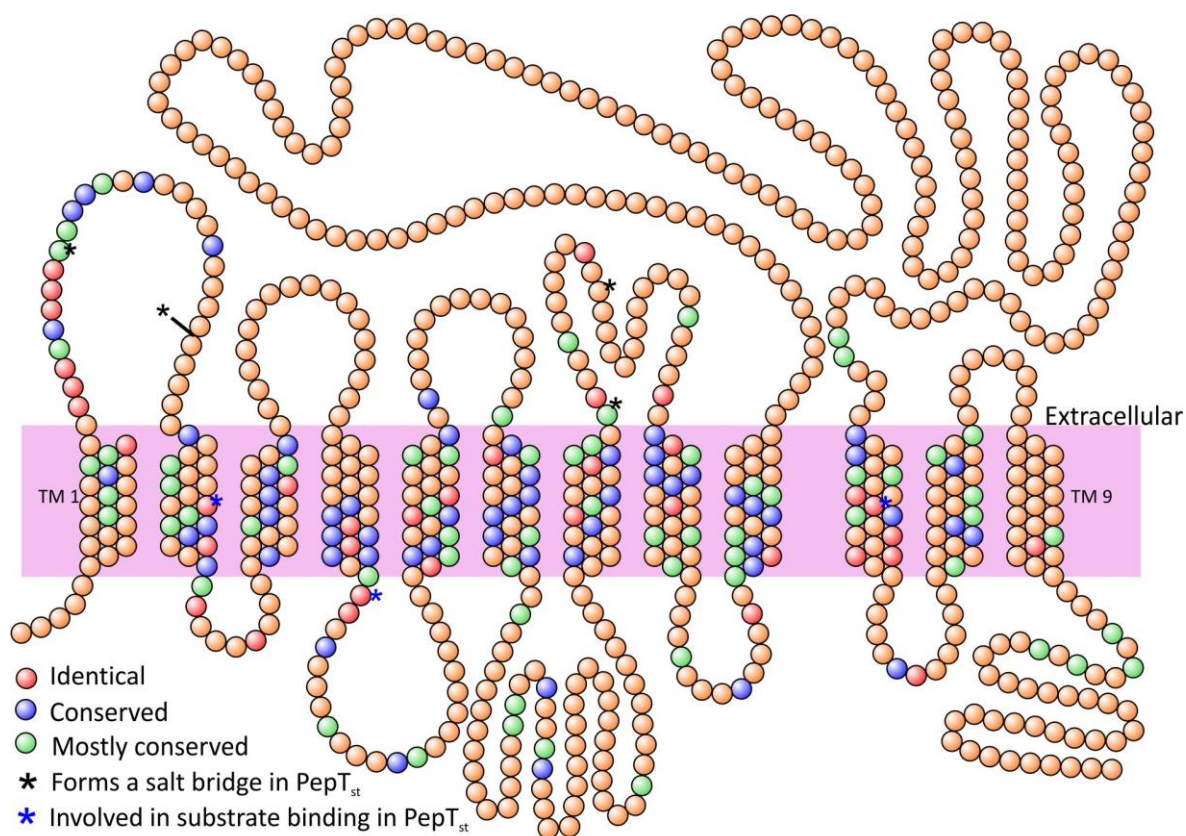


**Figure 10 Topology model showing amino acid residues similarities between; PepT1, PepT<sub>so</sub>, PepT<sub>st</sub>, GkPOT and PepT<sub>so2</sub>.**

### 1.3.6 Identifying PepT1 substrate structural features.

As there is no known structure for PepT1, the structural requirements of a PepT1 substrate have had to be ascertained through extensive *in vitro*, *in vivo* and *in-situ* screening.<sup>92</sup> This has hindered the structure-based approach to targeted drug discovery as computer models cannot be made of the binding site. This would allow investigation into the capacity of PepT1 for drugs of varying size, hydrophobicity and functional groups, although the crystallisation of both a dipeptide and tripeptide in PepT<sub>st</sub><sup>91</sup> is a promising development.

It was initially assumed that active transport was limited to compounds with structural resemblance to the products of dietary digestion. This was strengthened with the discovery that penicillin class  $\beta$ -lactam antibiotics, which contain an  $\alpha$  amino group, are PepT1 substrates. However, the discovery that cephalosporin class  $\beta$ -lactam antibiotics, which lack an  $\alpha$ -amino group are also transported, prompted research into other drugs that may be substrates. As a result ACE inhibitors, bestatin, thyrotropin-releasing hormone and some renin inhibitors were shown to be actively transported by PepT1 (Figure 11).

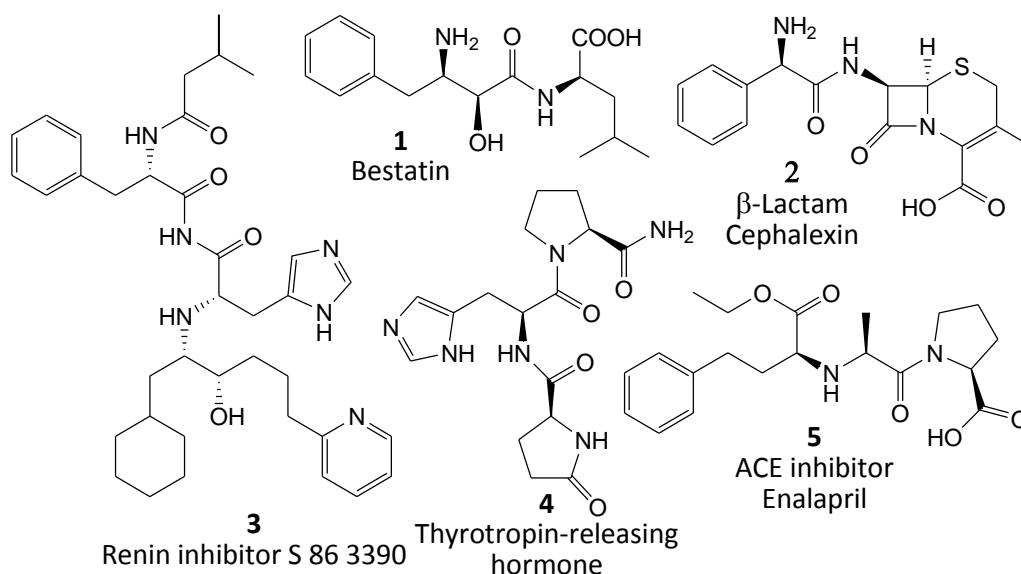


**Figure 11** Examples of the classes of drugs that are PepT1 substrates.

How closely a substrate must resemble a peptide and still be transported was further called into question with the discovery that 4-aminophenylacetic acid<sup>93</sup> and subsequently  $\omega$ -amino fatty acids<sup>80</sup> were able to bind and be transported by PepT1. This was the first indication that the presence of a peptide bond was also not a structural requirement for transport. Döring *et al.*<sup>80</sup> found that affinity of PepT1 for the substrates tested increased with increasing number of hydrogen bonding sites. To assess whether the *N*- or *C-terminus* played a role in transport, the terminal amino or carboxylic groups of known substrates were removed. No transport occurred although binding affinity was maintained, suggesting that they both play a role in substrate recognition.

The necessity of a terminal carboxylic acid group within a substrate was further investigated by Börner *et al.*<sup>94</sup> utilising peptidomimetic alanyl anilides. Removal of the terminal carboxylic group from known PepT1 substrates still resulted in molecules with medium binding affinities. The introduction of a phenyl group in the carboxy terminal region was shown to improve binding affinity, which was further improved with the introduction of nitro group or a second benzene group. This shows that carboxyl group is not necessary in this area and can be replaced with a group which can participate in hydrogen bonding. Interestingly, Börner also found that insertion of a CH<sub>2</sub> group between the peptide NH and benzene ring in alanine-4-nitroanilide (**7**) resulted in a greatly reduced binding affinity  $K_i = >30$  mM. This suggests that a directional vector of the carboxylate site may be important for high affinity binding.

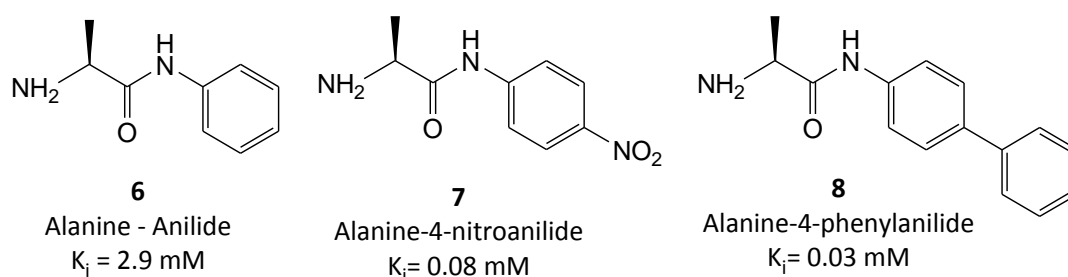


**Figure 12 Peptomimetics used by Börner<sup>94</sup> which are substrates of PepT1, but do not possess a free terminal carboxylic acid group.**



The necessity of a free amino *terminus* was demonstrated with the acetylation of the amino *terminus* of Phe-Tyr.<sup>95</sup> Upon acetylation, the binding affinity of phenylalanine-tyrosine was significantly reduced. The same molecules were also amidated at the carboxy *terminus*, resulting in a comparatively small decrease in transport affinity. This indicates that the amino *terminus* is the primary binding feature.

In an attempt to further assess the structural features required for transport Vig *et al.*<sup>96</sup> used high throughput screening to test 79 di- and tri-peptides and 2 amino acids for PepT1 activation. Surprisingly 20 of these did not induce PepT1, which contradicts the assumption that all di- and tri-peptides are PepT1 substrates. Of these five were dibasic, which encompasses all of the dibasic peptides tested except His-His. This suggests that the bulky side chains of Arg, Lys and Orn are responsible for their lack of transport, rather than their charge. Lys-Pro and Pro-Lys were also not transported. The study also attempts to suggest a model of the PepT1 channel by overlaying the lowest energy conformations of four dipeptides. They propose that substrates with aromatic side chains are subject to  $\pi$  stacking interactions with aromatic residues within the PepT1 binding site. This is found to occur in PepT<sub>st</sub>.

Within nature the *L* form of amino acids dominates. It is therefore assumed that di- and tri-peptides containing two and three *L*- amino acids respectively would have the highest affinity binding. Experimentally this has always been the case, with dipeptides which have *L*- stereochemistry at the *N-terminus* showing the highest affinity. To probe the reason behind this preference the Bailey group<sup>97</sup> synthesised and tested a series of constrained dipeptide analogues. In each case, surprisingly, the binding affinity was found to be higher in peptidomimetics with *D*- stereochemistry at the *N-terminus*. This suggests that high affinity binding is achieved when the amino group is directed to the back of the plane.

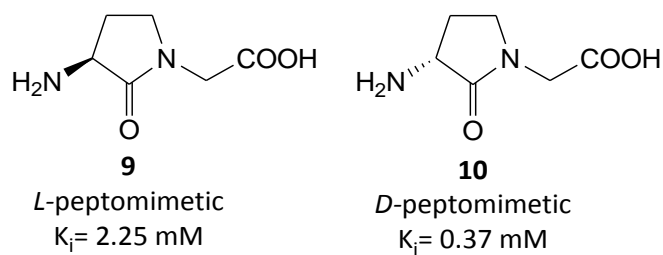


**Figure 13** The constrained dipeptide analogues used by Bailey<sup>97</sup> to demonstrate high affinity binding when the free *N-terminus* is directed back in the plane.

To further probe the reason for the low binding affinity seen in *D*-conformation *N-terminus* peptides, the half position of the *N-terminus* created by an  $\alpha$ -aminoisobutyric (Aib) peptide was investigated. Working on the assumption that the oxygen on the 3<sup>rd</sup> atom of the molecule in Figure 14 forms a salt bridge with a specific histidine residue, its positioning becomes fixed within the PepT1 central ligand binding site. The bond between atoms 2 and 3 must therefore rotate to find the optimum conformation of the three substituents on atom 2 within the binding site.

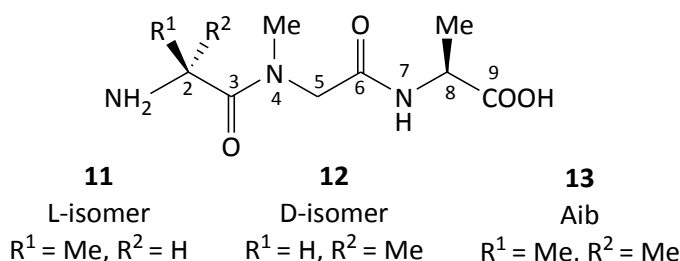


**Figure 14** The conformational arrangement of the *N-terminus D- or L- tripeptide conformational isomer* used in Baileys experiment.<sup>97</sup>

By placing a methyl group on atom 4 gauche interactions occur between that methyl group and the two functional groups on atom 2. To avoid this and minimise the energy of the system, rotation of the bond between atoms 2 and 3 must occur. This alters their optimum positioning within the binding pocket. Through the placement of either a hydrogen and a methyl or two methyl groups on atom 2 the *D-* or *L-* conformers or Aib analogue can be created. To avoid

gauche interactions and therefore reach an energy minimum, no rotation is required in the *L*-residue. However, a rotation of approximately 120° must occur in the *D*-residue and approximately 60° in the Aib analogue. In these rotated positions the amino group of the *L*-conformer (**11**) is in the experimentally deduced optimum position of being directed to the back of the plane; in the *D*-conformer (**12**) it is forward of the plane and in the Aib analogue (**13**) it is with the plane. It could therefore be assumed that the *L*-conformer (**11**) would have good binding affinity, the *D*-conformer (**12**) would have poor and the Aib analogue (**13**) would have a binding affinity somewhere between the two. However, no significant difference in binding affinity was seen between the *D*-conformer (**12**) and Aib analogue (**13**). This suggests that *D*-isomers have a lower binding affinity due to spatial constraints as the dipeptide makes its way down the binding pocket, not due to the positioning of the amino group.

When an amide bond is in its partial double bond form, rotation of the bond is inhibited and either the *cis* and *trans* isomer can form.<sup>98</sup> Rapid interconversion between these two isomers often occurs giving a specific *cis/trans* ratio. Favouritism for the *trans* isomer was first demonstrated by Brandsch *et al.*<sup>98</sup> By using a thiodipeptide to stabilise the peptide bond, they were able to show that the *trans* isomer was preferentially transported. Caco-2 cells were incubated with Ala(S)Pro in a 62% *trans*/38% *cis* ratio. After 60 minutes the intracellular content of the Caco-2 cells were analysed and found to contain 92% of the *trans* isomer. Reanalysed after 2 days the intracellular content was found to have re-equilibrated, showing that transport rates for the *trans* isomer are much higher than for the *cis* isomer. The findings of this study was supported by the Bailey group<sup>99</sup> using pH controlled thiodipeptides and Niida *et al.*<sup>100</sup> using fluoroalkene and alkene containing dipeptide mimics.

The presence of a *D*-amino acid at the carboxy *terminus* is tolerated, although lower transport rates are seen than if it is of the *L*-conformation.<sup>101</sup> If the positioning of the carboxylate is absolutely fixed due to hydrogen bonding a histidine residue, then the difference in binding affinities seen for *L*- and *D*- residues must be explained in the side chain positioning (Figure 15).

Under the assumption that the *L*-conformation at the *C-terminus* has the highest binding affinity, as there is no interaction of the side chain with the binding pocket, it can be proposed that the side chain points out of the binding pocket. The drop in binding affinity for the *D*-amino acids could therefore be proposed as being due to interaction of the side chain with the residues at the mouth of the binding pocket. Peptides that have pure *D*- stereochemistry have the lowest binding affinity of all enantiomers.<sup>97</sup>

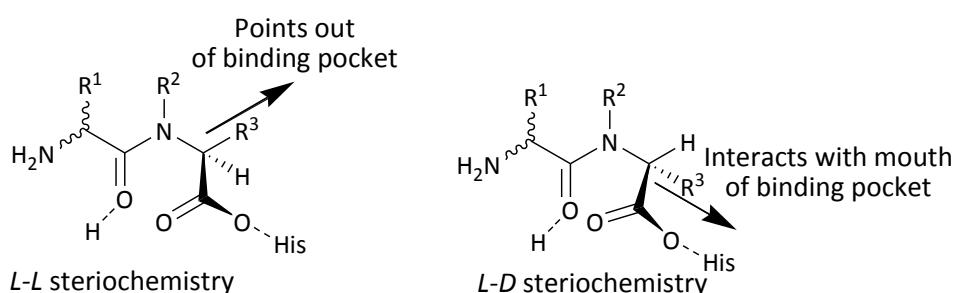


**Figure 15** Side chain positioning in *L*- and *D*- carboxy-terminus dipeptides.

The Bailey group was the first to collate all of the published PepT1 substrate data, enhancing the pool with *in vitro* investigations of over 100 substrates. This led to the first template that attempted to encompass all of the substrate specificities.<sup>102</sup> This work was later enhanced to give a predictive indication of how well a potential substrate would be transported by PepT1.<sup>103</sup>

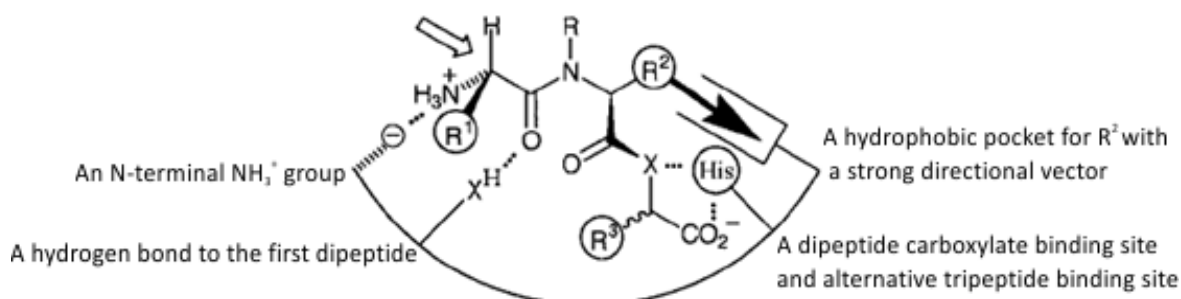


**Figure 16** The Bailey PepT1 substrate template, showing the four key binding sites.<sup>104</sup>

Reproduced with the kind permission of the publishers, ©2000 WILEY-BCH Verlag GmbH.

### 1.3.7 QSAR studies

Prior to Newstead *et al.*<sup>91</sup> determining the crystal structure of PepT<sub>so</sub> in complex with physiologically relevant di- and tri- peptides, quantitative structure affinity relationship (QSAR) modelling was used to assess the optimum binding conformation of a PepT1 substrate. Using a comparative molecular field analysis (CoMFA) and comparative molecular similarity indices analysis (CoMSIA), Gebauer *et al.*<sup>104</sup> developed a pharmacophore model, which is supported by independent study in 2005 by Våbenø *et al.*<sup>4</sup> Using CoMSIA standard deviation coefficient contour plots for steric properties, Gebauer was able to show that the poor binding affinity of *D*-conformers was due to the side chains occupying disfavoured steric regions (Figure 17). Binding affinity was found to increase with dipeptides which largely occupied favoured regions i.e. *L-trans* conformers with bulky side chains. These favoured regions correspond to the same positions as the two elongated cavities in the ligand binding site of PepT<sub>st</sub>. It was also found that at the carboxy *terminus* all that was required for appreciable affinity was an area of high electron density, rather than a specific carboxylate group. This is in keeping with previous groups work that alteration to the carboxy *terminus* has only a small affect on affinity. CoMSIA standard deviation coefficient contour plots, showing lipophilic properties, indicated an overlapping region with *C-terminus* sterically favoured region. This suggests, as in Bailey's template, that a *C-terminus* lipophilic side chain is favoured for high affinity binding.

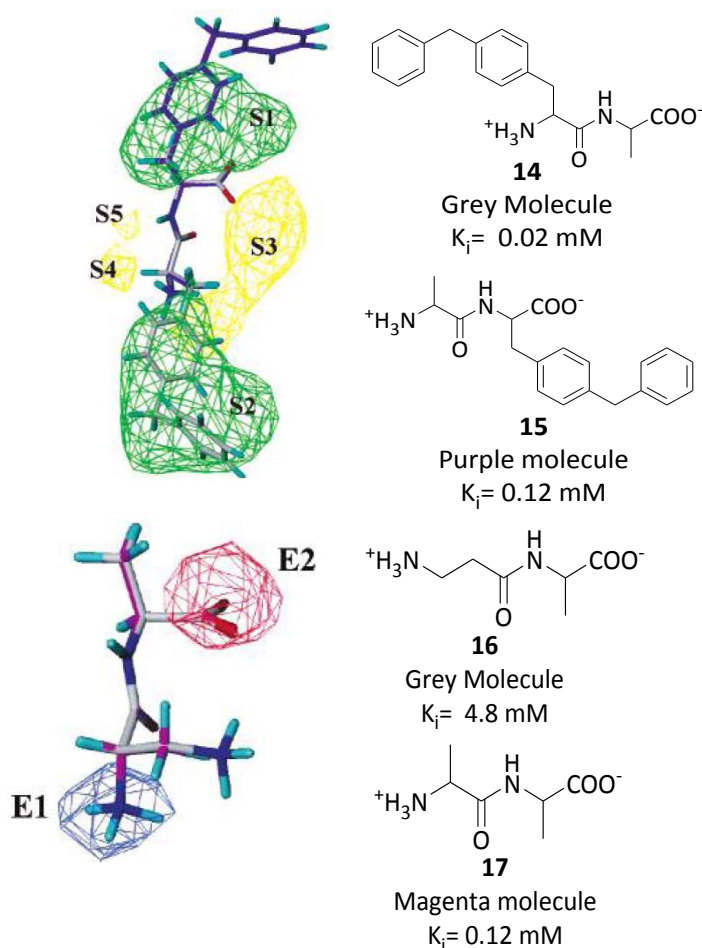


Figure 17 CoMISA standard deviation coefficient contour plots. Top: For steric properties. Green isopleths indicate regions where bulky groups enhance affinity. Yellow isopleths are regions that should be left unoccupied. Bottom: Electrostatic properties. The blue contour donates a region where positively charged groups enhance affinity. The red contour group donated a region where negatively charged groups increase affinity. Reproduced with the kind permission of the publishers, © 2015 American Chemical Society.<sup>104</sup>

# **Chapter 2**

## **Targeting drugs towards**

### **PepT1**

## Chapter Two Contents

2.1	Targeting drugs towards PepT1. ....	33
2.1.1	Changing the drug to make it a substrate.....	33
2.1.2	Attaching a substrate carrier. ....	35
2.2	Using thiodipeptides as carriers.....	37
2.3	Synthesis of thiodipeptide carriers. ....	41
2.4	Synthesis of alternatively protected thiodipeptide carrier.....	44
2.5	PepT1 targeted prodrugs using commercially available drugs. ....	47
2.5.1	Propofol.....	47
2.5.2	Ibuprofen .....	49
2.5.3	Aspirin. ....	50
2.6	AstraZeneca new chemical entities .....	57
2.6.1	Aurora kinase inhibitor .....	58
2.6.2	$\alpha 1\beta 5$ Integrin inhibitor.....	65
2.7	<i>In vitro</i> biological testing.....	73
2.7.1	Binding Affinity.....	74
2.7.2	Oocyte transport assay. ....	75
2.7.3	Caco-2 assays. ....	76
2.7.4	Biological results. ....	77



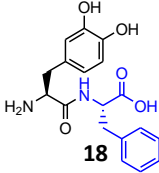
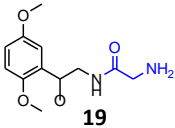
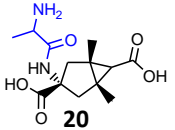
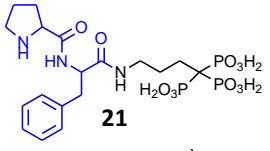
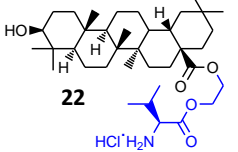
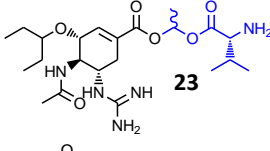
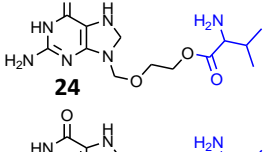
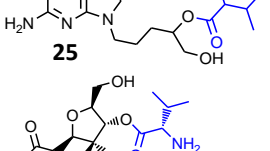
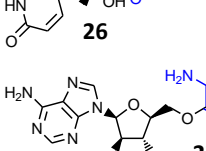
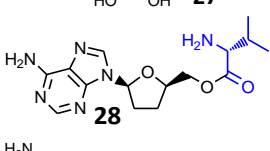
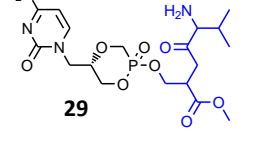

## 2.1 Targeting drugs towards PepT1.

There have been two major routes undertaken in an attempt to improve the bioavailability of drugs through PepT1 targeting. Both routes involve turning the drug in question into a prodrug. However, one approach focuses on turning the whole drug into a PepT1 substrate, whilst the other involves attaching the drug to a standardised hydrolysis resistant PepT1 substrate.

### 2.1.1 Changing the drug to make it a substrate.

Several successful PepT1 transported prodrugs have been created through the attachment of amino acids to drugs which already contain some peptidomimetic characteristics. *L*-dopa was one of the first drugs to which this prodrug method was applied. *L*-dopa is a naturally occurring psychoactive drug found in foods such as the velvet bean and is used primarily for the relief of Parkinson's disease symptoms. However, it undergoes metabolism by a decarboxylase enzyme in the gut wall causing variable bioavailability and poor absorption. Tamai *et al.*<sup>105</sup> attempted to improve the bioavailability of *L*-dopa by attaching it to *L*-phenylalanine. This created a dipeptide that was found to be recognised and transported in Caco-2 cells. Phenylalanine, the second amino acid moiety, can be metabolised by aromatic amino acid hydroxylases the body into *L*-dopa, and eventually to the target compound adrenaline. This means that by using phenylalanine, to create a PepT1 targeted prodrug, the number of *L*-dopa molecules per dose is doubled. This prodrug approach has also been applied to several other drugs displaying poor bioavailability, as summarised in Table 2. In most cases the PepT1 prodrug is created through the addition of an amino acid or dipeptide *via* an ester linkage. This involves time consuming and expensive high throughput screening of potential monoester and diester prodrugs. When using this strategy consideration must be given to whether the prodrug can undergo PepT1 transport, as well as to the stability of the prodrug linkage to enzymatic cleavage *in vivo* prior to transport.

**Table 2 Prodrugs which display improved bioavailability through PepT1 targeting. Parent drug displayed as black.** <sup>105-111</sup>

Parent name and bioavailability	Function	Prodrug name and bioavailability	Structure
<b>L-dopa</b> Variable <sup>105</sup>	Relieves Parkinson disease symptoms	<b>L-dopa-L-phenylalanine</b> x 40 uptake in Caco-2 <sup>105</sup>	 <b>18</b>
<b>DMAE</b> 50% <sup>106</sup>	Treats orthostatic hypotension	<b>Midodrine</b> 93% <sup>106</sup>	 <b>19</b>
<b>Eglumegad</b> 10% in rat <sup>106</sup>	Treats anxiety and drug addiction	<b>Talaglumetad</b> 84% in rat <sup>106</sup>	 <b>20</b>
<b>Alendronate</b> 1.7% in rat <sup>106</sup>	Used to treat and prevent osteoporosis	<b>Pro-Phe-alendronate</b> 75% in rat <sup>106</sup>	 <b>21</b>
<b>Olenolic acid</b> 0.7% <sup>107</sup>	Exhibits antitumor and antiviral properties	<b>L-valyl diester of olenolic acid</b> 2.21-fold improvement in rats <sup>107</sup>	 <b>22</b>
<b>Oseltamivir</b> 4% <sup>108</sup>	An antiviral licensed for influenza A+B virus	<b>GOC-L-Val</b> 48% in fasted and 23% in fed in mice <sup>108</sup>	 <b>23</b>
<b>Acyclovir</b> 12-20% <sup>106</sup>	Treatment of viral herpes	<b>Valacyclovir</b> 54% <sup>106</sup>	 <b>24</b>
<b>Ganciclovir</b> 6% <sup>106</sup>	Treatment of viral herpes	<b>Valganciclovir</b> 61% <sup>106</sup>	 <b>25</b>
<b>2'-C-methylcytidine</b> 10% <sup>109</sup>	Anti-viral	<b>Val-2'-C-methylcytidine</b> 34% <sup>109</sup>	 <b>26</b>
<b>Vidarabine</b> ~2% <sup>110</sup>	Anti-viral	<b>Vidarabine-Ile</b> x 10 uptake in Caco-2 <sup>110</sup>	 <b>27</b>
<b>Didanosine</b> 7.9% in rat <sup>106</sup>	Treatment of HIV	<b>L-valyl ester of Didanosine</b> 47.1% in rat <sup>106</sup>	 <b>28</b>
<b>Cidofovir</b> <5% <sup>111</sup>	Anti-viral	<b>MeSer-Val Cidofovir</b> x 20 uptake in rat perfusion <sup>111</sup>	 <b>29</b>

### 2.1.2 Attaching a substrate carrier.

As very few drugs resemble oligopeptides, turning the whole drug into a PepT1 substrate has limited applicability. Utilisation of an easily hydrolysable, standardised, PepT1 recognised attachment is a more pertinent approach. This concept was first put forward by Taub's group with the attachment of benzyl alcohols to the amino side chain of several dipeptides<sup>112-3</sup> (Figure 18). All dipeptides were transported by PepT1, with the *L*-dipeptides Glu(OBn)Sar (**30**) and Asp(OBn)Sar (**31**) having the highest affinity. However, *D*-Glu(OBn)Ala (**32**) and *D*-Asp(OBn)Ala (**33**) were found to be much more stable than their *L*-dipeptide counterparts. Both **32** and **33** were shown to qualitatively release benzyl alcohol as a result of hydrolysis, whereas both benzyl alcohol and cyclisation products were formed from **30** and **31**. This suggests that the *L*-dipeptides are hydrolysed by two parallel pathways.

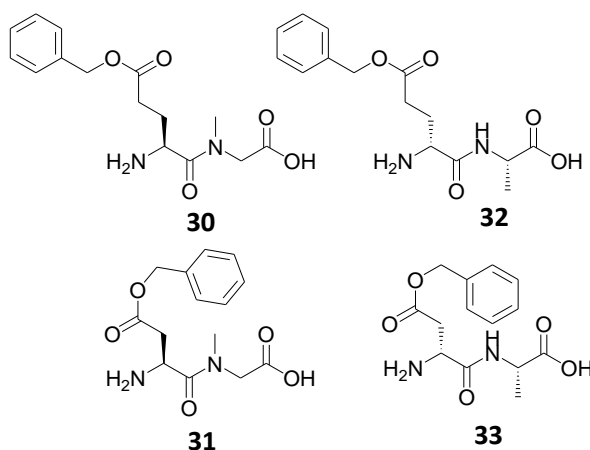


**Figure 18 Standardised dipeptide carriers investigated by Taub's group.**<sup>112, 113</sup>

In an attempt to examine if this method could be applied to larger molecules, the group expanded their research by attaching glucose-6-phosphatase inhibitors.<sup>114</sup> Glucose-6-phosphatase inhibitors of the 4-(4-chlororphenyl)-4,5,6,7-terahydrothieno[3,2-c]pyridin-5-yl-phenylmethanone (**34**) type (figure 19) are active inhibitors of G-6-Pase, but lack *in vivo* activity. This is thought to be due to physiochemical characteristics that prevent passive diffusion and/or give poor aqueous solubility. It was hoped that attaching of an enzymatically stable dipeptide would cause an

increase in permeability. A selection of derivatives were therefore synthesised and tested for G-6-Pase inhibitory activity. The modified compounds **36** and **37** (Figure 19) still showed significant inhibitory activity, whilst **38** did not. However, when tested using Caco-2 cells **38** was the only compound found to be transported. Interestingly, whilst compound **36** was not subjected to efflux, its parent compound was. Efflux is the mechanism by which compounds are removed from a cell and can seriously affect the oral bioavailability of a drug. This study suggests the attachment of a dipeptide to a compound can potentially alter the ability of the resultant prodrug to be recognised and transported by efflux pumps. The group did not pursue this method further, deeming that there is a restriction on the size of molecule that can be attached to a peptide whilst still being a PepT1 substrate.

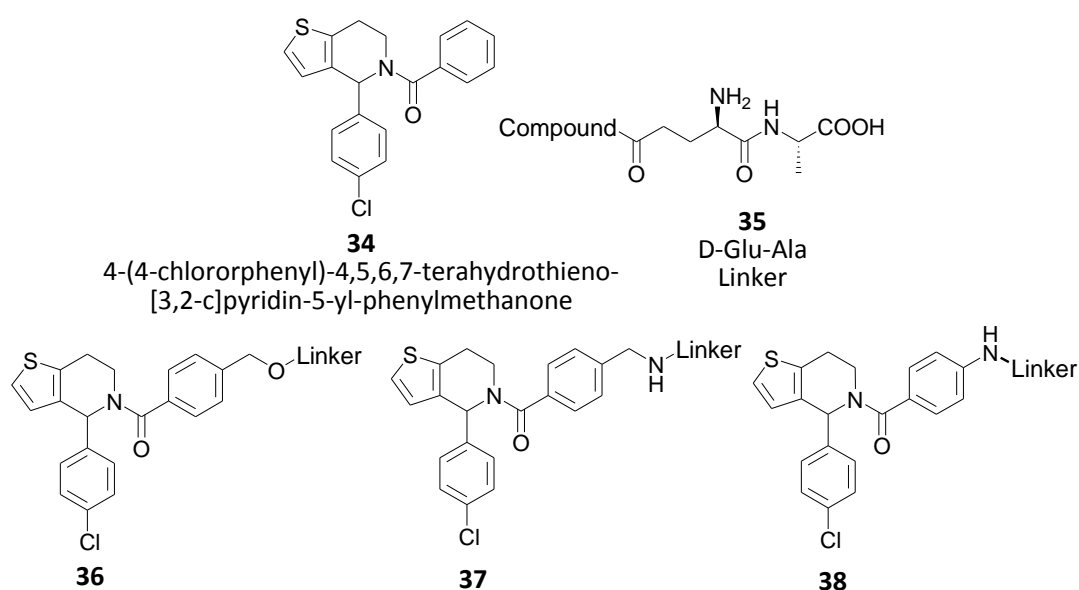


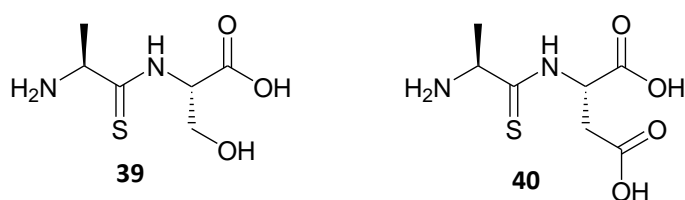
**Figure 19 The 4-(4-chlorophenyl)-4,5,6,7-tetrahydrothieno[3,2-C]pyridin-5-yl-phenylmethanone derivatives and their prodrug counterparts used by Taub.<sup>114</sup>**

The greatest limitation of this work was the use of a *D*-Glu-Ala linker. This was chosen as *N*-terminal *D*-amino acids are more enzymatically stable than their *L*- arranged counterparts. However, *N-terminus D*-amino acids are subject to spatial constraints as the peptide moves down the PepT1 binding pocket, resulting in lower binding affinities (section 1.3.6). The attachment of

the compound to the *N-terminus* R group means that the compound must be accommodated within the ligand binding site. Although a pocket has been shown to exist in this position in PepT<sub>st</sub><sup>91</sup> (section 1.3.5), it is much too small to accommodate the moieties attached in this case. This means that the required arrangement of the dipeptide within the binding pocket cannot occur preventing transport. If the linker chain was doubled back across the dipeptide, the attached moiety could be placed in a favourable region outside the PepT1 pocket. Although this is an unlikely high energy conformation it would allow the required arrangement of the dipeptide to take place and may have been why **38** was transported.

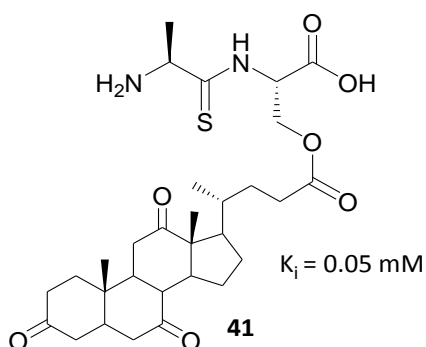
## 2.2 Using thiodipeptides as carriers.

The transport of thiodipeptides by PepT1 had been demonstrated in 1998 by Brandsch *et al.*<sup>98</sup> and later by our group (the Bailey group)<sup>99</sup> in experiments to understand if PepT1 could differentiate between the *cis-trans* isomers of dipeptides (section 1.3.6). During these experiments our group<sup>99</sup> found that the inclusion of a sulfur atom on the *N-terminus* amino acid had no significant effect on PepT1 binding affinities when compared to its oxygen counterpart. Our group went on to create a series of thiodipeptides which were patent protected in 2005.<sup>115</sup> We were surprised to find that not only did the thiodipeptides bind efficiently to PepT1, but they were rapidly transported *in vivo*. As thiodipeptides do not contain a 'classical' peptide bond they are resistant to hydrolysis by peptidases within the gastrointestinal tract. This eliminates the need to use an *N-terminal D-amino acid* to ensure that the dipeptide reaches the enterocytes intact. Two thiodipeptide analogues, Ala(S)Ser (**39**) and Ala(S)Asp (**40**), with good binding affinities were proposed for the use as carriers to improve the bioavailability of drugs.



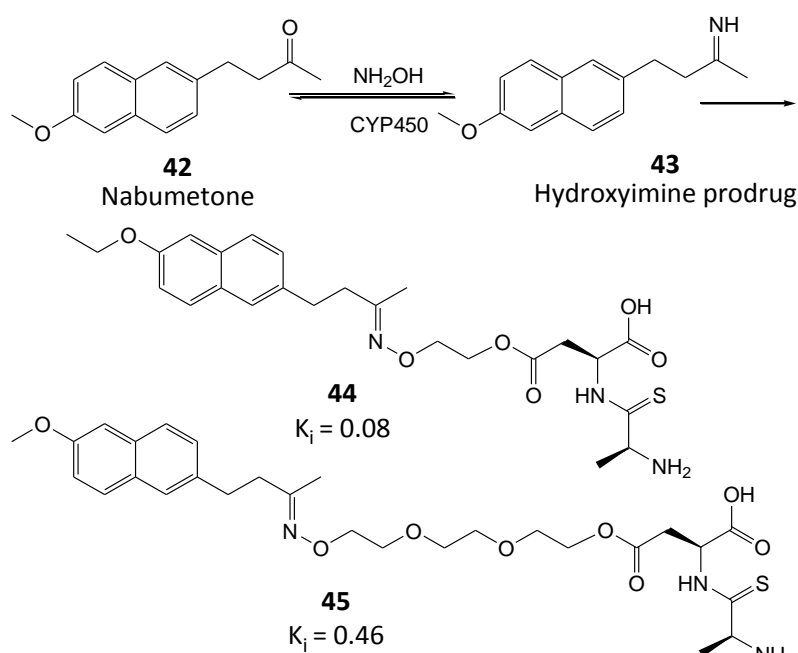
The carriers both display *L*-dipeptide configuration and have free *N*- and *C-terminus*. This allows optimum configuration within the PepT1 binding pocket, thereby increasing the chance of high binding affinity. Drug moieties can be attached *via* an ether or ester linkage through the R<sup>2</sup> position on the *C-terminus* amino acid. Both carriers were tested *in vivo* using a range of benzyl or cyclohexyl ester or ether analogues and were found to give favourable binding affinities.<sup>115</sup> To date **39** and **40** have been attached to several model drugs and commercially available drugs resulting in prodrugs which are transported by Pept1. Some of the work that had been completed within the group prior to the commencement of this project are highlighted below.

Attachment of poorly soluble dehydrocholic acid to the Ala(S)Ser carrier (**39**) by Dr. R. Pettecrew resulted in a prodrug (**41**) which was both recognised and transported by PepT1 (unpublished). This demonstrated for the first time the potential of the thiodipeptide prodrug method as a route for drug delivery. Unfortunately, the resultant prodrug was also poorly soluble, demonstrating that you cannot necessarily increase the solubility of a compound by attaching it to a dipeptide.



In order to activate the parent compound in the thiodipeptide prodrug, the ester or ether link between the carrier and the attached moiety must be hydrolysed *in vivo*. The toxicity of the carrier, as well as the parent drug, must therefore be assessed. Ala(S)Ser (**39**) was measured in rat using a single oral dose of 700 mg/kg. After 15 days no intercurrent deaths or weight loss occurred, suggesting that the carrier causes no negative pharmacodynamic effects.<sup>115</sup>

The first papers showing proof of concept with commercially available drugs were published by our group in 2009. In the first paper published, the carrier method was used in an attempt to improve the bioavailability of nabumetone (**42**) (Scheme 1).<sup>116</sup> An attempt to couple the hydroxyimine directly to the Ala(S)Asp carrier (**40**) resulted in a compound that was too unstable to isolate or use, so to circumvent this, a glycol spacer was used. Not only did this improve the water solubility of the prodrug, but it allowed investigation into the effect of chain length on transport.



**Scheme 1** The metabolism of the nabumetone hydroxyimine prodrug *in vivo* and the two nabumetone hydroxyimine-carrier prodrugs tested *in vitro*.

Prodrugs **44** and **45** were tested in *Xenopus laevis* oocytes expressing rabbit PepT1 and were found to competitively inhibit the transport of *D*-Phe-*L*-Gln. They were also both found to be transported by PepT1 in Caco-2 cells. The transport of both prodrugs was compared to the known thiodipeptide PepT1 substrate Thio-Phe-Ala. **44** was found to be transported 6.3 times faster than Thio-Phe-Ala and **45** 1.3 times faster. This is the first example of targeting a ketone drug towards PepT1.

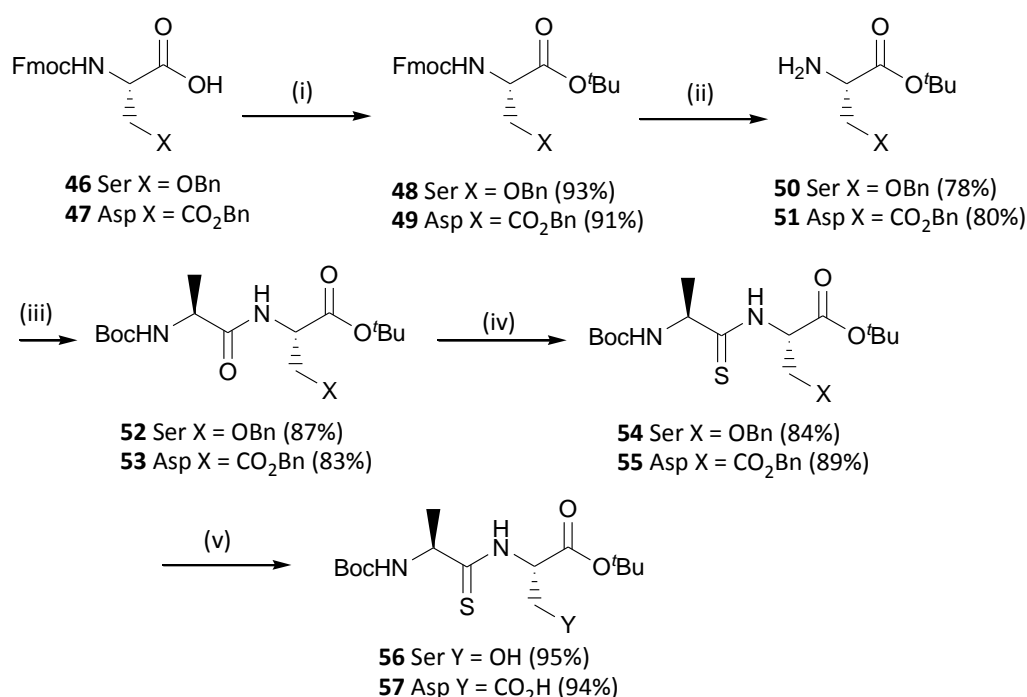
The use of a glycol spacer was further investigated by our group in a second 2009 paper.<sup>117</sup> We were intrigued that the use of a longer glycol chain in nabumetone prodrugs resulted in higher binding affinity and wished to explore this further. Benzoic acid and benzoic alcohol, separated from our carriers by various chain lengths, were assessed for binding affinity. The use of a triethylene glycol spacer between drug moiety and carrier significantly decreased transport rate when compared to the diethylene glycol spacer counterparts. This suggests that there is a limit in the tolerance of PepT1 to accommodate hydrophobic groups placed at considerable distance. Other than aiding the coupling of a drug to the carrier, a benefit of using a spacer may be to set the drug slightly away from the mouth of the binding pocket. Large drugs, especially if branched, attached directly to the carrier may cause negative interactions with the binding pocket. This may either decrease binding affinity or prevent transport from occurring. By setting the drug slightly away from the pocket PepT1 is likely to recognise the presence of only the carrier, not the attached drug. As a result, the mechanism of transport will already be in motion before the attached drug is detected and in a 'piggy backing' method the drug will be pulled through.

Our group believes that through the use of the PepT1 carrier method a wider range of pharmaceuticals may be brought to the market *via* the oral route. By determining the limits of the PepT1 transporter for drug moiety attachments it is hoped that not only can new drugs be formulated using this technique, but that existing drugs can be reassessed. With this in mind a collaboration was formed with AstraZeneca. The main purpose of the collaboration was not only to further explore the limits of a PepT1 substrate, but also to use the thio-dipeptide prodrug strategy in an attempt to improve the bioavailability of existing AstraZeneca compounds. This was the main focus of my research.



### 2.3 Synthesis of thiodipeptide carriers.

Ala(S)Asp (**40**) and Ala(S)Ser (**39**), the thiodipeptide carriers used in my research, were synthesised using methodology previously published by our group (Scheme 2).<sup>117</sup> Each carrier is synthesised on a multi-gram scale taking approximately two weeks. The first step in the synthesis is the protection of the free carboxylic acid in commercially available *N*-Fmoc side chain protected *O*-Bn amino acids. This is accomplished using *tert*-butyl 2,2,2-trichloroacetimidate in DCM:Et<sub>2</sub>O to give the *tert*-butyl ester. The free amine is generated through the removal of the Fmoc group with TBAF in THF. This is not the standard method of Fmoc deprotection, but must be employed as the use of pyridine had previously been found by the group to cause side reactions. Boc-Ala-OH is then coupled to the deprotected amino acid using DPPA/TEA in DMF. The amide carbonyl then undergoes selective sulfur-oxygen exchange using Lawesson's reagent in reflux conditions. The last step involves deprotection of the benzyl ether or ester using dissolving metal conditions.



**Scheme 2** Synthesis of the protected thiodipeptide carriers. (i) *tert*-butyl-2,2,2-trichloroacetimidate, DCM/Et<sub>2</sub>O, 3 days (ii) TBAF in THF, 3h (iii) Boc-Ala-OH, DPPA, TEA, DMF, 18h (iv) Lawesson's reagent, Toluene, 4h reflux (v) Na/NH<sub>3</sub> in THF, 2h, -78°C.

The preferred method of benzyl deprotection, hydrogenation, cannot be used due to the presence in the sulfur group in the thiodipeptides which would poison the catalyst. Although the dissolving metal reduction reaction used gives good yields and a clean compound, it is expensive and not suitable for scale up conditions. It was therefore speculated that benzyl hydrogenation may be performed prior to the sulphur exchange step. This was performed for both the Ala(S)Asp and Ala(S)Ser carriers, to yield the deprotected dipeptides in 90% yields. The deprotected dipeptides were then subjected to oxygen-sulfur exchange, using Lawesson's reagent. In both cases however, no desired thio-dipeptide product could be seen in the crude NMR, and column chromatography resulted in isolation of (4-methoxyphenyl)(thioxo)phosphane oxide and several very polar fractions. Upon the commencement of this project the column chromatography purification utilised in the purification of **48 & 49** and **54 & 55** involved the use of chlorinated solvents. Therefore, to make the process more 'green' the solvent system for **48 & 49** was changed to 2:8 EtOAc: petroleum ether and the solvent system for **54 & 55** was changed to 1:9 EtOAc: petroleum ether. Throughout this research project the use of chlorinated solvents has been avoided where possible.

In order to reduce the cost associated with making the thio-dipeptide carriers from di-protected amino acids an alternative route was envisioned involving the mono protection of the H-X(OBn)-OH starting material. This method had been successfully performed by AstraZeneca, using condensed isobutylene and catalytic H<sub>2</sub>SO<sub>4</sub> in Et<sub>2</sub>O and has been recently described for the protection of H-Ser(Bn)-OH in a patent lodged by Whomsley *et al.*<sup>118</sup> However, this method involves the shaking of the reaction mixture under pressure and these facilities were not available in our laboratory.

An alternative route using *tert*-butyl acetate was therefore considered. This involves the addition of catalytic perchloric acid to a cooled mixture of the amino acid and excess *tert*-butyl acetate. This method had been demonstrated using 2-bromo-2-phenylacetic acid by Arndt *et al.*<sup>119</sup> Initially this reaction was performed using H-Ser(OBn)-OH using the procedure as set out by

Arndt. However, a  $^1\text{H}$  NMR of the crude reaction mixture showed only starting material to be present. Attempts were made to change the reaction conditions by altering the number of equivalents of  $\text{HClO}_4$  used as well as the time and temperature (Table 3). Optimisation of these conditions gave H-Ser(OBn)-O<sup>t</sup>Bu in a near quantitative yield (99%) and use of these reaction conditions with H-Asp(OBn)-OH also gave the desired di-protected amino acid.

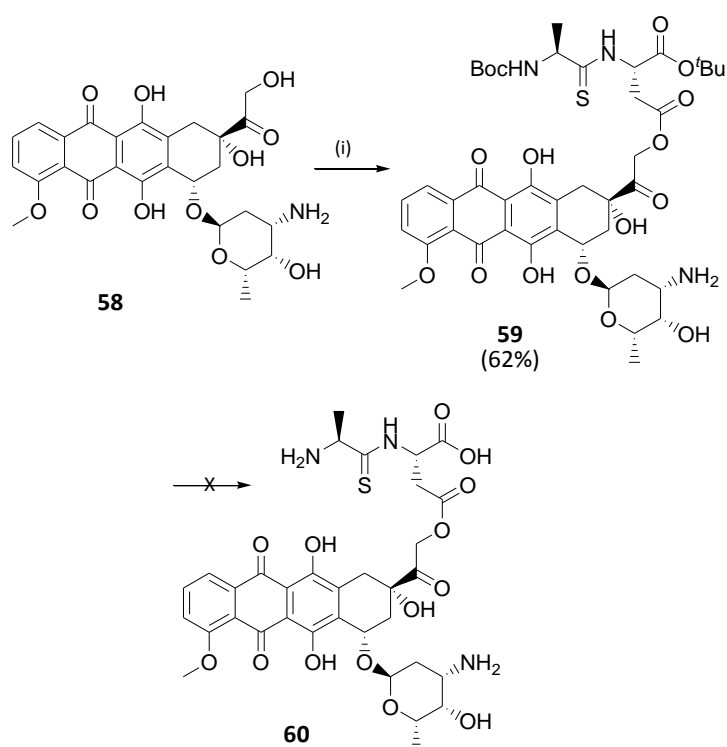
**Table 3 Reaction conditions tried in the mono protection of H-Ser(OBn)-OH**

eq of <i>t</i> -BuOAc	eq of $\text{HClO}_4$	Temperature (°C)	Time (h)	NMR	Time (h)	NMR	Time (h)	NMR
30	0.2	RT	24	Starting material	48	Starting material	72	Starting material
30	0.2	30	24	Starting material	48	Starting material	72	Starting material
30	0.2	50	24	Starting material	48	Starting material	72	Starting material
30	0.5	RT	24	Starting material	48	Starting material	72	Starting material
30	0.5	30	24	Starting material	48	Starting material	72	Starting material
30	0.5	50	24	Starting material	48	Starting material	72	Starting material
30	1.1	RT	24	Starting material	48	Starting material	72	Starting material
30	1.1	30	24	Starting material	48	Some product	72	Fully converted
30	1.1	50	24	Some product	48	Fully converted		

This optimised protection procedure gave an overall yield of ~69% in 5 days compared to the previous methodology of ~50% in 9 days. However, this method was not pursued due to a price increase of 280% for H-Asp(OBn)-OH (£422 per 25g) compared to Fmoc-Asp(OBn)-OH and a 500% increase for H-Ser(OBn)-OH (£660 per 25g) compared to Fmoc-Ser(OBn)-OH. This route may be pertinent should industrial scale up be required as amino acid costs would be reduced by buying in bulk. Any increased costs should be offset through both improved overall yield and the reduction of steps.

## 2.4 Synthesis of alternatively protected thiodipeptide carrier.

Doxorubicin (**58**) is an anthracycline antibiotic used in the treatment of haematological malignancies, carcinomas and soft tissue carcinomas. Poor bioavailability of the parent compound (5%) is due to low permeability, substrate specificity to the efflux pump P-gp and acid catalysed hydrolysis in the stomach.<sup>120</sup> This therefore necessitates intravenous administration. However, due to the wide usage as an oncology drug several strategies have been undertaken to deliver the drug orally.<sup>120</sup> As doxorubicin (**58**) is a known substrate of the P-gp transporter we were interested to assess whether the thiodipeptide prodrug method would allow this mechanism to be bypassed, therefore increasing bioavailability. This has been shown to be the case with quinidine which is actively effluxed by P-gp. *L*-valine-quinidine is both actively transported by PepT1 and is no longer a P-gp substrate.<sup>106</sup> Work to synthesise a Ala(S)Asp-doxorubicin prodrug was carried out by Dr R. Pathak and is summarised in scheme 3.



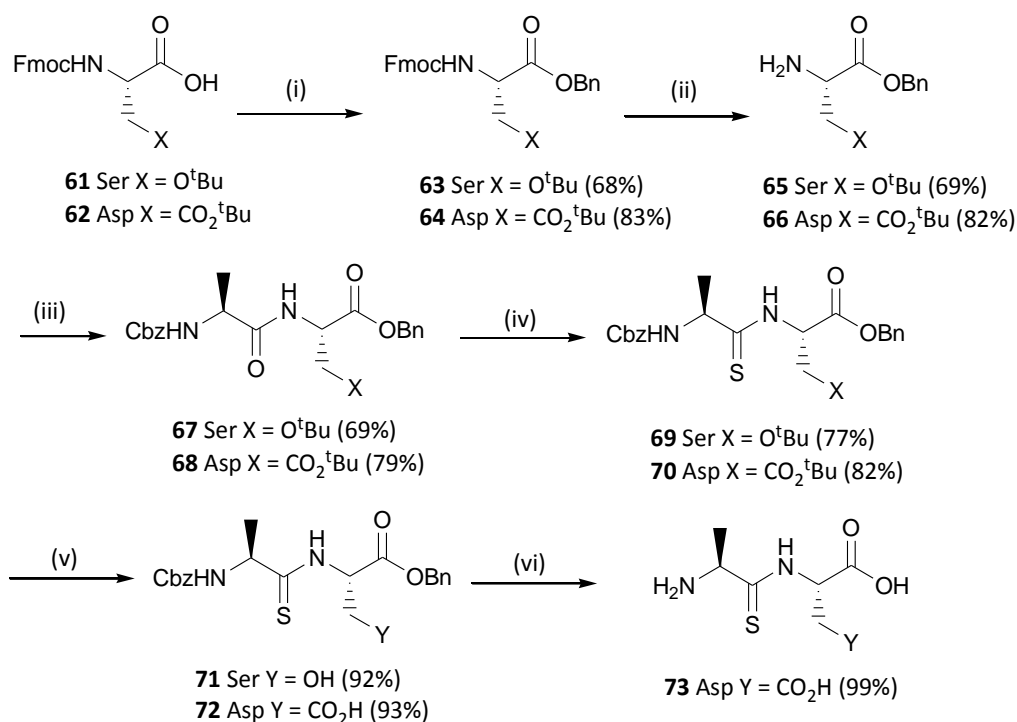
**Scheme 3** Attempted synthesis of Ala(S)Asp-doxorubicin prodrug by Dr. R. Pathak (i) (**57**), DCC, NHS, DIPEA, THF

Despite the utilisation of a variety of mild conditions, Dr Pathak encountered problems with the final deprotection of the prodrug due to the degradation of doxorubicin in acidic conditions. As these problems may be encountered in the future with other acid sensitive drugs, it was decided to establish methodology for our carriers utilising an alternative protecting group strategy. This work was carried out as part of this research project. The protecting groups chosen needed to be robust to the conditions used during the synthesis of the carriers and be cleaved cleanly using non acidic conditions in a single final step. Due to the commercial availability of serine and aspartate amino acids with *tert*-butyl protected side chains, these were used as the starting point for the synthesis. Several protecting groups were assessed for the protection of the amine and carboxylic groups. For the alanine amino acid Fmoc-Ala-OH was initially used as the *N*-terminus residue. However Fmoc deprotection occurred when DMAP was used as the base in the coupling reaction between alanine and the second residue. This could be mediated by using a base other than DMAP, but would severely limit the options available when coupling the carrier to drug. As alternative amino protecting groups, both methyl and ethyl carbonate were considered as they can be readily removed by KOH or K<sub>2</sub>CO<sub>3</sub>. For the serine or aspartate amino acid, the commercial availability of Cbz-Asp(O<sup>t</sup>Bu)-OH and Cbz-Ser(<sup>t</sup>Bu)-OH made us consider these protected amino acids as the starting point for the protection of carboxylic acid group. However, most carboxylic acid protecting groups are cleaved under acidic conditions, risking the deprotection of *tert*-butyl. We could not find a nontoxic carboxylic acid protecting group that would both withstand hydrogenation and cleave under KOH/ K<sub>2</sub>CO<sub>3</sub> conditions.

It was ultimately decided to use benzyl type protection as Cbz-Ala-OH is commercially available and benzyl protection of the free carboxylic acid on the second residue could be achieved using commercially available Fmoc-Asp(O<sup>t</sup>Bu)-OH or Fmoc-Ser(<sup>t</sup>Bu)-OH. Benzyl protection is robust enough to withstand the acidic conditions needed to cleave the *tert*-butyl side chain and the basic conditions used during coupling reactions. In our thiodipeptides the benzyl protection must be cleaved in the relatively harsh conditions of dissolving metal reduction.

This is due to the presence of a sulphur atom which would poison the catalyst. However, if this strategy is utilised in sulfur free alternative PepT1 carriers (Chapter 3) the usual mild conditions of hydrogenation with a palladium catalyst could be used.

Initial attempts were made to protect Fmoc-Asp(O<sup>t</sup>Bu)-OH using benzyl-2,2,2-trichloroacidimidate. This is a similar method used for the *tert*-butyl protection of Fmoc-Asp(OBn)-OH in the original synthesis ((i) in scheme 2). However, using this method after 4 days only a small amount desired product (6%) was obtained. This was thought to be due to an increase in the activation energy of reaction, as when this reaction is performed with *tert*-butyl-2,2,2-trichloroacidimidate high yields are only obtained after 3 days in a very concentrated solution. Benzyl bromide was therefore used to give the desired product (**64**) in a 83% yield. Fmoc deprotection of **64** was carried out using TBAF in THF to give **66**, followed by coupling with Cbz-Ala-OH using DPPA and TEA in DMF to give **68**. Sulphur-oxygen exchange was carried out using Lawesson's reagent prior to *tert*-butyl deprotection using TFA in DCM to give **72**. Deprotection of the benzyl type protecting groups was successfully carried out using dissolving metal reduction to give **73** (scheme 4). Unfortunately, when the stability of doxorubicin (**58**) to dissolving metal reduction conditions was assessed, degradation was found to occur and so this protecting group strategy could not be utilised in this case. It does however remain an option for acid sensitive drugs encountered in the future.

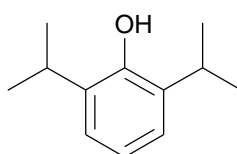


**Scheme 4** Synthesis of the benzyl protected thiodipeptide carriers. (i) BnBr, NaHCO<sub>3</sub>, DMF, 3 days (ii) TBAF in THF, 3h (iii) Cbz-Ala-OH, DPPA, TEA, DMF, 18h (iv) Lawesson's reagent, Toluene, 4h reflux (v) TFA in DCM, 8h (vi) Na/NH<sub>3</sub> in THF, 2h, -78°C.

## 2.5 PepT1 targeted prodrugs using commercially available drugs.

### 2.5.1 Propofol (2,6-diisopropylphenol).

Propofol (**74**) is used for the induction and maintenance of general anesthesia.<sup>121</sup> As it has a low solubility it is currently administered intravenously as an oil-in-water emulsion. If used at a sub-sedative dose there is evidence that propofol can be effective in treating: Delirium tremens associated with alcohol withdrawal;<sup>122</sup> trigeminal neuralgia;<sup>123</sup> spinal cord injury pain;<sup>124</sup> central post-stroke pain;<sup>125</sup> intractable migraines<sup>121</sup> and post-chemotherapeutic nausea and vomiting.<sup>121</sup>



**74**

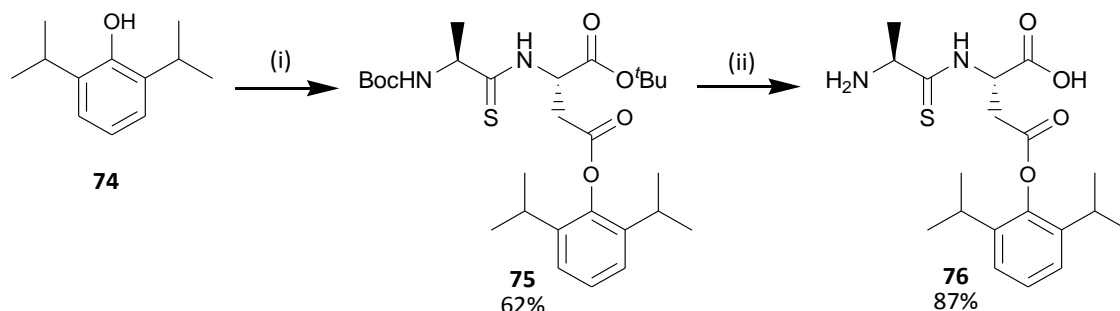
An oral formulation of propofol is therefore medically desirable. This has been attempted by the Xenoport incorporation<sup>121</sup> using amino acid and dipeptide attachments to target unspecified gastrointestinal transporters. The structurally unspecified amino acid attached prodrug, XP20925, has been shown, in a patent, to appear in *systemic* circulation in both rat and dog after oral administration<sup>126</sup> although no measure of bioavailability was given.

The Ala(S)Asp-2,6-diisopropylphenol prodrug (**76**) had previously been created within our group (Dr. R. Price and Dr. D. Foley, unpublished).<sup>127</sup> *In vitro* testing showed that the prodrug had high binding affinity for PepT1 and was transported moderately well in Caco-2 cells. Part of the collaboration between our group and AstraZeneca involved my use of their facilities for Caco-2 testing. Ala(S)Asp-2,6-diisopropylphenol was therefore synthesised to use as a standard to ensure consistency with Caco-2 work previously carried out at Oxford Brookes. In my hands, when propofol (**74**) was coupled to Boc-Ala(S)Asp(OH)-O<sup>t</sup>Bu using the established methodology<sup>127</sup> no desired product was obtained. Initial attempts were made to change the reaction conditions by increasing the equivalents of DMAP in both DMF and DCM. The use of DMAP as a full equivalent, rather than catalytically, often results in successful coupling conditions, despite its role as a catalyst in the reaction. Indeed, when the equivalents of DMAP used was increased from 0.15 to 1 and the coupling reagent was changed from DCC to EDC successful coupling was observed by crude NMR.

Purification was performed *via* dry loaded column chromatography using the established conditions; DCM followed by gradual change to 9:1 DCM: EtOAc. However, fractions collected showed the presence of propofol (**74**) as well as the desired product **75** which have very different R<sub>f</sub> values. Repeated attempts to optimise the eluting mixture still resulted in propofol being present in the fractions containing the product. It was therefore hypothesised that propofol was becoming “baked on” when absorbed onto the silica for dry loading. To counteract this, the volume of propofol added to the reaction mixture was reduced from 1.25 to 0.95eq and the crude reaction mixture wet loaded onto the column. Using a gradual change in the solvent system of



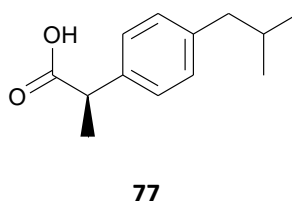
petroleum ether to 9:1 petroleum ether: EtOAc the product was successfully separated. Subsequent acidolysis of the Boc and *tert*-butyl protecting groups gave the desired prodrug.



**Scheme 5 Synthesis of Ala(S)-Asp-2,6-diisopropylphenol.** (i) (57), EDC, DMAP, DMF, rt, 3 days.  
(ii) HCO<sub>2</sub>H, reflux, 3h.

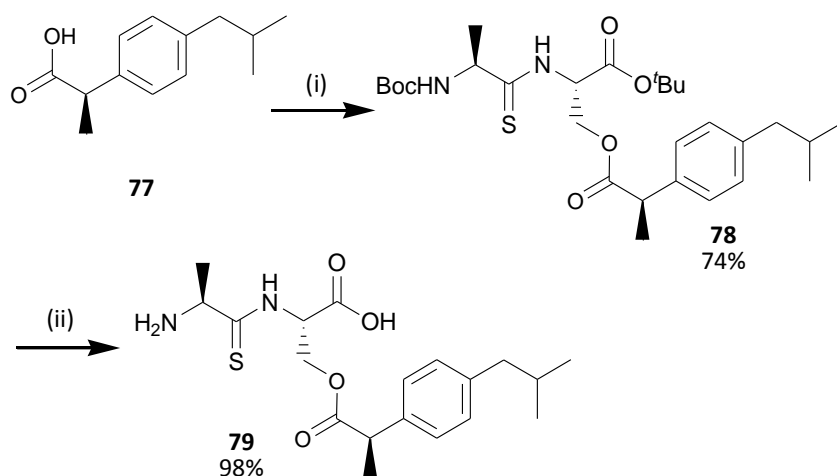
### 2.5.2 Ibuprofen

Unlike propofol, ibuprofen (**77**) does not suffer from low bioavailability. However, it can cause gastric and intestinal ulceration. This is especially prominent in patients on a long-term dose for chronic pain conditions.



By attaching a thiodipeptide carrier it was envisioned that gastric damage would be limited as, prior to uptake, the drug would not be available in its free form. A thiodipeptide prodrug of ibuprofen (**79**) had previously been created in our group.<sup>117</sup> *In vitro* testing had previously shown that the prodrug had high binding affinity for PepT1 and high permeability in Caco-2 cells. *In vivo* testing had shown that the prodrug is rapidly absorbed into circulation without any short term gastrointestinal or systemic toxicity (unpublished).<sup>127</sup> Ala(S)Ser-ibuprofen (**79**) was therefore synthesised (1.5g) for use in a full pharmacokinetic study and taste assessment

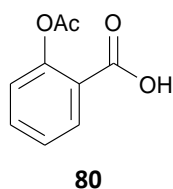
in rat (sections 3.3.1 and 3.3.2). Repeated difficulty was encountered with the final acidolysis step to give the desired prodrug **79**. It was found that the standard *tert*-butyl type deprotection conditions of TFA in DCM gave unpredictable results. Deprotection of the Boc and *tert*-butyl groups to give a pure sample is vital as the resulting deprotected prodrug salt is very polar and therefore cannot be separated from any impurities. Attempts to find conditions using TFA which consistently gave quantitative deprotection were made by reducing reaction times and distilling the TFA. Successful cleavage of the *tert*-butyl groups was hypothesised to be trace water dependent as certain bottles of TFA after a period of time would give quantitative deprotection. As the use of TFA could not guarantee a successful result, formic acid was used as an alternative reagent and consistently gave **79** in quantitative yields after 3 hours.



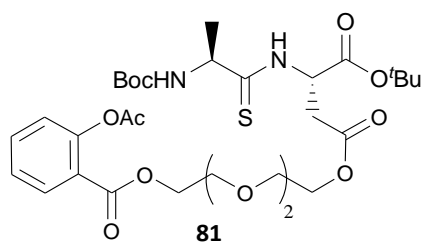
**Scheme 6 Synthesis of Ala(S)Ser-ibuprofen.** (i) (**56**), HBTU, DIPEA, DMF, rt, 4 days. (ii) HCO<sub>2</sub>H, reflux, 3h.

### 2.5.3 Aspirin.

Belonging to the same class of drugs (non-steroidal anti-inflammatory) as ibuprofen (**77**), aspirin (**80**) is also considerably toxic to the gastrointestinal tract. As well as for pain relief, aspirin (**80**) is widely used in primary and secondary preventive treatments of cardiovascular disease.



The development of a benign prodrug is therefore of considerable commercial interest. Ester and amide derivatives of aspirin (**80**) are expected to be less pernicious to the gastrointestinal tract.<sup>128</sup> Previous attempts in the group, by Dr. F. Foley, to attach aspirin (**80**) directly to the protected Ala(S)Ser carrier (**56**) using a variety of mild esterification conditions proved unsuccessful.<sup>127</sup> This was unsurprising as esters of aspirin reported in literature are generally made using an aspirin acid chloride, methodology we discounted as it would damage our carrier. A glycol ester of aspirin (**81**) was therefore synthesised by Dr. F. Foley, using concentrated Mitsunobu conditions and sonication. Although **81** showed good binding affinity *in vitro*, it was found to be unstable in acidic media.



*In vivo* aspirin ester prodrugs are hydrolysed by plasma butyrylcholinesterase (BuChE). This presents an obstacle to prodrug development as the competing hydrolysis to the salicylate ester (**84**) is usually the fastest pathway (Figure 20). This means that for an ester prodrug to successfully release aspirin (**80**), the ester must undergo hydrolysis at a greater rate than the acetyl group.

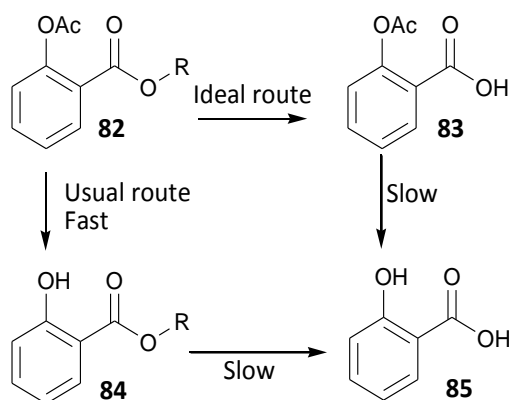
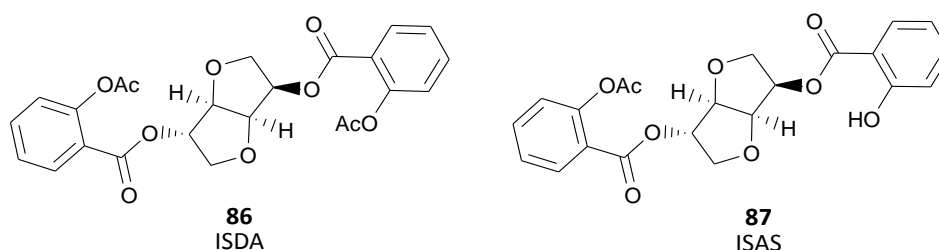
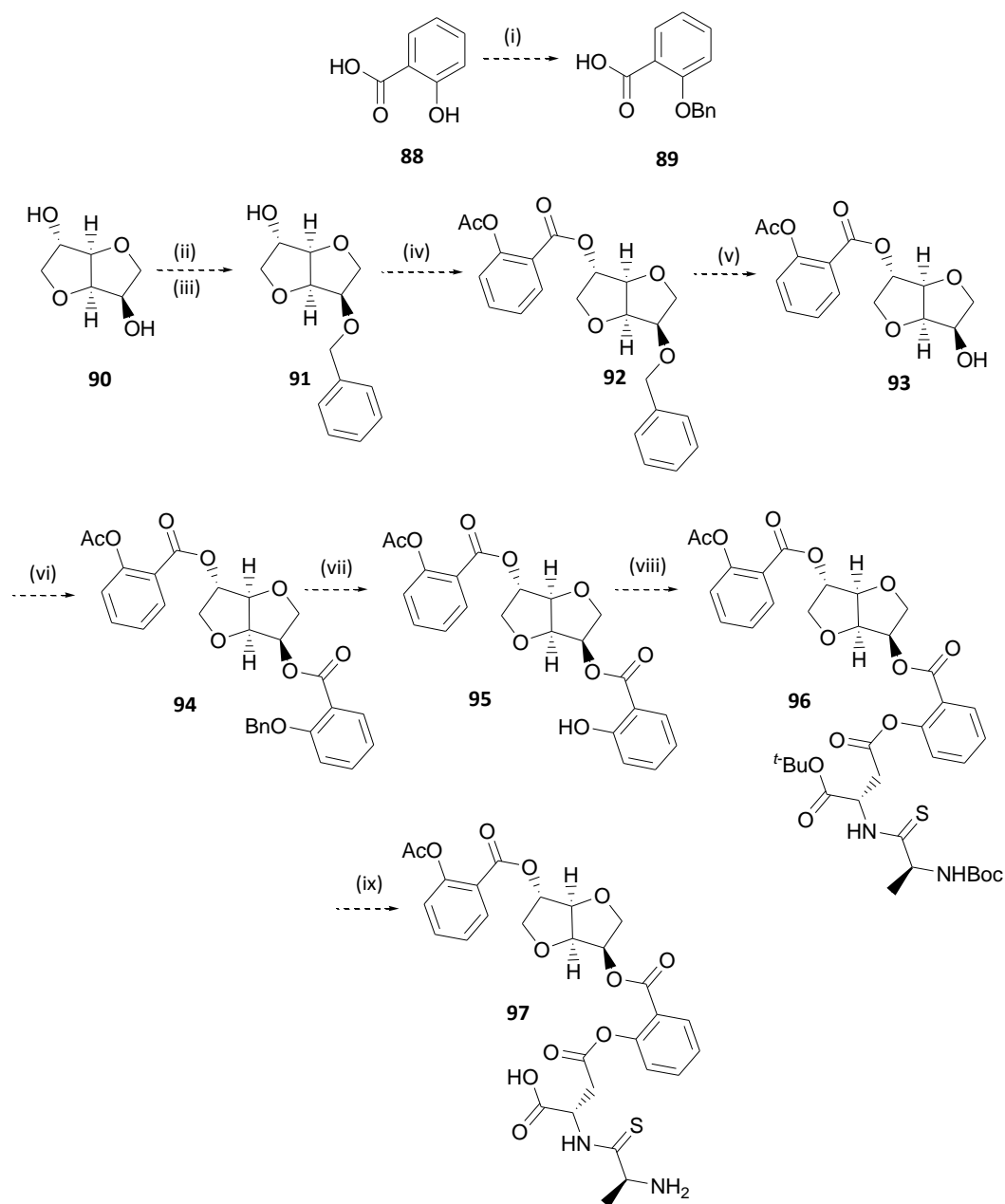


**Figure 20 Routes of aspirin ester hydrolysis. Adapted from Moriarty *et al.*<sup>128</sup>**

Recently a diasprinate ester of isosorbide has been published which has been shown to preferentially release acetyl salicylate (**83**) after interaction with BuChE. ISDA (**86**) has been shown to produce aspirin *in vivo*,<sup>128</sup> but due to competing hydrolysis pathways only 7% hydrolyses directly to aspirin (**80**).<sup>128</sup> This is due to the presence of two acetates and therefore two competing processes. Aspirin production is the result of either a direct hydrolysis of the isosorbide in either the 2 or 5 position, or hydrolysis of the resultant monoaspirinate. However, there is also a preferential competing pathway whereby either one or both of the aspirin moieties are hydrolysed to the salicylate ester. In this pathway the acetyl group of the 5-asprinate is hydrolysed first to give ISAS (**87**). When the hydrolysis pathways of ISAS were studied, surprisingly it was found to be an excellent substrate for BuChE. This outcompetes the usual fast route of the enzymes which hydrolyse the phenylacetate group. As a result ~70% of ISAS is directly hydrolysed to aspirin (**80**).

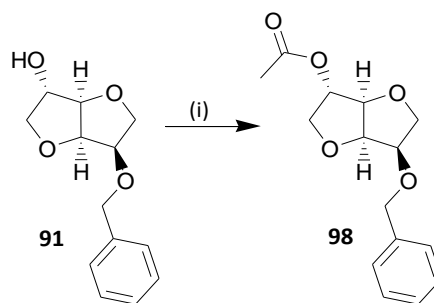


Although ISDA (**86**) has been shown to have oral bioavailability<sup>129</sup> this may not necessarily be the case with ISAS (**87**) as there is currently no published transport data. The presence of the free phenoxy group may also cause gastrointestinal toxicity, rendering the purpose of the prodrug futile. It was theorised that attachment of the Ala(S)Asp carrier (**40**) through the free phenoxy group may address both of these issues. The published synthesis for ISAS (**87**) is through isosorbide mononitrate, commonly used to treat angina. This is not commercially available due to the highly explosive isosorbide dinitrate also being formed during synthesis. The purpose of using isosorbide mononitrate in the published synthesis<sup>127</sup> appeared to be from a protecting group perspective only, so an alternative starting material was considered. Huynh *et al.*<sup>130</sup> had previously shown that the correct hydroxyl group on isosorbide (**90**) could be selected for monobenylation using LiH/LiCl. This presumably occurs through lithium ion chelation control as the use of sodium hydride preferentially selects for the *exo* hydroxyl group.<sup>131</sup> A synthetic route was therefore postured using isosorbide (**90**) as a starting material (Scheme 7).



**Scheme 7** Theorised synthesis of thiodipeptide aspirin prodrug. (i)  $K_2CO_3$ , TBAB, BnBr, THF, rt (ii) LiH, LiCl, DMSO (iii) BnCl (iv) (80), DCC, DMAP, DCM (v)  $H_2$ , Pd/C, rt (vi) (89), DCC, DMAP, DCM, rt (vii)  $H_2$ , Pd/C, rt (viii) (57), DCC, DMAP, DCM, rt (ix)  $HCO_2H$

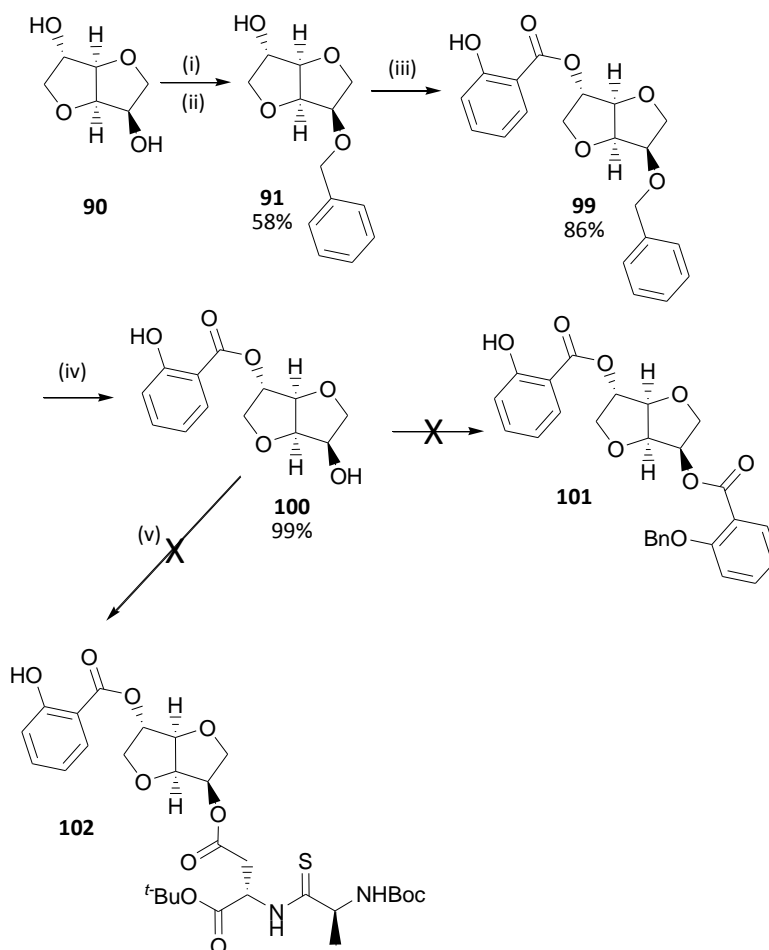
The monobenzylation of isosorbide (**90**) was successfully achieved in a 58% yield and no *exo* enantiomer was found to be present in the crude reaction mixture. However, upon coupling the monobenzylated isosorbide **91** to aspirin (**80**) using established methodology,<sup>129</sup> **92** was not obtained. Rather than the aspirin (**80**) coupling to the free hydroxyl group, deacetylation of the aspirin and acetylation of the isosorbide benzyl ester (**91**) was seen.



**Equation 1 Synthesis of 65 (i) Aspirin (**80**), DCC, DMAP, DCM.**

Pre-forming the DCC-isosorbide benzyl ester complex prior to the addition of aspirin (**80**) also resulted in transesterification occurring, with no coupled product seen. This method of performing a copupling reaction is called pre-charging method. When all of the reagents are added at the same time it is referred to the one-pot method.

DMAP can promote the acetylation of alcohols, so HOBt was used as an alternative base. Transesterification did not occur, but no desired ester was obtained. Using EDC and HATU as alternative coupling reagents also failed to give **92** as the desired product. Salicylic acid (**88**) was therefore used as the reactive species as acetylation to aspirin (**80**) could be undertaken subsequent to coupling (scheme 9). Using the pre-charged DCC DMAP conditions salicylic acid (**88**) was coupled to **91** in an 86% yield. Initial attempts were made to find conditions to acetylate **99** to give the desired aspirin product **92**. However, this avenue could not be fully explored due to this research being undertaken in the final few weeks of this research project.



**Scheme 8 Synthesis of modified salicylic prodrug.** (i) LiH, LiCl, DMSO (ii) BnCl (iii) Salicylic acid (88), DCC, DMAP, DCM (iv) H<sub>2</sub>, 10% Pd/C, MeOH:EtOAc rt (v) (57), DCC, DMAP, DCM, rt.

**99** was instead successfully deprotected using a 1:1 mix of MeOH: EtOAc as a solvent and 10% palladium on carbon as the catalyst to give **100**. As both the salicylic and isosorbide alcohols are deprotected in **100**, coupling of this compound to benzyl protected salicylic acid (**89**) would result in the formation of several products (scheme 8). It is therefore unlikely that the desired product **101** would be formed in the yields necessary to explore further synthesis using this intermediate. Therefore, in an effort to make a model aspirin like prodrug which could be used *in vitro* testing it was decided to couple the protected Ala(S)Asp carrier (**57**) directly attached to the free isosorbide alcohol on **100** (scheme 8). It was hoped that enough of **102** would be able to be isolated from the resultant mix of coupled products that, after deprotection, biological testing could be carried out.



Using pre-charged DCC conditions, the only product that could be isolated was the protected Ala(S)Asp carrier (**57**) attached both to the salicylic ester and the free isosorbide alcohol. This project was therefore abandoned due to the prioritisation of other work and the difficulties previously encountered in the group by Dr. Foley<sup>127</sup> in making a thiodipeptide aspirin prodrug. It is not known why in my hands transesterification was found to occur, when using DCC/DMAP conditions the Trinity college group successfully coupled aspirin (**80**) to a protected isosorbide. Perhaps the mononitrate group on the isosorbide used by Trinity plays a role other than as a convenient protecting group. Extensive screening of coupling conditions between aspirin (**80**) and mono-protected isosorbide to find a successful method which does not cause transesterification to occur would be the next step in moving this synthesis along. These same conditions could hopefully be used for all coupling reactions in the synthetic sequence. If this is achieved and the original target **97** is found to be a PepT1 substrate, *in vivo* work would need to be undertaken to assess whether aspirin is preferentially released.

## 2.6 AstraZeneca new chemical entities

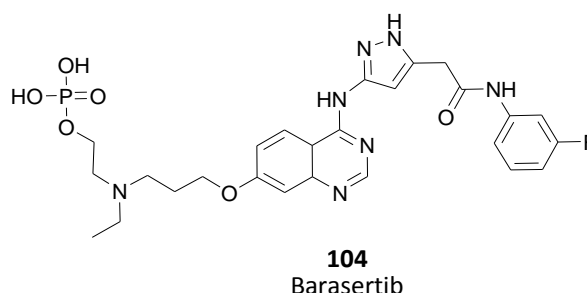
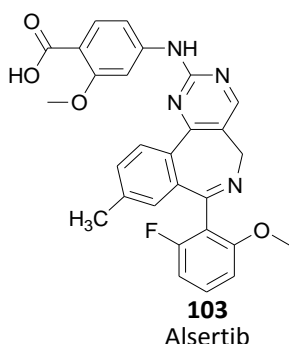
As the PepT1 prodrug strategy had been proven within the group for commercially available drugs, a collaboration was created with AstraZeneca to assess if existing new chemical entities could be taken further in the development process. Due to the financial cost involved in drug development, only the most promising candidates will be taken through drug discovery, pre-clinical research and into clinical trials. Designing a drug to have both favourable target efficacy and pharmacokinetics can be challenging and many valuable compounds are shelved due to bioavailability issues. Two AstraZeneca developed compounds were identified from two different classes of drugs to see if the PepT1 prodrug strategy could be successfully applied to improve their bioavailability. These are an Aurora kinase inhibitor and an  $\alpha 1\beta 5$  integrin inhibitor. Both of the structures are in the public domain and are not the lead development compounds, although they are of interest. The compounds are structurally very different from each other and from drug

moieties already attached to our carriers. This is to further assess PepT1's ability to transport drugs of varying size, hydrophobicity and functional groups.

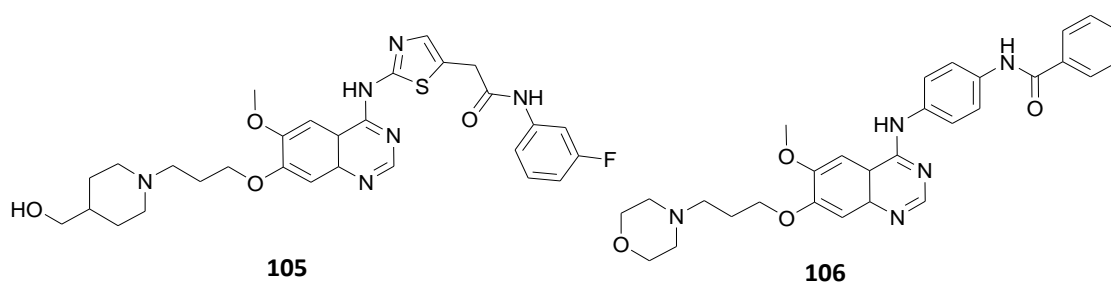
### 2.6.1 Aurora kinase inhibitor

Aurora kinase inhibitors play an important role in the regulation of mitosis and are highly expressed in the thymus, testis, spleen, intestine and bone marrow<sup>132</sup> and are commonly overexpressed in human tumours.<sup>133</sup> There are three Aurora kinase paralogues expressed in mammals, Aurora A, B and C. Aurora A regulates mitotic spindle assembly and stability from prophase to telophase. Overexpression of Aurora A has been shown to inhibit cytokinesis and overrides the mechanism that monitors spindle assembly.<sup>134</sup> Aurora B is a chromosome passenger protein which regulates chromosome segregation and cytokinesis. The function of Aurora C is still unknown, but it has the same subcellular location as Aurora B. It is overexpressed in somatic cancer tissues and hematologic cancers where it has been shown to interfere with the spindle checkpoint by promoting the degradation of Aurora B.<sup>135</sup> Disregulation of the Aurora kinase inhibitors ultimately leads to chromosome instability. This, combined with the overexpression of Aurora kinase inhibitors in cancer cells, suggests that they are involved in tumorigenesis.

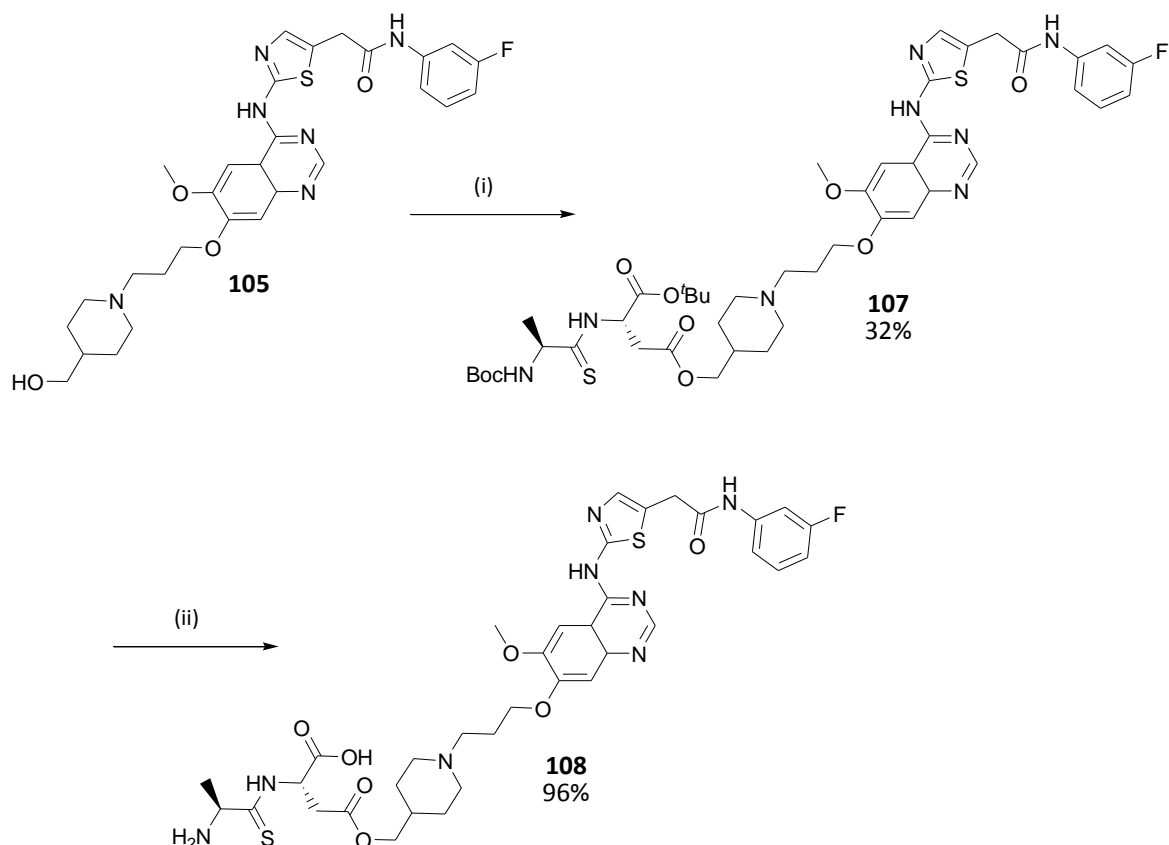
Several compounds have been reported to inhibit both Aurora A and B and have allowed the validation of Aurora kinases as a target for cancer drug discovery. The most advanced of these are Alisertib **103**, developed by Millennium, and Barasertib **104**, developed by AstraZeneca.



Alsertib (**103**) is currently in US and UK Phase-III clinical trials for relapsed or peripheral T-cell lymphoma. The half maximal inhibitory concentration ( $IC_{50}$ ) for Aurora A is  $0.0067\mu\text{m}$  and for Aurora B is  $1.534\mu\text{m}$ .<sup>136</sup> Barasertib (**104**) is an acetanilide-substituted pyrazole-amino-quinazoline prodrug and is in phase II/III clinical trials for acute myeloid leukaemia. The  $IC_{50}$ 's are  $1.369\mu\text{m}$  for Aurora A,  $0.00036\mu\text{m}$  for Aurora B and  $0.017\mu\text{m}$  for Aurora C.<sup>137</sup> Barasertib is the phosphate derivative of the structure activity relationship optimised analogue of **105**, which was based on one of the first reported Aurora kinase inhibitors ZM447439 (**106**).



**105** Suffers from low solubility ( $0.035\text{ mg/mL}$ ).<sup>132</sup> It was hoped that by attaching our carrier, solubility and therefore bioavailability would be improved. After an extensive range of coupling conditions were employed, the desired product was obtained with DCC and a combination of HOBt and DMAP as base. DMAP is generally needed in catalytic amounts in coupling conditions, although this has not been found to be the case in the course of this research. This was again found here with 0.5 equivalents only generating a trace of product (observed by TLC) that could not be isolated. Interestingly, reasonable yields (32%) were not achieved until 2 equivalents of HOBt were also used in the reaction. However, when used without DMAP no reaction was found to occur.

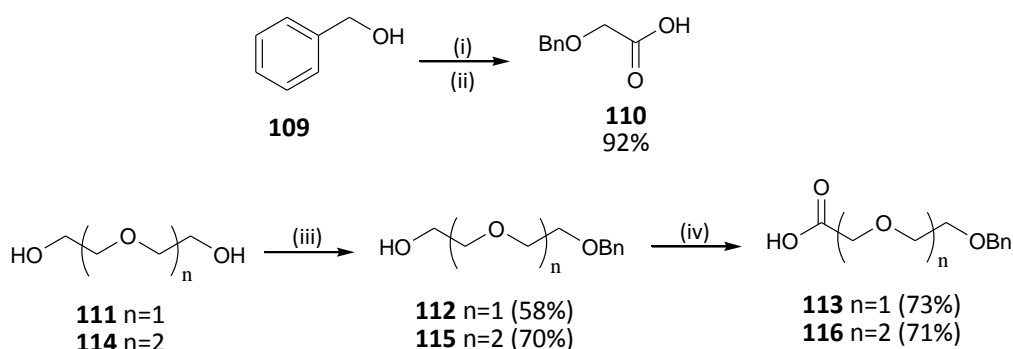


**Scheme 9 Synthesis of Aurora kinase inhibitor thiodipeptide prodrug. (i) (57), EDC, DMAP, HOBT, DMF, 3 days (ii) HCO<sub>2</sub>H, reflux, 3h.**

Solubility testing of **108** showed that solubility had been improved from 0.035mg/mL (**105**) to ~6 mg/ml. This was carried out by saturating 1ml of pH 7.4 HBSS/0.1% BSA/HEPES buffer with prodrug. Concentration of the centrifuged solution was then calculated based on mass spectrometer peak area assuming linearity at concentrations greater than the standards.

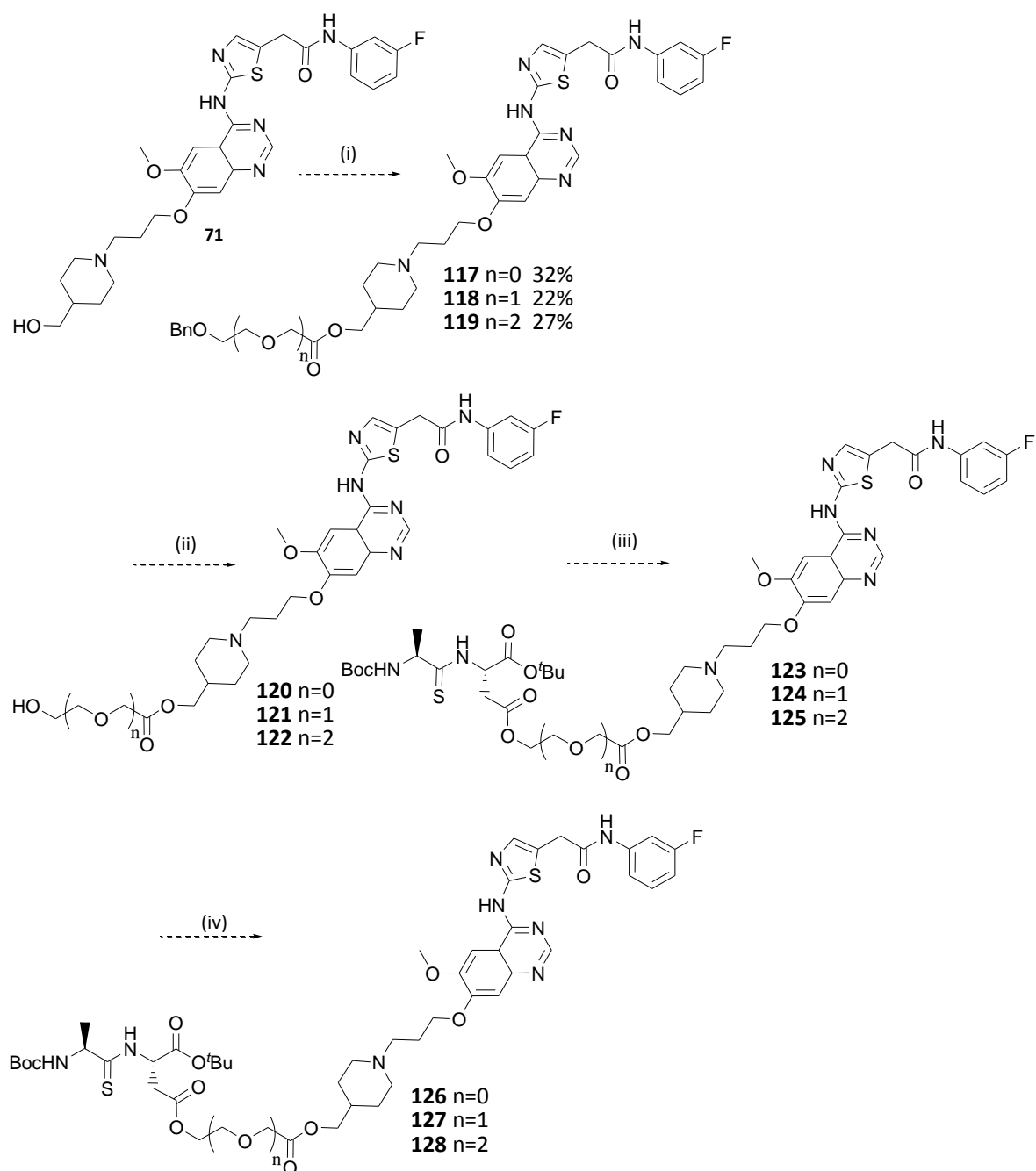
To assess the effect of chain length between the Aurora kinase inhibitor (**105**) and Ala(S)Asp carrier (**40**) on PepT1 transport, a series of polyethylene glycolic acid spacers were created. It was also hoped that solubility of the final prodrug would be improved, which had previously been seen when Dr. F. Foley attached glycol linkers between the Ala(S)Asp carrier (**40**) and nabumetone (**42**) (section 2.1.2). Benzyloxyacetic acid (**110**) was created from benzyl alcohol (**109**) and chloroacetic acid using modified Williamson ether synthesis (scheme 10). To synthesise

**113** and **116** the monobenzyl protected glycols **112** and **115** were first created from their corresponding glycols in good yields using standard sodium hydride based desymmetrisation chemistry (scheme 10). 2-(2-Phenylmethoxyethoxy)acetic acid (**111**) and 2-[2-(2-phenylmethoxyethoxy)ethoxy]acetic acid (**114**) were then synthesised through oxidation of their corresponding monobenzyl protected glycols with Jones oxidation.



**Scheme 10 Synthesis of glycol acid spacers. (i) Na, BnOH (ii) chloroacetic acid, BnOH (iii) NaH, KI, BnBr (iv) Cr<sub>3</sub>O, H<sub>2</sub>SO<sub>4</sub>, H<sub>2</sub>O, (CH<sub>3</sub>)<sub>2</sub>CO.**

Initial synthesis of an Aurora kinase glycol acid benzyl ether was attempted using **113** and the DCC, DMAP, HOBt conditions used to synthesise **108**, but unfortunately this failed to give the desired product **118**. After trying various coupling reagents a yield of 27% was achieved with 1eq DIPEA and 1.1eq HATU in DMF. This was then successfully applied to the other two glycol acid benzyl ethers (Scheme 11). It was envisioned that deprotection of the glycol benzyl ethers **117**, **118** and **119** could be achieved through palladium hydrogenation as the sulphur in the thiazole ring would be sufficiently conjugated to prevent poisoning of the catalyst, as is the case with the thiazolidine ring in penicillins.<sup>138</sup>



**Scheme 11** Intended synthesis of Ala(S)Asp glycol Aurora kinase prodrugs (i) (**126**, **127** or **128**), DIPEA, HATU, DMF (ii) Palladium hydrogenation (iii) (**57**), coupling conditions (iv)  $\text{HCO}_2\text{H}$ , reflux, 3h.

Attempts to remove the benzyl ether by hydrolysis were unsuccessful, with only starting material recovered from reactions. This was initially assumed to be the result of the starting materials being inert to the reaction conditions, so extensive screening of catalytic conditions was therefore carried out (Table 4). These could only be undertaken under atmospheric conditions as facilities for hydrogenation at multiple atmospheres were not available. The addition of a second quantity of 10% Pd(OH)<sub>2</sub>/C after 30 minutes to **118** when dissolved in ethanol and when dissolved in acetic acid gave a second spot by TLC. This could not be isolated due to scale (5 mg) as full conversion did not occur. It was theorised that poisoning of the catalysis was occurring so hydrogenation attempts were abandoned. The benzyl protecting group used in the synthesis of our thiodipeptide carriers is removed by dissolving metal reduction (section 2.3). However, when this method was used with **118** multiple products were observed by TLC. Literature searches of benzyl protected thiazole compounds showed that benzyl ether deprotection was most often undertaken with either boron trichloride or trimethylsilyl iodide. Due to the presence of other ether and ester bonds in **117**, **118** and **119** these methods could not be employed as they do not allow for selective hydrolysis. It was however hoped that the much milder condition of NaOH in MeOH would give the desired product. Multiple spots were seen on TLC after 15 minutes with **118**, but due to scale (5 mg) could not be isolated. As so much time had been dedicated to this research, with little success, it was decided to shelve this area of the research project to allow progression on other areas of work. If re-examined in the future, the use of *tert*-butyl ether rather than a benzyl ether on the glycolic acid linkers may afford a more easily hydrolysable product which could be removed using formic acid.

**Table 4 Hydrolysis conditions attempted to remove the benzyl ester protecting groups in compounds (117) and (118).**

Starting material	Solvent	Catalyst	Additive	Temperature	Result (TLC)
<b>117</b>	MeOH	10% Pd/C		Rt	Starting material
	EtOH	10% Pd/C		Rt/ Reflux	Second spot after second addition of catalyst
	AcOH	10% Pd/C		Rt	Starting material
	MeOH	10% Pd(OH) <sub>2</sub> /C		Rt	Starting material
	EtOH	10% Pd(OH) <sub>2</sub> /C		Rt/ Reflux	Starting material
	AcOH	10% Pd(OH) <sub>2</sub> /C		Rt	Second spot after second addition of catalyst
<b>118</b>	MeOH	Pd/C	HCl	Rt/ Reflux	Multiple spots
	MeOH	Pd/C	HCO <sub>2</sub> NH <sub>4</sub>	Rt	Starting material
	EtOH	Pd/C		Rt	Starting material
	AcOH	Pd/C		Rt/ Reflux	Multiple spots
	MeOH	5% Pd/C	AcOH	Rt/ Reflux	Starting material
	MeOH	5% Pd/C		Rt	Starting material
	AcOH	5% Pd/C		Rt	Starting material
	MeOH	10% Pd/C		Rt	Starting material
	MeOH	10% Pd/C	AcOH	Rt	Starting material
	EtOH	10% Pd/C		Rt/ Reflux	Starting material
	EtOAc	10% Pd/C		Rt	Starting material
	THF	10% Pd/C		Rt	Starting material
	AcOH	10% Pd/C		Rt	Starting material
		20%			
	MeOH	Pd(OH) <sub>2</sub> /C		Rt/ Reflux	Starting material
		20%			
	EtOH	Pd(OH) <sub>2</sub> /C		Rt/ Reflux	Starting material
		20%			
	EtOH	Pd(OH) <sub>2</sub> /C	AcOH	Rt/ Reflux	Starting material
		10%			
	MeOH	Pd(OH) <sub>2</sub> /C		Rt	Starting material
		10%			
	MeOH	Pd(OH) <sub>2</sub> /C	AcOH	Rt	Starting material
		10%			
	EtOH	Pd(OH) <sub>2</sub> /C		Rt	Starting material
		10%			
	EtOAc	Pd(OH) <sub>2</sub> /C		Rt	Starting material
		10%			
	AcOH	Pd(OH) <sub>2</sub> /C		Rt	Multiple spots
	DCM	Pd(OAc) <sub>2</sub>	1 eq Et <sub>3</sub> SiH, Cat. Et <sub>3</sub> N	Reflux	Starting material



### 2.6.2 $\alpha 1\beta 5$ Integrin inhibitor.

Integrins are transmembrane heterodimeric proteins which are present in a wide variety of cells and play a crucial role in normal cell function. Alongside other receptors, integrins modulate the signalling pathways of cells through microclimate sensing, thereby maintaining tissue homeostasis.<sup>139</sup> In mammals 24 subtypes have been identified, which are constituted from 18  $\alpha$  and 8  $\beta$  subunits. Many of these have been found to be overexpressed in cancer cells impacting proliferation, metastasis, resistance to therapies and recurrence.<sup>140</sup> Three of these;  $\alpha v\beta 3$ ,  $\alpha v\beta 5$  and  $\alpha 5\beta 1$  have been shown to mediate angiogenesis which is a key path physiology in cancer.<sup>141</sup> The increased nutrient and oxygen demands of an enlarging tumour necessitates new blood vessel formation, inhibiting this pathway would therefore have a significant effect on tumour progression. The overexpression of  $\alpha 5\beta 1$  in colon, breast, ovarian, lung and brain tumours is particularly associated with poor patient prognosis,<sup>139</sup> inhibition of this pathway is therefore an attractive target for cancer therapy.

Intracellular signalling by  $\alpha 5\beta 1$  is initiated through the formation of an adhesion complex with the extracellular matrix molecule fibronectin *via* the tripeptide motif Arg-Gly-Asp. Disruption of  $\alpha 5\beta 1$ -fibronectin binding has been investigated using three main classes of antagonists, specific antibodies, small peptides and Arg-Gly-Asp like molecules. Clinically the most advanced of these is voloximab, a chimeric antibody, which has completed phase II trials for advanced epithelial ovarian and peritoneal cancer in combination with liposomal doxorubicin.<sup>139</sup>

$\alpha 5\beta 1$ ,  $\alpha v\beta 3$  and  $\alpha 11b\beta 3$  are all able to recognise the Arg-Gly-Asp motif of fibronectin, making selective antagonist design a challenge. As a crystal structure of  $\alpha 5\beta 1$  in complex with fibronectin was not published until 2012<sup>142</sup> initial Arg-Gly-Asp like antagonists were developed using a homology model based on  $\alpha v\beta 3$ . This led to the development of several structure affinity relationship optimised non peptidic  $\alpha 5\beta 1$  antagonists by different pharmaceutical research groups.<sup>139</sup> One of these was by AstraZenca, using both a homology model and literature precedence of pharmacophores for  $\alpha 5\beta 1$  selectivity.<sup>143-4</sup> Structure affinity relationship

optimisation of the dibasic  $R^1$  group gave **131** and **132** as the most potent in an human immortalised myelogenous leukemia cell line (K562  $IC_{50}$  <0.003 and 0.007 $\mu$ m respectively with 2,6 dichlorophenyl (**130**)  $R^2$  group). Amide optimisation using **132** as the dibasic group gave **130**, **133**, **134** and **135** as the most potent amides.

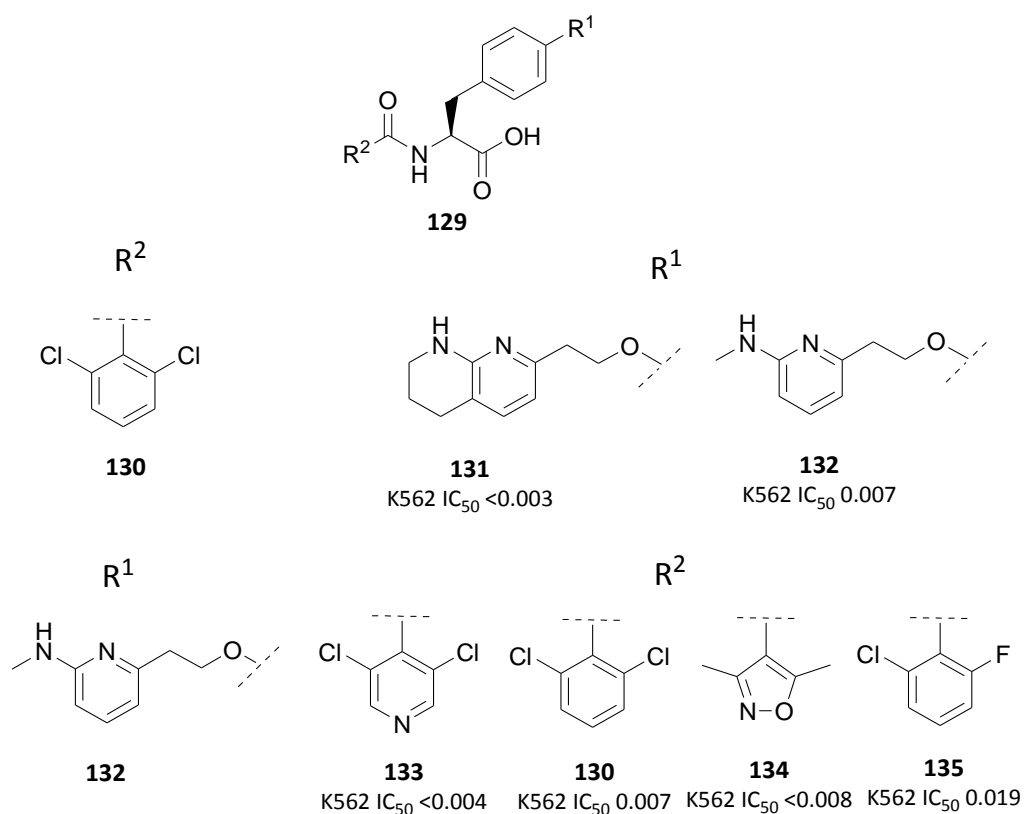


**Figure 21 Side chains identified through structure affinity optimisation of a non peptidic  $\alpha 5\beta 1$  antagonist.**<sup>143-4</sup>

The reaction scheme illustrates the synthesis of compound **138** from compound **136** in two steps:

**Step (i):** Compound **136** (a 6,7,8,9-tetrahydroquinoline derivative with a 4-(2-(2-chloro-3-fluorobenzamido)-2-hydroxyethyl)phenoxy group) reacts with a chiral auxiliary (BocHN-CH(CH<sub>3</sub>)-S-CH(CH<sub>3</sub>)-O-CO-CH<sub>2</sub>-CO<sub>2</sub>tBu) to form intermediate **137**. The auxiliary is attached to the hydroxyl group of **136** via an ester linkage.

**Step (ii):** Intermediate **137** is converted to compound **138** (a 6,7,8,9-tetrahydroquinoline derivative with a 4-(2-(2-chloro-3-fluorobenzamido)-2-aminoethyl)phenoxy group). The auxiliary is removed, and the hydroxyl group is replaced by an amino group.

67

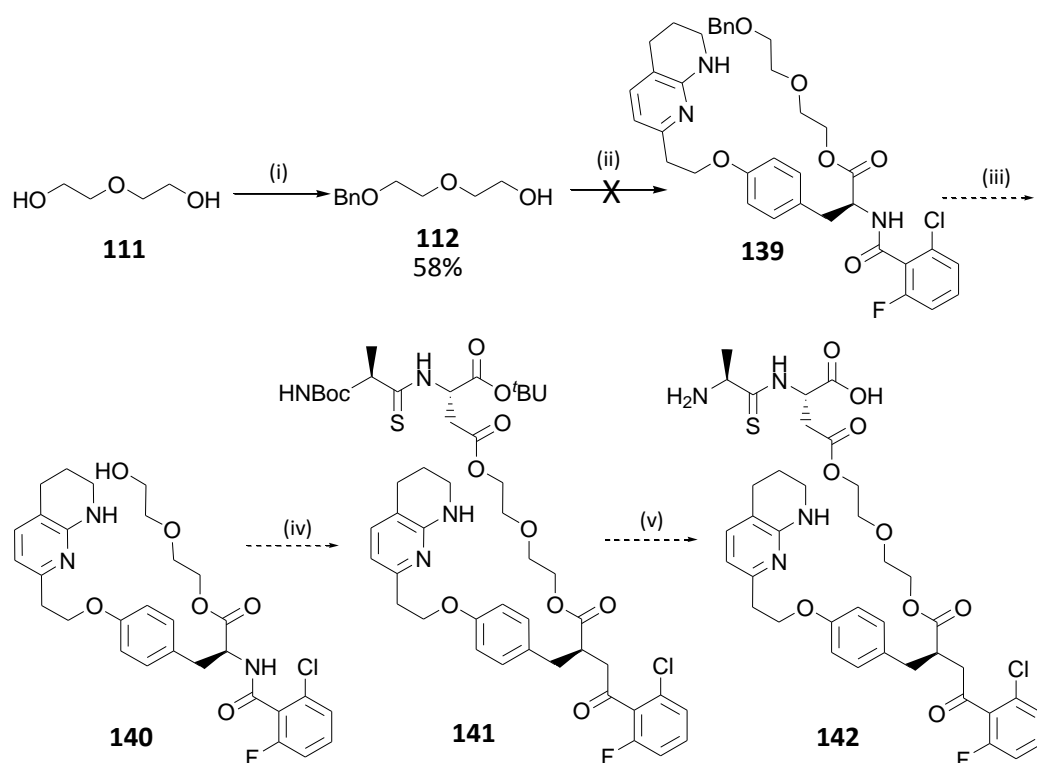
**Table 5 Conditions used for the coupling of Boc-Ala(S)Ser-OtBu (56) to the integrin inhibitor (136).**

<b>Coupling reagent</b>	<b>Eq.</b>	<b>Additive</b>	<b>Eq.</b>	<b>Additive</b>	<b>Eq.</b>	<b>Solvent</b>
<b>EDC</b>	1.1	DMAP	1			DMF
	1.2	DMAP	2			DMF
	1.1	DIPEA	2			DMF
	1.1	DMAP	1	HOBt	1	NMP
	1.1	DMAP	2	HOBt	2	DMF
	1.2	HOBt	1			EtOAc
<b>DCC</b>	1.1	DMAP	2			DMF
	1.1	DMAP	2	HOBt	1	DMF
	1.2	DIPEA	2	HOBt	1.1	DMF
	1.1	DIPEA	2	HOBt	1.1	THF
	1.2	HOBt	1.2			DMF
<b>COMU</b>		Oxyma				
	1.1	Pure	1.1			DMF
	1.2	DIPEA	1.5			DMF
<b>TBTU</b>	1.2	DIPEA	5			DMF
	1.1	HOBt	2	DIPEA	1.5	THF
	1.1	DIPEA	1.5			EtOAc
<b>HATU</b>	1.1	DIPEA	2			DMF
	1.2	DIPEA	2			DMF
	1.2	DIPEA	2	HOBt	2	DMF
	1.2	TEA	2			EtOAc
<b>HBTU</b>	3.5	TEA	3.5			DMSO
	1.2	TEA	2			DMF
	1.2	DIPEA	2			DMF
	1.2	DIPEA	2			THF
	1.2	DIPEA	5			DMF
<b>CDI</b>		m-				
	1.3	terphenyl	0.25	Imidazole	1.5	NMP
<b>DPPA</b>	1.2	TEA	1.2			THF
	1.1	TEA	2			DMF
<b>TFFH</b>	1	DIPEA	1			DMF
	1	DIPEA	2			DMF

Oxyma Pure has been brought to the market as a replacement additive in carbodiimide coupling reactions. This was in response to HOBt and HOAt being removed from sale due to explosive properties. It has been shown to possess coupling efficiency superior to that of HOBt and at least comparable to HOAt, whilst inhibiting racemisation.<sup>145</sup> COMU is an uronium salt derived from Oxyma Pure and contains morpholino group.<sup>146</sup> A benefit in using COMU is that the course of the reaction can be monitored due to a change in colour of the reaction mixture. The

other unusual reagent used was TFFH. TFFH is a non-hydroscopic salt fluorinating agent which, when used in conjunction with DIPEA, can be used to generate acid fluorides.<sup>147</sup> It is especially suited for the coupling of sterically hindered amino acids, which is why it was selected for use with the integrin inhibitor.

Despite extensive screening of coupling conditions for the coupling of Boc-Ala(S)Ser(OH)-O<sup>t</sup>Bu (**56**) to the integrin inhibitor (**136**), no successful condition could be found (Table 5). It was thought that this may be due to steric hindrance of the reaction site as both molecules are quite bulky. It was therefore theorised that coupling a less bulky polyethylene glycol linker to the integrin inhibitor may be more successful (Scheme 13).



**Scheme 13** Revised synthesis of Ala(S)Asp-linker-Integrin prodrug. (i) NaH, KI, BnBr (ii) (**136**), coupling conditions (iii) TosCl, pyridine, -5°C, 24h (iii) Pd(OH)<sub>2</sub>, MeOH (iv) (**57**), coupling conditions (v) HCO<sub>2</sub>H, reflux, 3h.

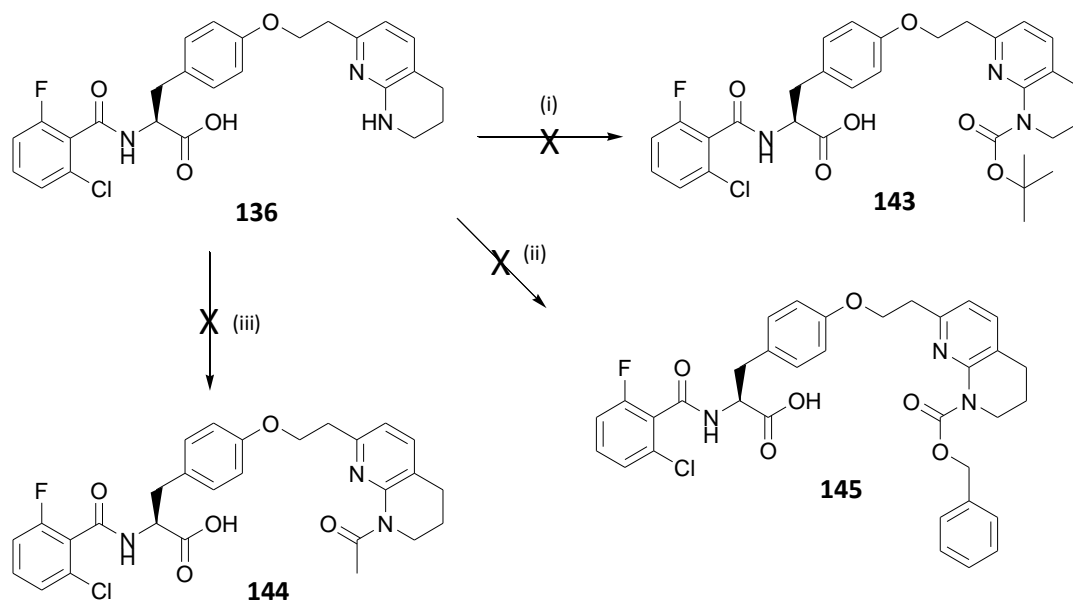
Adding a polyethylene linker to the integrin inhibitor would give the added benefit of assessing the effect of chain length on transport and hopefully improve the solubility of the very insoluble **136**. However again, extensive screening failed to give the desired product (Table 6).

**Table 6 Conditions used for the coupling of (112) to the integrin inhibitor (136).**

Coupling reagent	Eq.	Additive	Eq.	Additive	Eq.	Solvent
<b>EDC</b>	1.1	DMAP	2			DMF
	1.1	DMAP	3			DMF
	1.1	DIPEA	2			DMF
	1.1	DIPEA	2			EtOAc
	1.1	HOBt	2			EtOAc
<b>DCC</b>	1.1	DMAP	2			DMF
	1.1	DMAP	2	HOBt	1	DMF
	1.1	DIPEA	2			DMF
	1.1	DIPEA	2	HOBt	1	DMF
	1.1	HOBt	2			DMF
<b>COMU</b>	1.2	DIPEA	1.5			DMF
	1.1	HOBt	2			DMF
<b>TBTU</b>	1.1	HOBt	2			DMF
	1.1	DBU	2			DMF
	1.1	DIPEA	2			DMF
<b>HATU</b>	1.1	DIPEA	2			DMF
	1.1	DIPEA	3			DMF
	1.1	TEA	2			DMF
<b>HBTU</b>	3.5	TEA	3.5			DMSO
	1.1	TEA	2			DMF
	1.1	DIPEA	2			DMF
<b>TFFH</b>	1	TEA	5	DMAP	1	DMF

In addition to the coupling conditions listed (Table 6), Mitsunobu conditions (PPh<sub>3</sub> and DIAD) were utilised. It was thought that these reaction conditions may have failed due to the acid group on the integrin inhibitor being too sterically hindered to form a complex with the coupling reagent. Therefore, methyl protection was attempted on the carboxylic acid group. As methyl iodide is a very small molecule there should be no steric impediment to the reaction occurring. However, reaction conditions failed to give the methyl ester. In **136** the secondary amine on the 1,2,3,4-tetrahydro-1,8-naphthyridine is able to sit very close to the carboxylic acid, possibly participating in hydrogen bonding. This interaction would be eliminated through amine protection, hopefully enabling the carboxylic acid to react. Protecting the amine may also give the

added benefit of improving the solubility of **136**, allowing coupling to be carried out in a wider variety of solvents (Scheme 14).



**Scheme 14 Attempted secondary amide protection of integrin inhibitor. (i) *tert*-Butyl carbamate protection (ii) carboxybenzyl carbamate protection (iii) acetyl protection.**

Unfortunately, despite the utilisation of several protecting group strategies no conditions could be found to protect the amine (Table 7).

**Table 7 Conditions employed for the secondary amine protection of the integrin inhibitor (136).**

Protecting group	Reagent	Eq.	Additive	Eq.	Solvent	Temperature
<b>tert-Butyl carbamate</b>	Boc <sub>2</sub> O	1.2	DMAP	Cat.	THF	40°C
	Boc <sub>2</sub> O	1.2	DMAP	1	THF	Rt / 50°C
	Boc <sub>2</sub> O	1.2	DMAP	2	THF	Rt / 50°C
	Boc <sub>2</sub> O	2	TEA	10%	DMF	50°C
	Boc <sub>2</sub> O	2.5	NH <sub>2</sub> OH.HCl/ NaOH	2	Dioxane/ H <sub>2</sub> O	Rt / 40°C
	Boc <sub>2</sub> O	2	(CH <sub>3</sub> ) <sub>4</sub> NOH. 5H <sub>2</sub> O	1	CH <sub>3</sub> CN	Rt
	Boc-ON	1.1	LiHMDS	1	THF	Rt / 40°C
	Boc-ON	1.1	LiHMDS	2	DMF	Rt / 40°C
	Boc-ON	1.1	NaH	1	THF	Rt / 40°C
	Boc-ON	1.1	NaH	3	THF	Rt / 40°C/ reflux
<b>carboxybenzyl carbamate</b>	Cbz-Cl	1.5	NaHCO <sub>3</sub>	2	Dioxane/ H <sub>2</sub> O	Rt / 40°C
	Cbz <sub>2</sub> O	1.2	TEA	2	Dioxane/ H <sub>2</sub> O	Rt
<b>acetyl</b>	(CH <sub>3</sub> CO <sub>2</sub> ) <sub>2</sub> O	2	Pyridine	2	-	50°C

As so much time had been devoted to this project without fruition it was decided that this avenue of research should be shelved. It would be interesting to see if the conformation of **136** was the route of the synthetic issues experienced. Unfortunately the x-ray crystallography facilities at Keele were unavailable when this avenue was being explored.



## 2.7 *In vitro* biological testing

In order to determine whether the target compounds synthesised during the course of the project were PepT1 substrates, *in vitro* testing was carried out. This was initially carried out in *Xenopus laevis* oocytes by Dr D. Meredith at Oxford Brookes University. Binding affinity was first determined and then transport was confirmed using a *trans*-stimulation assay. Favourable compounds were then put forward for Caco-2 testing so that intestinal permeability could be assessed. As part of the collaboration with AstraZeneca, Caco-2 testing was identified as being best carried out by me using their facilities. This was due to their in house expertise being able to provide training and support in both cell line culture and the most appropriate methodology for the Caco-2 studies. This also meant that a validated Caco-2 cell line was available to use for occasional studies, without year round maintenance. Analysis of the samples generated would then be performed by LCMS experts in house. This would make analysis of the diverse range of compounds tested easier, as they would have the experience to identify suitable methodology. They kindly agreed that PepT1 potential substrates synthesised by others in the group would be able to be assayed as well as the ones synthesised by me.

Unfortunately this research project coincided with a time of restructuring within AstraZeneca. As a result expertise was lost from the company, facilities had to be relocated (necessitating a delay due to cell line re-validation) and in house projects were prioritised. Out of the five Caco-2 studies ran at AstraZeneca only one study yielded full results. The overall apparent permeability of the Aurora kinase inhibitor prodrug **108** was determined from the final study, of which this was the only prodrug able to be detected. The other studies failed to yield results due to issues arising after the Caco-2 studies had been performed, most notably from issues surrounding LCMS analysis. This was due to being unable to find suitable LCMS methodology to analyse compounds. Studies that failed to yield results include comparisons of the apparent permeability of the parent compound against its thiodipeptide prodrug, and studies to determine the PepT1 mediated component of permeability. Overall the experience collaborating with

AstraZeneca has been positive with the experts there going above and beyond, despite the difficulties, to try and mediate the issues and get useable results. It is unfortunate that the Caco-2 studies didn't work out. The precise experimental details for the *in vitro* assays can be found in section 6.1. The general methodology is given below, in depth evaluation in the use of these models to study the interaction of drugs and PepT1 is covered in an excellent review by Xia *et al.*<sup>148</sup>

### 2.7.1 Binding Affinity

*Xenopus laevis* oocytes have the capacity to translate exogenous mRNA, in this case expressing PepT1. Simple competitive inhibition assays can therefore be used to quickly determine the binding affinity of a potential PepT1 substrate. Increasing concentrations of prodrug were incubated with a set concentration (0.4 µl) of radiolabelled, hydrolysis resistant *D*-Phe-*L*-Gln. As PepT1 transport is an active process only one molecule of substrate can be transported at a time. This means that the rate of transport is limited by the concentration of PepT1 expression, as a result PepT1 substrates display concentration dependent kinetics (Michaelis-Menten Kinetics).<sup>149</sup> As the concentration of incubated test compound is increased, the concentration of radiolabelled compound transported into cells is reduced due to competitive inhibition, allowing binding affinity to be determined. PepT1 is a low affinity, high capacity transporter of substrates. Substrates with an affinity of less than 1 mM are classed as having high affinity for PepT1 and those with a binding affinity higher than 5 mM are classed as low affinity.

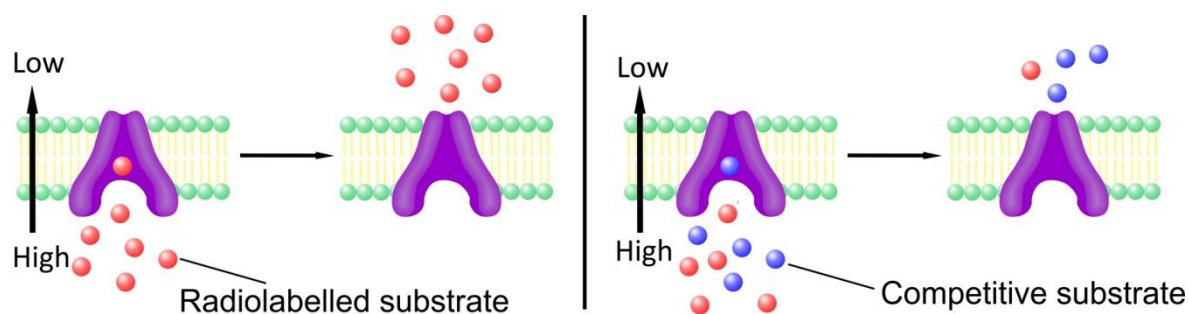


**Figure 22** Oocyte inhibition assay. Left: Determination of maximal uptake of radiolabelled substrate. Right: Reduced uptake of radiolabelled substrate in the presence of a competitive substrate.

### 2.7.2 Oocyte transport assay.

Although competitive inhibition assays can determine the binding affinity of a potential PepT1 substrate, whether the substrate is transported cannot be ascertained. This is because it is possible for a molecule to be recognised and have binding affinity for PepT1, but have unfavourable characteristics for transport (an inhibitor). Therefore transport is assessed with a *trans*-stimulation efflux assay (Figure 25).

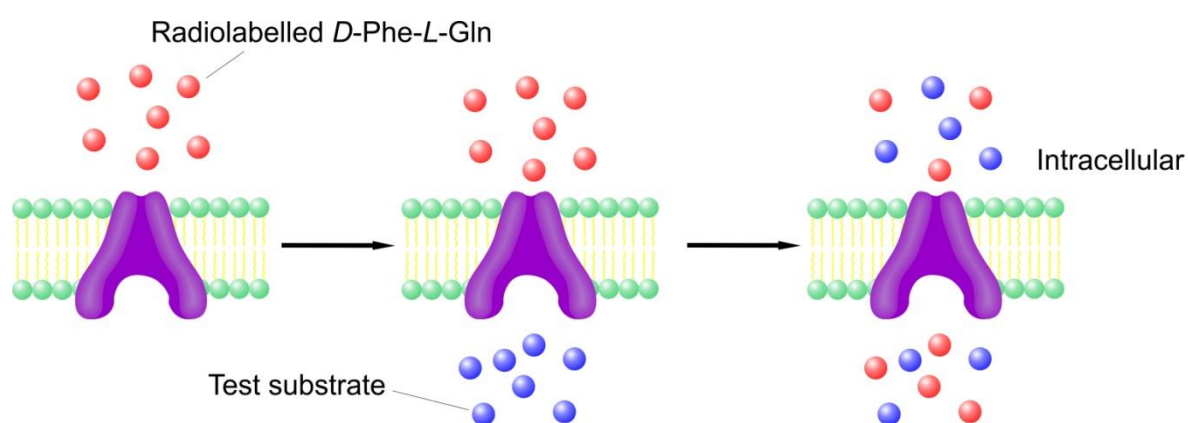


**Figure 23** Oocyte *trans*-stimulation assay. Left: oocytes injected with radiolabelled PepT1 substrate. Centre: oocytes incubated with test substrate. Right: *trans*-stimulated efflux of the radiolabel.

PepT1 mRNA expressing *Xenopus laevis* oocytes are injected with radiolabelled *D*-Phe-*L*-Gln (4.6 nL; 37.0 MBq mL<sup>-1</sup>) and incubated with the test compound. Once PepT1 has transported a molecule into the cell one of the ways it can reset itself is to efflux another substrate (the radiolabel) *via trans*-stimulation efflux. The intracellular radioactivity of the oocyte is measured after the incubation period and then compared to the decrease induced by the PepT1 substrate *L*-Gly-*L*-Gln.<sup>150</sup> If intracellular radioactivity of a *D*-Phe-*L*-Gln injected oocyte incubated with uptake media is taken as a control, then the percentage decrease in intracellular radioactivity seen when the oocyte is incubated with *L*-Gly-*L*-Gln can be used as a standard. Therefore, incubated test substrates which show an intracellular radioactivity decrease of 0-30% in comparison to Gly-Gln can be assessed as poorly transported, 30%-80% assessed as being moderately transported and 80%+ being excellently transported. Although you cannot get false positive results you can have a false negative result, as PepT1 has other pathways to reset.

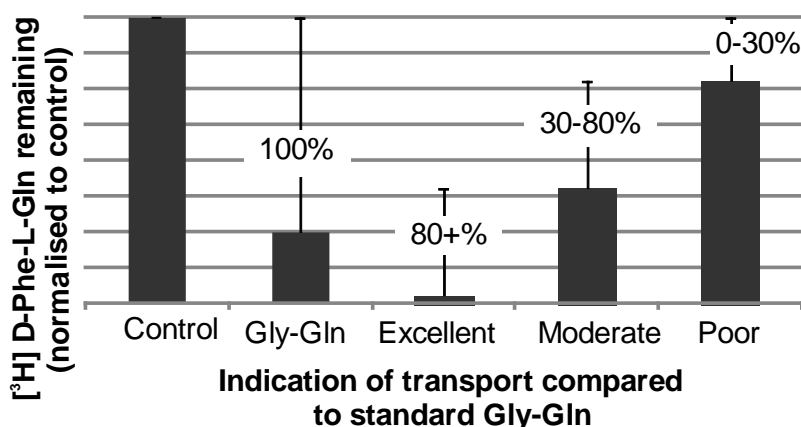


**Figure 24** A bar chart showing how transport is assessed using *trans*-stimulation data.

### 2.7.3 Caco-2 assays.

Caco-2 is an adenocarcinoma cell line and is widely accepted to be a good model for the small intestine and is the most extensively characterised model for examining the permeability of drugs.<sup>148</sup> The cell line expresses microvilli, tight-junctions, enzymes and transporters which resembles the small intestines morphology and functionality and has been shown to correlate

well with the *in vivo* absorption of orally administered drugs in man.<sup>151</sup> Prior to Caco-2 testing, the test compounds were assessed for stability against the enzymes on the apical cell surface of the Caco-2 monolayer. As well as assessing the overall permeability of a compound across a cell membrane, significance of the PepT1 mediated component can be identified by incubating the substrate with an excess of a known PepT1 substrate.

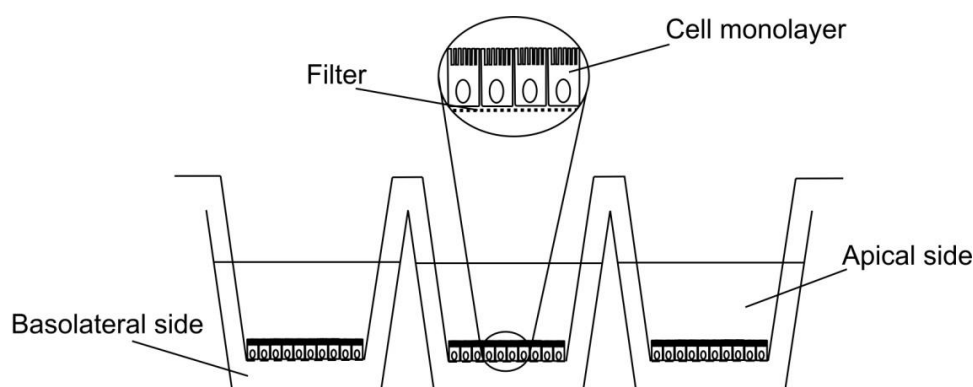


**Figure 25 A Caco-2 monolayer.**

#### 2.7.4 Biological results.

Binding affinity, *trans*-stimulation and apparent permeability had already been determined in the group for the thiodipeptide ibuprofen<sup>117</sup> (**79**) and propofol (**76**) (unpublished) prodrugs.<sup>127</sup> However, these compounds were re-analysed to ensure consistency between the Caco-2 data produced at AstraZeneca and Oxford Brookes. The binding affinity and *trans*-stimulation data for these prodrugs is also shown in Table 8.<sup>117,127</sup> Binding affinity, *trans*-stimulation efflux and overall apparent permeability for the Aurora Kinase inhibitor thiodipeptide prodrug **108** was generated during the course of this project. Studies to assess the PepT1 mediated component of substrate transport ran into problems with analysis of the samples generated from the studies. This had already been performed by Dr. Meredith's group for the thiodipeptide ibuprofen (**79**) and propofol (**76**) prodrugs and so is shown in Table 8 alongside the results obtained for prodrug **108**.

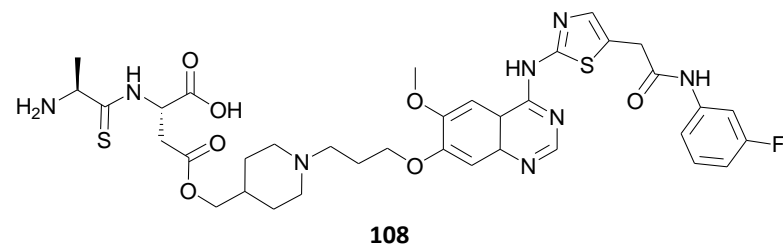
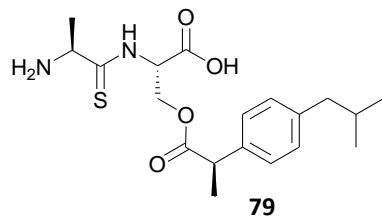
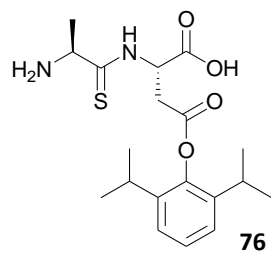


**Table 8** *In vitro* data for prodrugs (**76**), (**79**) and (**108**).

Compound	K <sub>i</sub>	<i>Trans</i> -stimulation	Overall P <sub>app</sub>	Overall P <sub>app</sub> previously found	PepT1 P <sub>app</sub> previously found
76	0.92 ± 0.19 mM	122%	0.40 ± 0.01 × 10 <sup>-6</sup> cm S <sup>-1</sup>	0.53 ± 0.05 × 10 <sup>-6</sup> cm S <sup>-1</sup>	0.52 ± 0.05 × 10 <sup>-6</sup> cm S <sup>-1</sup>
79	0.26 ± 0.03 mM	109%	3.97 ± 0.27 × 10 <sup>-6</sup> cm S <sup>-1</sup>	3.65 ± 0.22 × 10 <sup>-6</sup> cm S <sup>-1</sup>	2.10 ± 0.27 × 10 <sup>-6</sup> cm S <sup>-1</sup>
108	0.10 ± 0.02 mM	110%	0.31 ± 0.00 × 10 <sup>-6</sup> cm S <sup>-1</sup>	-	-

The thiodipeptide propofol prodrug (**76**) was found to have an apparent permeability of  $0.40 \pm 0.01 \times 10^{-6} \text{ cm S}^{-1}$  in Caco-2 cells, which is considered a moderate permeability. This data is similar to that previously found at Oxford Brookes ( $0.53 \pm 0.05 \times 10^{-6} \text{ cm S}^{-1}$ ). The binding affinity for PepT1 was found to be high (0.92 mM) and *trans*-stimulation was induced (122%), indicating that **76** is a PepT1 substrate. This is of significance as the parent drug propofol (**74**) has very low solubility and has to be administered intravenously as an oil-in-water emulsion, making this a potentially a prodrug of commercial interest.

The thiodipeptide ibuprofen prodrug (**79**) was found to have an apparent permeability of  $3.97 \pm 0.27 \times 10^{-6} \text{ cm S}^{-1}$ , which is considered to be a high permeability. This is similar to data previously generated at Oxford Brookes ( $3.65 \pm 0.57 \times 10^{-6} \text{ cm S}^{-1}$ ). This indicates that targeting ibuprofen (**77**) towards PepT1 through the attachment of a carrier still results in high permeability. This is an excellent result as there is in fact some evidence that parent ibuprofen (**77**) is a non-competitive inhibitor of PepT1.<sup>152</sup> Binding affinity was found to be excellent (0.26 mM) and *trans*-stimulation was induced (109%). This indicates that this prodrug should be investigated further to establish whether gastrointestinal side effects seen with the parent drug are reduced. Ibuprofen prodrug **79** was selected for a pharmacokinetic study and taste evaluation test in rat (chapter 3).

The Aurora kinase inhibitor prodrug **108** was found to have moderate apparent permeability ( $0.31 \pm 0.01 \times 10^{-6} \text{ cm S}^{-1}$ ). However this was generated from a single data point using parent compound detected on the basolateral side of the Caco-2 monolayer in apical to basolateral transport. The two other repeats were found to have an analytical response too low to detect. Very little of prodrug **108** was detected on the basolateral side, indicating that hydrolysis of the ester bond has occurred either during or subsequent to the assay. The parent Aurora kinase inhibitor (**105**) is slightly permeable through a Caco-2 monolayer ( $0.07 \pm 0.01 \times 10^{-6} \text{ cm S}^{-1}$ ), meaning that some of the parent prodrug (**105**) detected on the basolateral side may

have crossed the monolayer of cells if the prodrug was hydrolysed prior to transport. However, some of prodrug (**108**) must have been intact when moving from the apical to basolateral side of the cells for the apparent permeability to be as high as detected. To be sure of this result is reproducible Caco-2 testing should be performed again on this prodrug. Binding affinity was found to be high (0.10 mM) and *trans*-stimulation was induced (110%), indicating **108** is a PepT1 substrate.

Several prodrugs synthesised by Dr. Pathak were also assayed in Caco-2 cells at AstraZeneca. However, problems with analysis after the studies meant that apparent permeability could not be determined. For the purposes of assessing PepT1 for prodrug targeting the oocyte data generated by Dr. Meredith's team at Oxford Brookes (unpublished) is shown.

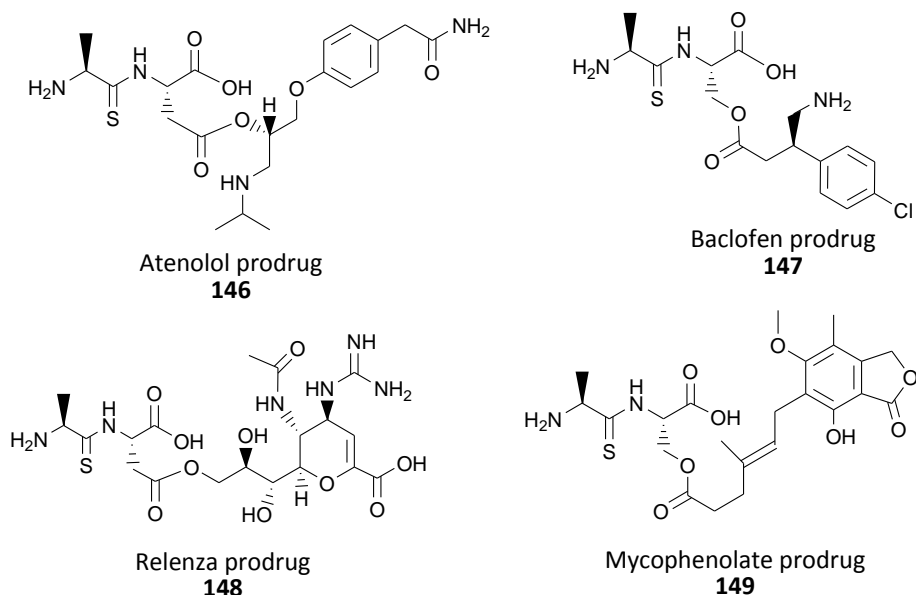


**Table 9** *In vitro* data for thiodipeptide prodrugs synthesised by R. Pathak (unpublished).

Compound	K <sub>i</sub>	<i>Trans</i> -stimulation
Atenolol prodrug <b>146</b>	0.44 ± 0.15 mM	70%
Baclofen prodrug <b>147</b>	1.87 ± 0.26 mM	25%
Relenza prodrug <b>148</b>	0.13 ± 0.02 mM	0%
Mycophenolate prodrug <b>149</b>	0.21 ± 0.08 mM	80%



Caco-2 data is needed to fully assess whether prodrugs **146-149** are transported by PepT1. The binding affinities for the thiopeptide atenolol (**146**) and mycophenolate (**149**) prodrugs are excellent, with both inducing moderately high *trans*-stimulation efflux. This suggests that both **146** and **149** are PepT1 substrates, but PepT1 mediated apparent permeability in Caco-2 cells will need to be determined to confirm this. Although the thiodipeptide relenza prodrug (**145**) has a high binding affinity, lack of *trans*-stimulation efflux suggests that it is an inhibitor of PepT1. The thiodipeptide baclofen prodrug **147** only showed moderate binding affinity and poor *trans*-stimulation efflux. This suggests that it is a very poor substrate of PepT1, which would be established with a PepT1 mediated apparent permeability Caco-2 assay.

# **Chapter 3**

## **Alternative carriers**

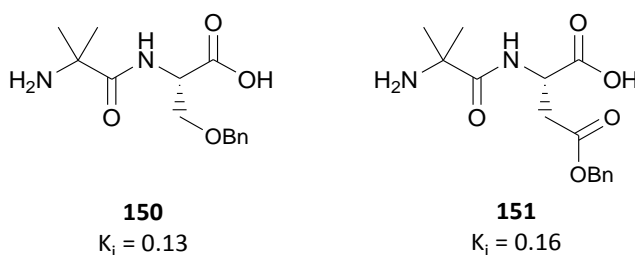
### Chapter Three Contents

3.1	Synthesis of carriers .....	84
3.2	<i>In vitro</i> biological testing .....	89
3.3	<i>In vivo</i> biological testing .....	92
3.3.1	Pharmacokinetic study .....	92
3.3.2	Taste assessment. ....	95

### 3.1 Synthesis of carriers

Previous work in our group has focused on the use of thiodipeptides as the carriers of choice when targeting drugs towards PepT1. These are favourable as the lack of peptide bond means they are resistant to hydrolysis in the gastrointestinal tract (section 2.4). Problems do however arise due to the presence of sulphur in the carriers. Synthetically the use of hydrogenation, once the carrier has undergone oxygen-sulphur exchange, is not possible due to poisoning of the catalyst. This limits the protecting group strategy that can be utilised in the synthesis of the desired prodrugs, which is particularly pertinent for acid or base sensitive drugs. The presence of sulphur in a drug can also drastically negatively alter taste, which can affect compliance especially in children. In the extreme this is demonstrated by the drug used to treat cystinosis, mercaptamine bitartrate, which has a very unpleasant taste. Finally the presence of a thiodipeptide in the final prodrug has often experimentally been found within our group to produce a non-crystalline product which presents a problem for formulation.

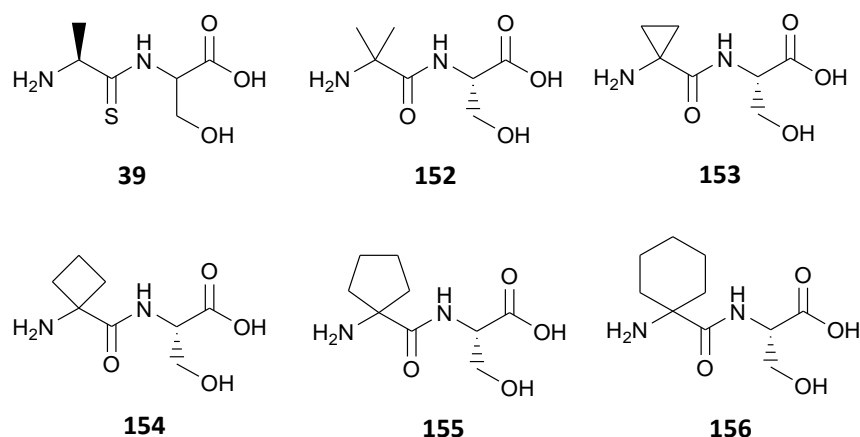
Previous work within our group (Dr D. Foley, unpublished)<sup>127</sup> showed that *N*-terminal  $\alpha,\alpha$ -disubstituted dipeptides **150** and **151** (shown with benzyl as a model drug moiety) had potential as alternative hydrolysis resistant carriers.



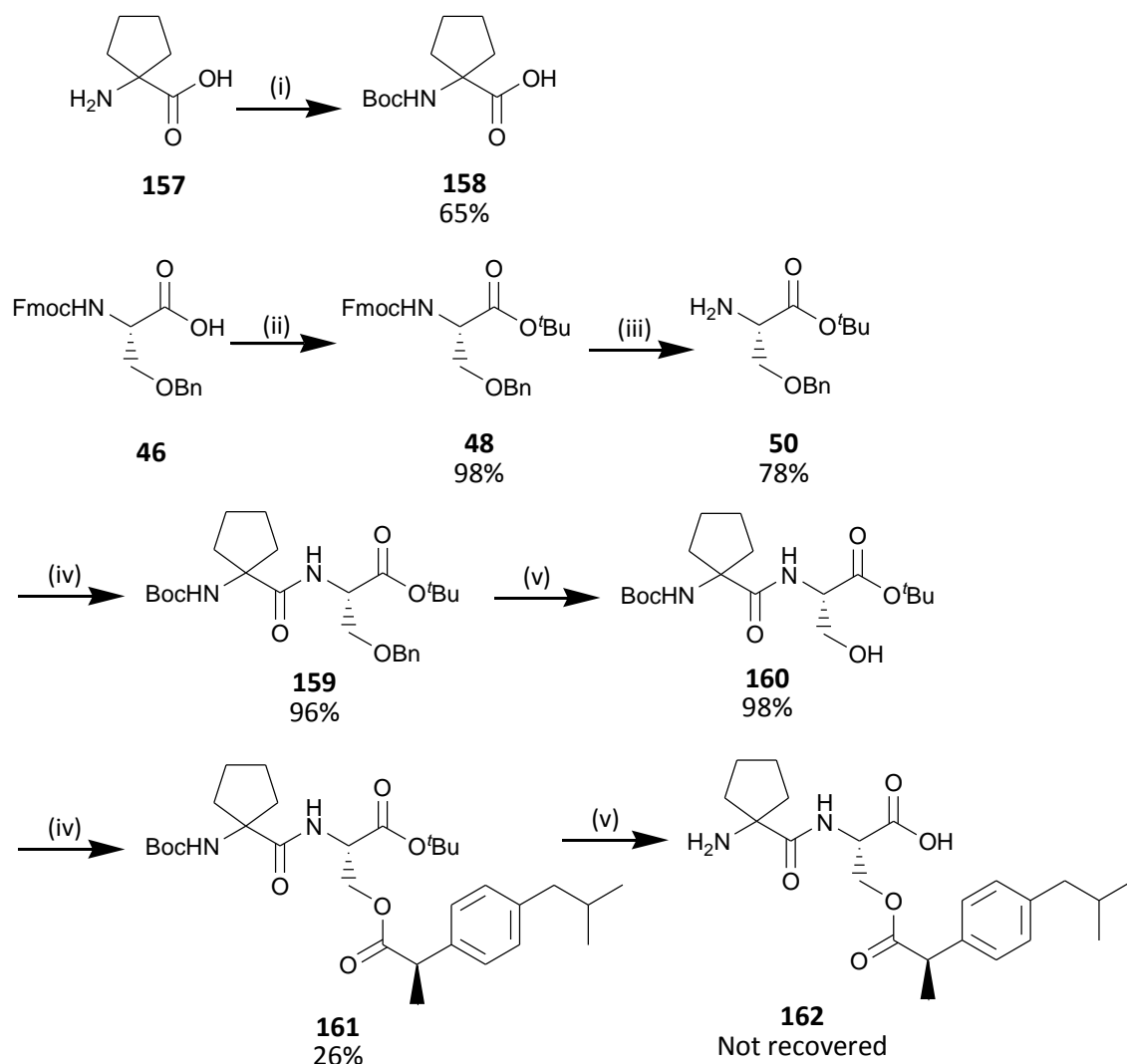
These results are consistent with the finding by Lyons *et al.*<sup>91</sup> that there is an elongated cavity in the *N*-terminal end of the ligand binding site in the prokaryotic POT transporter PepT<sub>so</sub>.<sup>89</sup> To explore the tolerance of PepT1 for bulk in this area a series of dipeptides were synthesised. The use of carbocyclic rings on the *N*-amino moiety allowed us to investigate this steric region, whilst having the added benefit of increasing the overall lipophilicity of resultant prodrugs due to

the added hydrocarbon bulk. Traditional prodrug strategies for poorly bioavailable drugs often involves increasing lipophilicity which can increase permeability.

By adding steric bulk to the *N*-terminal  $\alpha$ -carbon, access to the backside of the carbonyl group is reduced. This should prevent hydrolysis of the dipeptide in the gut and prevent the access of peptidases to the dipeptide. To gain the best understanding of how bulk in the *N*-terminal region affects PepT1 transport the data for *N*-terminal  $\alpha$ -monomethyl through to  $\alpha$ -cyclohexane must be assessed. This was achieved by comparing both the free carrier and carrier with moiety attachment through the *N*-terminal side chain. Benzyl was used to represent a small drug moiety and ibuprofen the real drug entity as it is a simple molecule to attach to a carrier due the presence of one functional group. This necessitated the use of serine as the second amino residue. The data for dipeptide **39**<sup>117</sup> and **152**<sup>127</sup> attached to both benzyl and ibuprofen had already been collected within the group, so dipeptides **153-156** were synthesised (Figure 30).



Synthetic work on this project was initiated by 3<sup>rd</sup> year student Lucy Richards, under my supervision, with the project target being cycloleucine-serine-ibuprofen (**162**) (Scheme 15). Due to the favourable price of cycloleucine (5g, £30), the project was initiated from this starting material rather than Boc-cycloleucine (1g, £20). This was to enable the student to gain experience in protecting group reactions and to economise the limited student project budget.



**Scheme 15** Initial synthesis of cycloleucine-Ser-ibuprofen. (i)  $\text{Boc}_2\text{O}$ , TEA, NaOH,  $\text{C}_2\text{H}_5\text{N}$ ,  $0^\circ\text{C} \rightarrow \text{rt}$ , 4h (ii) *tert*-butyl-2,2,2-trichloroacetimidate, DCM/ $\text{Et}_2\text{O}$ , 3 days (iii) TBAF in THF, 3h (iv) (158), DPPA, DIPEA, DMF,  $0^\circ\text{C}$ , 3 days (v) 10% Pd/C,  $\text{H}_2$ , MeOH, 24h (iv) HBTU, DIPEA, ibuprofen (77), DMF, 4 days (v)  $\text{HCO}_2\text{H}$ , reflux, 3h.

Traditional Boc-protection procedures (NaOH, dioxane,  $\text{H}_2\text{O}$  and  $\text{Boc}_2\text{O}$ ) failed to give the desired product **158**, so a bi-phasic procedure was utilised to give *N*-Boc-cycloleucine (**158**) in a 65% yield. NaOH enabled solvation of the cycloleucine, whilst acetonitrile enabled solvation of  $\text{Boc}_2\text{O}$  and TEA was used to activate  $\text{Boc}_2\text{O}$ . Synthesis of H-Ser(Bn)- $^t\text{Bu}$  (**50**) was carried out using the established methodology (*tert*-butyl protection of Fmoc-Ser(Bn)-OH (**46**) using *tert*-butyl-2,2,2-trichloroacetimidate, followed by Fmoc deprotection using TBAF) (Section 2.3). Synthesis of Boc-cycloleucine-Ser(Bn)-O $^t\text{Bu}$  (**159**) was initially carried out using the coupling conditions utilised

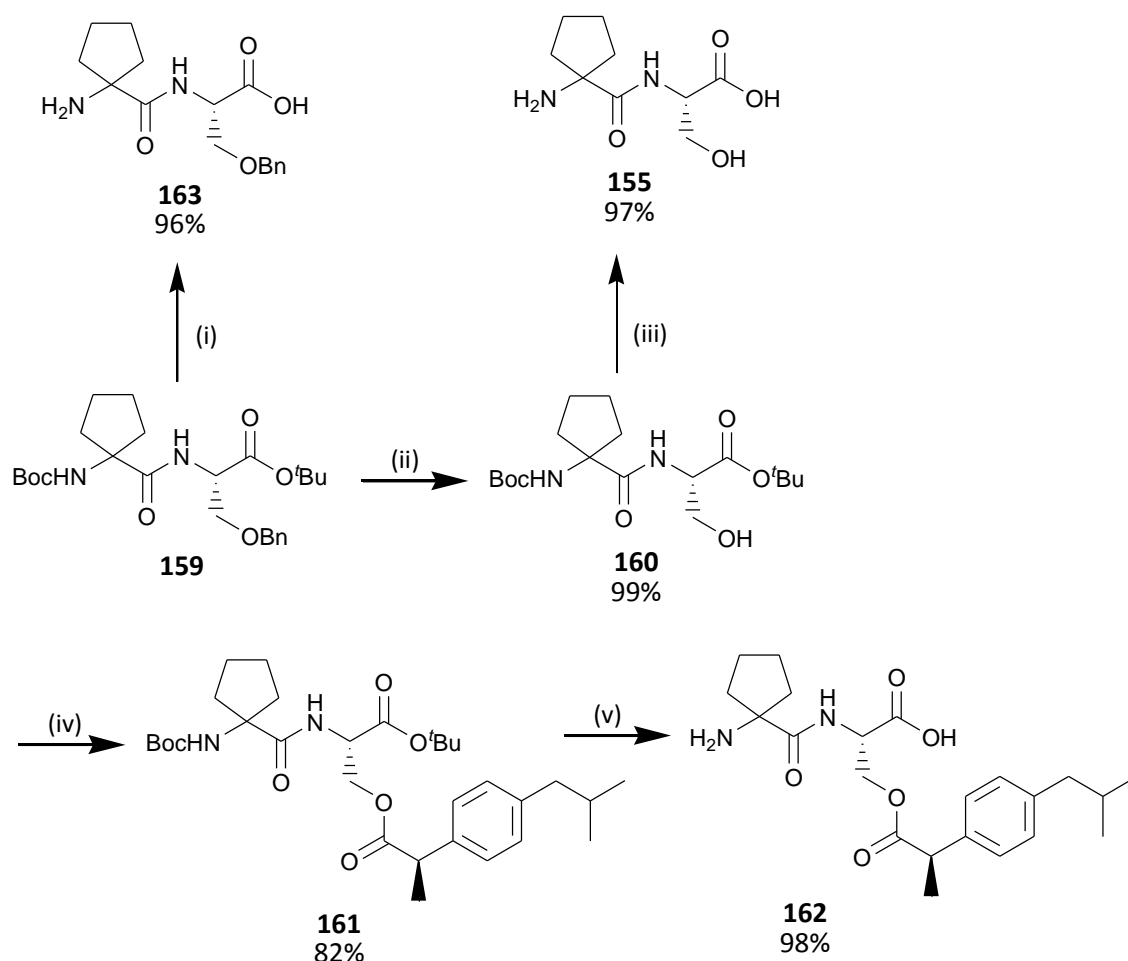
in the synthesis of our *tert*-butyl and Benzyl protected carriers (1.1 eq DPPA, 2 eq TEA in DMF) to give an expected yield of 78%. Although this is a good yield, to my knowledge no optimisation of this step had been carried out since the establishment of the original methodology. Therefore, to gain experience in synthesis optimisation and the different classes of coupling reagents, Lucy was asked to screen coupling conditions for this step (Table 10).

**Table 10 Optimisation of the coupling conditions for Boc-cycloleucine-Ser(Bn)-OtBu (159). All reactions carried out over 3 days at 0°C in DMF**

Excess amino acid (1.1 eq)	Coupling reagent	Eq.	Additive	Eq.	Yield
Boc-cycloleucine	DPPA	1.1	TEA	2	78%
Boc-cycloleucine	DPPA	1.1	DIPEA	1.5	61%
Boc-cycloleucine	DPPA	1.1	DIPEA	2	96%
Boc-cycloleucine	EDC	1.1	HOBt	2	49%
H-Ser(Bn)OtBu	EDC	1.1	HOBt	2	88%
Boc-cycloleucine	HBTU	1.1	DIPEA	2	35%

Benzyl deprotection of Boc-cycloleucine-Ser(Bn)-OtBu (**159**) was carried out using 10% Pd/C in MeOH to give **160**. **160** was then coupled to ibuprofen (**77**) using the previously established methodology of HBTU and DIPEA in DMF to give **161** in a 26% yield. Final deprotection of **161** was carried out in formic acid, but for some reason failed to give a clean product (**162**, Scheme 16).

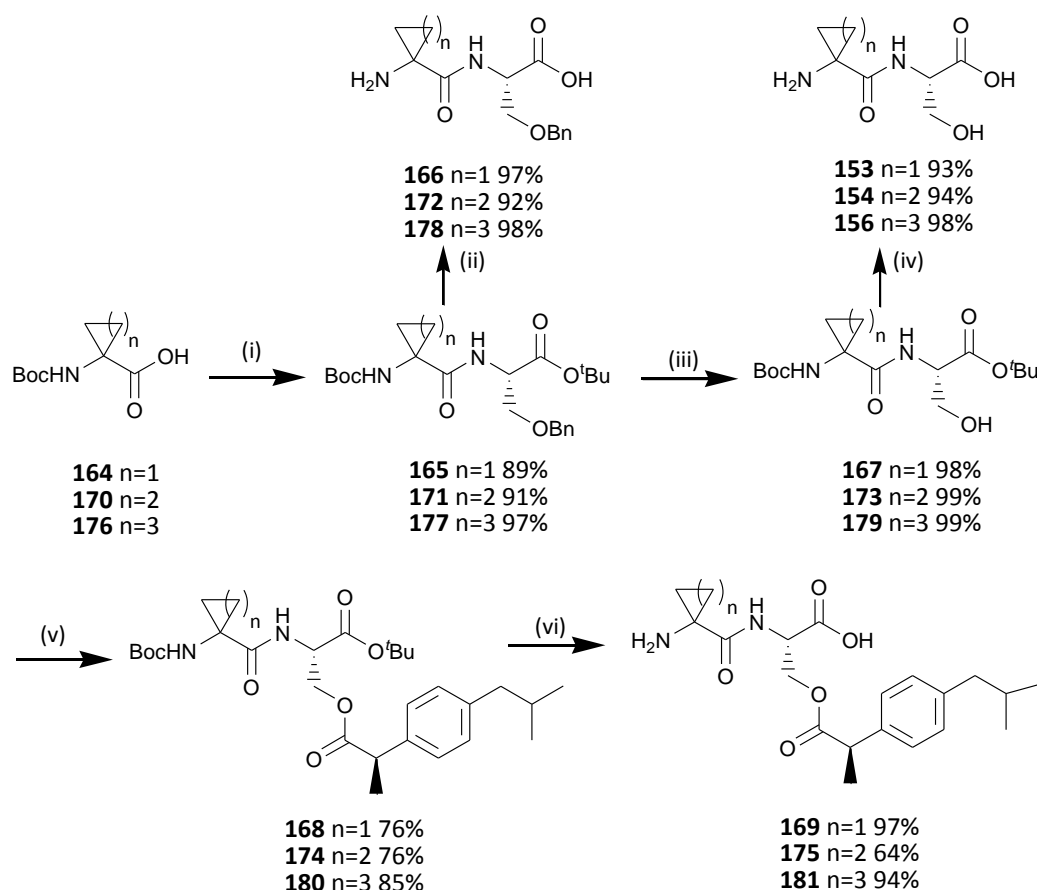
Although Lucy made good progress with the synthesis of protected cycloleucine-serine-ibuprofen (**161**), the target compound was not made. Therefore, to continue this project the free carrier, carrier with benzyl attachment and carrier with ibuprofen attachment were synthesised by me using stock **159** from Lucy's project. Due to low yield (26%) the coupling conditions used to synthesise **161** was optimised. DCC and DMAP in DCM was found to give the desired ibuprofen prodrug (**161**) in 82% yield (Scheme 16).



**Scheme 16** Synthesis of H-cycloleucine-Ser(Bn)-OH (**163**), H-cycloleucine-Ser(OH)-OH (**155**) and H-cycloleucine-Ser(ibuprofen)-OH (**162**). (i) HCO<sub>2</sub>H, reflux, 3h (ii) 10% Pd/C, H<sub>2</sub>, MeOH, 24h (iii) HCO<sub>2</sub>H, reflux, 3h (iv) DCC, DMAP, ibuprofen (**77**), DCM, 3 days (v) HCO<sub>2</sub>H, reflux, 3h.

Synthesis of the cyclopropane, cyclobutane and homocycloleucine carriers was carried out from their purchased Boc-amino acids (Scheme 17). The first set to be synthesised was the cyclopropane carrier derivatives. Difficulties were encountered upon the benzyl deprotection of **165** to give **167**, as 10% Pd/C in MeOH resulted in only starting material being obtained. It was only upon the addition of catalytic AcOH to Pd/C in MeOH that successful protection occurred to give **167**. The cyclobutane carrier derivatives and homocycloleucine carrier derivatives were synthesised using the same methodology (Scheme 17).



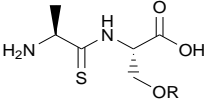
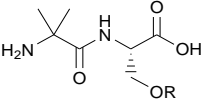
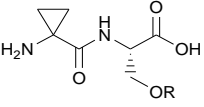
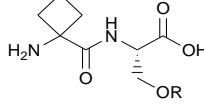
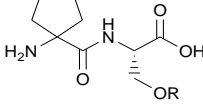
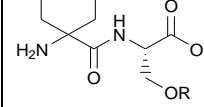


**Scheme 17** Synthesis the free carrier, carrier with benzyl attachment and carrier with ibuprofen attachment for the cyclopropane, cyclobutane and homocycloleucine carriers. (i) *N*-Boc amino acid, DPPA, DIPEA, DMF, 0°C, 3 days (ii) HCO<sub>2</sub>H, reflux, 3h (iii) AcOH, Pd/C, MeOH, 24h (iv) HCO<sub>2</sub>H, reflux, 3h (v) DCC, DMAP, ibuprofen, DCM, 3 days (vi) HCO<sub>2</sub>H, reflux, 3h.

### 3.2 *In vitro* biological testing

The synthesis of; H-Ala(S)Ser(Bn)-OH (**182**),<sup>117</sup> H-Ala(S)Ser(ibuprofen)-OH (**79**),<sup>117</sup> H-Aib-Ser(Bn)-OH (**150**)<sup>127</sup> (Dr. F. Foley) and H-Aib-Ser(ibuprofen)-OH (**183**) (Dr R. Pathak, unpublished) had previously been carried out by our group. Previously obtained oocyte data for these compounds are included in Table 11 for comparison purposes. Apparent permeability data for the ibuprofen attached carriers was attempted to be generated during the course of the project. Unfortunately data was not obtained from the Caco-2 studies, although the cycloleucine ibuprofen prodrug was found to fragment during stability testing, suggesting that this carrier is not hydrolysis resistant.

**Table 11 Binding affinity and *trans*-stimulation efflux for dipeptides.**

							
X= H	Oocytes $K_i$ <i>trans</i> -stimulation Compound No.	- - -	- - -	$0.79 \pm 0.41$ mM 117% <b>153</b>	$0.69 \pm 0.22$ mM 68% <b>154</b>	$0.66 \pm 0.26$ mM 68% <b>155</b>	$0.17 \pm 0.05$ mM 151% <b>156</b>
X= Bn	Oocytes $K_i$ <i>trans</i> -stimulation Compound No.	$0.25 \pm 0.05$ mM* 112% * <b>182</b>	$0.13 \pm 0.03$ mM* 0% * <b>151</b>	$0.25 \pm 0.12$ mM 166% <b>166</b>	$0.42 \pm 0.14$ mM 98% <b>172</b>	$0.26 \pm 0.08$ mM 117% <b>163</b>	$0.25 \pm 0.12$ mM 120% <b>178</b>
X= ibuprofen	Oocytes $K_i$ <i>trans</i> -stimulation Compound No.	$0.26 \pm 0.03$ mM 109% * <b>79</b>	$0.22 \pm 0.04$ mM* 82% * <b>183</b>	$0.23 \pm 0.05$ mM 55% <b>169</b>	$0.09 \pm 0.17$ mM 26% <b>175</b>	$0.16 \pm 0.06$ mM 173% <b>162</b>	$0.02 \pm 0.003$ mM 0% <b>181</b>

\* Previously generated data.

All dipeptides were shown to have excellent binding affinity for PepT1, this suggests that adding bulk to the *N*-terminal  $\alpha$ -carbon does not affect the ability of the compounds to bind to PepT1. For each dipeptide there a slight general trend of the binding affinity increasing as the size of the ligand attached to the serine alcohol increases H<Bn<ibuprofen. This can be explained by the fact the benzyl moiety and ibuprofen are hydrophobic and PepT1 has been shown to have a hydrophobic pocket with a strong directional vector in this region (section 1.3.8).

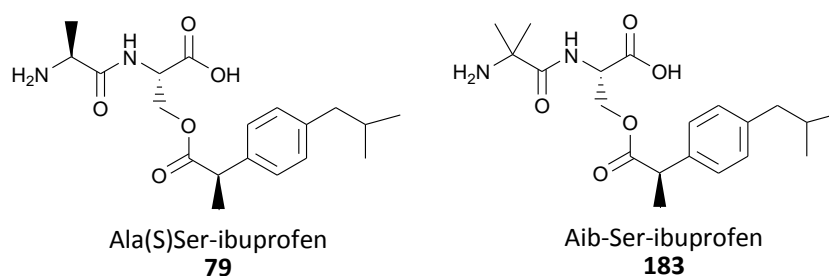
*Trans*-stimulation assays previously carried out by Dr D. Meredith on H-Aib(S)Ser(Bn)-OH (**150**), as part of Dr R. Pathak's research, failed to show efflux. Although false negatives should not occur in *trans*-stimulation assays transport has since been demonstrated in Caco-2 cells. This result is perhaps a result of abnormal oocytes. All dipeptides except cyclobutane-serine-ibuprofen (**175**) simulated moderate to excellent efflux in *trans*-stimulation assays. This is perhaps an anomalous result as both the free carrier and benzyl linked carrier stimulated efflux. Higher binding affinities were seen for the homocycloleucine carrier than the other carriers when as a free carrier or with drug moieties attached. This is surprising as the homocycloleucine carrier has the most *N*-terminal  $\alpha$ -carbon bulk and was expected to give the lowest binding affinity as a result. The lack of *trans*-stimulation and the high binding affinity seen for homocycloleucine-serine-ibuprofen (**181**) suggests that this may be an inhibitor for PepT1. Although the excellent *trans*-stimulation efflux seen for both the free homocycloleucine carrier and benzyl linker carrier indicates that these are in fact transported. This could be established though Caco-2 testing.

It is unfortunate that Caco-2 data could not be obtained for these molecules. It has been established that these molecules are recognised by PepT1, but not if they are able to be transported. Although apparent permeability data was not generated subsequent to Caco-2 testing, stability testing indicated that cycloleucine-serine-ibuprofen (**162**) was able to be hydrolysed. The ibuprofen-linked cyclopropane (**169**), cyclobutane (**175**) and homocycloleucine (**181**) carriers all seemed to be hydrolysis resistant. Further Caco-2 assays need to be performed on these molecules to assess the apparent permeability of the carriers. If found to be transported

well by PepT1, these carriers represent an attractive alternative to the thiodipeptide carriers currently used by the group.

### 3.3 *In vivo* biological testing.

Both the Ala(S)Ser (**79**) and Aib-Ser (**183**) ibuprofen prodrugs had previously been shown in the group to be substrates of PepT1. They were therefore selected for both an *in vivo* pharmacokinetic study and a taste tolerance study, performed in rat, by Saretuis Ltd. The object of the study was to assess whether the addition of the carriers significantly differed the pharmacokinetic profile for the prodrugs, when compared to ibuprofen. We were also interested in whether the presence of sulfur in prodrug **79** negatively affected its taste. Prodrug **79** was synthesised by myself for this study and prodrug **183** was synthesised by Dr. R. Pathak.



#### 3.3.1 Pharmacokinetic study

For the study Ala(S)Ser-ibuprofen (**79**) and Aib-Ser-ibuprofen (**183**) were prepared at 10 mg/Kg and ibuprofen was prepared at 6 mg/Kg in distilled water. This was administered orally to male CD rats (n=3). All compounds were well tolerated and no adverse events were reported. Plasma samples were collected 0.25, 0.5, 1, 2, 4, 8 and 24 h after dosing. An equal volume of heparinised saline was infused back into the rat to replace the blood volume taken from the animal, thus ensuring patency.

**Table 12 Summary of the mean calculated pharmacokinetic parameters. Each prodrug administered was detected both as the prodrug and parent ibuprofen.**

Parameter	Units	Ibuprofen (77)	Ala(S)Ser-ibuprofen (79)		Aib-Ser-ibuprofen (183)	
			prodrug	Ibuprofen	prodrug	Ibuprofen
T <sub>1/2</sub>	h	2.87	1.67	3.17	2.19	3.27
T <sub>max</sub>	h	0.66	1	1	0.66	1.83
C <sub>max</sub>	ng/mL	5664.13	199.7	207.20	31.40	3140.00
T <sub>last</sub>	h	8	3.33	8	3.33	16
C <sub>last</sub>	ng/mL	418.267	79.60	31.70	19.033	428.27
AUC <sub>last</sub>	h*ng/mL	14045.14	488.53	652.46	70.64	10363.16
AUC <sub>INF_obs</sub>	h*ng/mL	16111.45	790.34	799.62	125.64	12290.69

Ibuprofen (**77**) was found to be detectable in the plasma up to 8 hours after administration, with exposure levels consistent across all three rats. The mean peak serum concentration (C<sub>max</sub>) was determined as 5664.13 ± 0.64 µg/mL. The elimination of ibuprofen (**77**) was very similar for two of the rats, but an anomalous reading at the 8 hour time point in rat 1 generated a poorer fit. This suggests that the half life of Ibuprofen (**77**) is closer to 2 hours rather than 2.8 hours as generated by the mean.

Ala(S)Ser-ibuprofen (**79**) was detectable in plasma as the prodrug 3.3 hours after exposure and as the parent drug, ibuprofen (**77**), up to 8 hours after administration. Levels of compound exposure across the n=3 were consistent, a mean C<sub>max</sub> of 199.7 ± 35.9 ng mL for Ala(S)Ser-ibuprofen (**79**) was detected 1 hour after dosing. A mean C<sub>max</sub> of 207.20 ± 17.1 ng mL was detected for ibuprofen (**77**) 1 hour after dosing. As exposure levels were found to be low for one of the rats elimination curves were fitted for the data on an n=2 basis. Data from the n=2 to indicated a mean T<sub>1/2</sub> of approximately 1.67 hours for Ala(S)Ser-ibuprofen (**79**) and 3.17 hours for ibuprofen (**77**).

Aib-Ser-ibuprofen (**183**) was detectable in plasma as the prodrug or parent ibuprofen (**77**) up to 16 hours after administration. The levels of detection for Aib(S)Ser-ibuprofen (**183**) across the three treated rats were reasonably consistent although levels were very low.  $C_{max}$  occurred 0.66 hours after dosing and was determined as  $31.40 \pm 5.1$  ng/mL. Ibuprofen (**77**) was detected up to 16 hours after administration with  $C_{max}$  determined as  $1340 \pm 260.5$  ng/mL. Elimination curves could only be fitted to two of the three rats and the mean  $T_{1/2}$  was found to be 2.19 hours for Aib(S)Ser-ibuprofen (**183**) and 3.27 hours for ibuprofen (**77**).

Combining the prodrug and parent drug  $C_{max}$  for Ala(S)Ser-ibuprofen (**79**) results in a  $C_{max}$  of 406.9  $\mu$ g/mL which is only 0.07% of the  $C_{max}$  observed when ibuprofen (**77**) was administered (5664.13  $\mu$ g/mL). The parent drug, ibuprofen (**77**), was seen for up to 8 hours after administration, but  $C_{last}$  was very low indicating that this prodrug was not well absorbed. In contrast, if you combine the prodrug and parent drug  $C_{max}$  for Aib-Ser-ibuprofen (**183**) the  $C_{max}$  observed is 3171.4  $\mu$ g/mL. This is 56% of the  $C_{max}$  observed when ibuprofen (**77**) was administered (564.136  $\mu$ g/mL). However, the majority of the combined  $C_{max}$  observed for Aib-Ser-ibuprofen (**183**) comes from detected ibuprofen (**77**). This indicates that cleavage of the prodrug occurred prior to intestinal permeation or soon after the prodrug was in systemic circulation. The  $T_{max}$  was 3 times longer for Aib-Ser-ibuprofen (**183**) than when ibuprofen (**77**) was administered and elimination was twice as long. This indicates that Aib-Ser-ibuprofen (**183**) promotes a longer exposure duration than ibuprofen (**77**) and it is better absorbed than Ala(S)Ser-ibuprofen (**79**). This suggests that Aib-Ser-ibuprofen (**183**) may have therapeutic potential as an ibuprofen prodrug.

A 24 hour pharmacokinetic study for Ala(S)Ser-ibuprofen (**79**) had previously been performed in the group using a single male CD rat.<sup>117</sup> A 10 mg/kg dose of Ala(S)Ser-ibuprofen (**79**) resulted in a detected prodrug  $C_{max}$  of  $930 \pm 90$  ng/mL with a  $T_{max}$  of 1.33 hours. This  $C_{max}$  is much higher (4.6 times) than the result obtained here, although the  $T_{max}$  is roughly the same. This may be due to an anomalous rat as  $n=1$  rather than  $n=3$  was used the study. The study was also limited

as only the appearance of Ala(S)Ser-ibuprofen (**79**) in plasma was studied, rather than Ala(S)Ser-ibuprofen (**79**) and ibuprofen (**77**). This makes it hard to assess overall the transport and clearance of ibuprofen (**77**), both as the prodrug and parent drug.

### 3.3.2 Taste assessment.

To assess whether the presence of sulfur in the Ala(S)Ser carrier (**56**) negatively affected the taste of the resultant prodrug a taste assessment in rats was performed. In addition to Ala(S)Ser-ibuprofen (**79**), Aib-Ser-ibuprofen (**183**) was also assessed as it is not a sulfur containing prodrug, and ibuprofen (**77**). Rats were initially habituated in cages, for two days, with a choice of two identical water bottles, one containing ibuprofen (**77**) solution and one containing water. After this time the bottle which had contained water was replaced with either Ala(S)Ser-ibuprofen (**79**) solution or Aib-Ser-ibuprofen (**183**) solution. This meant that the rats now had a choice between a bottle containing an ibuprofen prodrug solution and a bottle containing an ibuprofen solution. This part of the experiment was carried out for three days and the water bottles were randomly switched each day to prevent preference.

When Ala(S)Ser-ibuprofen (**79**) solution was used as the prodrug solution there was a marked preference for the ibuprofen (**77**) solution. There was also a slight increase in the volume of ibuprofen (**77**) solution consumed during the three day test period than the volume of consumed during the 2 day acclimatisation period. When the Aib-Ser-ibuprofen (**183**) solution was used as the prodrug solution again more slightly more ibuprofen (**77**) was consumed over the three day test period than had been consumed in the 2 day acclimatisation period. There was also marked preference for the bottle containing ibuprofen (**77**) solution than the bottle containing Aib-Ser-ibuprofen (**79**) solution during the three day test period. When the volumes of the two prodrug test solutions consumed over the test period are compared, very little difference is seen. This indicates that the rats had no preference between these two prodrugs and therefore the presence of the sulfur atom in the carrier attached to the parent

drug does not make the taste significantly more unpalatable. However, the taste of both prodrug solutions is more unpalatable than ibuprofen solution.



# **Chapter 4**

## **Utilising the PepT1**

### **transporter for targeted drug delivery**

## Chapter Four Contents

4.1	PepT1 in cancer .....	99
4.2	Ala(S)Ser-ibuprofen .....	100
4.2.1	<i>In vitro</i> testing .....	101
4.2.2	Conclusions .....	105
4.3	Gemcitabine prodrugs .....	106
4.3.1	Gemcitabine prodrug synthesis. ....	110
4.3.2	<i>In vitro</i> testing .....	113
4.3.3	Conclusions .....	118

#### 4.1 PepT1 in cancer

The treatment of many cancers requires a chronic schedule. However, the oral bioavailability of many oncology drugs is both poor and highly variable. As well as being poorly absorbed, many anticancer drugs are substrate to efflux pumps such as P-gp which are designed to remove toxic substances from cells. This makes oral formulation difficult, although transmembrane targeting has been used as a tool to overcome this (Chapter 2).

Recently PepT1 has been shown to be over-expressed in several epithelial-derived cancer cell lines, where oligopeptide uptake is presumably necessary for rapid cell growth. These are; the malignant ductal pancreatic cancer cell lines AsPc-1 and Capan-2, human extrahepatic cholangiocarcinoma cell line SK-ChA-1,<sup>153</sup> human gastric cancer cell line MKN45<sup>154</sup> and human renal adenocarcinoma cell line VMRC-RCW.<sup>155</sup> This raises the possibility of using targeted PepT1 drug delivery as a tool in cancer therapy, potentially reducing side effects as off target delivery would be minimised. Once inside the cell the PepT1 recognised component of the prodrug would be cleaved from the oncology drug giving the active drug. The validity of this approach has been demonstrated in the constructed cell line HeLa-hPepT1. Bestatin, an oncology drug known to be transported by PepT1, was shown to inhibit HeLa-hPepT1 *in vitro*. *In vivo*, HeLa-hPepT1 tumours grown in mice were found to be suppressed and bestatin accumulated, following oral administration.<sup>155</sup>

Pancreatic cancer is particularly difficult to detect as symptoms often do not present until the cancer is relatively advanced. Although it is the 9<sup>th</sup> most common cancer in the UK, prognosis is poor with a 4% survival rate after 5 years.<sup>157</sup> Ductal pancreatic adenocarcinoma in particular can be resistant to chemotherapy due to the complex microenvironment that surrounds the pancreas.<sup>158</sup> The discovery that PepT1 is over-expressed in pancreatic cancer cell lines therefore enables research into the targeted delivery of cytotoxic drugs.

## 4.2 Ala(S)Ser-ibuprofen

The link between tumour growth and inflammation was first made in the 19<sup>th</sup> century and is now accepted as an underlying factor in the development of many cancers. Up to 20% of cancers are directly associated with microbial infection, with the causality of many others related to chronic infection, obesity, dietary factors and inhaled pollutants.<sup>159</sup> It has been shown that as a tumour develops it expresses phenotypes similar to inflammatory cells.<sup>160</sup> Inflammation has also been shown to play a role in both tumourgenesis and aggression of the resultant malignancy.<sup>161</sup> In fact the risk of developing prostate, colorectal and pancreatic cancers has been shown to increase in patients who have suffered chronic infection in those areas.<sup>161</sup> There are several excellent reviews into the research undertaken into understanding the inflammatory feedback mechanisms which can promote tumourgenesis.<sup>162-3</sup> This research has improved understanding into the molecular causation of cancer and opened up a new avenue of research into the use of anti-inflammatory drugs in the treatment of cancer.

Several studies have also shown the prophylactic benefit of taking nonsteroidal anti-inflammatory drugs (NSAID) for several cancers including, breast, colorectal, lung and ovarian cancers.<sup>161</sup> This was first demonstrated in patients with Gardner's syndrome, which causes intestinal polyps. When the patients were treated with the nonsteroidal anti-inflammatory drug sulindac, a reduction was seen in adenoma formation.<sup>164</sup> NSAID's are commonly used for the long term management of chronic pain conditions like arthritis and the preventive treatment of cardiovascular disease, allowing comparisons in the long term use and cancer incidents. Although this demonstrates the potential of NSAID's on a prophylactic basis, in most cases the side effects of long-time usage would outweigh any benefit in the reduction of incidence to the general population.

The use of anti-inflammatory drugs to treat established cancers, may however be an option. *In vitro*, proliferation in colorectal cell lines,<sup>165</sup> ovarian carcinoma cell lines<sup>166</sup> and lung cancer cell lines<sup>167</sup> has been demonstrated to reduce upon the treatment with a variety of NSAID's. *In vivo*, indomethacin has been shown to reduce the growth of both new and established spontaneous mammary tumors.<sup>168</sup> Diclofenac was shown to decrease pancreatic tumour growth.<sup>169</sup> Ibuprofen (**77**) and aspirin (**80**) have also been shown to reduce growth of colon cancer cells.<sup>169</sup> This shows the targeted use of nonsteroidal anti-inflammatory drugs may be of benefit as part of cancer therapy as toxicity would be minimised.

#### 4.2.1 *In vitro* testing

A collaboration with Prof. Randy Mersny at the University of Bath enabled a study into the use of PepT1 as a vehicle to deliver anti-inflammatory drugs into cancer cells. As anti-inflammatory drugs are only able to access the surface of cells efficacy is limited. By using PepT1 to deliver a NSAID into the cancerous cells it was hoped efficacy would be improved as the drug would be accumulated. Ibuprofen (**77**) was selected as the NSAID to be studied as its ability to reduce cell proliferation had been demonstrated<sup>170</sup> and the thiodipeptide prodrug had already been synthesised (section 2.5.2). The study was carried out by PhD student Ana Santos Cravo using the human pancreas adenocarcinoma cell line AsPC1, which has been shown to express PepT1. The studies were designed as a result of discussions between myself and Ana and any conclusions drawn from the studies are my own.

An AsPc1 PepT1 knockdown cell line was prepared by Ana for use as a control. Some cytosolic and nuclear expression of PepT1 was seen in the knock down cell line *via* immunoblot analysis (Figure 26). However, as this study is only concerned with PepT1 expressed at the cell surface this is not relevant.

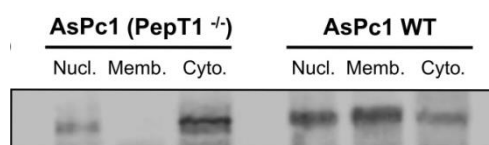


**Figure 26** Immunoblot assay showing absence of PepT1 at the cell surface of AsPc1 PepT1 <sup>-/-</sup> cells

To assess whether Ala(S)Ser-ibuprofen (**79**) would have an effect in reducing cell proliferation *via* PepT1 uptake, different concentrations of the prodrug was incubated with cells for 24 hours. Figure 27 shows that the AsPc1 cells expressing PepT1 displayed a statistically significant reduction in cell proliferation compared to AsPc1 knockdown cells. To confirm that the reduced proliferation seen was due to uptake of Ala(S)Ser-ibuprofen (**79**) *via* PepT1, rather than another mechanism, a competitive inhibition study was carried out (Figure 28). Different concentrations of Ala(S)Ser-ibuprofen (**79**) were incubated with AsPc1 PepT1 expressing cells in RPMI medium and a huge excess of Gly-Sar (50mM) for 24 hours. As Gly-Sar is a PepT1 substrate, this effectively blocks Ala(S)Ser-ibuprofen uptake into cells *via* the PepT1 transporter. Figure 28 shows that increased cell proliferation is seen in AsPc1 cells which have been supplemented with Gly-Sar, when compared to cells which have just been exposed to Ala(S)Ser-ibuprofen (**79**). This suggests PepT1 is involved in the uptake of Ala(S)Ser-ibuprofen (**79**) in AsPC1 cells.

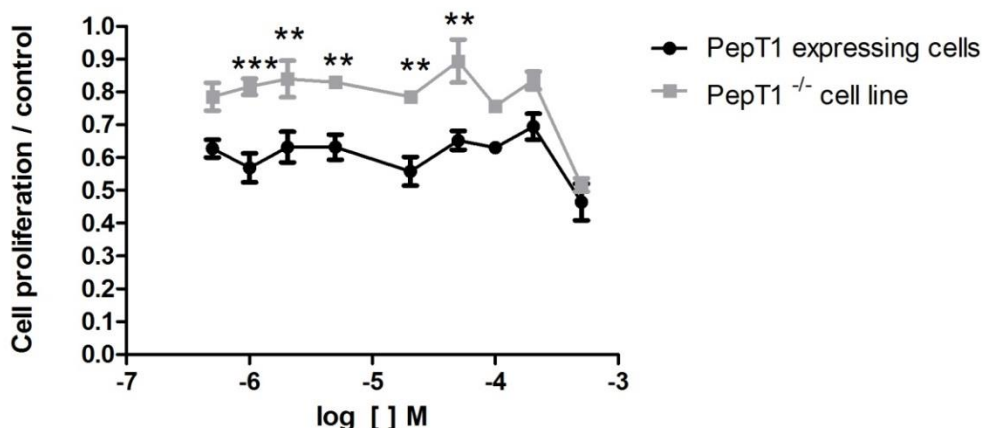


**Figure 27** Rate of proliferation in cells exposed to Ala(S)Ser-ibuprofen (**79**). Values are expressed as mean  $\pm$  SEM from 3 independent experiments; \*\*p < 0.01; \*\*\*p < 0.001.

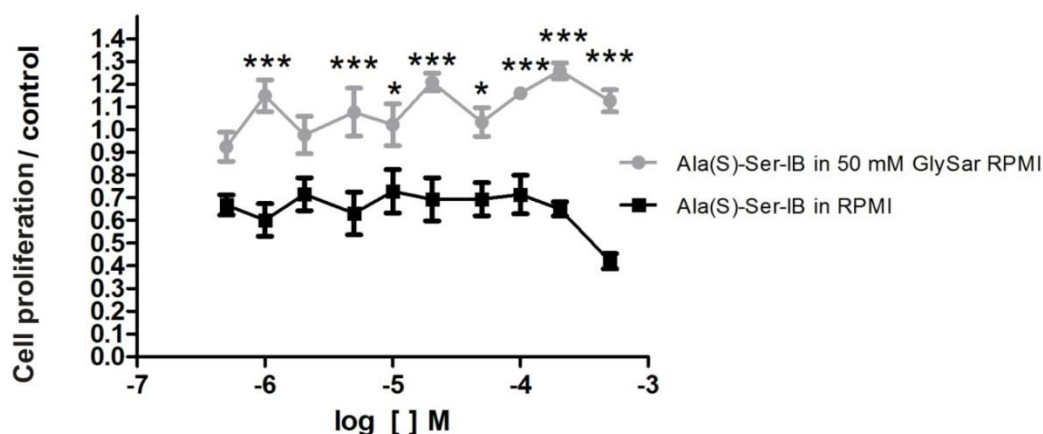


**Figure 28 Ala(S)Ser-ibuprofen (79) Competitive inhibition study. Values are expressed as mean  $\pm$  SEM from 3 independent experiments; \*\* $p < 0.01$ ; \*\*\* $p < 0.001$ .**

To assess whether Ala(S)Ser-ibuprofen (**79**) had an effect on cell viability as well as proliferation, a MTT assay was carried out. NAD(P)H-dependent cellular oxidoreductase enzymes in the cytosol of cells are able to reduce a colourless tetrazolium dye to a coloured formazan dye. Rapidly dividing cells display high cellular metabolism and therefore tetrazolium reduction is increased, resulting in a stronger colour. Cell viability can therefore be assessed as measure of colour. Different concentrations of Ala(S)Ser-ibuprofen (**79**) were incubated with cells for 24 hours. Figure 29 shows that the cell viability of AsPc1 cells was significantly decreased when compared to AsPc1 knockdown cells. This suggests that Ala(S)Ser-ibuprofen (**79**), once transported into cells, has an effect on cell viability either as the prodrug or the parent drug ibuprofen.

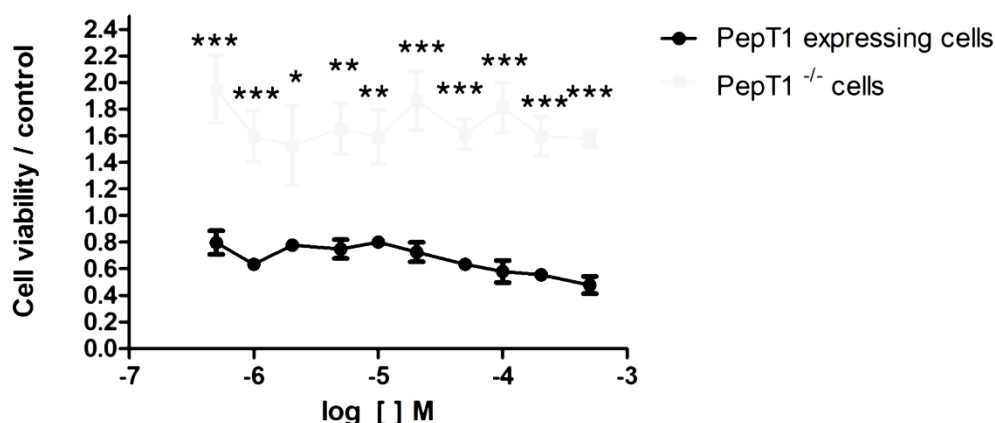


**Figure 29 MTT cell viability assay. Values are expressed as mean  $\pm$  SEM from 3 independent experiments; \*\*p< 0.01; \*\*\*p< 0.001.**

To my knowledge the reduced cell proliferation by an ibuprofen prodrug or ibuprofen in AsPc1 cells has not been previously reported, but is in line with the effect that has been described in other cancerous cell lines using alternative nonsteroidal anti-inflammatory drugs.<sup>165-70</sup> Cyclooxygenase-2 (COX-2) is one of the accepted pharmacological targets of ibuprofen and has been shown to be unregulated in several cancers, including pancreatic ductal adenocarcinomas. This is as a stress response induced by inflammatory cytokines, growth factors and oncogenes.<sup>171</sup> Disregulation of COX-2 results in increased biosynthesis of prostaglandin E<sub>2</sub> (PGE<sub>2</sub>) which has been shown to promote proliferation, angiogenesis, migration and inhibit apoptosis.<sup>164</sup> Therefore, one of the ways that ibuprofen may reduce proliferation is by inhibiting the COX-2/PGE<sub>2</sub> pathway.

To assess whether COX-2 levels in both AsPc1 and AsPc1 PepT1 knockdown cells were differentially affected by Ala(S)Ser-ibuprofen (**79**) than ibuprofen (**77**), an immunoblot assay was carried out subsequent to exposure for 24 hours. Figure 30 shows that COX-2 levels were significantly reduced in both cell lines after exposure to either ibuprofen (**77**) or the ibuprofen prodrug (**79**). However, COX-2 expression is eliminated in the ASPC1 cells expressing PepT1 that were exposed to Ala(S)Ser-ibuprofen (**79**). This may be explained by the accumulation of ibuprofen within the cells, which may have a bigger effect on disrupting the COX-2/PGE<sub>2</sub> pathway. In ASPC1 PepT1 knockdown cells incubated with Ala(S)Ser-ibuprofen (**79**), reduction in COX-2



expression was seen. This may be due to the ibuprofen prodrug (**79**) still being able to have a partial action in the prodrug form, alternatively some prodrug degradation could have occurred to give the free ibuprofen (**77**).

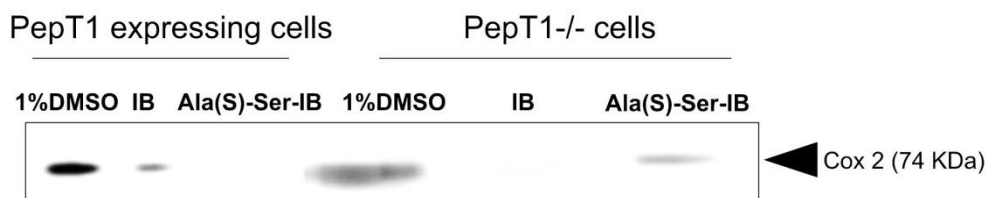


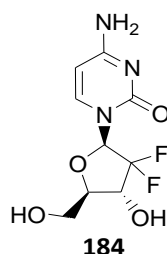
**Figure 30 Immunoblot assay showing COX-2 levels after AsPc1 and AsPc1 PepT1 -/- cells were exposed to Ala(S)Ser-ibuprofen (**79**).**

#### 4.2.2 Conclusions

Ala(S)Ser-ibuprofen (**79**) was shown to have a more pronounced effect on cell proliferation and vitality in AsPc1 cells expressing PepT1 compared to AsPc1 knockdown cells and affects COX-2 expression levels. The inhibitory affect of ibuprofen on cancerous cells which highly express COX-2 was recently demonstrated by Lichtenberger in colon cancer cells,<sup>170</sup> reflecting our results. Cell proliferation increased when uptake of Ala(S)Ser-ibuprofen (**79**) was blocked by Gly-Sar. This confirms that PepT1 involvement in the decreased proliferation and vitality in PepT1 expressing AsPc1 cells. The use of NSAID's in a prophylactic manor and as part of cancer therapy remains controversial due to the side effects reported from long-term use.<sup>161</sup> These side effects can be potentially mitigated through the use of active targeting. However, there is some indication that Ala(S)Ser-ibuprofen (**79**) may have some action in its prodrug form and this needs to be investigated further. Despite this, the reduction in proliferation and vitality of cells seen in this study justify the investigation Ala(S)Ser-ibuprofen (**79**) for efficacy in an *in vivo* oncology model.

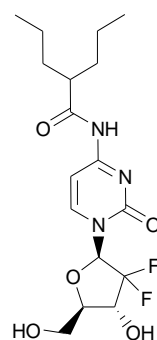
### 4.3 Gemcitabine prodrugs

As part of the collaboration with Prof. Mrsny the thiodipeptide prodrugs of gemcitabine (**184**) was also synthesised and assessed for efficacy in AsPc1 cells.



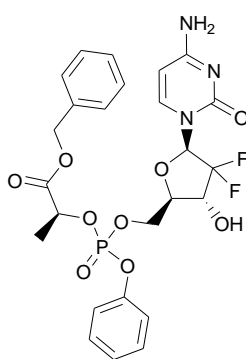
Gemcitabine (**184**) is a deoxycytidine analogue which has been licensed for the treatment of bladder cancer, breast cancer, non-small lung cancer and pancreatic cancer.<sup>172</sup> Gemcitabine (**184**) works by replacing one of the cytosine building blocks in DNA replication. As new nucleosides in the chain cannot be attached to gemcitabine (**184**) apoptosis is induced. As with other nucleoside analogues, gemcitabine suffers from low oral bioavailability. This is primarily due to extensive first pass metabolism of gemcitabine (**184**) by cytidine deaminase (CDA) to inactive 2,2-difluorodeoxyuridine.<sup>172</sup> As a result gemcitabine (**184**) is administered intravenously. There has been extensive research into oral formulations of gemcitabine (**184**), which would provide a more convenient dosing regimen. Currently gemcitabine (**184**) is injected over 30 minutes by a hospital professional.<sup>173</sup> It is however often used in combination with other orally formulated chemotherapy drugs such as capecitabine, making a combination oral formulation desirable.

There have been several strategies to improve the oral bioavailability of gemcitabine (**184**) both through increased lipophilicity and PepT1 targeting. The most clinically advanced gemcitabine prodrug is LY2334737 (**185**) developed by Eli Lilly and company, which is set to start phase II trials. The 4-amide linked valprolate prodrug blocks deamination of CDA thereby improving bioavailability and is hydrolysed slowly by carboxylesterase 2 leading to the sustained release of gemcitabine *in vivo*.<sup>174</sup>

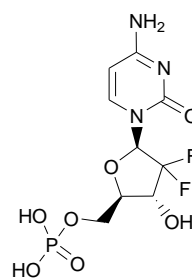


LY2334737  
**185**

Also in clinical trials is NUC-1031 (**186**), developed by the Cardiff School of Pharmacy.<sup>175</sup> This has been based on the premise that gemcitabine (**184**) must be activated by deoxycytidine kinase (dCK) to 5'-*O*-monophosphate-gemcitabine (**187**).<sup>175</sup> Down-regulation of this enzyme would therefore limit gemcitabine efficacy. To overcome this, a ProTide approach has been developed whereby a 5'-*O*-monophosphate group is protected by a biolabile group. NUC-1031 (**186**) has been shown to have a greater efficacy both *in vitro* and *in vivo* than gemcitabine (**184**), with an improved safety profile.<sup>175</sup>



NUC-1031  
**186**



5'-*O*-monophosphate-gemcitabine  
**187**

The oral bioavailability of several nucleoside drugs has been improved through PepT1 targeting. The most common method being the addition of a valine residue to create the amino acid ester prodrug (section 2.1.1). It is therefore unsurprising that this is a strategy that has been applied to gemcitabine (**184**), primarily by the Amidon research group. The most recent research

from this lab utilising this approach involves with the *in vitro* and *in vivo* testing of *L*- and *D*-valine (**188**, **189**) and *L*- and *D*-phenylalanine (**190**, **191**) 5'- mono acid ester prodrugs of gemcitabine (**184**) for transport *via* PepT1.<sup>176</sup>

**Table 13** Caco-2 and AsPc1 data for 5'-amino acid ester prodrugs of gemcitabine (**185**).<sup>176</sup>

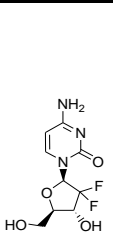
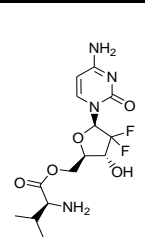
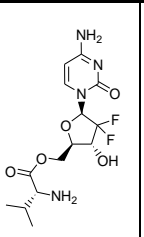
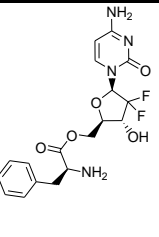
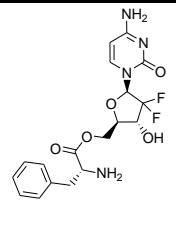
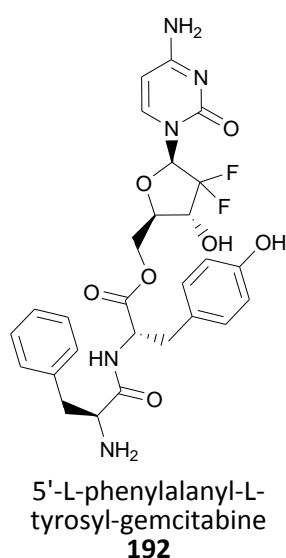
		 <b>184</b>	 5'- <i>L</i> -valyl <b>188</b>	 5'- <i>D</i> -valyl <b>189</b>	 5'- <i>L</i> -phenylalanyl <b>190</b>	 5'- <i>D</i> -phenylalanyl <b>191</b>
<b>Caco-2</b>	$P_{app}$ ( $\times 10^{-6}$ cm S <sup>-1</sup> )	1.0 ± 0.2	3.8 ± 0.9	4.5 ± 0.9	4.0 ± 0.1	3.9 ± 0.1
	approximate uptake (μM/ug of protein)	10	140	112	170	75
	Prodrug	-	82	69	85	90
	Gemcitabine	50	18	31	15	10
	Cytosine	50	0	0	0	0
<b>AsPc1</b>	approximate uptake (μM/ug of protein)	1	2.8	5.2	1.4	4.4
	Prodrug	-	6	12	69	19
	Gemcitabine	90	84	87	11	77
	Cytosine	10	10	1	20	4

Table 13 shows that, as expected, the 5'-*L*-amino acid ester prodrugs (**188**, **190**) displayed greater uptake in Caco-2 cells. This was also seen for mouse single-pass perfusion (not shown). Interestingly, overall uptake for AsPc1 was reduced (<6%). This could be attributed to a significantly higher amount and/or type of metabolising enzymes present in ASPC1 cells compared to Caco-2 cells. Therefore, much more prodrug degradation would occur in ASPC1 cells than in Caco-2 cells, limiting PepT1 transport. Interestingly, uptake of the *D*-amino acid ester prodrugs (**189**, **191**) in AsPc-1 cells was much greater than the *L*-amino acid ester prodrugs (**188**, **190**). This

is contrary to what is usually seen in PepT1. One explanation for this is the higher enzymatic stability of *D*-amino acid ester prodrugs, thereby allowing higher uptake prior to degradation. This does suggest that *D*-enantiomer prodrugs would be favourable for the active targeting of tumours which upregulate PepT1. One limitation of this study is that degradation of gemcitabine (**184**) to 2,2-difluorodeoxyuridine was not assessed. The validity of this prodrug approach to limit first pass metabolism into the inactive metabolite can therefore not be established. It would also be interesting to screen the AsPc1 cell line with known PepT1 substrates to assess whether the same transport profile is seen. This would confirm that the preference for *D*-amino acids seen in this case is due to prodrug degradation and not due to altered substrate specificity.

The Amidon group has also created a dipeptide monoester of gemcitabine.<sup>177</sup> 5'-*L*-phenylalanyl-*L*-tyrosyl-gemcitabine (**192**). This particular dipeptide was chosen as it has been experimentally shown to be hydrolysed by lysosomal cathepsin D,<sup>178</sup> which has been found to be unregulated in tumours. Being a dipeptide, *L*-phenylalanyl-*L*-tyrosyl is also a substrate for PepT1, thereby acting as a 'carrier' for attached drugs. This not only allows transport into cancerous cells, but ensures that prodrug activation can occur to give the free drug.

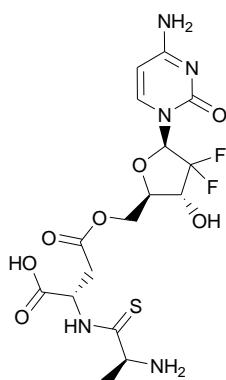


This is a similar approach to that used in our group, where cytosolic esterases release the attached drug. 5'-*L*-phenylalanyl-*L*-tyrosyl-gemcitabine (**192**) was shown to be taken up by Caco-2

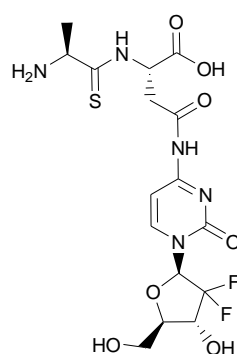
cells, but uptake was not inhibited by Gly-Pro, suggesting that a mechanism of uptake other than PepT1 is responsible. If this prodrug is assessed against a PepT1 substrate template (section 1.3.8) it can be seen that the stereochemistry of the tyrosine residue is not optimum. Although a hydrophobic entity with a strong directional vector at the *C-terminus* is present, which is necessary for transport, it is not in the optimum position and should be in line of the plane (the position occupied by gemcitabine (**184**)). In turn, bulk is best tolerated by PepT1 in the *C-terminus* side chain. Alteration of the *C-terminus* residue to *D*-tyrosine would give the required stereochemistry and may have resulted in PepT1 transport.

#### 4.3.1 Gemcitabine prodrug synthesis.

When creating an oral formulation of gemcitabine (**184**) several factors must be considered; 1) ability of the drug to be absorbed in the gastrointestinal tract, 2) stability of the prodrug to both intestinal epithelial cells and esterases in systemic circulation, 3) prevention of deamination to inactive 2,2-difluorodeoxyuridine, 4) resistance to enzymes at the cancerous cell surface, 5) ability to be transported into cancerous cells. Tackling these factors can be approached in different ways, as shown by different research groups. From a thiodipeptide prodrug perspective, two different gemcitabine prodrugs were synthesised to encompass the strategies utilised by previous groups (**193** and **194**).



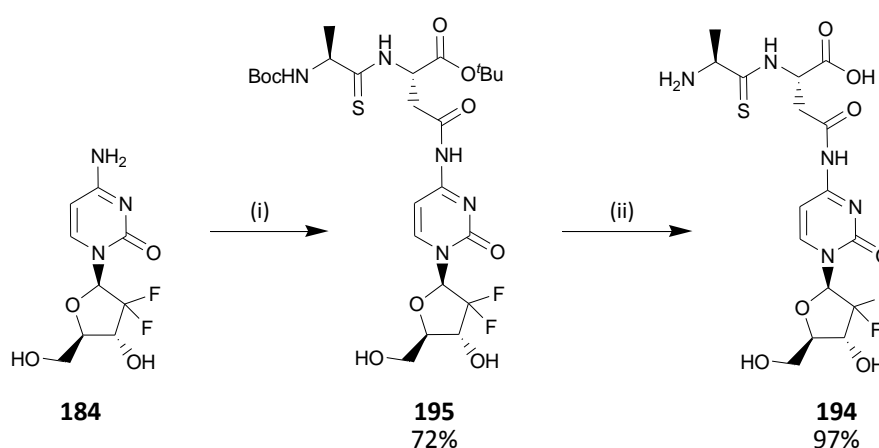
**193**



**194**

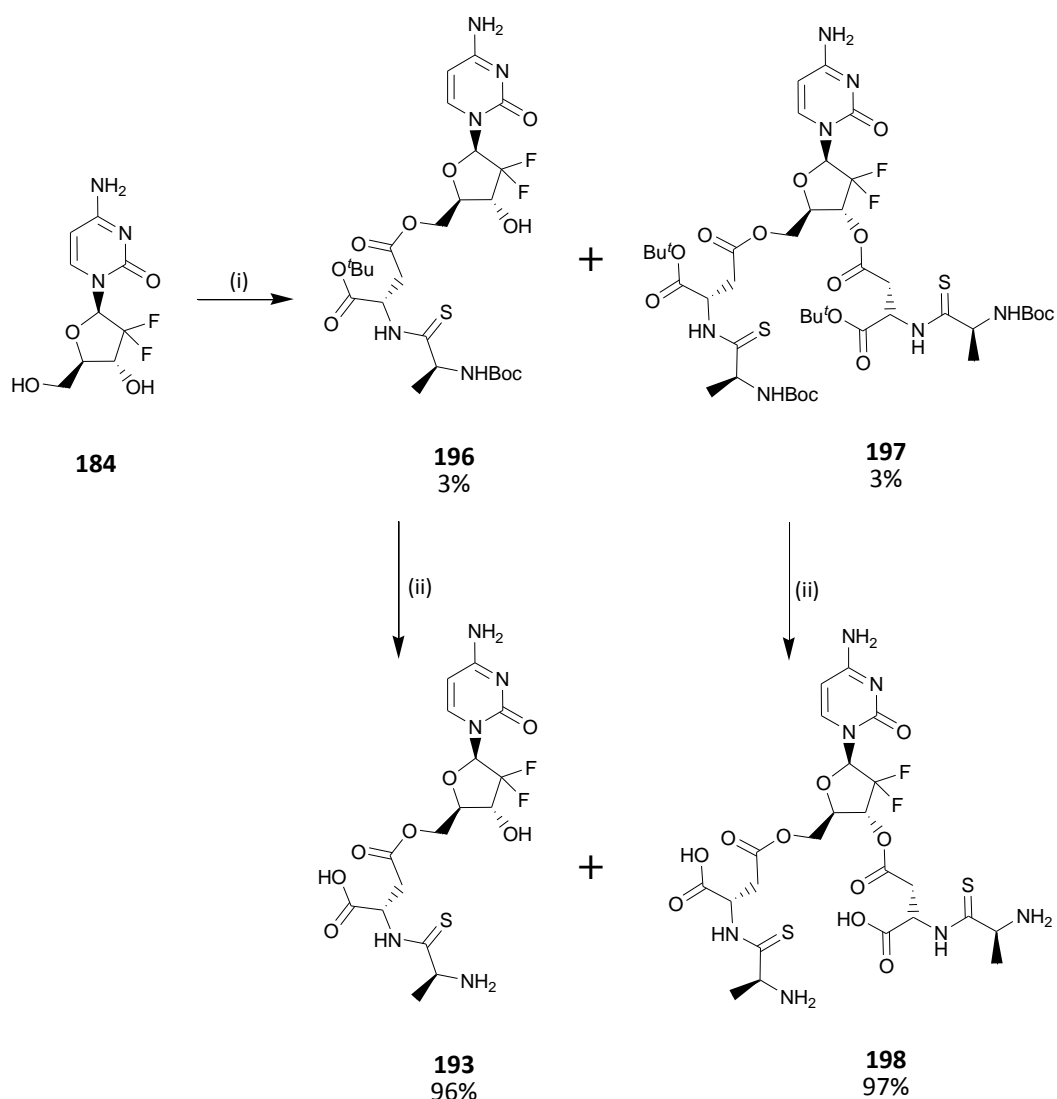
Prodrug **193**, 5'-O-Ala(S)Asp-gemcitabine, is in line with the prodrug strategy historically used by our group. The Ala(S)Asp carrier (**57**) is attached to gemcitabine (**184**) through the primary alcohol *via* an ester linkage. By attaching through the primary alcohol gemcitabine (**184**) is set slightly away from the carrier which has been found historically within our group to improve transport. Prodrug **194**, 4'-N-Ala(S)Asp-gemcitabine, attempts to solve the problem of the deamination of gemcitabine to 2,2-difluorodeoxyuridine. Protection of the amino group of gemcitabine has been shown in LY2334737 (**185**) to block deamination and give a prodrug with sustained release. This reduces the dosage needed for clinical efficacy and therefore reduces potential toxicity.

The synthesis of the 5'-monoester prodrug of gemcitabine (**193**) was initially carried out using the methodology published by the Amidon research group.<sup>176</sup> In their hands the use of Boc protected dipeptide, DCC (1.1eq), DMAP (0.1eq) and gemcitabine (**184**) in DMF gave the 3'-monoester, 5'-monoester and 3'-5'diester of gemcitabine after 24 hours. However, in my hands both the one pot method and pre-charging method gave *tert*-butyl protected 4'-N-Ala(S)Asp-gemcitabine (**195**) as the only product in a 72% yield (scheme 18). *Tert*-butyl deprotection was carried out using neat formic acid to give **194** in a near quantitative yield (97%).



**Scheme 18** Synthesis of 4'-N-Ala(S)Asp-gemcitabine (**194**). (i) (**57**), DCC, DMAP, DMF, 24h (ii) HCO<sub>2</sub>H, reflux, 3h.

Synthesis of the desired ester prodrugs of gemcitabine proved problematic with carbodiimide coupling reagents giving **195** as the only product. The utilisation of HATU and DIPEA in DMF also resulted in the formation of **195** (52%). However, the protected 5'-ester (**196**) and 3'-5'-diester (**197**) prodrugs were also synthesised, both in a 3% yield (scheme 19). Unexpectedly the 3'-monoester was not seen in the reaction mixture. Optimisation of this step was not carried out as enough material had been generated (after deprotection) to satisfy the quantities needed for characterisation and biological testing.



**Scheme 19** Synthesis of 5'-O-Ala(S)Asp-gemcitabine (**193**) and 3'-O-Ala(S)Asp-5'-O-Ala(S)Asp-gemcitabine (**198**). (i) (57), HATU, DIPEA, DMF (ii) HCO<sub>2</sub>H, reflux, 3h.



The efficacy of previously created gemcitabine prodrugs<sup>176</sup> has been potentially affected by degradation at the surface of pancreatic cancer cells, thereby limiting transport. The addition of two carriers to gemcitabine in **198** may prevent PepT1 in the gut from transporting the molecule. However, it should give added resistance to enzymes at the cell surface of tumours as cleavage of one of the carriers would give a prodrug still potentially transportable by PepT1. Biological testing of **198**, was therefore carried out alongside **193** and **194**.

#### 4.3.2 *In vitro* testing

Biological testing of **193**, **194** and **198** in AsPc1 and AsPc1 knockdown cells was one again carried out by Ana Santos Cravo at the University of Bath. Once again these studies were designed as a result of discussions between myself and Ana and any conclusions drawn are my own. The action of gemcitabine is through incorporation into the genome, blocking DNA synthesis. Therefore, the three gemcitabine prodrugs were initially assessed for cell viability response.

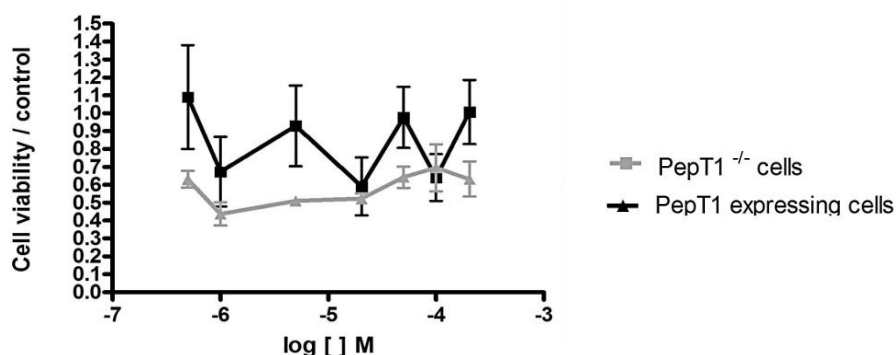


Figure 31 MTT cell viability assay. AsPc1 and AsPc1 knockdown cells were incubated with different concentrations of 4'-N-Ala(S)Asp-gemcitabine (**194**) for 24 hours. Values are expressed as mean  $\pm$  SEM from 3 independent experiments; \*\* $p < 0.05$ ; \*\*\* $p < 0.001$ .

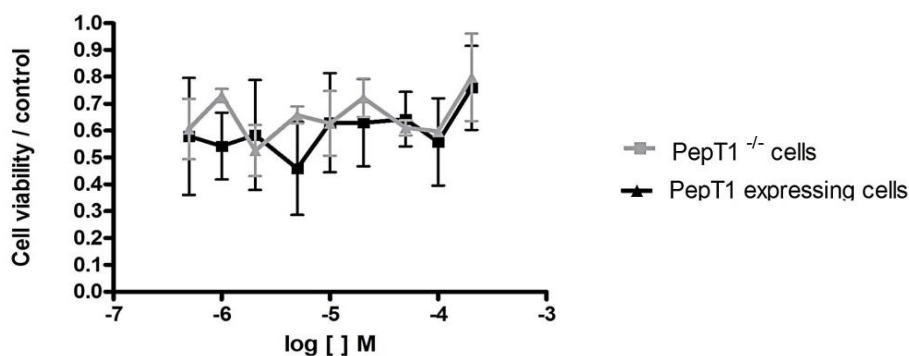


Figure 32 MTT cell viability assay. AsPc1 and AsPc1 knockdown cells were incubated with different concentrations of 5'-O-Ala(S)Asp-gemcitabine (193) for 24 hours. Values are expressed as mean  $\pm$  SEM from 3 independent experiments; \*\*p< 0.05; \*\*\*p< 0.001.

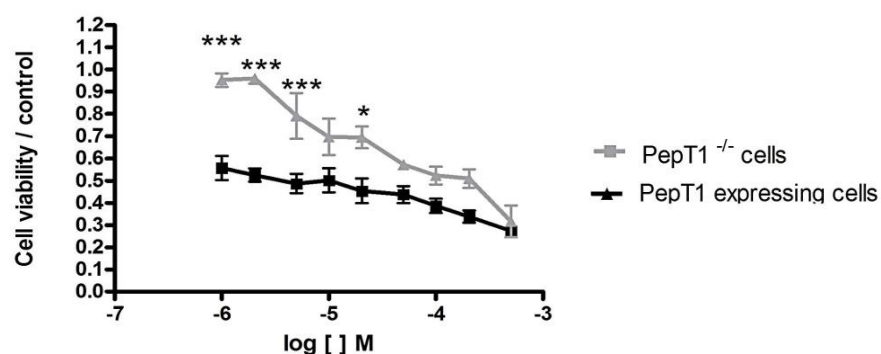
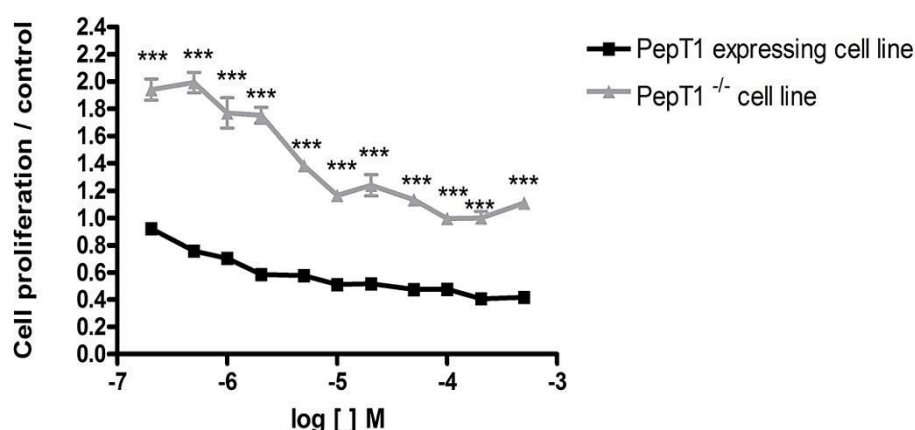


Figure 33 MTT cell viability assay. AsPc1 and AsPc1 knockdown cells were incubated with different concentrations of 3'-O-Ala(S)Asp-5'-O-Ala(S)Asp-gemcitabine (198) for 24 hours. Values are expressed as mean  $\pm$  SEM from 3 independent experiments; \*\*p< 0.05; \*\*\*p<0.05; \*\*\*p< 0.001.

Figure 31 shows a small decrease in cell viability in AsPc1 PepT1 expressing cells when compared AsPc1 knockdown cells. This suggests that PepT1 is transporting 4'-N-Ala(S)Asp-gemcitabine (**194**) in to the cell and some activation of the prodrug is occurring, most likely by carboxylesterases in the cytoplasm. Figure 32 shows no difference between the cell viability of AsPc1 PepT1 expressing cells and AsPc1 knockdown cells. This suggests that 5'-O-Ala(S)Asp-gemcitabine (**193**) is not transported by PepT1, or more likely that degradation of the prodrug is occurring prior to transport as occurred in the 5'-amino acid ester prodrugs of gemcitabine created by the Amidon group.<sup>171</sup> Figure 33 shows that 3'-O-Ala(S)Asp-5'-O-Ala(S)Asp-gemcitabine

(198) was the most effective at decreasing AsPc1 cell viability in both AsPc1 PepT1 expressing cells and AsPc1 knockdown cells. Cell viability is significantly reduced in AsPc1 expressing cells compared knockdown cells, suggesting that PepT1 plays a part in the reduction of cell viability. This is surprising as we theorised that 3'-O-Ala(S)Asp-5'-O-Ala(S)Asp-gemcitabine (198) would be the least likely to be transported, due to the presence of the two carrier motifs.

Cell proliferation in AsPc1 and AsPc1 knockdown cells after exposure to 3'-O-Ala(S)Asp-5'-O-Ala(S)Asp-gemcitabine (198) was then assessed. Figure 34 shows that in AsPc1 PepT1 expressing cells there is a statistically significant reduction in cell proliferation when compared to AsPc1 knockdown cells. This suggests that the selective growth inhibition of AcPc1 expressing cells is due to 3'-O-Ala(S)Asp-5'-O-Ala(S)Asp-gemcitabine (198) transport by PepT1.



**Figure 34** Rate of proliferation in cells exposed to different concentrations of 3'-O-Ala(S)Asp-5'-O-Ala(S)Asp-gemcitabine (198) after 48 hours. Values are expressed as mean  $\pm$  SEM from 3 independent experiments; \*\*\*p< 0.001.

To evaluate the role of PepT1 in the uptake of 3'-O-Ala(S)Asp-5'-O-Ala(S)Asp-gemcitabine (198) a competitive inhibition study was carried out. Different concentrations of 3'-O-Ala(S)Asp-5'-O-Ala(S)Asp-gemcitabine (198) were incubated with AsPc1 PepT1 expressing cells in RPMI medium and a huge excess of Gly-Sar (50 mM) for 48 hours. As can be seen in Figure 35 some increase in cell viability is seen when PepT1 uptake is blocked by Gly-Sar, suggesting that PepT1 is

involved in the uptake of 3'-O-Ala(S)Asp-5'-O-Ala(S)Asp-gemcitabine (**198**). However, a decrease in cell viability is also seen with increasing concentration when PepT1 transport is blocked, suggesting that the uptake of 3'-O-Ala(S)Asp-5'-O-Ala(S)Asp-gemcitabine (**198**) also occurs *via* an alternative mechanism.

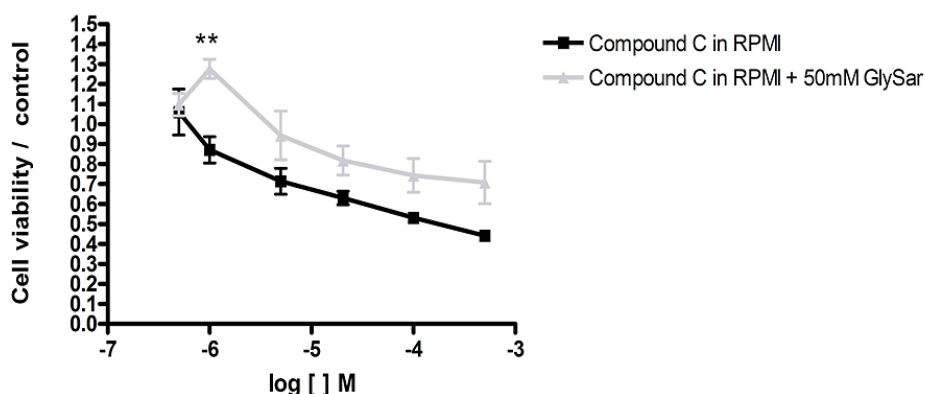


**Figure 35** Competitive inhibition study of 3'-O-Ala(S)Asp-5'-O-Ala(S)Asp-gemcitabine (**198**).

Values are expressed as mean  $\pm$  SEM from 3 independent experiments; \*\* $p < 0.01$ .

The cytotoxic potential of 3'-O-Ala(S)Asp-5'-O-Ala(S)Asp-gemcitabine (**198**) was compared to its parent drug gemcitabine. Figure 36 shows that 3'-O-Ala(S)Asp-5'-O-Ala(S)Asp-gemcitabine (**198**) displayed significantly lower cell vitality than its parent compound gemcitabine (**184**).

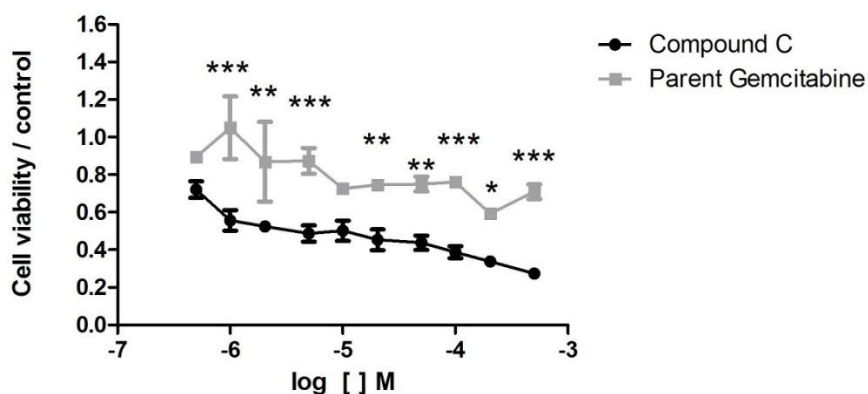
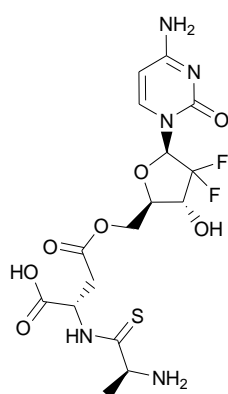
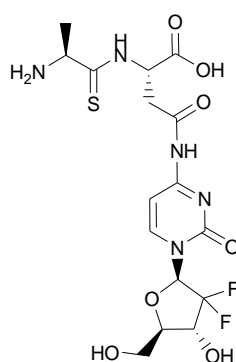


**Figure 36** MTT cell viability assay. AsPc1 cells were incubated with different concentrations of 3'-O-Ala(S)Asp-5'-O-Ala(S)Asp-gemcitabine (**198**) or gemcitabine (**184**) for 48h. Data presented as mean of 3 independent experiments  $\pm$  SEM; \* $p < 0.05$ ; \*\*  $p < 0.01$ ; \*\*\*  $< 0.01$ ; \*\*\*\*  $< 0.001$ .

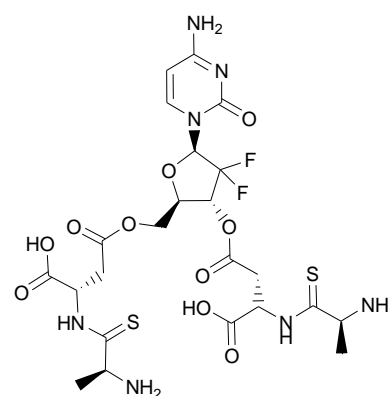
The binding affinity and *trans*-stimulation efflux for the gemcitabine prodrugs was also assessed in oocytes. 4'-*N*-Ala(S)Asp-gemcitabine (**194**) was shown to have a binding affinity of 1.37 mM meaning that it moderately binds to PepT1, however *trans*-stimulation efflux was poorly induced with only a 35% reduction of intracellular radiation when compared to the control dipeptide Gly-Gln which is known to be transported by PepT1. 3'-*O*-Ala(S)Asp-5'-*O*-Ala(S)Asp-gemcitabine (**198**) and 5'-*O*-Ala(S)Asp-gemcitabine (**193**) in contrast were found to have very high binding affinities. The binding affinity for 5'-*O*-Ala(S)Asp-gemcitabine (**193**) was found to be 0.07 mM, however *trans*-stimulation efflux in oocytes was not induced. The binding affinity for 3'-*O*-Ala(S)Asp-5'-*O*-Ala(S)Asp-gemcitabine (**198**) was found to be 0.04 mM and with only 0.07% *trans*-stimulation efflux induced when compared to Gly-Gln. This suggests that both **193** and **198** are able to be recognised, but not transported by PepT1.



**193**  
 $K_i = 0.07 \pm 0.03$  mM  
*Trans*-stimulation = 0%



**194**  
 $K_i = 1.37 \pm 0.40$  mM  
*Trans*-stimulation = 0.07%



**198**  
 $K_i = 0.04 \pm 0.2$  mM  
*Trans*-stimulation = 35%

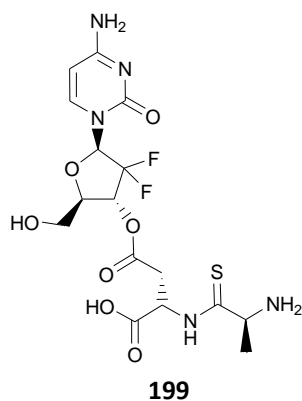
#### 4.3.3 Conclusions

5'-*O*-Ala(S)Asp-gemcitabine (**193**) was not found to decrease cell viability in AsPc1 cells when compared to AsPc1 knock down cells. This suggests that it is not transported by PepT1 and is supported by the lack of *trans*-stimulation efflux induced in oocytes. Alternatively degradation of the prodrug by AsPc1 cell surface enzymes could be occurring prior to transport, as was seen by the Amidon group.<sup>175</sup> This could be assessed both through a Caco-2 study and an AsPc1 cell surface enzyme stability assessment.

4'-N-Ala(S)Asp-gemcitabine (**194**) shows a small reduction in cell viability in AsPc1 cells expressing PepT1 compared to AsPc1 knockdown cells, but efficacy is limited by the rate of activation. Activation is expected to occur by carboxylesterase 2, which has been shown to activate LY2334737 *in vivo*.<sup>174</sup> However, only certain cell lines have been shown to express carboxylesterase 2 at high levels, such as the ovarian cancer cell line SKOV3. It would therefore be interesting to test 4'-N-Ala(S)Asp-gemcitabine within this cell line to see if activation does occur. If so then 4'-N-Ala(S)Asp-gemcitabine may be a candidate for a prodrug of gemcitabine which is resistant to deamination and like LY2334737 gives sustained release of gemcitabine. Although only a moderate binding affinity and poor *trans*-stimulation efflux was seen in oocytes, full Caco-2 testing would assess whether the same poor permeability is seen in this cell line.

3'-*O*-Ala(S)Asp-5'-*O*-Ala(S)Asp-gemcitabine (**198**) decreases cell viability and proliferation in AsPc1 cells expressing PepT1 compared to AsPc1 knockdown cells and is more cytotoxic than gemcitabine. Transport into AsPc1 cells has been shown to occur *via* a separate mechanism as well as by PepT1. This is supported by the poor *trans*-stimulation efflux induced in oocytes, indicating that is perhaps only once the prodrug is hydrolysed to a single carrier attachment that PepT1 transport can occur. If 5'-*O*-Ala(S)Asp-gemcitabine (**193**) is not found to be transported across a Caco-2 monolayer of cells it would indicate that perhaps 3'-*O*-Ala(S)Asp-gemcitabine (**199**) is a PepT1 substrate. 3'-*O*-Ala(S)Asp-gemcitabine (**199**) could be synthesised by *N*-Boc

protecting the cytosine amine and *tert*-butyl protecting the primary alcohol on gemcitabine (**184**) prior to coupling.



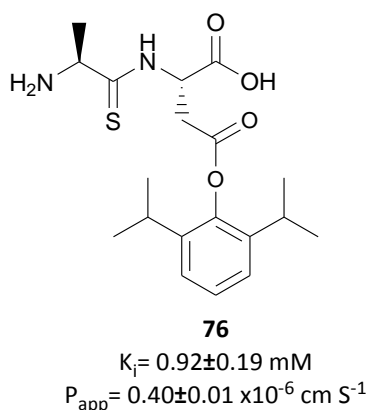
The targeted use of oncology drugs *via* up-regulated nutrient pathways shows promise as a novel cancer therapy tool. Currently there have been abnormal function of PepT1 reported, highlighting this protein as target for rational drug design and delivery. However, the secondary toxicity of PepT1 targeted anti-cancer drugs in organs where the protein is normally rather than pathologically expressed must be considered.

# **Chapter 5**

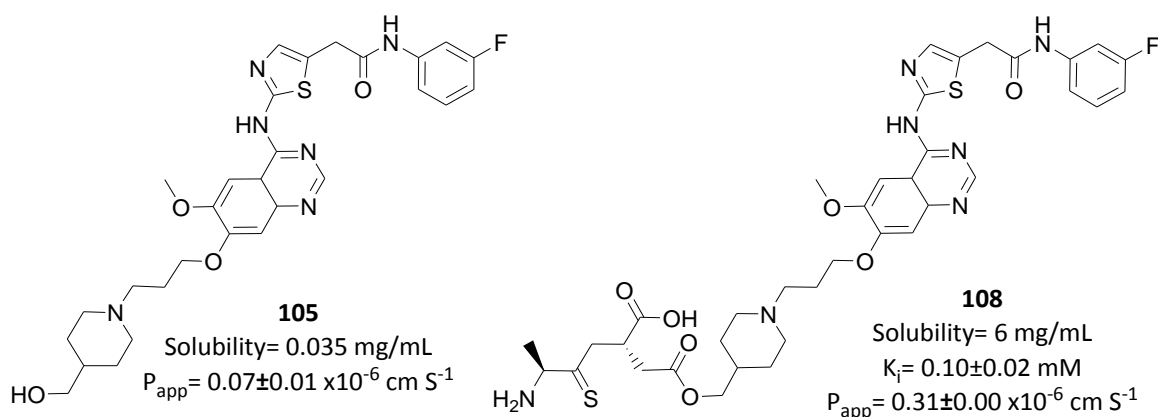
## **Conclusions**



The highly hydrophobic drug propofol (**74**), which was re-examined in this research, showed a marked improvement in solubility when attached to our carriers. New methodology was developed for the synthesis of the propofol prodrug (**76**), as the previous methodology<sup>127</sup> failed to couple propofol (**74**) to the carrier (**40**) and the purification procedure failed to cleanly isolate the prodrug. The resultant prodrug **76** has been found to have an excellent binding affinity for PepT1 and be transported well through Caco-2 cells.



Attachment of our thiodipeptide carrier (**40**) to the Aurora kinase inhibitor (**71**), supplied by AstraZeneca, also resulted in a marked improvement in solubility compared to the parent drug. The solubility of **105** was improved from 0.35 mg/mL to approximately 6 mg/mL when our Ala(S)Asp carrier (**40**) was attached to create prodrug **108**.



Although **108** was found to have a high affinity for the PepT1 transporter ( $0.10 \pm 0.02$  mM), apparent permeability in Caco-2 cells was moderate  $0.31 \pm 0.00 \times 10^{-6} \text{ cm S}^{-1}$ . This is however slightly higher than the apparent permeability of the parent drug **105** indicating the PepT1 plays a small role in the permeation of **108** across Caco-2 cells. The use of a glycol spacer between our carrier and the attached drug had previously been shown by our group to improve the water solubility of the resultant nabumetone prodrug.<sup>116</sup> The use of a glycol spacer may also improve the transport of the resultant prodrug. By setting the drug slightly away from the mouth of the binding pocket in PepT1, only the carrier motif of the prodrug is likely to be recognised. As a result the PepT1 transport mechanism may already be in motion before the attached drug is detected. The use of glycol spacers to improve the apparent permeability of **108** was therefore investigated. Unfortunately one of the acetic acid glycol linkers had been coupled to **105**, the benzyl ether protecting the other end of the linker could not be removed (Figure 37).

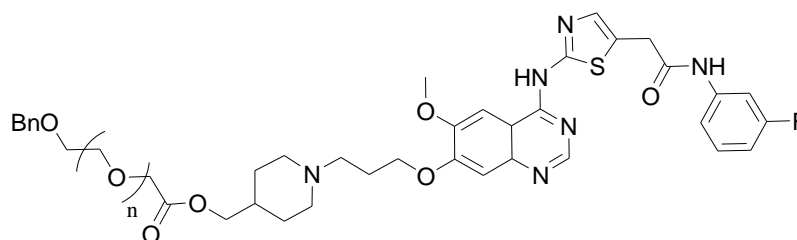
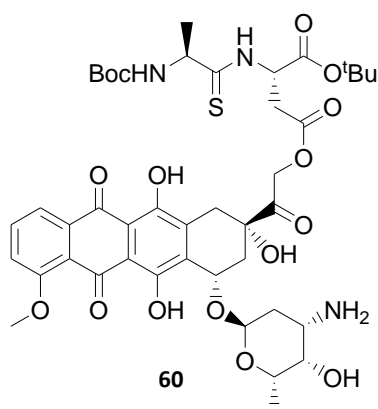


**Figure 37 Acetic acid glycol linkers attached to (105)**

Failure to remove the benzyl protecting group with palladium hydrogenation only highlights the difficulty of working with sulfur containing chemicals. It was initially thought that in the thiazole ring would be sufficiently conjugated to prevent poisoning of the catalyst. However, this was not found to be the case. The presence of ether and ester bonds in the molecule also prevented benzyl deprotection with boron trichloride or trimethylsilyl iodide and mild esterification methods also gave multiple products. Use of an alternative protecting group which can withstand coupling conditions and be selectively deprotected in the presence of a methyl ether would allow the desired linker prodrugs to be synthesised.

The presence of a thioamide in our carriers prevents hydrolysis of the prodrug by peptidases in the gastrointestinal tract. *Tert*-butyl type protection of our carrier is traditionally used, as after coupling of our carrier to a drug, they can be cleaved cleanly in one step in the presence of a sulfur atom. When this final step was performed by Dr R. Pathak with the protected thiodipeptide prodrug of doxorubicin (**60**), it was found that the doxorubicin was unstable to acid conditions.

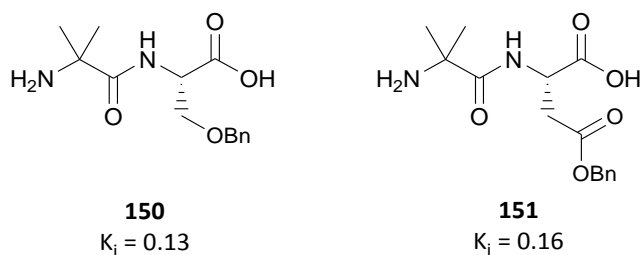


In an attempt to broaden the classes of drugs that can be targeted to PepT1 to include acid sensitive drugs, alternatively protected thiodipeptide carriers were created. The serine or aspartate component of the dipeptide must be differentially protected to allow selective deprotection of both the amine and R<sup>2</sup> group during synthesis of the carrier. Finding protecting groups which would allow this, withstand coupling conditions and are cleaved with one step after coupling of the carrier to a selected drug in the presence of sulfur proved a challenge. Benzyl type protection was ultimately chosen as although they must be deprotected in the relatively harsh conditions of dissolving metal reduction in the presence of sulfur, if this atom is not present hydrogenation can be used. The use of alternative carriers, which do not contain a sulfur atom, was also explored in this research project.

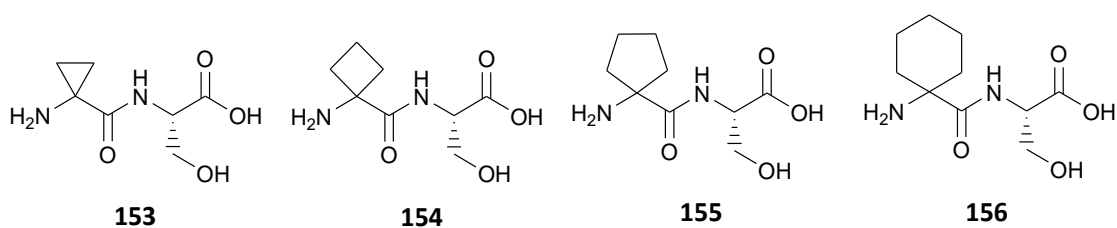
Alternative routes to synthesis the *tert*-butyl protected carriers were explored. Mono-protection of the aspartate and serine amino acids to give H-X(OBn)-O<sup>t</sup>Bu eliminated the need for one of the steps in the synthesis of the carriers. This increased the overall yield to ~69% in 5 days, compared to the established methodology of ~50% in 9 days. However, the prohibitive cost of the

new starting material compared to that in the established methodology meant this method of synthesis was not pursued. The established method for the synthesis of the *tert*-butyl protected carriers was however improved through the elimination of halogenated solvents during purification procedures. Halogenated solvents have a much larger environmental impact than non-halogenated solvents and were avoided during the course of this research where possible.

The presence of a thiodipeptide in carriers has often been found to result in non-crystalline prodrugs being synthesised, which can present a problem for formulation. We were also worried about the presence of the sulfur atom negatively affecting the taste of any prodrugs taken forward in development. R<sup>1</sup>  $\alpha,\alpha$ -disubstituted dipeptides **150** and **151** (shown with benzyl as a model drug moiety) had previously been explored for use as alternative carriers (Dr D. Foley, unpublished).<sup>127</sup> Both displayed excellent binding affinities for PepT1 and had been found to be transported across a Caco-2 cell line much better than their thiodipeptide counterparts.



Newstead *et al.*<sup>89</sup> had recently shown that there is an elongated cavity ( 16 x 7 x 11 Å) in the *N*-terminal end of the ligand binding site in the prokaryotic POT transporter PepT<sub>so</sub>. This is where R<sup>1</sup> would be positioned when the carrier is 'docked' in the substrate binding pocket of PepT1. Therefore in an attempt to find a second alternative PepT1 carrier, as well as explore the tolerance of PepT1 for bulk in this area, a series of dipeptides were synthesised (**153-156**).

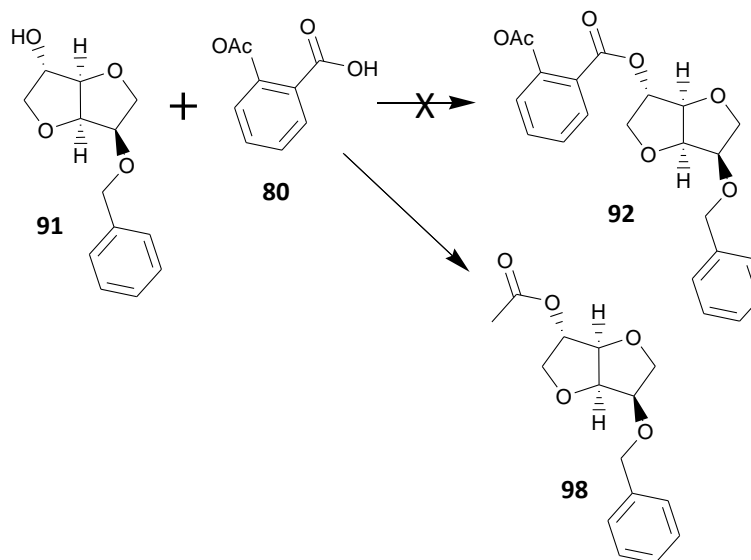


The use of cyclic groups on the *N*-terminal  $\alpha$ -carbon allowed the presence of bulk in this region to be assessed, whilst preventing hydrolysis by peptidases as access to the backside of the carbonyl group is reduced. The addition of hydrocarbon bulk to the dipeptides also has the added benefit of increasing overall lipophilicity. This is of benefit as traditional prodrug strategies for poorly bioavailable drugs often include increasing lipophilicity as permeability will be increased.

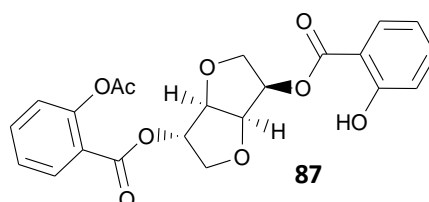
All carriers (with no moiety attached in the R<sup>2</sup> position, or with benzyl or ibuprofen attached) were found to have excellent binding affinity in oocytes. *Trans*-stimulation data was also favourable with only homocycloleucine-serine-ibuprofen (**181**) failing to induce efflux. This may be an anomalous result as both the free dipeptide and benzyl attached dipeptide were transported, or it may be an inhibitor of PepT1. During stability testing of the ibuprofen linked carriers, only the cycloleucine carrier (**155**) was found to fragment, suggesting this carrier is not hydrolysis resistant. The results obtained for the cyclopropane (**153**), cyclobutane (**154**) and cyclohexane (**156**) carriers indicates that in addition to the Aib carrier, these may be promising alternative carriers. Full Caco-2 testing will need to be undertaken to confirm this.

Caco-2 permeability was attempted to be generated for the ibuprofen linked carriers during the course of this research. Unfortunately analysis of the samples generated from the Caco-2 study could not be carried out. This has been a theme across this research and is primarily attributed to unfortunate timing of this project with a time of restructuring at AstraZeneca. In many ways the collaboration with AstraZeneca has been excellent with free access to facilities and expertise being provided, as well as the kind supply of the equipment, chemicals and cells needed for Caco-2 testing. In addition new chemical entities developed by AstraZeneca were kindly donated for use in this project and support was freely offered when synthetic problems were encountered. Everyone involved at AstraZeneca, both past and present, went out of their way to try and mediate the problems encountered during the course of this project.

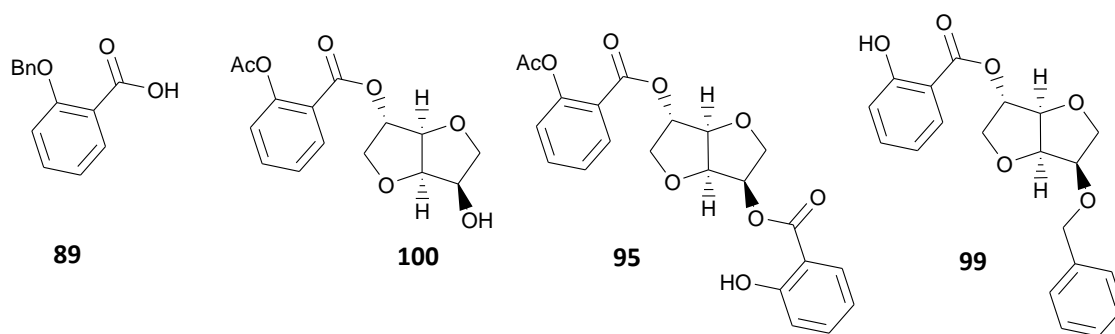
Synthesis of an aspirin (**80**) prodrug hit a barrier when the coupling of aspirin (**80**) to **91** resulted in **98** rather than **92**. Alternative coupling methods were investigated, but each time transesterification occurred.



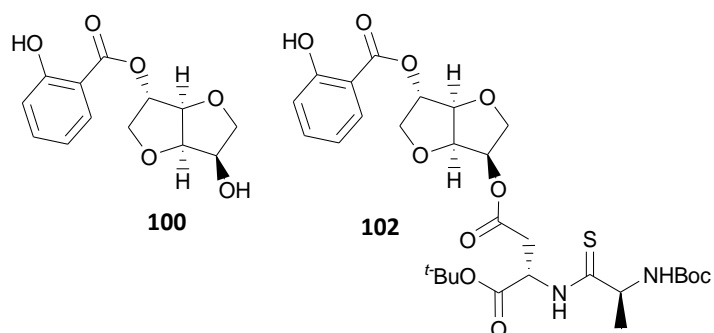
This is surprising as the synthetic conditions utilised were based on conditions employed by the group at Trinity College<sup>130</sup> to make the aspirin prodrug ISAS (**87**).



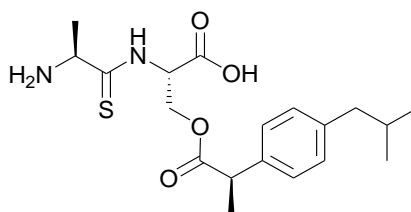
In an attempt to overcome this salicylic acid was used as an alternative to aspirin. Using pre-charged coupling conditions **99** was achieved in good yields (86%). Due to this work being undertaken at the very end of this research project the acetylation of **99** was not investigated as deacetylation could possibility occur when **100** was coupled to **89** or **95** was coupled to our carrier.



In an attempt to make a carrier coupled prodrug that would be useful for the *in vitro* testing of a model aspirin like prodrug, our protected carrier (**57**) was coupled directly to **100**. Unfortunately **102** could not be isolated from the reaction mixture, with carrier attached to both alcohols on salicylic-isosorbide (**100**) the only compound separated from the reaction mixture. This project was abandoned due to the prioritisation of other work and the difficulties previously encountered in the group by Dr. Foley<sup>127</sup> in making a thiodipeptide aspirin prodrug. If successful conditions are found to couple aspirin to isosorbide-benzyl or to acetylate salicylic-isosorbide-benzyl then hopefully no further problems should be encountered in the synthetic route.



The Ala(S)Ser-ibuprofen prodrug **79** had previously been created in our group<sup>117</sup> and had been shown to have both favourable binding affinity and Caco-2 permeability. The apparent permeability for this prodrug was also assessed in the course of this research and was found to closely resemble reported data.



**79**

$$K_i = 0.26 \pm 0.03 \text{ M}$$

$$P_{app} = 3.97 \pm 0.27 \times 10^{-6} \text{ cm S}^{-1}$$

An *in vivo* pharmacokinetic test of **79** had been previously carried out. Plasma detection of a 10 mg/kg dose in rat gave a  $C_{max}$  of  $930 \pm 90$  ng/mL with a  $T_{max}$  of 1.33 hours.<sup>117</sup> It was therefore decided to perform full pharmacokinetic analysis **79** in rat, detecting both the presence of prodrug and parent in plasma. Synthesis of **79** was therefore undertaken using the reported coupling conditions.<sup>117</sup> Problems with the *tert*-butyl final deprotection step using TFA necessitated a switch to formic acid. This was used as the standard deprotection conditions for the rest of this project. As Aib carriers had previously been shown to be promising sulfur free hydrolysis resistant alternatives to our thiodipeptides, the Aib-seine prodrug of ibuprofen (**183**) was also tested. This was synthesised by Dr R. Pathak who also synthesised the prodrug for the taste assessment study.

In contrast to the previous *in vivo* result found for Ala(S)Ser-ibuprofen (**79**), in this study it was not found to be well absorbed in rat. The  $C_{max}$  value obtained was approximately similar for both **79** and parent ibuprofen (**77**) (~200 ng/mL, after 1 hour), which is much less than the  $C_{max}$  when an equivalent dose of ibuprofen was given (5664 ng/mL, after 1 hour). Ibuprofen (**77**) was able to be detected in plasma 8 hours after dosing of **79**, which is how long parent ibuprofen (**77**) was detected after an equivalent dose was given. Aib-Ser-ibuprofen (**183**) was found to have a longer exposure profile than ibuprofen (**77**), with a  $T_{last}$  of 16 hours compared to 8 hours for ibuprofen (**77**). The  $C_{max}$  for Aib-Ser-ibuprofen (**183**) was very low (32 ng/ mL, after 1 hour) indicating that either prodrug breakdown was occurring prior to transport or very quickly once in systemic circulation. The Ala(S)Ser-ibuprofen prodrug **79** was also synthesised to assess whether rats preferred ibuprofen prodrugs with and without a sulfur atom. It was found that rats did not



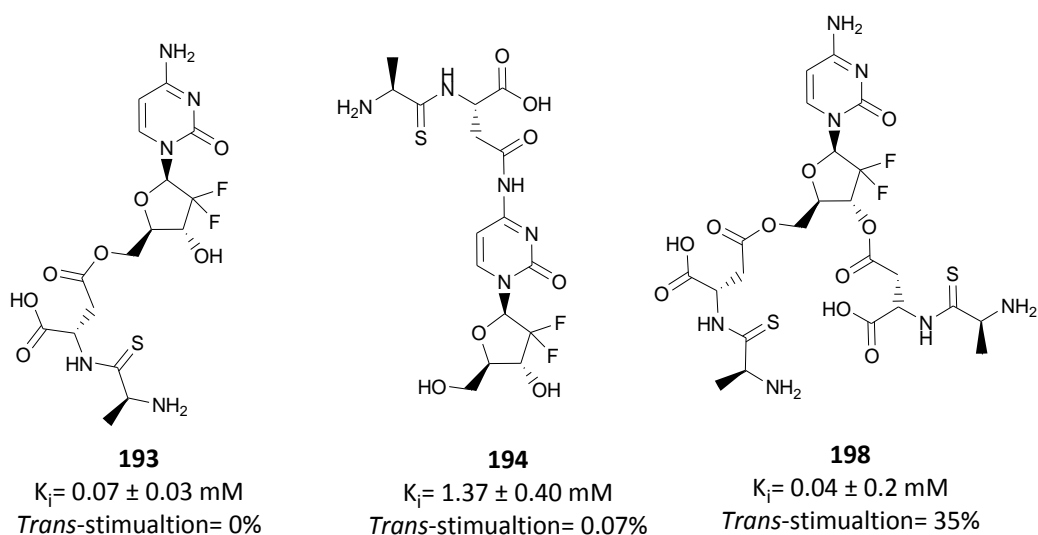
care for either the Ala(S)Ser-ibuprofen (**79**) or Aib-Ser-ibuprofen (**183**) prodrugs and instead preferentially consumed parent ibuprofen.

The discovery that PepT1 is over-expressed in pancreatic adenocarcinoma cell lines, AsPc-1 and Capan-2,<sup>153</sup> has also led to research being undertaken into PepT1 targeted anti-cancer therapy. Pancreatic cancer often has a poor prognosis, with only a 5% survival rate 5 years after diagnosis,<sup>157</sup> this highlights the need for treatment options in this area. The use of PepT1 targeting could potentially reduce the side effects experienced during cancer therapy, as off target delivery would be minimised. Cell proliferation in several cancerous cell lines<sup>165-7</sup> had been shown to reduce upon the treatment of a variety of nonsteroidal anti-inflammatory drugs. As these drugs can only access the surface of these cells efficacy is limited. We were therefore intrigued to see if our PepT1 targeted ibuprofen prodrug **79** would have an increased efficacy over parent ibuprofen (**77**) due to its ability to be transported into cells.

Testing was carried out by Prof R. Mrsny's group at the University of Bath in AsPc1 cells. As a control AsPc1 knockdown cells which did not express PepT1 were used. This meant the PepT1 component of any results seen could be assessed. Ala(S)Ser-ibuprofen (**79**) was shown to have a more pronounced effect on cell proliferation and vitality in AsPc1 cells expressing PepT1 than AsPc1 knockdown cells. In both cell lines Ala(S)Ser-ibuprofen (**79**) also showed a more pronounced effect on cell proliferation and vitality than ibuprofen (**77**). To my knowledge this is the first time that reduced cell proliferation by an ibuprofen prodrug or ibuprofen (**77**) in AsPc1 cells has been reported. One of the ways that ibuprofen (**79**) may reduce proliferation is by inhibiting the COX-2/PGE<sub>2</sub> pathway, which if dysregulated has been shown to result in cell proliferation, angiogenesis, migration and inhibit apoptosis.<sup>164</sup> COX-2 is an accepted pharmacological target of ibuprofen (**77**). Its expression in AsPc1 (PepT1) cells was assessed after treatment with either ibuprofen prodrug (**79**) or ibuprofen (**77**). Although levels of COX-2 were reduced by ibuprofen (**77**), it was eliminated by Ala(S)Ser-ibuprofen (**79**). This suggests that the prodrug **79** was accumulating in cells therefore having a greater effect on COX-2 expression.

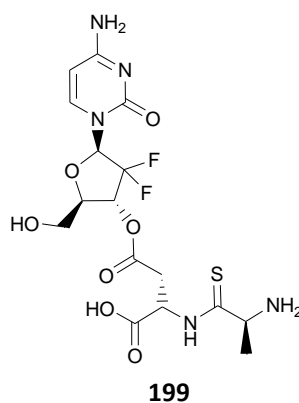
Through the active targeting of ibuprofen (**77**) the side effects normally reported with long term ibuprofen (**77**) use may be mitigated.<sup>161</sup> This opens up the possibility of use as part of cancer therapy and in a prophylactic manor. The efficacy of Ala(S)Ser-ibuprofen (**79**) or indeed Aib-Ser-ibuprofen (**183**) in an *in vivo* oncology model should therefore be assessed.

Gemcitabine (**184**) is a nucleoside drug licensed for the treatment of bladder cancer, breast cancer, non-small lung cancer and pancreatic cancer.<sup>172</sup> As with other nucleoside analogues, gemcitabine (**184**) suffers from low oral bioavailability due to extensive first pass metabolism to an inactive metabolite. As part of the collaboration with Prof. Mersny it was decided to synthesise thiodipeptide prodrugs of gemcitabine (**184**) to assess for efficacy in AsPc1 cells. It was hoped that as was seen for the ibuprofen prodrug **79**, the active targeting of gemcitabine (**184**) towards PepT1 would result in accumulation of gemcitabine (**184**) within cells. This would hopefully result in increased efficacy. The oral bioavailability of several nucleoside drugs have been improved through PepT1 targeting (section 2.1.1) so we were hopeful that a prodrug that was both recognised and transported by PepT1 could be created.



Out of the three prodrugs synthesised only **198** was shown to reduce viability and proliferation in AsPc1 cells. However, a Gly-Sar blocking study still showed a reduction in cells vitality indicating that this prodrug is entering cells both by PepT1 and *via* an alternative route.

Poor *trans*-stimulation data in oocytes indicated that the prodrug was not being transported into cell intact. However, the significantly lower cell vitality in AsPc1 cells seen for **198** compared to gemcitabine (**184**) indicating that accumulation of **198** in cells was occurring. Most likely degradation of **198** by enzymes on the surface of AsPc 1 cells was resulting in gemcitabine (**184**) linked to a single carrier being transported into cells. If 5'-*O*-Ala(S)Asp-gemcitabine (**193**) is not found to be transported across a Caco-2 monolayer of cells it would indicate that perhaps 3'-*O*-Ala(S)Asp-gemcitabine (**199**) is the gemcitabine prodrug responsible for the reduced cell vitality seen.



Although PepT1 can be used as a tool to improve oral bioavailability, the use of PepT1 as a tool for targeted cancer therapy is where PepT1 research should be focused. Although PepT1 targeting has been shown to improve the oral bioavailability of drugs, both through the use of our thiodipeptide and amino acid attachment, drug choice is perhaps limited to the existing physiochemical properties of the parent drug. Although solubility of propofol was improved through attachment our carrier, this has not always been the case with other drugs. The previously created thiodipeptide prodrug of poorly soluble dehydrocholic acid (Dr. R. Pettecrew, unpublished), was both recognised and transported by PepT1 but solubility was not significantly improved. This has again been demonstrated during this project with the synthesis of Aurora Kinase inhibitor **105**. Although solubility was increased 200 fold when compared to the parent drug, only a 50  $\mu$ M solution in buffer could be created for Caco-2 testing. The issue of 'brick dust' compounds was also highlighted by the failure of the planned  $\alpha$ 1 $\beta$ 5 Integrin inhibitor prodrug.

These are compounds in pharmaceutical development that may have found to have good target efficacy, but are shelved due to less than optimum solubility properties.

If however, poor oral bioavailability is a result of active efflux, PepT1 targeting is an attractive option. Quinidine which is actively effluxed by P-gp was found to no longer be a substrate when turned into the PepT1 substrate *L*-valine-quinidine.<sup>106</sup> As most oncology drugs are also P-gp substrates, bypassing this mechanism is an important step in improving oral bioavailability. There is also the third class of drugs which may benefit from PepT1 targeting. Drugs such as ibuprofen (**77**) and aspirin (**80**) cause gastrointestinal side effects but there are benefits to patients in their long term use. Although difficulties have been encountered both in the project and by a previous group member in making a PepT1 targeted aspirin prodrug, the thiodipeptide and Aib-serine prodrugs of ibuprofen have been synthesised (**79**, **80**). More work is needed to assess the stability of these ibuprofen prodrugs *in vivo* although favourable binding affinity and transport in Caco-2 has been demonstrated. Assessment would also need to be undertaken to ensure that these drugs are not active in their prodrug form.

The targeted use of oncology drugs *via* up-regulated nutrient pathways shows promise as a novel cancer therapy tool. However, this is certainly not without its challenges. Cell surface enzymes on cancer cells are more likely to hydrolyse PepT1 targeted prodrugs before they reach the PepT1 transporter than is found in the small intestines. This necessitates the use of a more robust method to link the drug to a PepT1 recognised motif. Unless pathways are present in the cell to active the resulting prodrug, this attachment must be approached with the view of keeping the resultant prodrug active. Although this would allow for accumulation of drug within cells and therefore higher efficacy, off target delivery would not necessarily be minimised. There has also been mutations in PepT1 reported for several cancers.<sup>179</sup> The substrate specificity of PepT1 which has been upregulated in cancer cells has yet to be assessed. It may be found that a slightly different transport profile is seen requiring a different carrier.

# **Chapter 6**

## **Experimental**

## Chapter Six Contents

6.1	General methods .....	135
6.1.1	Oocyte binding affinity.....	135
6.1.2	Oocyte <i>trans</i> -stimulation assay.....	135
6.1.3	Caco-2 assay.....	136
6.1.4	AcPc1 assay .....	137
6.1.5	Pharmacokinetic study in rat .....	137
6.1.7	Synthetic materials .....	138
6.1.8	Characterisation.....	139
6.2	Synthesis of Benzyl type protected carriers (section 2.4).....	140
6.3	Synthesis of PepT1 targeted prodrugs using commercial drugs (section 2.5).....	151
6.3.1	Propofol prodrug (section 2.5.1).....	151
6.3.2.	Ibuprofen prodrug (section 2.5.2).....	154
6.3.3	Aspirin prodrug (section 2.5.3). ....	156
6.4	Synthesis of polyethylene glycol based linkers (section 2.6.1).....	160
6.5	Synthesis of Aurora Kinase inhibitor prodrug (section 2.6.1).....	165
6.6	Synthesis of alternative carriers section (3.1).....	172
6.6.1.	Serine component (section 2.3 and 3.1).....	172
6.6.2.	Cycloleucine-serine carrier (section 3.1).....	176
6.6.3.	Cyclopropane-serine carrier (section 3.1).....	183
6.6.4.	Cyclobutane carrier (section 3.1).....	189
6.6.5.	Homocycloleucine carrier (section 3.1). ....	195
6.7	Synthesis of gemcitabine prodrugs (section 4.3.1).....	201

## 6.1 General methods

### 6.1.1 Oocyte binding affinity

Six solutions of test substrate between 0 and 5 mM were prepared from serial dilution of a 10 mM test compound in pH 5.5 uptake media stock solution. An n=5 was performed for each concentration of test solution by adding a 50  $\mu$ L aliquot of test solution to 50  $\mu$ L of radiolabelled [ $^3$ H]-D-Phe-L-Gln (0.4  $\mu$ M, 37.0 MBq mL<sup>-1</sup>) in a 96 well plate. An n=5 was also performed for a blank control using pH 5.5 uptake media stock solution. A *Xenopus laevis* oocytes expressing rabbit PepT1 was added to each well and incubated for one hour. After one hour the oocytes were removed from the test solution and washed with five 1 mL portions of ice-cold uptake media, transferred to individual scintillation vials, lysed and tested. Binding affinity ( $K_i$ ) was obtained from a plot of fractional uptake versus substrate concentration, using standard Michaelis-Menten kinetics. Carried out by Dr. Meredith or Anish Senan at Oxford Brookes University.

### 6.1.2 Oocyte *trans*-stimulation assay

A 10 mM solution in pH 5.5 uptake media was made for each test compound and a 100  $\mu$ L aliquot was added to a 96 well plate to give an n=5 for each test compound. An n=5 was also performed for a blank control using pH 5.5 uptake media stock solution and a 10mM solution of L-Gly-L-Gln in pH 5.5 uptake media. A rabbit PepT1 *Xenopus laevis* oocyte injected with 4.6 nM of [ $^3$ H]-D-Phe-L-Gln (37.0 MBq mL<sup>-1</sup>), which had been pre incubated for 15 minutes with pH 5.5 uptake media, was added to each well and incubated for 90 minutes. After 90 minutes the oocytes were removed from the test solution and washed with five 1 mL portions of ice-cold uptake media, transferred to individual scintillation vials, lysed and tested. *Trans*-stimulation efflux was measured as a reduction in radioactivity of the test solution incubated oocyte compared to the control. This is then compared to the decrease in radiation induced by the PepT1 substrate L-Gly-L-Gln. Carried out by Dr. Meredith or Anish Senan at Oxford Brookes University.

### 6.1.3 Caco-2 assay

Caco-2 cells (supplied at passage number 17) were purchased from American Type Culture Collection and were used for transport studies at passage 28-35, the count of which was continued from the received passage. For the transport studies the Caco-2 cells were grown on BD Falcon™ 24-multiwell insert systems with polyethylene terephthalate membranes (1 mm pore size, 0.3 cm<sup>2</sup> surface area) with BD Falcon™ 24-multiwell companion plates in a cell culture medium consisting of Dulbecco's Modified Eagle's Medium supplemented with 20% (w/v) foetal bovine serum and 1% (v/v) non-essential amino acids until confluent (16-18 days, *trans*-epithelial electrical resistance (TEER) > 1000 Ω cm<sup>-2</sup>).

650 μM solutions of each test compound (except Aurora kinase inhibitor **108** which was made to 50 μM due to solubility issues) were made in pH 5.5 (Hanks Balanced salt solution, (v/v) 0.1% bovine serum albumin, MES 25 mM ) and 7.4 buffer solution (Hanks Balanced salt solution, (v/v) 0.1% bovine serum albumin, HEPES 25 mM). 1% DMSO was added to all stock solutions to maintain consistency with the test compounds which did not dissolve well in buffer. Stability of the test compounds was assessed by incubating them for 30 minutes in pH 5.5 buffer solution which had been aspirated from the apical surface of Caco-2 cells.

All solutions were heated to 37°C prior to use on cells. The cells incubated in buffer solution at 37°C for 25 minutes prior to use in the study (apical pH 5.5, basolateral pH 7.4) and then aspirated. For apical to basolateral transport 200 μL of pH 5.5 test compound solution was aliquoted on the apical side of the monolayer (n=3) and 600 μL of pH 7.4 buffer aliquoted on the basolateral side. For basolateral to apical transport 200 μL of pH 5.5 buffer solution was aliquoted on the apical side of the monolayer and 600 μL of pH 7.4 test compound solution buffer aliquoted on the basolateral side (n=3). The plates were incubated for 60 minutes (37°C, 50 cycles min<sup>-1</sup>), before 50 μL of solution was removed from both the apical and basolateral compartments, placed in separate LCMS vials, frozen (-20°C) and sent for LCMS analysis. As an integrity marker



for the cells  $^{14}\text{C}$  Mannitol (100 KBq/mL) was prepared in pH 5.5 buffer (apical to basolateral plate) and pH 7.4 (basolateral to apical plate) and assayed on each plate (n=3). After incubation 50  $\mu\text{L}$  of solution was removed, vortex mixed with UltimaGold scintillation fluid (2 mL) and counted using a Tricarb 2300LTR counter using a dual dpm protocol. Mannitol is transported through cells *via* the paracellular route so  $P_{\text{app}}$  values exceeding  $1 \times 10^6 \text{ cm s}^{-1}$ , would indicate that the tight junctions were not properly formed.

For PepT1 transport component studies only apical to basolateral transport was measured and 2000  $\mu\text{M}$  Gly-Sar was added to each pH 5.5 test solution. Studies were performed under the guidance and assistance of Kate Harris at AstraZeneca in Charnwood and Alderley Park. LCMS analysis was performed by either Sarah Kelly at Alderley Park or Constanze Hilgendorf at AstraZeneca Mölndal.

#### 6.1.4 AcPc1 assay

AsPc1 WT and AsPc1 PepT1<sup>-/-</sup> cells were plated in 96 well plates at a cell density of 500 cells per well. 50 mM in DMSO stock solutions of the ibuprofen and gemcitabine prodrugs were serially diluted to; 500  $\mu\text{M}$ , 200  $\mu\text{M}$ , 100  $\mu\text{M}$ , 50  $\mu\text{M}$ , 20  $\mu\text{M}$ , 10  $\mu\text{M}$ , 5  $\mu\text{M}$  and 1  $\mu\text{M}$  in buffer. After incubation, cell viability was assessed using the MTS reagent. To assess the PepT1 mediated component of transport the cell culture media was supplemented with 50 mM Gly-Sar. These assays were carried out by Ana Maria Cravo at the University of Bath.

#### 6.1.5 Pharmacokinetic study in rat

Ibuprofen (**77**) was prepared in distilled water at 1.2 mg/mL which gave a dose of 6 mg/kg with a dose volume of 5 mL/kg. The ibuprofen prodrugs were prepared in distilled water at 2 mg/mL which gave a dose of 10 mg/kg (equivalent ibuprofen does of 6 mg/kg) with a dose volume of 5 mL/kg.

Nine male CD (Sprague Dawley equivalents) rats (251-281 g at the time of dosing, Charles River, UK) were housed singly following jugular vein cannulation, maintained under a 12 hour light/dark cycle and allowed free access to food and water. An n=3 was performed for each test compound and blood samples (~ 230 µL) were collected 0.25, 0.5, 1, 2, 4, 8 and 24 h after dosing, with an equal volume of heparinised saline was then infused back into the rat thus ensuring patency.

Blood samples were added to an Eppendorf 1.5 mL tube containing 5 µL heparin (25,000 IU in 5 mL), shaken and centrifuged (Biofuge Pico, Kendro Lab Products) at 10,000 rpm for 3 minutes. 80 µL of plasma was extracted and added to 10 µL of water and 810 µL acetonitrile. The sample was then centrifuged at 13,000 rpm for 5 minutes at 4°C and 500 µL of the supernatant was extracted and added to 500 µL water. This sample was then diluted 20 fold by mixing a 50 µL aliquot with 950 µL of water. Samples were then analysed by LC-MS/MS on a 50 x 2.0 mm C18 Gemini 5 µM column. Carried out by Saretius Ltd at the University of Reading.

#### 6.1.7 Synthetic materials

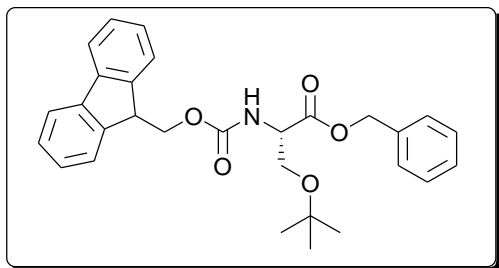
All solvents used were commercial grade. Dichloromethane was distilled over calcium hydride and tetrahydrofuran was distilled over sodium metal and benzophenone to make anhydrous. Anhydrous dimethyl sulfoxide and anhydrous dimethylformamide were purchased from Sigma Aldrich and used without further treatment. All chemicals purchased from suppliers were used without further purification (Sigma Aldrich, Flurochem, Tokyo Chemicals Limited, AGTC Bioproducts, Acros Organics). Aurora Kinase Inhibitor *N*-(3-fluorophenyl)-2-(2-(7-(3-(4-(hydroxymethyl)piperidin-1-yl)propoxy)-6-methoxyquinazolin-4-ylamino)thiazol-5-yl)acetamide and α1β5 Integrin inhibitor (S)-2-(2-chloro-6-fluorobenzamido)-3-(4-(2-(5,6,7,8-tetrahydro-1,8-naphthyridin-2-yl)ethoxy)phenyl)propanoic acid was kindly supplied by AstraZeneca and after structure confirmation were used without further purification. Flash column chromatography was carried out on silica gel 60 (40-63 µm mesh).

#### 6.1.8 Characterisation

Analytical TLC was performed on Macherey-Nagel aluminium sheet silica gel 60 UV<sub>254</sub> plates. Spots were visualised with a UV lamp, potassium permanganate stain or vanillin stain. Retention factors ( $R_f$ ) are quoted to the nearest 0.01.  $^1\text{H}$  and  $^{13}\text{C}$  NMR spectra were recorded on a Bruker Advance DPX 300 spectrometer at 300 MHz and 75 MHz respectively. Splitting patterns are recorded as follows: chemical shift, multiplicity, integration and atom. Multiplicity is described as singlet (s), doublet (d), triplet (t), quartet (q), quintet (quin), multiplet (m), broad (br), or any combination thereof. AB refers to secondary splitting effects where the chemical shift between protons is large. Coupling constants ( $J$ ) are stated in Hz to the nearest 0.01 Hz. Infrared spectra were recorded on a Thermo Nicolet Nexus FT-IR spectrometer. Optical rotations were measured using a Rudolph Research Analytical Autopol I automatic polarimeter with sodium D light ( $\lambda = 589$  nm).  $[\alpha]_D^{25}$  values are recorded in units of  $10^{-1} \text{ deg cm}^2 \text{ g}^{-1}$  and concentrations are stated in g per mL of solvent. Mass spectra were recorded on a Thermofisher LTQ Orbitrap XL spectrometer using nano-electrospray. Melting points were determined on a Stuart SMP30 Digital Advance machine and are uncorrected.

## 6.2 Synthesis of Benzyl type protected carriers (section 2.4)

### (S)-benzyl-2-fluorenylmethoxycarbonyl-3-*tert*-butoxypropanoate (63).



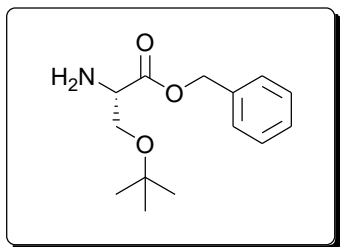
*N*-(9-Fluorenylmethoxycarbonyl)-*O*-(*tert*-butyl)-*L*-serine (**61**) (15.150 g; 39.51 mM) and sodium bicarbonate (6.638 g; 79.02 mM) was dissolved in 20 mL of anhydrous DMF under a nitrogen atmosphere. Benzyl bromide (18.77 mL; 158.04 mM) was added dropwise and the reaction stirred for 72 hours at room temperature. The solvent was removed *in vacuo* to yield a clear oil. The oil was dissolved in 20 mL EtOAc and washed with three 20 mL portions of water followed by 20 mL of brine, dried over anhydrous MgSO<sub>4</sub> and filtered. 200 mL of cyclohexane was added and the reaction left to stand overnight to yield a white solid, which was collected by filtration. The white solid was recrystallised from 200 mL cyclohexane to yield 12.788 g of **63** as a white solid (27.00 mM, 68%).

R<sub>f</sub>: 0.61 (EtOAc:Pet ether 4:6). <sup>1</sup>H NMR (300 MHz, chloroform-*d*) δ ppm 1.13 (s, 9H, CH<sub>3</sub> *tert*-butyl), 3.63 (ABdd, *J*=9.04 Hz, 1H, CH<sub>2</sub> serine), 3.88 (ABdd, *J*=8.67 Hz, 1H, CH<sub>2</sub> serine), 4.28 (t, *J*=7.20 Hz, 1H, CH Fmoc), 4.32-4.48 (m, 2H, CH<sub>2</sub> Fmoc), 4.57 (t, 1H, *J*=8.95, 2.86 Hz, CH serine), 5.24 (qAB, *J*=1.00 Hz, 2H, CH<sub>2</sub>-benzyl), 5.73 (d, *J*=9.04 Hz, 1H, NH), 7.29-7.46 (m, 9H, CH benzyl, CH Fmoc), 7.64 (d, *J*=7.16 HZ, 2H, CH Fmoc), 7.79 (d, *J*=7.16Hz, 2H, CH Fmoc). <sup>13</sup>C NMR (75 MHz, chloroform-*d*) δ ppm 27.27, 47.12, 54.70, 62.13, 67.12, 67.21, 73.47, 119.99, 125.18, 125.23, 127.09, 127.71, 128.25, 128.36, 128.55, 135.51, 141.28, 143.79, 144.00, 156.16, 170.60. *u*<sub>max</sub> (thin film, cm<sup>-1</sup>): 3430, 3035-2874, 1723, 1499, 1333, 1102, 1088, 739. [α]<sub>D</sub><sup>25</sup> (CHCl<sub>3</sub>; c = 0.103): - 3.88.

MS: C<sub>29</sub>H<sub>31</sub>NO<sub>5</sub>, *m/z* (ES<sup>+</sup>) 474.23 [M+H]<sup>+</sup>. HRMS: Calculated C<sub>14</sub>H<sub>22</sub>NO<sub>3</sub> 474.2275, found 474.2266.

MP: 84°C

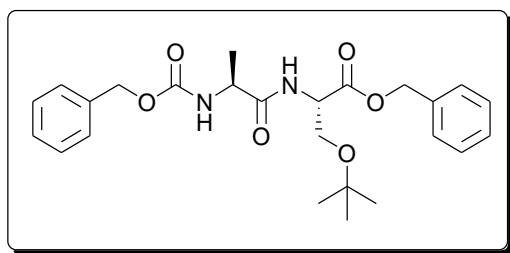
**(S)-benzyl-2-amino-3-*tert*-butoxypropanoate (65).**



**63** (4.052 g; 8.56 mM) was dissolved in 20 mL of anhydrous THF under a nitrogen atmosphere. The reaction was cooled to 0°C and a 1.0 M solution of TBAF in THF (9.41 mL) was added dropwise. The reaction was stirred at 0°C for 30 minutes, and allowed to proceed a further 2-3 hours at room temperature, monitored by TLC. The solvent was removed *in vacuo* to yield a sticky pink residue which was taken up into 20 mL of water. The pH of the solution was adjusted to pH 2 using 2 M HCl, and 20 mL of EtOAc added. The aqueous layer was separated and extracted with a further two 10 mL portions of EtOAc. The aqueous phase was adjusted to pH 8-9 using 2 M NaOH, and extracted with one 20 mL and two 10 mL portions of EtOAc. The EtOAc portions from the basic aqueous extraction were combined, dried over anhydrous MgSO<sub>4</sub> and filtered. The solvent was reduced *in vacuo* to give 1.493g of **65** as a brown oil (5.94mM, 69%).

R<sub>f</sub>: 0.43 (EtOAc:Pet ether 4:6). <sup>1</sup>H NMR (300 MHz, chloroform-*d*) δ ppm 1.13 (s, 9H, CH<sub>3</sub> *tert*-butyl), 3.56-3.63 (m, 2H, CH<sub>2</sub> serine), 3.64-3.71 (m, 1H, CH serine), 5.23 (qAB, *J*=1 Hz, 2H, CH<sub>2</sub> benzyl), 7.30-7.45 (m, 5H, CH benzyl). <sup>13</sup>C NMR (75 MHz, chloroform-*d*) δ ppm 27.36, 55.24, 63.72, 66.64, 73.08, 128.21, 128.54, 135.82, 174.22. *u*<sub>max</sub> (thin film, cm<sup>-1</sup>): 3384, 3033-2875, 1737, 1363, 1137, 1081, 880, 735, 697. [α]<sub>D</sub><sup>25</sup> (CHCl<sub>3</sub>; *c* = 0.138): - 17.39. MS: C<sub>14</sub>H<sub>21</sub>NO<sub>3</sub>, *m/z* (ES<sup>+</sup>) 252.16 [M+H]<sup>+</sup>. HRMS: Calculated C<sub>14</sub>H<sub>22</sub>NO<sub>3</sub> 252.1600, found 252.1594.

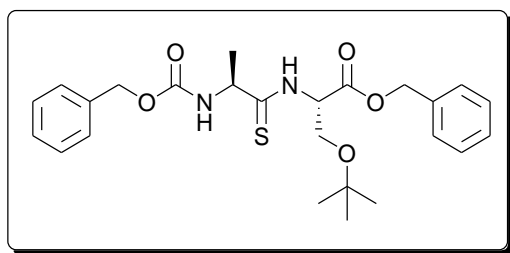
**(S)-benzyl-2-((S)-2-benzylloxycarbonylpropanamino)-3-tert-butoxypropanoate (67).**



**65** (2.027 g; 8.07 mM) and *N*-(carboxybenzyl)-*L*-alanine (1.980 g; 8.87 mM) was dissolved in 10 mL of anhydrous DMF under nitrogen and cooled to 0°C. TEA (2.25 mL; 16.13 mM) was added dropwise and the reaction stirred for 10 minutes. DPPA (1.91 mL; 8.87 mM) was added dropwise and the reaction stirred for 18 hours at 0°C. The solvent was removed *in vacuo* to give a pale brown oil. The oil was dissolved in 30 mL EtOAc and washed with two 15 mL portions of NH<sub>4</sub>Cl, two 15 mL portions of Na<sub>2</sub>CO<sub>3</sub> and one 15 mL portion of brine. The organic layer was dried over anhydrous MgSO<sub>4</sub> to yield 2.528 g of **67** as a pale brown oil which solidified upon refrigeration to an off white sticky solid (5.54 mM, 69%).

R<sub>f</sub>: 0.35 (EtOAc:Pet ether 4:6). <sup>1</sup>H NMR (300 MHz, chloroform-*d*) δ ppm 1.08 (s, 9H, CH<sub>3</sub> *tert*-butyl), 1.40 (d, *J*=7.16 Hz, 3H, CH<sub>3</sub> alanine), 3.54 (ABdd, *J*=8.85, 3.01 Hz, 1H, CH<sub>2</sub> serine), 3.84 (ABdd, *J*=9.04, 2.64 Hz, 1H, CH<sub>2</sub> serine), 4.30 (quin, *J*=7.44 Hz, 1H, CH alanine), 4.74 (dt, *J*=8.48, 2.83 Hz, 1H, CH serine), 5.04 - 5.28 (m, 4H, CH<sub>2</sub> benzyl), 5.43 (d, *J*=6.78 Hz, 1H, NH alanine), 6.64 (d, *J*=8.48 Hz, 1H, NH serine), 7.32 - 7.37 (m, 10H, CH aromatic). <sup>13</sup>C NMR (75 MHz, chloroform-*d*) δ ppm 19.06, 27.23, 50.43, 52.83, 61.74, 66.96, 67.17, 73.42, 73.50, 128.07, 128.18, 128.27, 128.39, 128.55, 135.40, 136.20, 136.25, 155.72, 170.10, 172.80.  $\nu_{\max}$  (thin film, cm<sup>-1</sup>): 3357, 3281, 2975, 1735, 1654, 1507, 1355, 1243, 1044, 744, 696.  $[\alpha]_D^{25}$  (CHCl<sub>3</sub>; *c* = 0.117): - 4.51. MS: C<sub>25</sub>H<sub>32</sub>N<sub>2</sub>O<sub>6</sub>, *m/z* (ES<sup>+</sup>) 457.23 [M+H]<sup>+</sup>. HRMS: Calculated C<sub>25</sub>H<sub>33</sub>N<sub>2</sub>O<sub>6</sub> 457.2339, found 457.2346. MP: 69.7°C

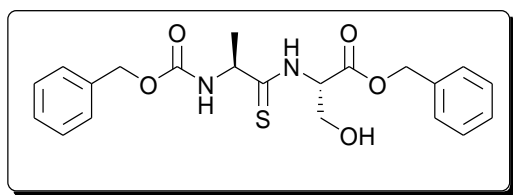
**(S)-benzyl-2-((S)-2-benzyloxycarbonylpropanethioamino)-3-tert-butoxypropanoate (69).**



**67** (2.528 g; 5.54 mM) and Lawesson's reagent (1.148 g; 2.84 mM) was dissolved in 30 mL anhydrous toluene. The reaction was refluxed under nitrogen at 115°C for 4 hours. The solution was allowed to return to room temperature, the solvent removed *in vacuo* and the residue dissolved onto silica. Purification was obtained by flash chromatography (DCM followed by 9:1 Pet ether: EtOAc) to give 2.016 g of **69** as a yellow oil (4.27 mM, 77%).

R<sub>f</sub>: 0.29 (EtOAc:Pet ether 4:6). <sup>1</sup>H NMR (300 MHz, chloroform-*d*) δ ppm 1.14 (s, 9H, CH<sub>3</sub> *tert*-butyl), 1.43 (d, *J*=7.14 Hz, 3H, CH<sub>3</sub> alanine), 3.92 (m, *J*=5.46, 2.83 Hz, 2H, CH<sub>2</sub> serine), 4.79 (m, 1H, CH alanine), 4.91 (m, 1H, CH serine), 5.08 - 5.32 (m, 4H, CH<sub>2</sub> benzyl), 5.48 (d, *J*=6.15 Hz, 1H, NH alanine), 7.18 - 7.44 (m, 10H, CH aromatic), 8.49 (d, *J*=7.91 Hz, 1H, NH serine). <sup>13</sup>C NMR (75 MHz, chloroform-*d*) δ ppm 20.47, 27.95, 56.24, 58.24, 64.92, 68.12, 68.57, 73.52, 128.21, 128.34, 128.69, 128.91, 136.27, 136.41, 155.14, 171.82, 204.27. *u*<sub>max</sub> (thin film, cm<sup>-1</sup>): 3293, 2976, 1404, 1506, 1192, 1045, 743, 695. [α]<sub>D</sub><sup>25</sup> (CHCl<sub>3</sub>; *c* = 0.0324): - 0.31. MS: C<sub>25</sub>H<sub>32</sub>N<sub>2</sub>O<sub>5</sub>S, *m/z* (ES<sup>+</sup>) 473.21 [M+H<sup>+</sup>]. HRMS: Calculated C<sub>25</sub>H<sub>33</sub>N<sub>2</sub>O<sub>5</sub>S 473.2110, found 473.2107.

**(S)- benzyl-2-((S)-2-benzyloxycarbonylpropanethioamido)-3-hydroxypropanoate (71).**

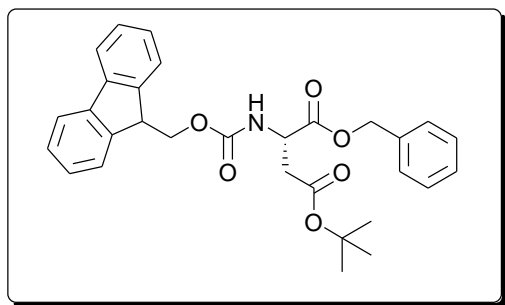


**69** (483 mg; 1.02 mM) was dissolved in 30 mL of 33% TFA in DCM under a nitrogen atmosphere. After 1 hour a further 20 mL portion of 33% TFA in DCM was added to give a final ratio of ~1 mL 33% TFA in DCM per 10 mg of starting material. The reaction was allowed to proceed for 5 hours before the solvent was removed *in vacuo* and the residue dissolved in 50 mL water, filtered through glass wool and extracted with 20 mL Et<sub>2</sub>O. The aqueous layer was lyophilised to give 391 mg of **71** as a yellow oil (0.94 mM; 92%).

R<sub>f</sub>: 0.21 (EtOAc:Pet ether 6:4). <sup>1</sup>H NMR (300 MHz, chloroform-*d*) δ ppm 1.41 (d, *J*=7.14 Hz, 3H, CH<sub>3</sub> alanine), 3.91 ABdd, *J*=8.94, 3.11 Hz, 1H, CH<sub>2</sub> serine), 4.23 (ABdd, *J*=9.02, 2.67 Hz, 1H, CH<sub>2</sub> serine), 4.79 (m, 1H, CH alanine), 4.87 (m, 1H, CH serine), 5.11 - 5.32 (m, 4H, CH<sub>2</sub> benzyl), 5.51 (d, *J*=6.15 Hz, 1H, NH alanine), 7.15 - 7.44 (m, 10H, CH aromatic), 8.42 (d, *J*=7.94 Hz, 1H, NH serine). <sup>13</sup>C NMR (75 MHz, chloroform-*d*) δ ppm 21.36, 56.14, 58.36, 64.83, 67.93, 68.84, 128.21, 128.30, 128.42, 136.31, 136.52, 155.32, 172.18, 203.96. *ν*<sub>max</sub> (thin film, cm<sup>-1</sup>): 3335, 2977, 2932, 1683, 1367, 1248, 1154, 1053. [α]<sub>D</sub><sup>25</sup> (CHCl<sub>3</sub>; *c* = 0.0094): + 12.23. MS: C<sub>21</sub>H<sub>24</sub>N<sub>2</sub>O<sub>5</sub>S, *m/z* (ES<sup>+</sup>) 417.15 [M+H]<sup>+</sup>. HRMS: Calculated C<sub>21</sub>H<sub>25</sub>N<sub>2</sub>O<sub>5</sub>S 417.1484, found 417.1487.



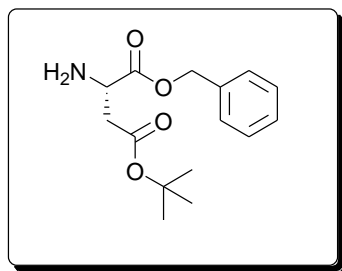
**(S)-1-benzyl-4-tert-butyl-2-fluorenylmethoxycarbonylsuccinate (64).**



*N*-(9-Fluorenylmethoxycarbonyl)-*O*-(*tert*-butyl)-*L*-aspartic acid (**62**) (15.005 g; 36.47 mM) and sodium bicarbonate (6.131 g; 72.91 mM) was dissolved in 30 mL anhydrous DMF under a nitrogen atmosphere. Benzyl bromide (17.33 mL; 145.87 mM) was added dropwise and the reaction stirred for 72 hours at room temperature. The solvent was removed *in vacuo* to yield a clear oil. The oil was dissolved in 50mL EtOAc washed three times with 50mL water and once with 20mL brine, dried over anhydrous MgSO<sub>4</sub> and filtered. 200mL of petroleum ether was added and the reaction stirred for 30 minutes to yield a white precipitate which was collected by filtration. 100mL of 10% EtOAc in petroleum ether was added to the filtrate, stirred and the white precipitate collected *via* filtration. 15.254 g of **64** was collected as a white solid (30.41 mM, 83%).

R<sub>f</sub>: 0.47 (EtOAc:Pet ether 4:6). <sup>1</sup>H NMR (300 MHz, chloroform-*d*) δ ppm 1.44 (s, 9H, CH<sub>3</sub> *tert*-butyl), 2.81, (ABdd, *J*=4.10 Hz, 1H, CH<sub>2</sub> aspartate), 3.02 (ABdd, *J*=4.50 Hz, 1H, CH<sub>2</sub> aspartate), 4.26 (t, *J*=7.20 Hz, 1H, CH Fmoc), 4.30-4.49 (m, 2H, CH<sub>2</sub> Fmoc), 4.64-4.71 (m, 1H, CH aspartate), 5.23 (qAB, *J*=12.06 Hz, 2H, CH<sub>2</sub>-benzyl), 5.87 (d, *J*=8.67 Hz, 1H, NH), 7.29-7.47 (m, 9H, CH benzyl, CH Fmoc), 7.62 (d, *J*=7.54 Hz, 2H, CH Fmoc), 7.79 (d, *J*=7.54Hz, 2H, CH Fmoc). <sup>13</sup>C NMR (75 MHz, chloroform-*d*) δ ppm 28.01, 37.75, 47.07, 50.61, 67.31, 67.51, 81.94, 120.01, 125.17, 125.22, 127.10, 127.74, 128.29, 128.46, 128.62, 135.24, 141.29, 143.70, 143.92, 156.02, 170.04, 170.86 (C=O).  $\nu_{\max}$  (thin film, cm<sup>-1</sup>): 3416, 3186-2857, 1735, 1723, 1493, 1341, 1180, 1026, 739, 728.  $[\alpha]_{\text{D}}^{25}$  (CHCl<sub>3</sub>; *c* = 0.105): + 15.23. MS: C<sub>30</sub>H<sub>31</sub>NO<sub>6</sub>, *m/z* (ES<sup>+</sup>) 502.22 [M+H]<sup>+</sup>. HRMS: Calculated C<sub>30</sub>H<sub>32</sub>NO<sub>6</sub> 502.2224, found 502.2213. MP: 126°C.

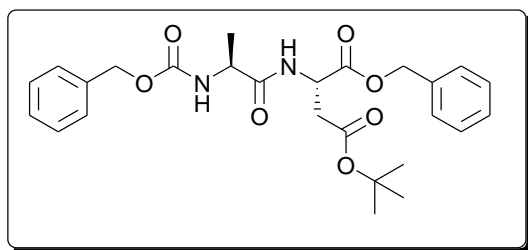
**(S)- 1-benzyl-4-tert-butyl-2-aminosuccinate (66).**



**64** (4.202 g; 8.38 mM) was dissolved in 20 mL of anhydrous THF under a nitrogen atmosphere and cooled to 0°C. A 1.0 M solution of TBAF in THF (9.22 mL, 0.92 mM) was added dropwise. The solution stirred at 0°C for 30 minutes and allowed to proceed a further 2-3 hours at room temperature, monitored by TLC. The solvent was removed *in vacuo* to yield a sticky pink residue which was taken up into 20 mL of water. The pH of the solution was adjusted to pH 2 using 2 M HCl, and 20 mL of EtOAc was added. The aqueous layer was separated and extracted with a further two 10 mL portions of EtOAc. The aqueous phase was adjusted to pH 8-9 using 2 M NaOH, and extracted with one 20 mL and two 10 mL portions of EtOAc. The EtOAc portions from the basic aqueous extraction were combined, dried over anhydrous MgSO<sub>4</sub> and then filtered. The solvent was reduced *in vacuo*, to give 1.926 g of **66** as a clear oil (6.87 mM, 82%).

R<sub>f</sub>: 0.43 (EtOAc:Pet ether 4:6). <sup>1</sup>H NMR (300 MHz, chloroform-*d*) δ ppm 1.42 (s, 9H, CH<sub>3</sub> *tert*-butyl), 2.67-2.73 (m, 2H, CH<sub>2</sub> aspartate), 3.72-3.81 (m, 1H, CH aspartate), 5.06-5.30 (m, 2H, CH<sub>2</sub>-benzyl), 7.30-7.45 (m, 5H, CH benzyl). <sup>13</sup>C NMR (75 MHz, chloroform-*d*) δ ppm 28.29, 39.87, 47.07, 64.84, 66.97, 81.29, 128.29, 128.60, 141.43, 170.34, 174.33.  $\nu_{\max}$  (thin film, cm<sup>-1</sup>): 3106-2852, 1722, 1671, 1456, 1392, 1148, 852, 735, 697.  $[\alpha]_D^{25}$  (CHCl<sub>3</sub>; c = 0.110): - 4.55. MS: C<sub>15</sub>H<sub>21</sub>NO<sub>4</sub>, *m/z* (ES<sup>+</sup>) 280.15 [M+H]<sup>+</sup>. HRMS: Calculated C<sub>15</sub>H<sub>22</sub>NO<sub>4</sub> 280.1543, found 280.1542.

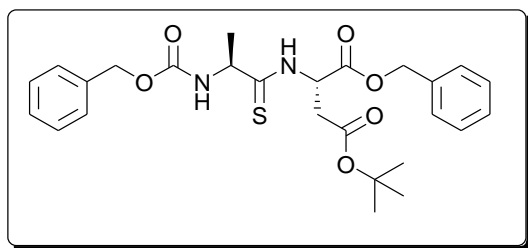
**(S)- 1-benzyl-4-tert-butyl-2-((S)-2-tert-benzylloxycarbonylpropanamido)succinate (68).**



**66** (2.498 g; 8.94 mM) and *N*-(carboxybenzyl)-*L*-alanine (2.200 g; 9.84 mM) was dissolved in 10 mL of anhydrous DMF under nitrogen and cooled to 0°C. TEA (2.50 mL; 17.90 mM) was added dropwise and the reaction stirred for 10 minutes. 1.1eq DPPA (2.12 mL; 9.84 mM) was added dropwise and the reaction stirred for 18 hours at 0°C. The solvent was removed in *vacuo* to yield a pale brown oil. The oil was dissolved in 30 mL EtOAc and washed with two 15 mL portions of NH<sub>4</sub>Cl, two 15 mL portions of Na<sub>2</sub>CO<sub>3</sub> and one 15 mL portion of brine. The organic layer was dried over anhydrous MgSO<sub>4</sub> to yield 3.437 g of **68** as a pale brown oil which solidified upon refrigeration to an orange sticky solid (7.07mM, 79%).

R<sub>f</sub>: 0.37 (EtOAc:Pet ether 4:6). <sup>1</sup>H NMR (300 MHz, chloroform-*d*) δ ppm 1.36 (s, 3H, CH<sub>3</sub> alanine), 1.40 (s, 9H, CH<sub>3</sub> *tert*-butyl), 2.75 (ABm, *J*=4.33 Hz, 1H, CH<sub>2</sub> aspartate), 2.96 (ABm, *J*=4.52 Hz, 1H, CH<sub>2</sub> aspartate), 4.32 (m, *J*=6.59 Hz, 1H, CH alanine), 4.86 (dq, *J*=8.38, 4.36 Hz, 1H, CH aspartate), 5.07 - 5.27 (m, 4H, CH<sub>2</sub> benzyl), 5.65 (d, *J*=7.54 Hz, 1H, NH alanine), 7.08 - 7.16 (m, 1H, NH aspartate), 7.34 (s, 10H, CH aromatic). <sup>13</sup>C NMR (75 MHz, chloroform-*d*) δ ppm 18.74, 18.87, 27.93, 27.96, 37.18, 37.18, 48.71, 48.80, 50.45, 66.91, 67.00, 67.47, 81.84, 81.93, 128.09, 128.16, 128.19, 128.26, 128.30, 128.46, 128.53, 128.60, 135.16, 136.20, 136.28, 155.83, 155.91, 169.85, 170.10, 170.52, 170.57, 172.25, 172.33.  $\nu_{\max}$  (thin film, cm<sup>-1</sup>): 3673, 3361, 3293, 2980, 1701, 1646, 1360, 1217, 1056, 695.  $[\alpha]_D^{25}$  (CHCl<sub>3</sub>; *c* = 0.092): +8.66. MS: C<sub>26</sub>H<sub>32</sub>N<sub>2</sub>O<sub>7</sub>, *m/z* (ES<sup>+</sup>) 485.23 [M+H<sup>+</sup>]. HRMS: Calculated C<sub>26</sub>H<sub>33</sub>N<sub>2</sub>O<sub>7</sub> 485.2288, found 485.2293. MP: 94.9°C

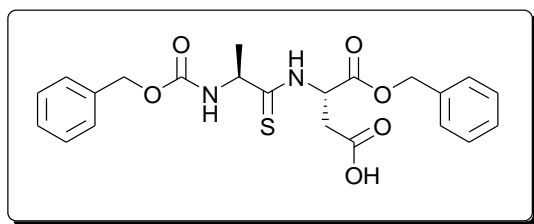
**(S)- 1-benzyl-4-tert-butyl-2-((S)-2-tert-benzylloxycarbonylpropanethioamido)succinate (70).**



**68** (3.437 g; 7.07 mM) and Lawesson's reagent (1.465 g; 3.63 mM) was dissolved in 30 mL anhydrous toluene. The reaction was refluxed at 115°C for 4 hours, under nitrogen. The solution was allowed to return to room temperature, the solvent removed *in vacuo* and the residue dissolved onto silica. Purification was achieved by flash chromatography (DCM followed by 8:2 Pet ether: EtOAc) to give 2.914 g of **70** as a yellow oil (5.82 mM; 82%).

R<sub>f</sub>: 0.32 (EtOAc:Pet ether 4:6). <sup>1</sup>H NMR (300 MHz, chloroform-*d*) δ ppm 1.34 - 1.40 (m, 9H, CH<sub>3</sub> *tert*-butyl), 1.44 (d, *J*=6.78 Hz, 3H, CH<sub>3</sub> alanine), 3.00 (m, *J*=4.43 Hz, 2H, CH<sub>2</sub> aspartate), 4.56 (quin, *J*=6.88 Hz, 1H, CH alanine), 5.03 - 5.29 (m, 4H, CH<sub>2</sub> benzyl), 5.35 - 5.48 (m, 1H, CH aspartate), 5.69 (d, *J*=6.22 Hz, 1H, NH alanine), 7.34 (s, 10H, CH aromatic), 8.65 (d, *J*=7.72 Hz, 1H, NH aspartate). <sup>13</sup>C NMR (75 MHz, chloroform-*d*) δ ppm 22.25, 27.96, 35.51, 35.80, 53.86, 56.80, 67.02, 67.12, 67.72, 82.12, 82.26, 128.09, 128.17, 128.37, 128.54, 128.57, 128.64, 134.96, 136.21, 155.45, 169.60, 169.70, 169.87, 170.04, 204.59, 205.34. *u*<sub>max</sub> (thin film, cm<sup>-1</sup>): 3279, 2977, 1704, 1498, 1148, 1047, 735, 695, 583. [α]<sub>D</sub><sup>25</sup> (CHCl<sub>3</sub>; *c* = 0.098): + 31.48. MS: C<sub>26</sub>H<sub>32</sub>N<sub>2</sub>O<sub>6</sub>S, *m/z* (ES<sup>+</sup>) 501.21 [M+H]<sup>+</sup>. HRMS: Calculated C<sub>26</sub>H<sub>33</sub>N<sub>2</sub>O<sub>6</sub>S 501.2059, found 501.2062.

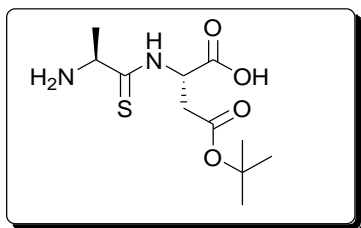
**(S)- 4-benzyloxy-3-((S)-2-*tert*-benzyloxycarbonylpropanethioamido)-4-oxobutanoic acid (72).**



**70** (500 mg; 1.00 mM) was dissolved in 30 mL of 33% TFA in DCM under a nitrogen atmosphere. After 1 hour a further 20 mL portion of 33% TFA in DCM was added to give a final ratio of ~1 mL 33% TFA in DCM per 10 mg of starting material. The reaction was allowed to proceed for 5 hours before the solvent was removed *in vacuo* and the residue dissolved in 50 mL water, filtered through glass wool and extracted with 20 mL Et<sub>2</sub>O. The aqueous layer was lyophilised to give 413 mg of **72** as a pale yellow oil (0.93 mM; 93%).

R<sub>f</sub>: 0.42 (DCM:MeOH 19:1). <sup>1</sup>H NMR (300 MHz, chloroform-*d*) δ ppm 1.32 (d, *J*=6.59 Hz, 3H, CH<sub>3</sub> alanine), 2.98 - 3.22 (ABdq, 2H, CH<sub>2</sub> aspartate), 4.81 - 5.21 (m, 5H, CH<sub>2</sub> benzyl, CH alanine), 5.47 (br. s., 1H, CH aspartate), 5.88 (d, *J*=8.48 Hz, 1H, NH alanine), 7.21 - 7.36 (m, 10H, CH aromatic), 9.07 (d, *J*=7.72 Hz, 2H, NH aspartate). <sup>13</sup>C NMR (75 MHz, chloroform-*d*) δ ppm 22.28, 35.47, 35.82, 53.89, 56.74, 67.03, 67.52, 128.19, 128.43, 128.56, 128.69, 135.21, 136.81, 155.41, 169.82, 170.60, 205.42. ν<sub>max</sub> (thin film, cm<sup>-1</sup>): 3306, 2978, 2930, 1715, 1506, 1393, 1367, 1246, 1153, 910. [α]<sub>D</sub><sup>25</sup> (CHCl<sub>3</sub>; c = 0.0102): + 67.93. MS: C<sub>22</sub>H<sub>24</sub>N<sub>2</sub>O<sub>6</sub>S, *m/z* (ES<sup>+</sup>) 445.14 [M+H<sup>+</sup>]. HRMS: Calculated C<sub>22</sub>H<sub>25</sub>N<sub>2</sub>O<sub>6</sub>S 445.1433, found 445.1428.

**(S)- 2-((S)-2-aminopropanethioamido)succinic acid (**73**).**



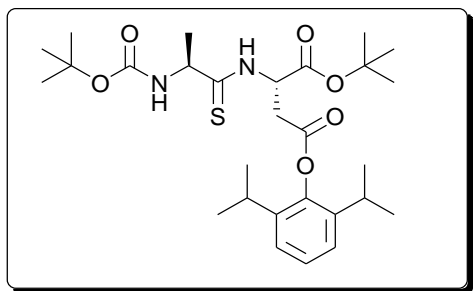
**72** (1.023g, 2.04 mM) was dissolved in 10 ml anhydrous THF and cooled to -78°C. Approximately 10 ml of liquid ammonia was added, the mixture stirred for 10 minutes and then sodium metal (188 mg, 8.17 mM) added in small portions to form a dark blue solution. The reaction was stirred under nitrogen for 3 hours, before being quenched with  $\text{NH}_4\text{Cl}_{(\text{s})}$  and warmed to room temperature. The solvent was removed *in vacuo*, the residue taken up in 20ml of EtOAc and washed with two 10ml portions of water. The aqueous phase was acidified to pH 2 with 2M HCl and extracted with two 20ml portions of EtOAc and one 20ml portion of  $\text{CH}_3\text{Cl}$ . The organic phases were combined, dried with  $\text{MgSO}_4$ , filtered, and the solvent reduced *in vacuo* to give 520 mg of **73** as a clear oil (1.88 mM, 92%).

$R_f$ : 0.32 (1:9:90  $\text{NH}_4\text{OH}:\text{MeOH}:\text{DCM}$ )  $^1\text{H}$  NMR (300 MHz, methanol- $d_4$ )  $\delta$  ppm 1.36-1.43 (m, 9.5H,  $\text{CH}_3$  *tert*-butyl,  $\text{CH}_3$  alanine\*), 1.51 (d,  $J=6.81$  Hz, 2.5H,  $\text{CH}_3$  alanine), 2.98-3.03 (m, 2H,  $\text{CH}_2$  aspartate), 4.39 (quin,  $J=6.94$  Hz, 1H,  $\text{CH}$  alanine), 5.54 (t,  $J=5.83$  Hz, 1H,  $\text{CH}$  aspartate). \* minor rotamer.  $^{13}\text{C}$  NMR (75 MHz, methanol- $d_4$ )  $\delta$  ppm 19.80, 27.96, 34.92, 54.21, 55.98, 82.18, 170.83, 171.92, 202.74. MS:  $\text{C}_{11}\text{H}_{20}\text{N}_2\text{O}_4\text{S}$   $m/z$  (ES+) 277.12  $[\text{M}+\text{H}]^+$ . HRMS: Calculated  $\text{C}_{11}\text{H}_{21}\text{N}_2\text{O}_4\text{S}$  277.1222, found 277.1228.

### 6.3 Synthesis of PepT1 targeted prodrugs using commercially available drugs (section 2.5).

#### 6.3.1 Propofol prodrug (section 2.5.1).

**(S)-1-tert-butyl-4-(2,6-diisopropylphenyl)-2-((S)-2-tert-butoxycarbonylpropanethioamido) succinate (75).**



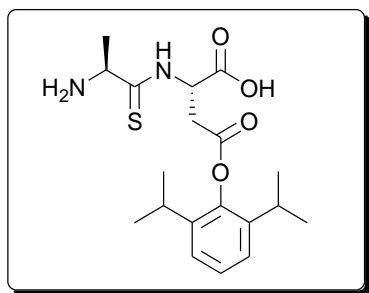
**57** (222 mg; 0.59 mM), EDC.HCl (124 mg; 0.65 mM), DMAP (72 mg; 0.59 mM) and 2,6-diisopropylphenol (**74**) (104  $\mu$ l; 0.56 mM) were stirred in 3 mL anhydrous DMF for one hour at 0 °C. The solution was warmed to room temperature and stirred for 72 hours. The solvent was removed *in vacuo* and the residue purified by flash column chromatography (petroleum ether to 9:1 Pet ether:EtOAc) to give 188mg of **75** as a yellow oil (0.35 mM; 62%).

R<sub>f</sub>: 0.73 (EtOAc:Pet ether 1:9). <sup>1</sup>H NMR (300 MHz, chloroform-*d*)  $\delta$  ppm 1.03 - 1.16 (m, 12H, CH(CH<sub>3</sub>)<sub>2</sub>), 1.34 (s, 3H, CH<sub>3</sub> alanine), 1.35 - 1.44 (m, 18H, CH<sub>3</sub> Boc, CH<sub>3</sub> *tert*-butyl), 2.65 - 2.87 (m, 2H, CH(CH<sub>3</sub>)<sub>2</sub>), 3.32 (m, 1H, CH<sub>2</sub> aspartate), 3.43 - 3.64 (m, 1H, CH<sub>2</sub> aspartate), 4.32 - 4.48 (m, 1H, CH alanine), 4.99 - 5.11 (m, 1H, NH alanine), 5.15 - 5.29 (m, 1H, CH aspartate), 6.95 - 7.22 (m, 3H, CH aromatic), 8.44 - 8.53 (m, 0.1H, NH aspartate\*), 8.61 (d, *J*=7.16 Hz, 0.9H, NH aspartate) \* minor rotamer. <sup>13</sup>C NMR (75 MHz, chloroform-*d*)  $\delta$  ppm 22.14, 23.86, 27.62, 27.82, 28.26, 33.90, 53.88, 56.39, 80.40, 83.55, 124.04, 126.83, 140.05, 145.20, 154.75, 168.16, 170.29, 204.91.  $\nu_{\text{max}}$  (thin film, cm<sup>-1</sup>): 3323, 2959-2856, 1689, 1504, 1439, 1150, 746. MS: C<sub>28</sub>H<sub>44</sub>N<sub>2</sub>O<sub>6</sub>S *m/z* (ES+) 537.30 [M+H]<sup>+</sup>. HRMS: Calculated C<sub>28</sub>H<sub>45</sub>N<sub>2</sub>O<sub>6</sub>S 537.2998, found 537.2996.

This compared to data previously recorded by Price (unpublished) in the group.

$^1\text{H}$  NMR (500 MHz, chloroform-*d*)  $\delta$  ppm 1.18 (d, 12H), 1.50-1.41 (m, 21H), 2.95-2.70 (m, 2H), 3.44-3.35 (m, 1H), 3.66-3.55 (m, 1H), 4.49 (t,  $J = 6.5$ , 1H), 5.13 (s, 1H), 5.28 (s, 1H), 7.15 (d,  $J = 7.5$ , 2H), 7.22 (t,  $J = 7.5$ , 1H), 8.56 (br. s., 0.2 H)\*, 8.69 (d,  $J = 7.0$ , 0.8H).  $^{13}\text{C}$  NMR (100 MHz, chloroform-*d*)  $\delta$  ppm 22.1, 22.8-24.4, 27.8, 28.2, 34.2, 53.7, 53.9, 83.4, 124.0, 126.8, 140.0, 145.2, 155.1, 168.1, 170.3, 204.9. \* minor rotamer.  $\nu_{\text{max}}$  (thin film,  $\text{cm}^{-1}$ ): 3323, 2980, 2934, 1728, 1514, 1396, 1370, 1335, 1248, 1158, 1053, 912, 846, 734.  $[\alpha]_{\text{D}}^{31}$  ( $\text{CHCl}_3$ ;  $c = 3.00$ ): +60.20.

**(S)-2-((S)-2aminopropanethioamido)-4-(2,6-diisopropylphenoxy)-4-oxobutanoic acid (76).**



**75** (103 mg; 0.19 mM) was dissolved in 5 mL 97% formic acid and the solution refluxed at 100 °C for three hours. The reaction was cooled to room temperature and the formic acid removed *in vacuo*. The residue was taken up in 5 mL distilled water, filtered through a pipette plugged with glass wool and extracted with 2 mL  $\text{Et}_2\text{O}$ . The aqueous layer was lyophilised to give 70 mg of **76** as a white solid in formate salt form (0.16 mM; 87%).

$^1\text{H}$  NMR (300 MHz, methanol- $d_4$ )  $\delta$  ppm 1.04 - 1.12 (d,  $J=6.78$  Hz, 12H,  $\text{CH}(\text{CH}_3)_2$ ), 1.37 - 1.43 (m, 1.4H,  $\text{CH}_3$  alanine\*), 1.50 (d,  $J=6.78$  Hz, 1.6H,  $\text{CH}_3$  alanine), 2.83 - 2.93 (m, 1H,  $\text{CH}(\text{CH}_3)_2$ ), 3.27 (d,  $J=5.65$  Hz, 2H,  $\text{CH}_2$  aspartate), 4.23 (m,  $J=6.78$  Hz, 1H, CH alanine), 5.41 (dt,  $J=9.42$ , 5.56 Hz, 0.2H, CH aspartate\*), 5.48 (t,  $J=5.65$  Hz, 0.8H, CH aspartate), 7.02 - 7.18 (m, 3H, CH aromatic), 7.90 (br. s., 1H, NH aspartate). \* minor rotamer.  $^{13}\text{C}$  NMR (75 MHz, methanol- $d_4$ )  $\delta$  ppm 20.80,



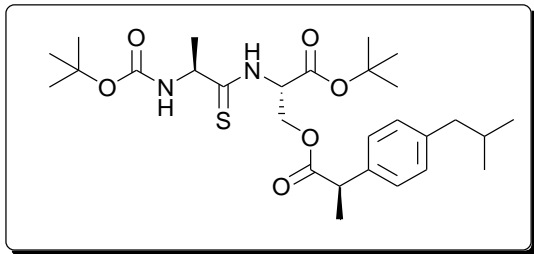
23.23, 28.18, 28.56, 31.71, 35.59, 37.04, 55.53, 56.15, 125.00, 127.88, 141.71, 146.69, 170.99, 171.84, 202.17.  $\nu_{\max}$  (thin film,  $\text{cm}^{-1}$ ): 3379, 2967, 2522, 1660, 1453, 1385, 1364, 1140. MS:  $\text{C}_{19}\text{H}_{28}\text{N}_2\text{O}_4\text{S}$   $m/z$  (ES+) 381.1  $[\text{M}+\text{H}]^+$ . HRMS: Calculated  $\text{C}_{19}\text{H}_{29}\text{N}_2\text{O}_4\text{S}$  381.1843, found 381.1846.

This compared to data previously recorded by Price (unpublished) in the group, so no further characterisation was carried out.

$^1\text{H}$  NMR (500 MHz, methanol- $d_4$ )  $\delta$  ppm 1.17 (s, 6H), 1.18 (s, 6H), 1.49 (d,  $J = 6.5$ , Ala- $\text{CH}_3$ , 3H), 2.85-3.05 (m, 2H), 3.22-3.55 (m, 2H), 4.27 (q,  $J = 7.0$ , 1H Ala- $\alpha$ -CH), 5.53 (br. s., 1H), 7.15-7.23 (m, 3H).  $^{13}\text{C}$  NMR (100 MHz, methanol- $d_4$ )  $\delta$  ppm 20.9, 23.5, 24.2, 28.3, 28.7, 35.7, 55.2, 55.7, 125.1, 127.9, 141.8, 146.8, 171.1, 171.9, 202.3. MS:  $\text{C}_{19}\text{H}_{28}\text{N}_2\text{O}_4\text{S}$   $m/z$  (ES $^+$ ) 381.1  $[\text{M}+\text{H}^+]$ . HRMS: Calculated  $\text{C}_{19}\text{H}_{29}\text{N}_2\text{O}_4\text{S}$ : 381.1843, found: 381.1836. \* minor rotamer.

6.3.2. Ibuprofen prodrug (section 2.5.2).

**(S)-2-((S)-2-*tert*-butoxycarbonylpropanethioamido)-3-((R)-2-(4-isobutylphenyl)propionyloxy)-propanoic acid *tert*-butyl ester (78).**

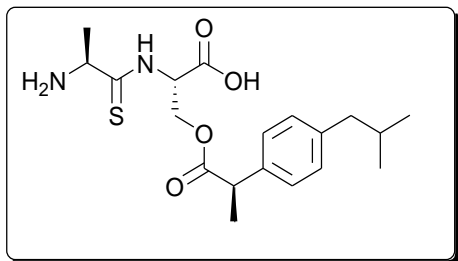


Published data: Foley *et al.*<sup>117</sup>

Ibuprofen (**77**) (848 mg; 4.11 mM) and HBTU (1.870 g; 4.93 mM) were dissolved in 10 mL anhydrous DMF under a nitrogen atmosphere. DIPEA (1.22 mL; 6.99 mM) was added dropwise and the solution stirred at room temperature for 30 minutes. **56** (1.146 g; 3.29 mM) was dissolved in 5 mL anhydrous DMF was added and the solution stirred at room temperature for three days. The solvent was removed *in vacuo* and the residue purified by flash column chromatography (a gradient of 2:8 to 7:3 EtOAc:Pet ether) to give 1.307 g of **78** as a yellow oil (2.44 mM; 74%).

R<sub>f</sub>: 0.57 (EtOAc:Pet ether 4:6). <sup>1</sup>H NMR (300 MHz, chloroform-*d*) δ ppm 0.86 - 0.92 (m, 6H, CH(CH<sub>3</sub>)<sub>2</sub>), 1.26 (d, *J*=6.97 Hz, 3H, CH<sub>3</sub> alanine) 1.35 (s, 3H, Ibu-CH<sub>3</sub>), 1.45-1.51 (m, 18H, CH<sub>3</sub> Boc, CH<sub>3</sub> *tert*-butyl), 1.76 - 1.91 (m, 1H, CH(CH<sub>3</sub>)<sub>2</sub>), 2.44 (d, *J*=7.16 Hz, 2H, Ibu-CH<sub>2</sub>), 3.57 - 3.80 (m, 1H, Ibu-CH), 4.41 (m, 2H, CH alanine, CH<sub>2</sub> serine), 4.64 (ABdd, *J*=2.60, 11.49, 1H, CH<sub>2</sub> serine), 4.95 (br. s., 0.2H, NH alanine\*), 5.07 - 5.25 (m, 0.8H, NH alanine), 6.95 - 7.31 (m, 4H, CH aromatic), 8.26 - 8.38 (d, *J*=6.41 Hz, 0.7H, NH serine), 8.41 - 8.56 (d, *J*=6.59 Hz, 0.3H, NH serine\*). \* minor rotamer. <sup>13</sup>C NMR (75 MHz, chloroform-*d*) δ ppm 18.16, 18.45, 27.76, 27.87, 28.28, 30.19, 44.79, 44.97, 45.04, 57.11, 57.23, 62.87, 83.49, 127.29, 129.40, 129.50, 137.07, 137.27, 140.76, 140.83, 167.30, 174.08, 180.49, 205.22, 205.44.  $\nu_{\max}$  (thin film, cm<sup>-1</sup>): 3307, 2977, 2931, 1715, 1614, 1505, 1394, 1368, 1248, 1157, 778. MS: C<sub>28</sub>H<sub>44</sub>N<sub>2</sub>O<sub>6</sub>S *m/z* (ES+) 537.30 [M+H]<sup>+</sup>. HRMS: Calculated C<sub>28</sub>H<sub>45</sub>N<sub>2</sub>O<sub>6</sub>S 537.2998, found 537.3003.

**(S)-2-((S)-2-aminopropanethioamido)-3-((R)-2-(4-isobutylphenyl)propionyloxy)-propanoic acid  
(79).**



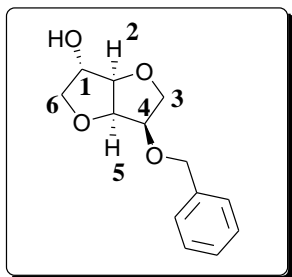
Published data: Foley *et al.*<sup>117</sup>

**78** (532 mg; 0.99 mM) was dissolved in 15 mL 97% formic acid and refluxed at 100°C for three hours. The reaction mixture was cooled to room temperature and the formic acid removed *in vacuo*. The residue was taken up in 15 mL distilled water, filtered through a pipette plugged with glass wool and extracted with 7 mL Et<sub>2</sub>O. The aqueous layer was lyophilised to give 414 mg of **79** as a yellow resin in formate salt form (0.97 mM; 98%).

<sup>1</sup>H NMR (300 MHz, methanol-*d*<sub>4</sub>) δ ppm 0.86 - 0.95 (m, 6H, CH(CH<sub>3</sub>)<sub>2</sub>), 1.45 (dd, *J*=7.16, 1.70 Hz, 5H, CH<sub>3</sub>-ibuprofen, CH<sub>3</sub> alanine), 1.54 (d, *J*=6.59 Hz, 1H, CH<sub>3</sub>-alanine\*), 1.79 - 1.92 (m, 1H, CH(CH<sub>3</sub>)<sub>2</sub>), 2.46 (d, *J*=6.97 Hz, 2H, CH<sub>2</sub>-ibuprofen), 3.62 - 3.81 (m, 1H, CH-ibuprofen), 4.15 (q, *J*=6.91 Hz, 1H, CH-alanine), 4.56 (m, *J*=4.71 Hz, 2H, CH<sub>2</sub>-serine), 5.09 (dd, *J*=4.62, 3.30 Hz, 1H, CH serine), 7.08 - 7.14 (m, 2H, CH aromatic), 7.16 - 7.27 (m, 2H, CH aromatic). \* minor rotamer <sup>13</sup>C NMR (75 MHz, methanol-*d*<sub>4</sub>) δ ppm 19.11, 20.40, 22.72, 31.49, 56.20, 60.71, 65.12, 128.23, 130.28, 130.37, 139.83, 142.3, 176.18, 200.58.  $\nu_{\max}$  (thin film, cm<sup>-1</sup>): 3152, 2953, 1732, 1614, 1507, 1455, 1381, 1165, 779. MS: C<sub>19</sub>H<sub>28</sub>N<sub>2</sub>O<sub>4</sub>S *m/z* (ES<sup>+</sup>) 381.1 [M+H]<sup>+</sup>. HRMS: Calculated C<sub>19</sub>H<sub>29</sub>N<sub>2</sub>O<sub>4</sub>S 381.1848, found 381.1845.

### 6.3.3 Aspirin prodrug (section 2.5.3).

#### (3S,3aR,6R,6aR)-6-(benzyloxy)-hexahydrofuro[3,2-b]furan-3-ol (**91**).

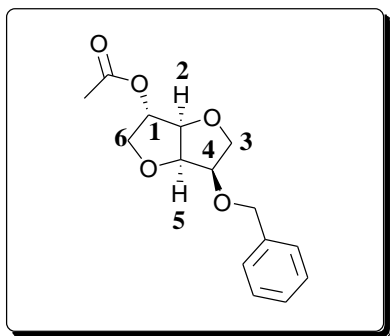


Published data: Huynh *et al.*<sup>130</sup>

Isosorbide (**90**) (20.00g, 136.88 mM), lithium hydride (1.088 g, 136.88 mM), and lithium chloride (5.800 g, 136.88 mM) were dissolved in 65 mL anhydrous DMSO and stirred at 90°C for 20 min under a nitrogen atmosphere. Benzyl chloride (15.75 mL, 136.88 mM) was added dropwise and the reaction stirred for 18 h. The pH of the solution was adjusted to pH 2 with 2 M HCl and extracted with three 50 mL portions of EtOAc. The organic phases were combined and dried over anhydrous MgSO<sub>4</sub> and filtered. The solvent was evaporated *in vacuo* and the residual oil was purified by flash column chromatography (1:1; 3:7; 1.5:8.5 EtOAc:Pet ether) to give 18.767 g of **91** as a tan solid (79.43 mM; 58%).

R<sub>f</sub>: 0.13 (EtOAc:Pet ether 6:4). <sup>1</sup>H NMR (300 MHz, dimethyl sulfoxide-*d*<sub>6</sub>) δ ppm 3.42 (t, *J*=8.19 Hz, 1H, CH<sub>2(ax)</sub>-isosorbide **3**), 3.68 - 3.82 (m, 3H, CH<sub>2(eq)</sub>-isosorbide **3**, CH<sub>2</sub>-isosorbide **6**), 4.01 - 4.11 (m, 2H, CH-isosorbide **1**, CH-isosorbide **4**), 4.28 (d, *J*=4.14 Hz, 1H, CH-isosorbide **5**), 4.44 - 4.52 (ABd, 1H, CH<sub>2</sub>-benzyl), 4.60 - 4.68 (m, 2H, CH<sub>2</sub>-benzyl, CH-isosorbide **2**), 5.18 (s, 1H, OH), 7.25 - 7.41 (m, 5H, CH-benzyl). <sup>13</sup>C NMR (75 MHz, chloroform-*d*) δ ppm 72.17, 74.41, 77.73, 78.31, 81.97, 82.53, 90.60, 129.90, 130.13, 130.43, 140.40. [α]<sub>D</sub><sup>25</sup> (CHCl<sub>3</sub>; c = 0.0133): + 91.80. *u*<sub>max</sub> (thin film, cm<sup>-1</sup>): 3416, 2960-2873, 1368, 1063, 979, 833, 739. MS: C<sub>13</sub>H<sub>16</sub>O<sub>4</sub> *m/z* (ES<sup>+</sup>) 237.11 [M+H]<sup>+</sup>. HRMS: Calculated C<sub>13</sub>H<sub>17</sub>O<sub>4</sub> 237.1127, found: 237.1125. MP: 93.9°C

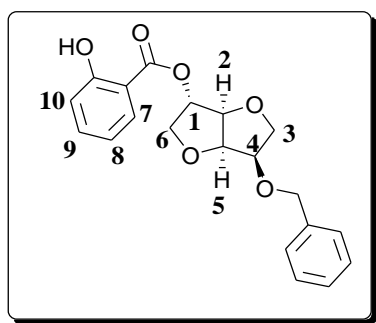
**(3S,3aR,6R,6aR)-6-(benzyloxy)-hexahydrofuro[3,2-b]furan-3-yl acetate (**98**).**



Aspirin (**80**) (2.000 g, 11.10 mM), DCC (2.520 g, 12.21 mM) and DMAP (0.136 g, 1.10 mM) were dissolved in 20 mL anhydrous DCM under a nitrogen atmosphere at 0°C and left to stir for 1 hour. **91** (2.617 g, 11.10 mM) in 10 mL anhydrous DCM was added and reaction mixture stirred at room temperature for 18 hours. The solution was filtered and the DCM removed *in vacuo*. The resultant oil was purified by flash column chromatography (a gradient of 1:1 to 2:4; EtOAc:Pet ether) to give 2.914 g of **98** as an orange oil (10.48 mM, 94%).

R<sub>f</sub>: 0.28 (EtOAc:Pet ether 6:4). <sup>1</sup>H NMR (300 MHz, chloroform-*d*) δ ppm 2.06 (s, 3H, CH<sub>3</sub>-acetyl), 3.64 (dd, *J*=8.67, 7.72 Hz, 1H, CH<sub>2(ax)</sub>-isosorbide **3**), 3.87 (dd, *J*=8.85, 6.59 Hz, 1H, CH<sub>2(eq)</sub>-isosorbide **3**), 3.97 - 4.15 (m, 3H, CH<sub>2</sub>-isosorbide **6**, CH-isosorbide **4**), 4.49 (d, *J*=4.33 Hz, 1H, CH-isosorbide **5**), 4.56 (ABd, *J*=11.87 Hz, 1H, CH<sub>2</sub>-benzyl), 4.68 (t, *J*=4.52 Hz, 1H, CH-isosorbide **2**), 4.76 (ABd, *J*=11.68 Hz, 1H, CH<sub>2</sub>-benzyl), 5.16 (d, *J*=3.77 Hz, 1H, CH-isosorbide **1**), 7.28 - 7.40 (m, 5H, CH benzyl). <sup>13</sup>C NMR (75 MHz, chloroform-*d*) δ ppm 20.94, 70.35, 72.47, 73.75, 76.76, 77.18, 77.61, 78.58, 79.06, 80.57, 85.87, 127.95, 128.49, 137.65, 170.01. *u*<sub>max</sub> (thin film, cm<sup>-1</sup>): 2874, 1743, 1369, 1237, 1102, 1056, 740. [α]<sub>D</sub><sup>25</sup> (CHCl<sub>3</sub>; *c* = 0.0354): + 101.98. MS: C<sub>15</sub>H<sub>18</sub>O<sub>5</sub> *m/z* (ES<sup>+</sup>) 279.12 [M+H]<sup>+</sup>. HRMS: Calculated C<sub>15</sub>H<sub>19</sub>O<sub>5</sub> 279.1233, found: 279.1234.

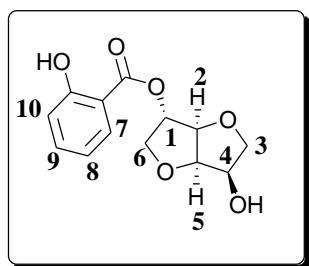
**(3S,3aR,6R,6aR)-6-(benzyloxy)-hexahydrofuro[3,2-b]furan-3-yl 2-hydroxybenzoate (**99**).**



Salicylic acid (**88**) (2.925 g, 21.18 mM), DCC (4.806 g, 23.29 mM) and DMAP (2.587 g, 21.18 mM) were dissolved in 20 mL anhydrous DCM under a nitrogen atmosphere at 0°C and left to stir for 30 minutes. **91** (5.00 g, 21.18 mM in 10 mL anhydrous DCM) was added and reaction mixture stirred at room temperature for 18 hours. The solution was filtered and the filtrate washed with one 30 mL portion of 1 M HCl, one 30 mL portion of saturated aqueous Na<sub>2</sub>HCO<sub>3</sub> and three 30 mL portions of water. The organic layer was dried over anhydrous MgSO<sub>4</sub> and the solvent removed *in vacuo*. The resultant colourless oil was purified by flash column chromatography (a gradient of 3:7 to 7:3 Pet ether: EtOAc) to give 6.538 g of **99** as a cream solid (18.26 mM, 86%).

R<sub>f</sub>: 0.70 (EtOAc:Pet ether 6:4). <sup>1</sup>H NMR (300 MHz, chloroform-*d*) δ ppm 3.68 - 3.78 (m, 1H, CH<sub>2(ax)</sub>-isosorbide **3**), 3.93 (dd, *J*=8.85, 6.59 Hz, 1H, CH<sub>2(eq)</sub>-isosorbide **3**), 4.07 - 4.29 (m, 3H, CH<sub>2</sub>-isosorbide **6**, CH-isosorbide **4**), 4.60 (d, *J*=11.87 Hz, 1H, ABd, 1H, CH<sub>2</sub>-benzyl), 4.66 (d, *J*=4.33 Hz, 1H, CH-isosorbide **5**), 4.76 - 4.83 (m, 2H, CH<sub>2</sub>-benzyl, CH-isosorbide **2**), 5.44 (d, *J*=3.77 Hz, 1H, CH-isosorbide **1**), 6.89 (ddd, *J*=8.10, 7.16, 1.13 Hz, 1H, CH-salicylic **8**), 6.96 - 7.02 (m, 1H, CH-salicylic **10**), 7.28 - 7.41 (m, 5H, CH-benzyl), 7.48 (ddd, *J*=8.48, 7.16, 1.88 Hz, 1H, CH-salicylic **9**), 7.79 - 7.85 (m, *J*=1.70, 0.38 Hz, 1H, CH-salicylic **7**). <sup>13</sup>C NMR (75 MHz, chloroform-*d*) δ ppm 70.54, 72.59, 73.51, 76.63, 79.02, 79.45, 80.70, 85.91, 111.84, 117.75, 119.26, 127.99, 128.04, 128.56, 129.94, 136.22, 137.58, 161.87, 169.25. *ν*<sub>max</sub> (thin film, cm<sup>-1</sup>): 3212, 2962-2877, 1674, 1483, 1141, 1077, 1017, 747, 696, 529. [α]<sub>D</sub><sup>25</sup> (CHCl<sub>3</sub>; *c* = 0.0074): + 95.68. MS: C<sub>20</sub>H<sub>20</sub>O<sub>6</sub> *m/z* (ES<sup>+</sup>) 357.13 [M+H]<sup>+</sup>. HRMS: Calculated C<sub>20</sub>H<sub>21</sub>O<sub>6</sub> 357.1338, found: 357.1341. MP: 59.7°C

**(3S,3aR,6R,6aR)-6-hydroxy-hexahydrofuro[3,2-b]furan-3-yl 2-hydroxybenzoate (**100**).**

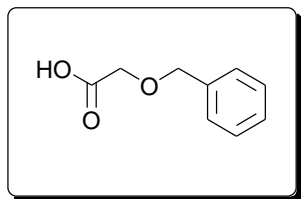


**99** (3.046 g, 8.51 mM) was dissolved in 10 mL 1:1 MeOH:EtOAc. 10% Pd/C (300 mg) was added and the suspension stirred under a hydrogen atmosphere at room temperature for 24 hours. The reaction mixture was filtered through a Celite<sup>®</sup> bed and the organic solvent removed *in vacuo*. 2.245 g of **100** was obtained as a clear oil (8.43 mM, 99%).

R<sub>f</sub>: 0.65 (EtOAc:Pet ether 6:4). <sup>1</sup>H NMR (300 MHz, chloroform-*d*) δ ppm 3.65 (dd, *J*=9.51, 5.93 Hz, 1H, CH<sub>2(ax)</sub>-isosorbide **3**), 3.96 (dd, *J*=9.42, 6.03 Hz, 1H, CH<sub>2(eq)</sub>-isosorbide **3**), 4.11 - 4.27 (m, 2H, CH<sub>2</sub>-isosorbide **6**), 4.38 (q, *J*=5.71 Hz, 1H, CH-isosorbide **4**), 4.66 (d, *J*=4.52 Hz, 1H, CH-isosorbide **5**), 4.71 - 4.78 (m, 1H, CH-isosorbide **2**), 5.51 (d, *J*=3.58 Hz, 1H, CH-isosorbide **1**), 6.86 - 6.95 (m, 1H, CH-salicylic **8**), 6.97 - 7.05 (m, 1H, CH-salicylic **10**), 7.50 (ddd, *J*=8.52, 7.11, 1.70 Hz, 1H, CH-salicylic **9**), 7.83 (dd, *J*=8.01, 1.79 Hz, 1H, CH-salicylic **7**). <sup>13</sup>C NMR (75 MHz, chloroform-*d*) δ ppm 72.33, 73.37, 73.63, 79.19, 82.12, 85.57, 111.72, 117.78, 119.31, 129.91, 136.32, 161.88, 169.16. *u*<sub>max</sub> (thin film, cm<sup>-1</sup>): 3484, 2977-2858, 1189, 1488, 1304, 1077, 1007, 748, 529. [α]<sub>D</sub><sup>25</sup> (CHCl<sub>3</sub>; *c* = 0.0286): + 53.49. MS: C<sub>13</sub>H<sub>14</sub>O<sub>6</sub> *m/z* (ES<sup>+</sup>) 267.09 [M+H]<sup>+</sup>. HRMS: Calculated C<sub>13</sub>H<sub>15</sub>O<sub>6</sub> 267.0869, found: 267.0874. MP: 93.9°C

#### 6.4 Synthesis of polyethylene glycol based linkers (section 2.6.1).

##### 2-benzyloxyacetic acid (**110**).



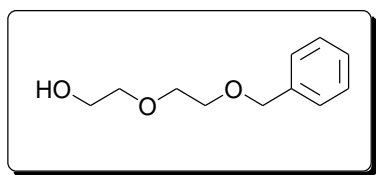
Published data: Yamashita *et al.*<sup>180</sup>

Sodium metal (3.040 g; 132.28 mM) was added in small portions to 22 ml benzyl alcohol (**109**) at 0°C. The reaction was allowed to warm to room temperature before being heated to 100°C. When no sodium metal was visible the reaction was cooled to room temperature and chloroacetic acid (5 g; 52.91 mM) in benzyl alcohol (5.5 mL) was added dropwise. The solution was refluxed at 210°C for 2 hours. Once cooled 30 mL water was added and washed with five 20 mL portions of Et<sub>2</sub>O. The pH of the aqueous layer was adjusted to pH 2 with 2M HCl solution and extracted with five 20 mL portions of Et<sub>2</sub>O. The organic layers were combined and washed with three 20 mL portions of water, one 20 mL portion of brine, dried over anhydrous MgSO<sub>4</sub> and filtered. The solvent was reduced *in vacuo*. The resultant clear oil was purified with flash column chromatography (a gradient of 19:1 to 7:3 Pet ether: EtOAc) to give 8.096g of **110** as a pale yellow oil (48.72 mM, 92%).

R<sub>f</sub>: 0.43 (EtOAc:Pet ether 6:4). <sup>1</sup>H NMR (300 MHz, chloroform-*d*) δ ppm 3.91 - 4.35 (m, 2H, CH<sub>2</sub>COOH), 4.45 - 4.78 (m, 2H, CH<sub>2</sub> benzyl), 7.09 - 7.54 (m, 5H, CH benzyl), 8.60 (br. s., 1H, COOH). <sup>13</sup>C NMR (75 MHz, chloroform-*d*) δ ppm 60.86, 67.41, 130.01135.34, 136.71, 170.52, 175.19.  $\nu_{\max}$  (thin film, cm<sup>-1</sup>): 3030, 1732, 1208, 1120, 632, 534, 498.  $[\alpha]_D^{25}$  (CHCl<sub>3</sub>; c = 0.0965): 0.00. MS: C<sub>9</sub>H<sub>10</sub>O<sub>3</sub> *m/z* (ES<sup>+</sup>) 167.07 [M+H]<sup>+</sup>. HRMS: Calculated C<sub>9</sub>H<sub>11</sub>O<sub>3</sub> 167.0707, found: 167.0706.



## 2-(2-(benzyloxy)ethoxy)ethanol (**112**).

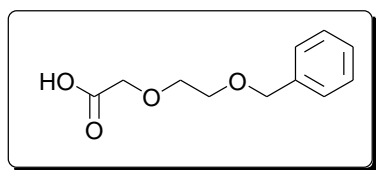


Published data by the group: Foley *et al.*<sup>116</sup>

60% NaH in mineral oil (1.327 g; 33.19 mM) was suspended in 50 mL anhydrous THF under a nitrogen atmosphere. Diethylene glycol (**111**) (3.00 mL; 31.61 mM) was added dropwise and the reaction stirred at room temperature for 1 hour. Benzyl bromide (3.76 mL, 31.61 mM) was added dropwise and the white suspension stirred for 48 hours at room temperature. 100 mL DCM and 50 mL 10% (w/v) K<sub>2</sub>CO<sub>3</sub> was added. The organic layer was separated and washed with one 50 mL portion of water, dried over anhydrous MgSO<sub>4</sub> and filtered. The solvent was reduced *in vacuo* to give a brown oil which was purified by flash column chromatography (a gradient of 4:1 to 0:1 Pet ether:EtOAc) to give 3.614 g of **112** as a yellow oil (18.42 mM; 58%).

R<sub>f</sub>: 0.40 (EtOAc:Pet ether 6:4). <sup>1</sup>H NMR (300 MHz, chloroform-*d*) δ ppm 2.92 (br. s., 1H, OH), 3.24 - 4.08 (m, 8H, CH<sub>2</sub> glycol), 4.42 - 4.72 (m, 2H, CH<sub>2</sub> benzyl), 7.03 - 7.57 (m, 5H, CH benzyl). <sup>13</sup>C NMR (75 MHz, chloroform-*d*) δ ppm 61.63, 69.41, 70.32, 72.58, 73.25, 73.27, 73.30, 127.78, 127.86, 128.44. ν<sub>max</sub> (thin film, cm<sup>-1</sup>): 3346, 2866, 1661, 1494, 1367, 1315, 1066, 630. [α]<sub>D</sub><sup>25</sup> (CHCl<sub>3</sub>; c = 0.0817): 0.00. MS: C<sub>11</sub>H<sub>16</sub>O<sub>3</sub> *m/z* (ES<sup>+</sup>) 197.12 [M+H]<sup>+</sup>. HRMS: Calculated C<sub>11</sub>H<sub>17</sub>O<sub>3</sub> 197.1172, found: 197.1171.

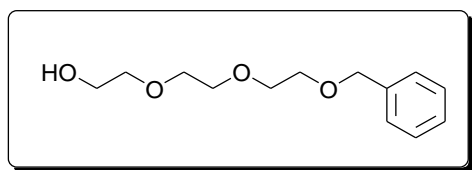
**2-(2-(benzyloxy)ethoxy)acetic acid (**113**).**



**112** (534 mg; 2.72 mM) was dissolved in 15 mL acetone at 0°C. Chromic trioxide (0.463 mg; 4.63 mM) in 4.6 mL 0.25 M H<sub>2</sub>SO<sub>4</sub> was added dropwise and the reaction stirred at room temperature for 24 hours, during which the reaction turned dark green. 2-propanol (10 mL) was added and the reaction stirred vigorously for 10 minutes. The solution was extracted with five 10 mL portions of EtOAc, which were combined and washed with two 10 mL portions of water. The organic layer was extracted with five 10 mL portions of saturated NaHCO<sub>3</sub>, which were combined and the pH adjusted to pH 2 with 5 M HCl. The acidified solution was washed with five 10 mL portions of EtOAc, which were combined, dried over anhydrous MgSO<sub>4</sub> and filtered. The solvent was removed *in vacuo* to give 416 mg of **113** as a colourless oil (1.98 mM, 73%)

R<sub>f</sub>: 0.22 (EtOAc:Pet ether 6:4). <sup>1</sup>H NMR (300 MHz, chloroform-*d*) δ ppm 3.52 - 3.84 (m, 6H, CH<sub>2</sub> glycol), 4.08 - 4.30 (m, 2H, CH<sub>2</sub>COOH), 4.45 - 4.65 (m, 2H, CH<sub>2</sub> benzyl), 7.27 - 7.49 (m, 5H, CH benzyl). <sup>13</sup>C NMR (75 MHz, chloroform-*d*) δ ppm 68.63, 69.20, 70.32, 70.66, 71.17, 73.31, 127.77, 127.89, 124.44, 137.90, 173.50.  $\nu_{\max}$  (thin film, cm<sup>-1</sup>): 3500, 2869, 1731, 1453, 1353, 1208, 1088.  $[\alpha]_D^{25}$  (CHCl<sub>3</sub>; c = 0.0107): 0.00. MS: C<sub>11</sub>H<sub>14</sub>O<sub>3</sub> *m/z* (ES<sup>+</sup>) 211.10 [M+H]<sup>+</sup>. HRMS: Calculated C<sub>11</sub>H<sub>15</sub>O<sub>3</sub> 211.0970, found: 211.0974.

**2-(2-(2-(benzyloxy)ethoxy)ethoxy)ethanol (**115**).**

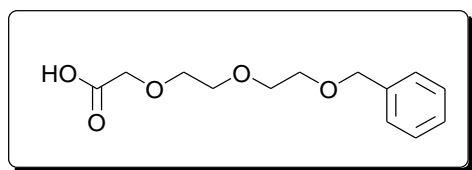


Published data by the group: Foley *et al.*<sup>116</sup>

Ag<sub>2</sub>O (11.708 g; 50.52 mM) was suspended in 50 mL anhydrous THF under a nitrogen atmosphere in a flask made light impenetrable. Triethylene glycol (**114**) (4.5 mL; 33.68 mM) was added dropwise and the reaction stirred at room temperature for 1 hour. Benzyl bromide (4.01 mL, 33.68 mM) was added dropwise and the suspension stirred for 72 hours at room temperature. The reaction mixture was filtered through a Celite<sup>®</sup> bed and the organic solvent removed *in vacuo* to give a brown oil. The oil was purified by flash column chromatography (a gradient of 4:1 to 0:1 Pet ether:EtOAc) to give of 5.648 g of **115** as a colourless oil (23.50 mM, 70%).

R<sub>f</sub>: 0.25 (EtOAc:Pet ether 6:4). <sup>1</sup>H NMR (300 MHz, chloroform-*d*) δ ppm 3.22 (s, 1H, OH), 3.52 - 3.78 (m, 12H, CH<sub>2</sub> glycol), 4.56 (s, 2H, CH<sub>2</sub> benzyl), 7.22 - 7.39 (m, 5H, CH benzyl). <sup>13</sup>C NMR (75 MHz, chloroform-*d*) δ ppm 61.2, 63.99, 68.90, 69.21, 69.30, 70.24, 70.58, 72.60, 73.24, 127.82, 128.39, 138.00. ν<sub>max</sub> (thin film, cm<sup>-1</sup>): 3419, 2866, 1748, 1455, 1351, 1205, 1136. [α]<sub>D</sub><sup>25</sup> (CHCl<sub>3</sub>; c = 0.0614): 0.00. MS: C<sub>13</sub>H<sub>20</sub>O<sub>4</sub> *m/z* (ES<sup>+</sup>) 241.14 [M+H]<sup>+</sup>. HRMS: Calculated C<sub>11</sub>H<sub>17</sub>O<sub>3</sub> 241.1440, found: 241.1392.

**2-(2-(2-(benzyloxy)ethoxy)ethoxy)acetic acid (**116**).**

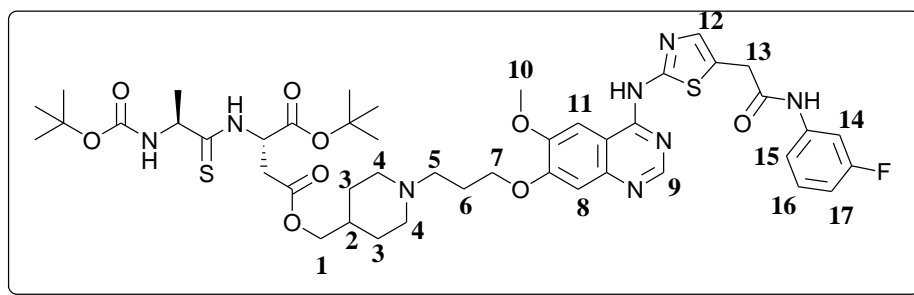


**115** (1.014 g; 4.22 mM) was dissolved in 25 mL acetone at 0°C. Chromic trioxide (0.717 mg; 7.17 mM) in 7.2 mL 0.25 M H<sub>2</sub>SO<sub>4</sub> was added dropwise and the reaction stirred at room temperature for 24 hours, during which the reaction turned dark green. 2-propanol (15 mL) was added and the reaction stirred vigorously for 10 minutes. The solution was extracted with five 20 mL portions of EtOAc, which were combined and washed with two 20 mL portions of water. The EtOAc was extracted with five 20 mL portions of saturated NaHCO<sub>3</sub>, which were combined and the pH adjusted to pH 2 with 5 M HCl. The acidified solution was washed with five 20 mL portions of EtOAc, which were combined, dried over anhydrous MgSO<sub>4</sub> and filtered. The solvent was removed *in vacuo* to give 764 mg of **116** as a colourless oil (3.00 mM, 71%).

R<sub>f</sub>: 0.49 (EtOAc:Pet ether 6:4). <sup>1</sup>H NMR (300 MHz, chloroform-*d*) δ ppm 3.56 - 3.80 (m, 8H, CH<sub>2</sub> glycol), 4.08 - 4.24 (m, 2H, CH<sub>2</sub>COOH), 4.51 - 4.60 (m, 2H, CH<sub>2</sub> benzyl), 7.28 - 7.38 (m, 5H, CH benzyl). <sup>13</sup>C NMR (75 MHz, chloroform-*d*) δ ppm 68.57, 69.17, 70.31, 70.60, 71.05, 73.29, 127.77, 127.90, 128.44.  $\nu_{\max}$  (thin film, cm<sup>-1</sup>): 3419, 2866, 1748, 1455, 1351, 1205, 1136.  $[\alpha]_D^{25}$  (CHCl<sub>3</sub>; c = 0.0112): 0.00. MS: C<sub>13</sub>H<sub>18</sub>O<sub>5</sub> *m/z* (ES<sup>+</sup>) 255.12 [M+H]<sup>+</sup>. HRMS: Calculated C<sub>13</sub>H<sub>19</sub>O<sub>5</sub> 255.1232, found: 255.1237.

## 6.5 Synthesis of Aurora Kinase inhibitor prodrug (section 2.6.1)

**(S)-1-tert-butyl-4-(1-(3-(4-(5-(2-(3-fluorophenylamino)-2-oxoethyl)thiazol-2-ylamino)-6-methoxy-4a,8a-dihydroquinazolin-7-yloxy)propyl)piperidin-4-yl)methyl-2-((S)-2-(tert-butoxycarbonylpropanethioamido)succinate (107).**

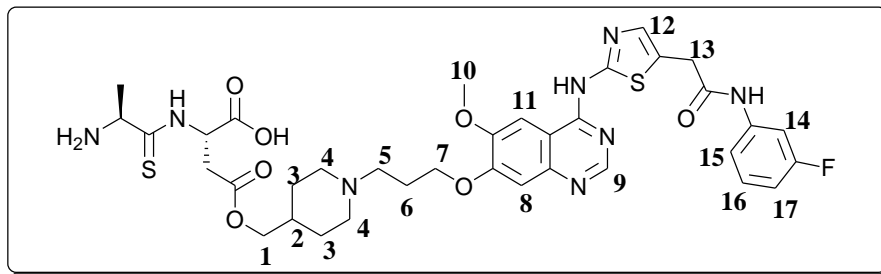


**57** (142 mg; 0.38 mM), EDC.HCl (79 mg; 0.41 mM), DMAP (46 mg; 0.38 mM) and HOBT (102 mg; 0.76 mM) were stirred in 5 mL anhydrous DMF for one hour at 0 °C under a nitrogen atmosphere. **105** (200 mg; 0.34 mM) dissolved in 2 mL anhydrous DMF was added dropwise. The solution was warmed to room temperature and stirred for 72 hours. The solvent was removed *in vacuo* and the residue purified by flash column chromatography (1:9:90 NH<sub>4</sub>OH:MeOH:DCM) to give 103 mg of **107** as an orange resin (0.11 mM; 32%).

R<sub>f</sub>: 0.57 (NH<sub>4</sub>OH:MeOH:DCM 1:9:90). <sup>1</sup>H NMR (300 MHz, methanol-*d*<sub>4</sub>) δ 1.20 - 1.31 (m, 1H, piperidine-CH **2**), 1.39 (d, *J*=6.97 Hz, 3H, CH<sub>3</sub> alanine), 1.44 (s, 9H, CH<sub>3</sub> Boc), 1.47 (s, 9H, CH<sub>3</sub> *tert*-butyl), 1.59 - 1.75 (m, 3H, piperidine-CH<sub>(ax)</sub> **3**), 2.02 (d, *J*=10.74 Hz, 2H, piperidine-CH<sub>(eq)</sub> **3**), 2.29 - 2.37 (m, 2H, CH<sub>2</sub> **6**), 3.01 (t, *J*=5.56 Hz, 3H, CH<sub>2</sub> aspartate, piperidine-CH<sub>(ax)</sub> **4**), 3.06 - 3.10 (m, 1H, piperidine-CH<sub>(ax)</sub> **4**), 3.33 (dt, *J*=3.34, 1.62 Hz, 2H, piperidine-CH<sub>2</sub> **5**), 3.68 (d, *J*=12.81 Hz, 2H, piperidine-CH<sub>(eq)</sub> **4**), 3.93 (br. s., 2H, thiazole-CH<sub>2</sub> **13**), 3.95 (s, 3H, O-CH<sub>3</sub> **10**), 4.07 (d, *J*=5.09 Hz, 2H, piperidine-CH<sub>2</sub> **1**), 4.17 (t, *J*=5.56 Hz, 2H, O-CH<sub>2</sub> **7**), 4.45, (q, *J*=7.16 Hz, 1H, CH alanine), 5.30 (q, *J*=6.47 Hz, 1H, CH aspartate), 6.80 - 6.89 (m, 1H, fluoroaniline **16**), 6.98 (s, 1H, thiazole **12**), 7.30 - 7.35 (m, 2H, fluoroaniline **17**, quinazoline **11**), 7.36 (s, 1H, fluoroaniline **14**), 7.60 (s, 1H, fluoroaniline **15**), 7.62 - 7.66 (m, 1H, quinazoline **8**), 8.53 (s, 1H, quinazoline **9**). <sup>13</sup>C NMR (75 MHz, chloroform-

*d*)  $\delta$  ppm 22.06, 25.01, 27.22, 28.21, 28.78, 34.27, 35.88, 36.04, 53.53, 55.91, 56.93, 57.86, 67.72, 80.66, 83.81, 102.90, 107.39, 107.91, 180.26, 111.55, 111.83, 116.46, 131.32, 131.44, 141.58, 141.72, 150.90, 155.22, 162.66, 165.89, 170.01, 170.79, 171.59, 196.23, 208.14.  $\nu_{\max}$  (thin film,  $\text{cm}^{-1}$ ): 3306, 2977-2874, 1722, 1645, 1504, 1365, 1247, 1156, 1070, 884, 750.  $[\alpha]_{\text{D}}^{25}$  ( $\text{CHCl}_3$ ;  $c = 0.0082$ ): + 11.70. MS:  $\text{C}_{36}\text{H}_{59}\text{FN}_8\text{O}_9\text{S}_2$   $m/z$  ( $\text{ES}^+$ ) 939.39  $[\text{M}+\text{H}]^+$ . HRMS: Calculated  $\text{C}_{36}\text{H}_{60}\text{FN}_8\text{O}_9\text{S}_2$  939.3903, found: 939.3919. MP: 56.2°C

(S)-2-((S)-2-aminopropanethioamido)-4-((1-(3-(4-(5-(2-(3-fluorophenylamino)-2-oxoethyl)thiazol-2-ylamino)-6-methoxy-4a,8a-dihydroquinazolin-7-yloxy)propyl)piperidin-4-yl)methoxy)-4-oxobutanoic acid (**108**).

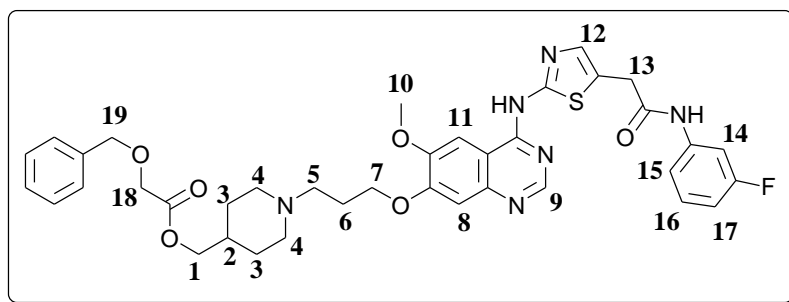


**107** (52 mg, 0.06 mM) was dissolved 5 mL 97% formic acid and refluxed at 100°C for three hours. The reaction was cooled to room temperature and the formic acid removed *in vacuo*. The residue was taken up in 5 mL distilled water, filtered through a pipette plugged with glass wool and extracted with 2 mL Et<sub>2</sub>O. The aqueous layer was lyophilised to give 44 mg of **108** as an orange resin in formate salt form (0.05 mM; 96%).

<sup>1</sup>H NMR (300 MHz, methanol-*d*<sub>4</sub>) δ ppm 1.24 - 1.36 (m, 1H, piperidine-CH **2**), 1.51 (d, *J*=6.78 Hz, 1H, CH<sub>3</sub> alanine\*), 1.57 (d, *J*=6.59 Hz, 2H, CH<sub>3</sub> alanine), 1.61 - 1.77 (m, 2H, piperidine-CH<sub>(ax)</sub> **3**), 2.00 - 2.13 (m, 2H, piperidine-CH<sub>(eq)</sub> **3**), 2.41 (br. s., 2H, CH<sub>2</sub> **6**), 3.06 (m, 2H, CH<sub>2</sub> aspartate), 3.37 - 3.46 (m, 2H, piperidine-CH<sub>(eq)</sub> **4**), 3.77 (d, *J*=12.81 Hz, 2H, piperidine-CH<sub>(ax)</sub> **4**), 3.98 (s, 2H, thiazole-CH<sub>2</sub> **13**), 4.04 (s, 3H, O-CH<sub>3</sub> **10**), 4.06 - 4.13 (m, 2H, piperidine-CH<sub>2</sub> **1**), 4.25 - 4.33 (m, 1H, CH alanine), 4.33 - 4.41 (m, 2H, O-CH<sub>2</sub> **7**), 5.43 (t, *J*=5.75 Hz, 1H, CH aspartate), 6.87 (t, *J*=8.57 Hz, 1H, fluoroaniline **16**), 7.18 - 7.38 (m, 3H, thiazole **12**, quinazoline **11**, fluoroaniline **17**), 7.50 (s, 1 H, fluoroaniline **14**), 7.60 (d, *J*=11.87 Hz, 1H, fluoroaniline **15**), 7.90 - 7.96 (m, 1H, quinazoline **8**), 8.81 - 8.85 (m, 1H, quinazoline **9**) *u*<sub>max</sub> (thin film, cm<sup>-1</sup>): 3401, 1669, 1442, 1182, 1124, 801, 724. MS: C<sub>36</sub>H<sub>43</sub>FN<sub>8</sub>O<sub>7</sub>S<sub>2</sub> *m/z* (ES<sup>+</sup>) 783.28 [M+H]<sup>+</sup>. HRMS: Calculated C<sub>36</sub>H<sub>44</sub>FN<sub>8</sub>O<sub>7</sub>S<sub>2</sub> 783.2758, found: 783.2757.

<sup>13</sup>C NMR was attempted in methanol-*d*<sub>4</sub>, water-*d*<sub>2</sub> and dimethyl sulfoxide-*d*<sub>6</sub> but could not be obtained due to solubility issues.

(1-(3-(4-(5-(2-(3-fluorophenylamino)-2-oxoethyl)thiazol-2-ylamino)-6-methoxy-4a,8a-dihydroquinazolin-7-yloxy)propyl)piperidin-4-yl)methyl 2-(benzyloxy)acetate (**117**).



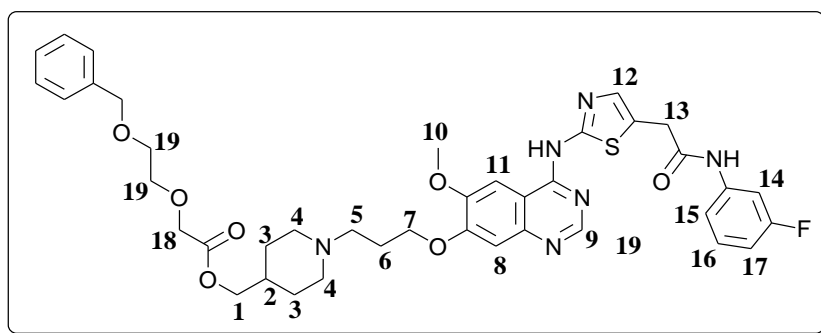
**110** (28 mg; 0.17 mM), HATU (65 mg; 0.17 mM) and DIPEA (27  $\mu$ L; 0.15 mM) were stirred in 3 mL anhydrous DMF for one hour at 0 °C under a nitrogen atmosphere. **105** (90 mg; 0.15 mM) dissolved in 2 mL anhydrous DMF was added dropwise. The solution was warmed to room temperature and stirred for 72 hours. The solvent was removed *in vacuo* and the residue purified by flash column chromatography (1:9:90  $\text{NH}_4\text{OH}:\text{MeOH}:\text{DCM}$ ) to give 27 mg of **117** as an orange resin (0.04 mM; 24%).

$R_f$ : 0.17 ( $\text{NH}_4\text{OH}:\text{MeOH}:\text{DCM}$  1:9:90).  $^1\text{H}$  NMR (300 MHz, methanol- $d_4$ )  $\delta$  ppm 0.92-0.98 (m, 1H, piperidine-CH **2**), 1.42 (m, 2H, piperidine-CH<sub>(ax)</sub> **3**), 1.73 - 1.83 (m, 2H, piperidine-CH<sub>(eq)</sub> **3**), 2.07 - 2.15 (m, 2H, CH<sub>2</sub> **6**), 2.16 - 2.28 (m, 2H, piperidine-CH<sub>2</sub> **4H**<sub>(ax)</sub>), 2.69 - 2.77 (m, 2H, piperidine-CH<sub>2</sub> **5**), 3.09 - 3.17 (m, 1H, piperidine-CH<sub>2</sub> **4**<sub>(eq)</sub>), 3.21 (q,  $J=7.41$  Hz, 1H, piperidine-CH<sub>2</sub>(eq) **4**), 3.71 (dt,  $J=13.33, 6.62$  Hz, 2H, CH<sub>2</sub> **18**), 3.90 (d,  $J=0.75$  Hz, 2H, thiazole-CH<sub>2</sub> **13**), 3.99 (s, 3H, O-CH<sub>3</sub> **10**), 4.06 (d,  $J=5.84$  Hz, 2H, piperidine-CH<sub>2</sub> **1**), 4.16 (m, 2H, O-CH<sub>2</sub> **7**), 4.61 (s, 2H, CH<sub>2</sub> benzyl), 6.80 - 6.88 (m, 1H, fluoroaniline **16**), 7.10 (s, 1H, thiazole **12**), 7.27 - 7.38 (m, 8H, CH benzyl, fluoroaniline **14**, fluoroaniline **17**, quinazoline **11**), 7.56 (m, 1H, fluoroaniline **15**), 7.73 (s, 1H, quinazoline **8**), 8.57 (s, 1H, quinazoline **9**).  $^{13}\text{C}$  NMR (75 MHz, chloroform- $d$ )  $\delta$  ppm 13.30, 18.04, 26.74, 28.91, 35.85, 43.71, 48.73, 49.30, 49.87, 54.12, 55.68, 56.44, 56.86, 68.00, 68.31, 69.58, 74.30, 106.13, 106.84, 111.24, 117.01, 129.03, 129.18, 129.46, 139.23, 139.84, 149.63, 155.84, 160.82, 166.25, 170.66, 170.92, 174.88, 197.51, 207.36.  $\nu_{\text{max}}$  (thin film,  $\text{cm}^{-1}$ ): 3070, 2904, 1678, 1613, 1520, 1454, 1397,



1265, 1209, 1139, 849, 657. MS: C<sub>38</sub>H<sub>41</sub>FN<sub>6</sub>O<sub>6</sub>S *m/z* (ES<sup>+</sup>) 729.29 [M+H]<sup>+</sup>. HRMS: Calculated C<sub>38</sub>H<sub>42</sub>FN<sub>6</sub>O<sub>6</sub>S 729.2871, found: 729.2872. MP: 62.4 °C

**(1-(3-(4-(5-(2-(3-fluorophenylamino)-2-oxoethyl)thiazol-2-ylamino)-6-methoxy-4a,8a-dihydroquinazolin-7-yloxy)propyl)piperidin-4-yl)methyl 2-(2-benzyloxy)ethoxy)acetate (118).**

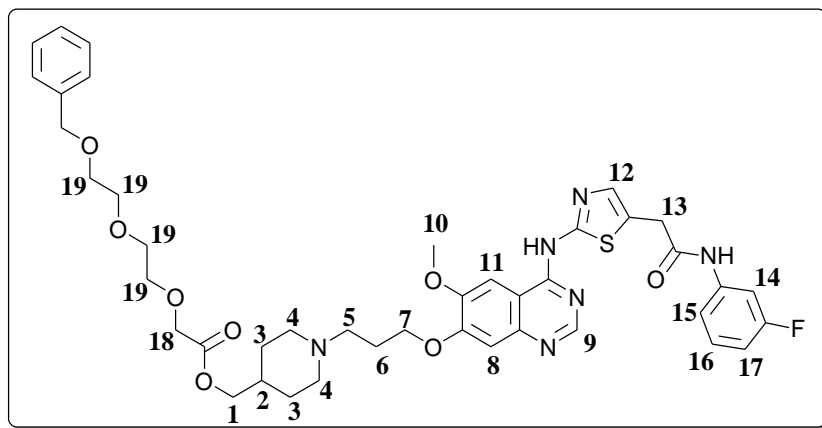


**113** (40 mg; 0.19 mM), HATU (72 mg; 0.19 mM) and DIPEA (30 µL; 0.17 mM) were stirred in 3 mL anhydrous DMF for one hour at 0 °C under a nitrogen atmosphere. **105** (100 mg; 0.17 mM) dissolved in 2 mL anhydrous DMF was added dropwise. The solution was warmed to room temperature and stirred for 72 hours. The solvent was removed *in vacuo* and the residue purified by flash column chromatography (1:9:90 NH<sub>4</sub>OH:MeOH:DCM) to give 36 mg of **118** as a sticky orange resin (0.05 mM; 27%).

R<sub>f</sub>: 0.22 (NH<sub>4</sub>OH:MeOH:DCM 1:9:90). <sup>1</sup>H NMR (300 MHz, chloroform-*d*) δ ppm 0.98-1.09 (m, 2H, piperidine-CH **2**), 1.14 - 1.34 (m, 2H, piperidine-CH<sub>(ax)</sub> **3**), 1.61 (d, *J*=10.74 Hz, 2H, piperidine-CH<sub>(eq)</sub> **3**), 1.80 - 1.93 (m, 2H, piperidine-CH<sub>(ax)</sub> **4**), 1.95 - 2.09 (m, 2H, CH<sub>2</sub> **6**), 2.44 (t, *J*=7.16 Hz, 2H, piperidine-CH<sub>2</sub> **5**), 2.79 - 2.91 (m, 2H, piperidine-CH<sub>(eq)</sub> **4**), 3.53 - 3.72 (m, 4H, CH<sub>2</sub> **19**), 3.79 (s, 2H, thiazole-CH<sub>2</sub> **13**), 3.84 (br. s., 3H, O-CH<sub>3</sub> **10**), 3.93 (d, *J*=6.03 Hz, 1H, piperidine-CH<sub>2</sub> **1**), 4.06 - 4.17 (m, 4H, O-CH<sub>3</sub> **10**, CH<sub>2</sub> **18**), 4.48 (s, 2H, CH<sub>2</sub> benzyl), 6.43 (d, *J*=5.46 Hz, 1H, quinazoline **11**), 6.70 (br. s., 1H, fluoroaniline **16**), 7.06 - 7.34 (m, 8H, thiazole **12**, CH benzyl, fluoroaniline **14**, fluoroaniline **17**), 7.44 (d, *J*=9.80 Hz, 1H, fluoroaniline **15**), 8.17 (br. s., 1H,

quinazoline **8**), 8.60 - 8.96 (m, 1H, quinazoline **9**).  $^{13}\text{C}$  NMR (75 MHz, chloroform-*d*)  $\delta$  ppm 24.96, 25.57, 26.44, 28.88, 33.69, 35.29, 35.68, 39.07, 49.17, 53.27, 55.16, 56.28, 67.69, 68.59, 69.09, 69.37, 70.67, 70.93, 73.25, 106.71, 107.26, 107.60, 108.56, 110.93, 111.22, 115.22, 127.63, 128.38, 129.92, 130.04, 138.17, 139.60, 149.36, 149.94, 154.33, 164.51, 167.97, 170.61.  $\nu_{\text{max}}$  (thin film,  $\text{cm}^{-1}$ ): 2926, 2850, 1601, 1540, 1272, 1193, 1104, 892, 739, 697. MS:  $\text{C}_{40}\text{H}_{45}\text{FN}_6\text{O}_7\text{S}$   $m/z$  ( $\text{ES}^+$ ) 773.31  $[\text{M}+\text{H}]^+$ . HRMS: Calculated  $\text{C}_{40}\text{H}_{46}\text{FN}_6\text{O}_7\text{S}$  733.3133, found: 733.3138.

(1-(3-(4-(5-(2-(3-fluorophenylamino)-2-oxoethyl)thiazol-2-ylamino)-6-methoxy-4a,8a-dihydroquinazolin-7-yloxy)propyl)piperidin-4-yl)methyl-2-(2-(2-benzyloxy)ethoxy)ethoxy)acetate (**119**).



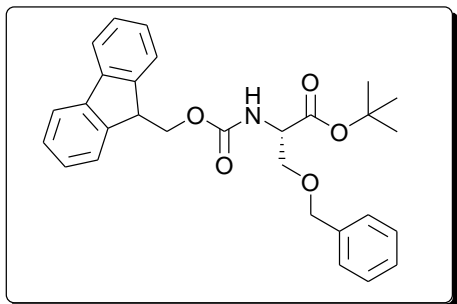
**116** (53 mg; 0.21 mM), HATU (79 mg; 0.21 mM) and DIPEA (33  $\mu\text{L}$ ; 0.19 mM) were stirred in 3 mL anhydrous DMF for one hour at 0  $^{\circ}\text{C}$  under a nitrogen atmosphere. **105** (110 mg; 0.19 mM) dissolved in 2 mL anhydrous DMF was added dropwise. The solution was warmed to room temperature and stirred for 72 hours. The solvent was removed *in vacuo* and the residue purified by flash column chromatography (1:9:90  $\text{NH}_4\text{OH}:\text{MeOH}:\text{DCM}$ ) to give 44 mg of **119** as a sticky orange resin (0.05 mM; 28%).

R<sub>f</sub>: 0.28 (NH<sub>4</sub>OH:MeOH:DCM 1:9:90). <sup>1</sup>H NMR (300 MHz, chloroform-*d*) δ ppm 0.81 - 0.91 (m, 1H, piperidine-CH **2**), 1.26 (m, 2H, piperidine-CH<sub>(ax)</sub> **3**), 1.33 (d, *J*=9.80 Hz, 2H, piperidine-CH<sub>(eq)</sub> **3**), 1.65 - 1.74 (m, 2H, piperidine-CH<sub>(ax)</sub> **4**), 1.92 - 2.13 (m, 3H, CH<sub>2</sub> **6**, piperidine-CH<sub>(eq)</sub> **4**), 2.55 (t, *J*=6.97 Hz, 2H, piperidine-CH<sub>2</sub> **5**), 2.96 (d, *J*=10.93 Hz, 1H, piperidine-CH<sub>(eq)</sub> **4**), 3.59 - 3.80 (m, 8H, CH<sub>2</sub> **19**), 3.86 (br. s., 2H, thiazole-CH<sub>2</sub> **13**), 4.00 (d, *J*=5.65 Hz, 3H, O-CH<sub>3</sub> **10**), 4.07 - 4.20 (m, 4H, piperidine-CH<sub>2</sub> **1**, CH<sub>2</sub> **18**), 4.55 (s, 2H, CH<sub>2</sub> benzyl), 6.77 (m, 1H, fluroaniline **16**), 7.06 - 7.38 (m, 9H, fluroaniline **14**, fluroaniline **17**, thiazole **12**, quinazoline **11**, CH benzyl), 7.51 (d, *J*=9.98 Hz, 1H, fluroaniline **15**), 7.92 - 8.11 (m, 1H, quinazoline **8**), 8.57 - 8.82 (m, 1H, quinazoline **9**). <sup>13</sup>C NMR (75 MHz, chloroform-*d*) δ ppm 14.20, 21.09, 26.20, 28.59, 35.10, 50.65, 53.16, 53.48, 55.11, 56.18, 60.46, 67.53, 68.54, 68.93, 69.35, 70.63, 70.90, 73.25, 107.27, 107.62, 111.04, 115.27, 127.65, 127.78, 128.38, 129.97, 130.09, 138.10, 149.88, 161.24, 164.48, 168.02, 170.61, 171.29. *u*<sub>max</sub> (thin film, cm<sup>-1</sup>): 2924, 2850, 1646, 1541, 1272, 1194, 1086, 892, 697. MS: C<sub>42</sub>H<sub>49</sub>FN<sub>6</sub>O<sub>8</sub>S *m/z* (ES<sup>+</sup>) 817.34 [M+H]<sup>+</sup>. HRMS: Calculated C<sub>42</sub>H<sub>49</sub>FN<sub>6</sub>O<sub>8</sub>S 817.3395, found: 817.3403.

## 6.6 Synthesis of alternative carriers section (3.1).

### 6.6.1. Serine component (section 2.3 and 3.1).

#### (S)- 9-Fluorenylmethoxycarbonyl-*O*-benzyl-*L*-aspartic acid-*tert*-butyl ester (**48**).



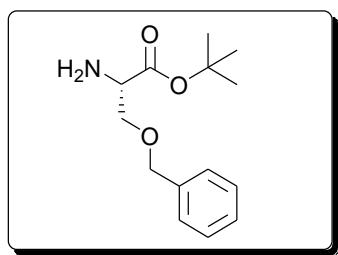
*N*-9-Fluorenylmethoxycarbonyl-*O*-*tert*-butyl-*L*-aspartic acid (**46**) (4.998 g; 11.97 mM) was dissolved in 10 ml anhydrous DCM under a nitrogen atmosphere at room temperature. *Tert*-butyl-2,2,2-trichloroacidimide (4.29 mL; 23.95 mM) was added dropwise, followed by 5ml Et<sub>2</sub>O. The reaction mixture was stirred for 72 days at room temperature, before being cooled to -20°C and left unstirring for 30 minutes. The reaction was filtered to remove the white precipitate and the solvent reduced *in vacuo* to give a brown foam. Purification was attained by flash column chromatography (1:4 Pet ether: EtOAc) to give 5.574 g of **48** as a white solid (11.77 mM; 98%).

R<sub>f</sub>: 0.62 (EtOAc:Pet ether 4:6). <sup>1</sup>H NMR (300 MHz, chloroform-*d*) δ ppm 1.49 (s, 9H, CH<sub>3</sub> *tert*-butyl), 3.73 (ABdd, *J*=8.70, 3.60 Hz, 1H, CH<sub>2</sub>-serine), 3.92 (dd, *J*=9.32, 2.92 Hz, 1H, CH<sub>2</sub>-serine), 4.26 (t, *J*=7.54 Hz, 1H, CH-Fmoc), 4.35 - 4.48 (m, 2H, CH<sub>2</sub>-Fmoc, CH-serine), 4.49 - 4.66 (AB, 2H, CH<sub>2</sub>-benzyl), 5.75 (d, *J*=8.67 Hz, 1H, NH), 7.26 - 7.48 (m, 9H, CH aromatic) 7.65 (d, *J*=6.59 Hz, 2H, CH-Fmoc aromatic), 7.79 (d, *J*=7.35 Hz, 2H, CH-Fmoc aromatic). <sup>13</sup>C NMR (75 MHz, chloroform-*d*) δ ppm 28.02, 47.13, 50.89, 54.87, 67.17, 70.24, 73.41, 119.99, 125.24, 127.10, 127.73, 127.87, 128.46.

This compared to data previously recorded by Foley *et al.* in the group, so no further characterisation was carried out.<sup>116,117</sup>

R<sub>f</sub>: 0.48 (CHCl<sub>3</sub>). <sup>1</sup>H NMR (300 MHz, chloroform-*d*) δ ppm 1.49 (s, 9H), 3.90 (ABdd, *J* = 9.4 & 2.6, 2H), 4.25 (t, *J* = 7.2, 1H), 4.53-4.38 (m, 3H), 4.57 (ABd, *J* = 12.1, 2H), 5.72 (d, *J* = 6.8, 1H), 7.45-7.26 (m, 9H), 7.68-7.62 (m, 2H), 7.81-7.76 (m, 2H). <sup>13</sup>C NMR (75 MHz, chloroform-*d*) δ ppm 28.4, 47.5, 55.31, 67.5, 70.6, 73.8, 82.7, 120.3, 125.6, 127.5-127.8, 138.0, 141.7-144.4, 156.4, 169.7.  $\nu_{\max}$  (thin film, cm<sup>-1</sup>): 3340, 3053, 2974, 1726, 1515, 1247, 1153.  $[\alpha]_{\text{D}}^{25}$  (CHCl<sub>3</sub>; *c* = 0.54): + 7.0. MS: C<sub>29</sub>H<sub>31</sub>NO<sub>5</sub> *m/z* (ES<sup>+</sup>) 496.2 [M+Na]<sup>+</sup>. HRMS: Calculated for C<sub>29</sub>H<sub>31</sub>NNaO<sub>5</sub> 496.2100, found 496.2115.

**(S)-benzyl-2-amino-3-tert-butoxypropanoate (50).**



Previously published data by the group: Foley *et al.*<sup>116,117</sup>

**Method 1** (section 2.3 and section 3.1).

**48** (2.513 g; 5.31 mM) was dissolved in 10 mL of anhydrous THF under a nitrogen atmosphere. The reaction was cooled to 0°C and a 1.0 M solution of TBAF in THF (5.84 mL) was added dropwise. The reaction was stirred at 0°C for 30 minutes, and allowed to proceed a further 2-3 hours at room temperature, monitored by TLC. The solvent was removed *in vacuo* to yield a sticky pink residue which was taken up into 20 mL of water. The pH of the solution was adjusted to pH 2 using 2 M HCl, and 20 mL of EtOAc added. The aqueous layer was separated and extracted with a further two 10mL portions of EtOAc. The aqueous phase was adjusted to pH 8-9 using 2 M NaOH, and extracted with one 20 mL and two 10 mL portions of EtOAc. The EtOAc portions from the basic aqueous extraction were combined, dried over anhydrous MgSO<sub>4</sub> and filtered. The solvent was reduced *in vacuo*, to give 1.043 g of **50** as a clear oil (4.15 mM; 78%).

**Method 2** (section 2.3)

*O*-benzyl-*L*-aspartic acid (100 mg; 0.45 mM) was dissolved in 1.8ml of *tert*-butyl acetate under a nitrogen atmosphere. Perchloric acid (30 µL; 0.49 mM) was added dropwise, the reaction heated to 50°C and stirred for 2 days. The solution was diluted with 20 mL water and the pH of the solution adjusted to pH 8-9 using 2 M NaOH, and extracted with one 20 mL and two 10 mL portions of EtOAc. The EtOAc were combined, dried over anhydrous MgSO<sub>4</sub> and then filtered. The solvent was reduced *in vacuo*, to give 111 mg of **50** as a clear oil (0.44 mM; 99%).

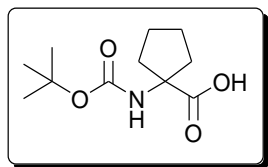
R<sub>f</sub> 0.43 (EtOAc:Pet ether 4:6). <sup>1</sup>H NMR (300 MHz, methanol-*d*<sub>4</sub>) δ ppm 1.46 (s, 9H, CH<sub>3</sub> *tert*-butyl), 3.50 (dd, *J*=4.52, 3.96 Hz, 1H, CH serine), 3.61 - 3.80 (m, 2H, CH<sub>2</sub> serine), 4.54 (m, *J*=9.98 Hz, 2H, CH<sub>2</sub>-benzyl), 7.15 - 7.44 (m, 5H, CH aromatic). <sup>13</sup>C NMR (75 MHz, methanol-*d*<sub>4</sub>) δ 28.29, 55.99, 73.11, 74.33, 82.52, 128.76, 128.89, 129.38, 139.37, 173.92.

This compared to data previously recorded by Foley *et al.* in the group, so no further characterisation was carried out.<sup>116,117</sup>

R<sub>f</sub>: 0.35 (95:5 CHCl<sub>3</sub>:CH<sub>3</sub>OH). <sup>1</sup>H NMR (400 MHz, chloroform-*d*) δ ppm 1.47 (s, 9H), 3.68-3.48 (m, 1H), 3.79-3.68 (m, 2H), 4.55 (AB, *J* =12.6, 2H), 7.40-7.28 (m, 5H). <sup>13</sup>C NMR (100 MHz, chloroform-*d*) δ ppm 28.4, 55.8, 72.8, 73.7, 81.7. 128.0, 128.1, 128.8, 138.4, 173.4. [α]<sub>D</sub><sup>25</sup> (CHCl<sub>3</sub>; c = 1.08): – 5.9. *u*<sub>max</sub> (thin film, cm<sup>–1</sup>): 3382, 2988, 2924, 2864, 1729, 1601, 1377, 1242, 1164. MS: C<sub>14</sub>H<sub>21</sub>NO<sub>3</sub> *m/z* (ES<sup>+</sup>) 251.2 [M+H]<sup>+</sup>. HRMS: Calculated for C<sub>14</sub>H<sub>22</sub>NO<sub>3</sub> 252.1599, found 252.1590.

6.6.2. Cycloleucine-serine carrier (section 3.1).

**1-(tert-butoxycarbonyl)cyclopentanecarboxylic acid (**158**).**

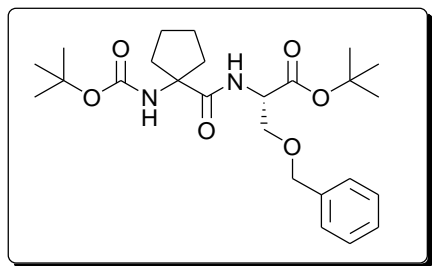


Cycloleucine (**157**) (2.000 g; 15.48 mM) was dissolved in 20ml acetonitrile at 0°C. TEA (10.79 mL; 77.41 mM) was added dropwise, followed by 1 M NaOH (15.48 mL; 15.48 mM) and the reaction stirred for 10 minutes. After the addition of di-*tert*-butyl dicarbonate (5.069 g; 23.22 mM), the reaction was brought to room temperature and stirred vigorously for 4 hours, during which time a white precipitate formed. The solvent was removed *in vacuo* to give a white solid which was dissolved in 100 mL EtOAc:water (1:1). The organic phase was separated and washed with three 20 mL portions of water. The aqueous phases were combined and the pH adjusted to pH 2 with 2 M HCl. The acidified aqueous phase was extracted with three 20 mL portions of EtOAc, which were combined and washed with one 20 mL portion of water and one 10 mL portion of brine. The organic phase was dried over anhydrous MgSO<sub>4</sub>, filtered and reduced *in vacuo* to give 2.311 g of **158** as a white solid (1.00 mM, 65%).

R<sub>f</sub>: 0.425 (EtOAc:MeOH 9:1). <sup>1</sup>H NMR (300 MHz, chloroform-*d*) δ ppm 1.44 (s, 9H, CH<sub>3</sub> Boc), 1.76 (dt, *J* = 7.35, 3.49 Hz, 4H (CH<sub>2</sub>)<sub>2</sub> cycloleucine), 1.90 - 2.01 (m, 2H, CH-CH<sub>2</sub>-CH<sub>2</sub>-CH cycloleucine), 2.09 - 2.23 (m, 2H, CH-CH<sub>2</sub>-CH<sub>2</sub>-CH cycloleucine). <sup>13</sup>C NMR (75 MHz, methanol-*d*<sub>4</sub>) δ 25.4, 28.8, 38.15, 66.9, 80.1, 157.6, 178.6. ν<sub>max</sub> (thin film, cm<sup>-1</sup>): 3244, 2971, 2502, 1698, 1643, 1403, 1260, 1156, 942, 776, 669. [α]<sub>D</sub><sup>25</sup> (CHCl<sub>3</sub>; c = 0.0157): + 10.19 MS: C<sub>11</sub>H<sub>19</sub>NO<sub>4</sub>, *m/z* (ES<sup>+</sup>) 228.12 [M-H]<sup>+</sup>. HRMS: Calculated for C<sub>11</sub>H<sub>19</sub>NO<sub>4</sub> 229.1314, found 228.1236. MP 137°C (Lit: 129-135-Sigma Aldrich).



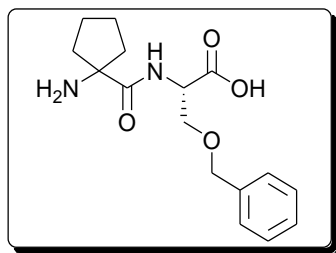
**(S)-tert-butyl 3-(benzyloxy)-2-(1-(tert-butoxycarbonyl)cyclopentanecarboxamido)propanoate**  
**(159).**



**158** (254 mg; 1.11 mM) and **50** (253 mg; 1.01 mM) were dissolved in 5 mL anhydrous DMF under nitrogen atmosphere at 0°C. DIPEA (351  $\mu$ L; 2.01 mM) was added dropwise and the reaction stirred for 10 minutes prior to the dropwise addition of DPPA (239  $\mu$ L; 1.11 mM). The solution was stirred at 0°C for 72 hours after which the solvent was removed *in vacuo*. The residue was dissolved in 20 mL EtOAc and washed with two 10 mL portions of NH<sub>4</sub>Cl, two 10 mL Na<sub>2</sub>CO<sub>3</sub> and one 20 mL portion of brine. The organic layer was dried over anhydrous MgSO<sub>4</sub>, filtered and the solvent removed *in vacuo* to give 451 mg of **159** as a white solid (0.97 mM; 96%).

R<sub>f</sub>: 0.50 (EtOAc:Pet ether 4:6). <sup>1</sup>H NMR (300 MHz, methanol-*d*<sub>4</sub>)  $\delta$  ppm 1.42 (s, 9H, CH<sub>3</sub> Boc), 1.45 (s, 9H, CH<sub>3</sub> *tert*-butyl) 1.68 - 1.78 (m, 4H, (CH<sub>2</sub>)<sub>2</sub> cycloleucine), 1.83 - 1.98 (m, 2H, CH-CH<sub>2</sub>-CH<sub>2</sub> CH-cycloleucine), 2.09 - 2.27 (m, 2H, CH-CH<sub>2</sub>-CH<sub>2</sub>-CH cycloleucine), 3.67 (ABdd, *J*=9.42, 3.01 Hz, 1H, CH<sub>2</sub> serine), 3.82 (ABdd, *J*=9.42, 3.58 Hz, 1H, CH<sub>2</sub> serine), 4.45 - 4.59 (m, 3H, CH serine, CH<sub>2</sub>-benzyl), 7.17 - 7.42 (m, 5H, CH benzyl), 7.50 - 7.63 (m, 1 H, NH serine). <sup>13</sup>C NMR (75 MHz, methanol -*d*<sub>4</sub>)  $\delta$  25.35, 25.41, 28.34, 28.86, 37.35, 38.05, 54.83, 67.87, 71.05, 74.35, 80.66, 83.22, 121.32, 124.51, 128.87, 129.44, 130.31, 139.15, 157.06, 170.58, 177.02.  $\nu_{\max}$  (thin film, cm<sup>-1</sup>): 3310, 2977-2867, 1681, 1520, 1389, 1250, 1152, 1099, 732.  $[\alpha]_D^{25}$  (CHCl<sub>3</sub>; *c* = 0.0128): + 16.22. MS: C<sub>25</sub>H<sub>38</sub>N<sub>2</sub>O<sub>6</sub>, *m/z* (ES<sup>+</sup>) 463.28 [M+H]<sup>+</sup>. HRMS: Calculated C<sub>25</sub>H<sub>39</sub>N<sub>2</sub>O<sub>6</sub> 463.2730, found 463.2795. MP: 72.3°C

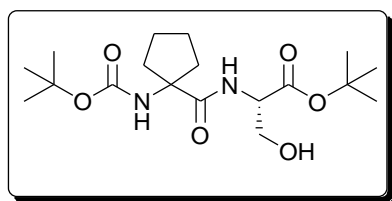
**(S)-2-(1-aminocyclopentanecarboxamido)-3-(benzyloxy)propanoic acid (**163**).**



**159** (50 mg, 0.11 mM) was dissolved 5 mL 97% formic acid and refluxed at 100°C for three hours. The reaction was cooled to room temperature and the formic acid removed *in vacuo*. The residue was taken up in 5 mL distilled water, filtered through a pipette plugged with glass wool and extracted with 2 mL Et<sub>2</sub>O. The aqueous layer was lyophilised to give 35 mg of **163** as a white solid in formate salt form (0.10 mM; 96%).

<sup>1</sup>H NMR (300 MHz, methanol-*d*<sub>4</sub>) δ ppm 1.68 - 1.86 (m, 2H, CH-CH<sub>2</sub>-CH<sub>2</sub>-CH cycloleucine), 1.95 (m, 4H, (CH<sub>2</sub>)<sub>2</sub> cycloleucine), 2.07 - 2.48 (m, 2H, CH-CH<sub>2</sub>-CH<sub>2</sub>-CH cycloleucine), 3.68 - 3.94 (m, 2H, CH<sub>2</sub> serine), 3.99 - 4.13 (m, 1H, CH serine), 4.43 - 4.68 (m, 2H, CH<sub>2</sub>-benzyl), 7.25 - 7.44 (m, 5H, CH benzyl). <sup>13</sup>C NMR (75 MHz, methanol-*d*<sub>4</sub>) δ ppm 25.77, 25.87, 26.51, 37.26, 37.65, 37.82, 38.10, 55.78, 67.54, 71.55, 74.05, 128.73, 128.95, 129.13, 129.38, 129.55, 139.54, 165.37, 172.73. *u*<sub>max</sub> (thin film, cm<sup>-1</sup>): 2955, 2870, 1654, 1584, 1385, 1100, 737. MS: C<sub>16</sub>H<sub>22</sub>N<sub>2</sub>O<sub>4</sub>, *m/z* (ES<sup>+</sup>) 306.16 [M+H]<sup>+</sup>. HRMS: Calculated C<sub>16</sub>H<sub>23</sub>NO<sub>4</sub> 307.1658, found 307.1652.

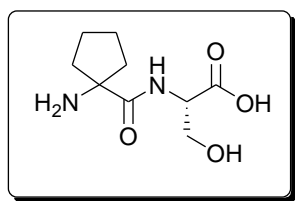
**(S)-tert-butyl 2-(1-(tert-butoxycarbonyl)cyclopentanecarboxamido)-3-hydroxypropanoate (160).**



**159** (998 mg, 2.16 mM) was dissolved in 5 mL MeOH. 10% Pd/C (100 mg) was added and the suspension stirred under a hydrogen atmosphere at room temperature for 24 hours. The reaction mixture was filtered through a Celite® bed and the organic solvent removed *in vacuo*. 796 mg of **160** was obtained as a white solid (2.13 mM, 99%).

R<sub>f</sub>: 0.32 (EtOAc:Pet ether 4:6). <sup>1</sup>H NMR (300 MHz, methanol-*d*<sub>4</sub>) δ ppm 1.45 (s, 9H, CH<sub>3</sub> Boc), 1.49 (s, 9H, CH<sub>3</sub> *tert*-butyl), 1.75 (dt, *J*=7.21, 3.46 Hz, 4H, (CH<sub>2</sub>)<sub>2</sub> cycloleucine), 1.84 - 1.97 (m, 2H, CH-CH<sub>2</sub>-CH<sub>2</sub>-CH cycloleucine), 2.10 - 2.33 (m, 2H, CH-CH<sub>2</sub>-CH<sub>2</sub>-CH cycloleucine), 3.84 (ABq, *J*=3.77 Hz, 2H, CH<sub>2</sub>-benzyl), 4.28 - 4.38 (m, 1H, CH serine), 7.59 (d, *J*=7.16 Hz, 1H, NH serine). <sup>13</sup>C NMR (75 MHz, methanol-*d*<sub>4</sub>) δ ppm 25.36, 28.29, 28.76, 37.55, 37.91, 56.87, 62.99, 67.97, 80.80, 83.14, 160.30, 170.93, 177.12. *ν*<sub>max</sub> (thin film, cm<sup>-1</sup>): 3306, 2976, 1682, 1514, 1367, 1158, 734. [α]<sub>D</sub><sup>25</sup> (CHCl<sub>3</sub>; *c* = 0.0143): +11.23. MS: C<sub>18</sub>H<sub>32</sub>N<sub>2</sub>O<sub>6</sub>, *m/z* (ES<sup>+</sup>) 373.23 [M+H]<sup>+</sup>. HRMS: Calculated for C<sub>18</sub>H<sub>33</sub>N<sub>2</sub>O<sub>6</sub> 373.2339, found 373.2330. MP: 117.4°C

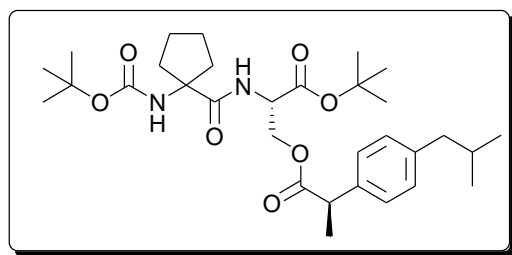
**(S)-2-(1-aminocyclopentanecarboxamido)-3-hydroxypropanoic acid (155).**



**160** (52 mg, 0.14 mM) was dissolved in 5 mL 97% formic acid and refluxed at 100°C for three hours. The reaction was cooled to room temperature and the formic acid removed *in vacuo*. The residue was taken up in 5 mL distilled water, filtered through a pipette plugged with glass wool and extracted with 2 mL Et<sub>2</sub>O. The aqueous layer was lyophilised to give 29 mg of **155** as a white solid in formate salt form (0.14 mM; 97%).

<sup>1</sup>H NMR (300 MHz, methanol-*d*<sub>4</sub>) δ ppm 1.67 - 1.88 (m, 2H, CH-CH<sub>2</sub>-CH<sub>2</sub>-CH cycloleucine), 1.95 (m, 4H, (CH<sub>2</sub>)<sub>2</sub> cycloleucine), 2.07 - 2.49 (m, 2H, CH-CH<sub>2</sub>-CH<sub>2</sub>-CH cycloleucine), 3.69 - 3.95 (m, 2H, CH<sub>2</sub> serine), 4.54 (m, 1H, CH serine). <sup>13</sup>C NMR (75 MHz, methanol-*d*<sub>4</sub>) δ ppm 25.78, 25.92, 26.50, 37.22, 37.65, 37.83, 38.10, 55.92, 68.32, 74.16, 165.21, 172.84. *u*<sub>max</sub> (thin film, cm<sup>-1</sup>): 3239, 2943, 1396, 742, 621, 517. MS: C<sub>9</sub>H<sub>16</sub>N<sub>2</sub>O<sub>4</sub>, *m/z* (ES<sup>+</sup>) 217.19 [M+H]<sup>+</sup>. HRMS: Calculated C<sub>9</sub>H<sub>16</sub>N<sub>2</sub>O<sub>4</sub> 217.1188, found 217.1186.

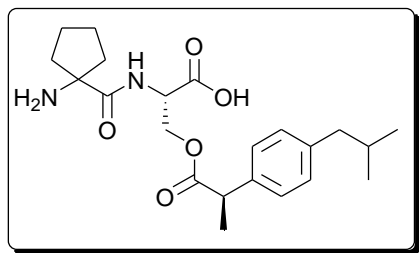
**(S)-2-(1-(*tert*-butoxycarbonylcyclopentanecarboxamido)-3-((R)-2-(4 isobutylphenyl)propanoyloxy) propanoic acid *tert*-butyl ester (161).**



Ibuprofen (**77**) (150 mg, 0.71 mM), DCC (165 mg, 0.80 mM) and DMAP (88 mg, 0.71 mM) were dissolved in 5 mL anhydrous DCM under a nitrogen atmosphere at 0°C and left to stir for 30 minutes. **160** (284 mg, 0.76 mM) in 2 mL anhydrous DCM was added and reaction mixture stirred at room temperature for 72 hours. The solution was filtered and the solvent removed *in vacuo*. The resultant white solid was purified by flash column chromatography (a gradient of 2:8 to 7:3 EtOAc: pet ether) to give 328 mg of **161** as a colourless oil (0.58 mM, 82%).

R<sub>f</sub>: 0.68 (EtOAc:Pet ether 4:6). <sup>1</sup>H NMR (300 MHz, methanol-*d*<sub>4</sub>) δ ppm 0.92 (d, *J*=6.59 Hz, 6H, Ibu-CH(CH<sub>3</sub>)<sub>2</sub>), 1.42 (s, 9H, CH<sub>3</sub> *tert*-butyl), 1.45 (s, 9H, CH<sub>3</sub> Boc), 1.47 (s, 3H, Ibu-CH<sub>3</sub>), 1.68 - 1.78 (m, 4H, (CH<sub>2</sub>)<sub>2</sub>-cycloleucine), 1.80 - 1.92 (td, *J*=13.42, 6.50 Hz, 1H, Ibu-CH(CH<sub>3</sub>)<sub>2</sub>), 1.96 - 2.08 (m, 2H, CH-CH<sub>2</sub>-CH<sub>2</sub>-CH cycloleucine), 2.13 - 2.28 (m, 2H, CH-CH<sub>2</sub>-CH<sub>2</sub>-CH cycloleucine), 2.47 (d, *J*=7.16 Hz, 2H, Ibu-CH<sub>2</sub>CH), 3.73 (q, *J*=7.10 Hz, 1H, Ibu-CHCH<sub>3</sub>), 4.40 (m, *J*=3.77 Hz, 2H, CH<sub>2</sub> serine), 4.47 - 4.53 (m, 1H, CH serine), 7.10 - 7.23 (m, 4H, Ibu-CH aromatic), 7.54 (br. s., 1H, NH serine). <sup>13</sup>C NMR (75 MHz, methanol-*d*<sub>4</sub>) δ ppm 19.14, 22.79, 25.30, 25.32, 28.18, 28.79, 31.52, 37.24, 46.08, 46.23, 54.21, 64.82, 67.84, 80.74, 83.71, 128.35, 130.52, 139.04, 169.74, 175.78. *ν*<sub>max</sub> (thin film, cm<sup>-1</sup>): 2956, 2471, 1738, 1367, 1153, 759, 497. MS: C<sub>31</sub>H<sub>48</sub>N<sub>2</sub>O<sub>7</sub>, *m/z* (ES<sup>+</sup>) 561.35 [M+H]<sup>+</sup>. HRMS: Calculated C<sub>31</sub>H<sub>49</sub>N<sub>2</sub>O<sub>7</sub> 561.3534, found 561.3531.

(S)-2-(1-aminocyclopentanecarboxamido)-3-((R)-2-(4-isobutylphenyl)propanoyloxy)propanoic acid (**162**).

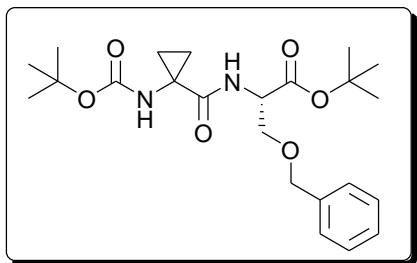


**161** (214 mg, 0.38 mM) was dissolved 5 mL 97% formic acid and refluxed at 100°C for three hours. The reaction was cooled to room temperature and the formic acid removed *in vacuo*. The residue was taken up in 5 mL distilled water, filtered through a pipette plugged with glass wool and extracted with 2 mL Et<sub>2</sub>O. The aqueous layer was lyophilised to give 168 mg of **162** as a white solid in formate salt form (0.37 mM; 98%).

<sup>1</sup>H NMR (300 MHz, methanol-*d*<sub>4</sub>) δ ppm 0.91 (d, *J*=6.59 Hz, 6H, Ibu-CH(CH<sub>3</sub>)<sub>2</sub>), 1.44 (d, *J*=7.16 Hz, 3H, Ibu-CH<sub>3</sub>), 1.68 - 2.00 (m, 7H, CH<sub>2</sub> cycloleucine, Ibu-CH(CH<sub>3</sub>)<sub>2</sub>), 2.18 - 2.34 (m, 2H, CH<sub>2</sub> cycloleucine), 2.46 (d, *J*=7.16 Hz, 2H, Ibu-CH<sub>2</sub>CH), 3.74 (q, *J*=6.97 Hz, 1H, Ibu-CHCH<sub>3</sub>), 4.35 - 4.59 (m, 3H, CH<sub>2</sub> serine, CH serine), 7.01 - 7.28 (m, 4H, Ibu-CH aromatic). <sup>13</sup>C NMR (75 MHz, methanol-*d*<sub>4</sub>) δ ppm 18.87, 22.77, 25.81, 25.92, 31.51, 37.21, 38.08, 46.03, 46.08, 55.21, 65.57, 67.29, 128.38, 130.44, 139.22, 176.37. *u*<sub>max</sub> (thin film, cm<sup>-1</sup>): 2954-2868, 1738, 161, 1488, 1393, 1328, 1151, 1066, 545. MS: C<sub>22</sub>H<sub>35</sub>N<sub>2</sub>O<sub>5</sub>, *m/z* (ES<sup>+</sup>) 403.22 [M+H]<sup>+</sup>. HRMS: Calculated C<sub>22</sub>H<sub>34</sub>N<sub>2</sub>O<sub>5</sub> 403.2238, found 403.2230.

6.6.3. Cyclopropane-serine carrier (section 3.1).

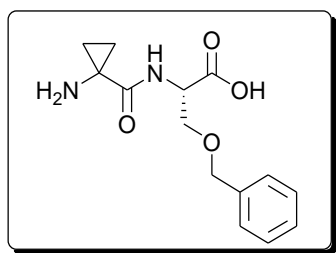
**(S)-tert-butyl 3-(benzyloxy)-2-(1-(tert-butoxycarbonyl)cyclopropanecarboxamido)propanoate  
(165)**



1-(*tert*-butoxycarbonyl)cyclopropanecarboxylic acid (**164**) (501 mg; 2.49 mM) and **50** (569 mg; 2.26 mM) were dissolved in 5 mL anhydrous DMF under nitrogen atmosphere at 0°C. DIPEA (788  $\mu$ L; 4.53 mM) was added dropwise and the reaction stirred for 10 minutes prior to the dropwise addition of DPPA (537  $\mu$ L; 2.49 mM). The solution was stirred at 0°C for 72 hours after which the solvent was removed *in vacuo*. The residue was dissolved in 20 mL EtOAc and washed with two 10 mL portions of  $\text{NH}_4\text{Cl}$ , two 10 mL portions of  $\text{Na}_2\text{CO}_3$  and one 20 mL portion of brine. The organic layer was dried over anhydrous  $\text{MgSO}_4$ , filtered and the solvent removed *in vacuo* to give 871 mg of **165** as a white solid (2.00 mM; 89%).

$R_f$ : 0.40 (EtOAc:Pet ether 4:6).  $^1\text{H}$  NMR (300 MHz, methanol- $d_4$ )  $\delta$  ppm 1.02 - 1.09 (m, 2H, CH-CH cyclopropane), 1.44 (s, 9H,  $\text{CH}_3$  Boc), 1.46 (s, 11H,  $\text{CH}_3$  *tert*-butyl, CH-CH cyclopropane), 3.70 (ABdd,  $J=9.42, 3.20$  Hz, 1H,  $\text{CH}_2$  serine), 3.90 (ABdd,  $J=9.42, 3.39$  Hz, 1H,  $\text{CH}_2$  serine), 4.45 - 4.61 (m, 3H,  $\text{CH}_2$ -benzyl, CH serine), 7.25 - 7.39 (m, 5H, CH benzyl), 7.61 (d,  $J=7.72$  Hz, 1H, NH serine).  $^{13}\text{C}$  NMR (75 MHz, methanol- $d_4$ )  $\delta$  ppm 17.80, 28.29, 28.70, 36.09, 55.07, 70.96, 74.35, 81.11, 83.36, 128.83, 129.44, 139.16, 158.09, 170.41, 174.72.  $\nu_{\text{max}}$  (thin film,  $\text{cm}^{-1}$ ): 2977-2841, 2446, 1721, 1648, 1443, 1390, 1365, 1256, 1160, 1111, 746.  $[\alpha]_D^{25}$  ( $\text{CHCl}_3$ ;  $c = 0.0122$ ): + 5.63. MS:  $\text{C}_{23}\text{H}_{34}\text{N}_2\text{O}_6$ ,  $m/z$  ( $\text{ES}^+$ ) 435.25  $[\text{M}+\text{H}]^+$ . HRMS: Calculated  $\text{C}_{23}\text{H}_{35}\text{N}_2\text{O}_6$  435.2495, found 435.2493. MP: 73.2°C

**(S)-2-(1-aminocyclopropanecarboxamido)-3-(benzyloxy)propanoic acid (**166**).**

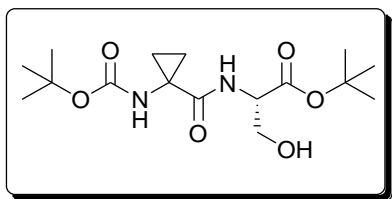


**165** (92 mg, 0.21 mM) was dissolved in 5 mL 97% formic acid and refluxed at 100°C for three hours. The reaction was cooled to room temperature and the formic acid removed *in vacuo*. The residue was taken up in 5 mL distilled water, filtered through a pipette plugged with glass wool and extracted with 2 mL Et<sub>2</sub>O. The aqueous layer was lyophilised to give 67 mg of **166** as a yellow resin in formate salt form (0.21 mM; 97%).

<sup>1</sup>H NMR (300 MHz, chloroform-*d*) δ ppm 0.98 - 1.12 (m, 2H, CH-CH cyclopropane), 1.39 - 1.58 (m, 2H, CH-CH cyclopropane), 3.69 - 3.98 (m, 2H, CH<sub>2</sub> serine), 4.49 - 4.66 (m, 3H, CH<sub>2</sub> serine, CH serine), 7.20 - 7.42 (m, 5H, CH benzyl). <sup>13</sup>C NMR (75 MHz, chloroform-*d*) δ ppm 17.30, 34.62, 71.15, 74.19, 126.67, 129.13, 139.28, 165.13, 173. *u*<sub>max</sub> (thin film, cm<sup>-1</sup>): 3293-2868, 1654, 1508, 1392, 1199, 1098, 735, 696. MS: C<sub>14</sub>H<sub>18</sub>N<sub>2</sub>O<sub>4</sub>, *m/z* (ES<sup>+</sup>) 279.13 [M+H<sup>+</sup>]. HRMS: Calculated C<sub>14</sub>H<sub>19</sub>N<sub>2</sub>O<sub>4</sub> 279.1345, found 279.1345



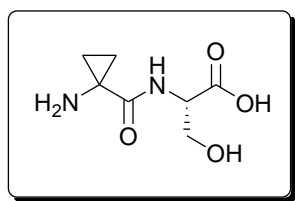
**(S)-tert-butyl 2-(1-(tert-butoxycarbonyl)cyclopropanecarboxamido)-3-hydroxypropanoate (167).**



**165** (600 mg, 1.38 mM) was dissolved in 5 mL MeOH. 10% Pd/C (100 mg) was added and the suspension stirred under a hydrogen atmosphere at room temperature for 24 hours. The reaction mixture was filtered through a Celite<sup>®</sup> bed and the organic solvent removed *in vacuo*. 466 mg of **167** was obtained as a yellow solid (1.35 mM, 98%).

R<sub>f</sub>: 0.05 (EtOAc:pet ether 4:6). <sup>1</sup>H NMR (300 MHz, methanol-*d*<sub>4</sub>) δ ppm 1.06 (d, *J*=3.20 Hz, 2H, CH –CH cyclopropane), 1.45 (d, *J*=3.58 Hz, 2H, CH –CH cyclopropane), 1.49 (s, 9H, CH<sub>3</sub> Boc), 1.50 (s, 9H, CH<sub>3</sub> *tert*-butyl), 3.78 - 3.95 (ABq, 2H, CH<sub>2</sub> serine), 4.34 (br. s., 1H, CH serine), 7.63 (d, *J*=6.03 Hz, 1H, NH serine). <sup>13</sup>C NMR (75 MHz, methanol-*d*<sub>4</sub>) δ ppm 17.29, 18.13, 28.31, 28.71, 36.11, 57.03, 62.90, 81.29, 83.34, 158.33, 170.73, 174.71. *u*<sub>max</sub> (thin film, cm<sup>-1</sup>): 3313, 2973, 1679, 1515, 1366, 1280, 1157, 847. [α]<sub>D</sub><sup>25</sup> (CHCl<sub>3</sub>; *c* = 0.0194): + 25.73. MS: C<sub>16</sub>H<sub>28</sub>N<sub>2</sub>O<sub>6</sub>, *m/z* (ES<sup>+</sup>) 345.120 [M+H]<sup>+</sup>. HRMS: Calculated C<sub>16</sub>H<sub>29</sub>N<sub>2</sub>O<sub>6</sub> 345.2026, found 345.2029. MP: 112.6°C

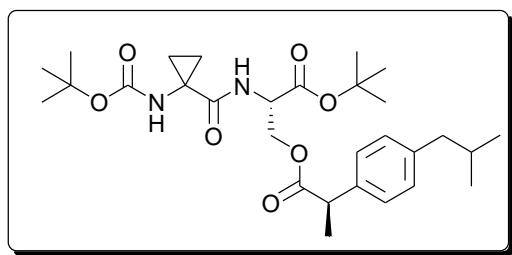
**(S)-2-(1-aminocyclopropanecarboxamido)-3-hydroxypropanoic acid (153).**



**167** (66 mg, 0.19 mM) was dissolved in 5 mL 97% formic acid and refluxed at 100°C for three hours. The reaction was cooled to room temperature and the formic acid removed *in vacuo*. The residue was taken up in 5 mL distilled water, filtered through a pipette plugged with glass wool and extracted with 2 mL Et<sub>2</sub>O. The aqueous layer was lyophilised to give 42 mg of **153** as a yellow resin in formate salt form (0.18 mM; 93%).

<sup>1</sup>H NMR (300 MHz, methanol-*d*<sub>4</sub>) δ ppm 1.10 (m, *J*=3.58 Hz, 2H, CH-CH cyclopropane), 1.20 (m, *J*=3.58 Hz, 1H, CH cyclopropane), 1.44 - 1.58 (m, 2H, CH-CH cyclopropane), 3.75 - 4.07 (m, 2H, CH<sub>2</sub> serine), 4.41 - 4.55 (m, 1H, CH serine), 8.16 (s, 1H, NH serine). <sup>13</sup>C NMR (75 MHz, methanol-*d*<sub>4</sub>) δ ppm 17.51, 17.69, 34.6, 55.31, 62.91, 165.47, 173.53. *u*<sub>max</sub> (thin film, cm<sup>-1</sup>): 2953, 2874, 1648, 1518, 1383, 1208, 1046. MS: C<sub>7</sub>H<sub>12</sub>N<sub>2</sub>O<sub>4</sub>, *m/z* (ES<sup>+</sup>) 189.09 [M+H]<sup>+</sup>. HRMS: Calculated C<sub>7</sub>H<sub>13</sub>N<sub>2</sub>O<sub>4</sub> 189.0875, found 189.0872.

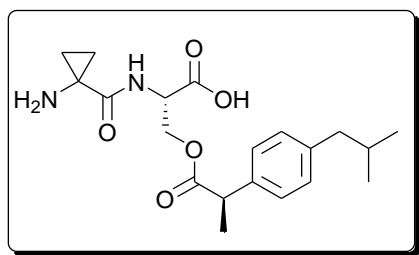
**(S)-2-(1-(*tert*-butoxycarbonylcyclopropanecarboxamido)-3-((R)-2-(4-isobutylphenyl)propanoyloxy)propanoic acid *tert*-butyl ester (168).**



Ibuprofen (**77**) (228 mg, 1.10 mM), DCC (251 mg, 1.22 mM) and DMAP (135 mg, 1.10 mM) were dissolved in 5 mL anhydrous DCM under a nitrogen atmosphere at 0°C and left to stir for 30 minutes. **167** (400 mg, 1.16 mM) in 2 mL anhydrous DCM was added and reaction mixture stirred at room temperature for 72 hours. The solution was filtered and the solvent removed *in vacuo*. The resultant white solid was purified by flash column chromatography (a gradient of 2:8 to 7:3 EtOAc: pet ether) to give 457 mg of **168** as a colourless oil (0.86 mM, 76%).

R<sub>f</sub>: 0.58 (EtOAc:Pet ether 4:6). <sup>1</sup>H NMR (300 MHz, methanol-*d*<sub>4</sub>) δ ppm 0.92 (d, *J*=6.6, 6H, Ibu-CH(CH<sub>3</sub>)<sub>2</sub>), 1.05 (m, 2H, CH–CH cyclopropane), 1.33 (s, 2H, CH–CH cyclopropane), 1.41 (s, 9H, CH<sub>3</sub> Boc), 1.43 - 1.51 (m, 12H, CH<sub>3</sub> *tert*-butyl, Ibu-CH<sub>3</sub>), 1.86 (dt, *J*=13.54, 6.88 Hz, 1H, Ibu-CH(CH<sub>3</sub>)<sub>2</sub>), 2.47 (d, *J*=7.16 Hz, 2H, Ibu-CH<sub>2</sub>CH), 3.73 (m, 1H, Ibu-CHCH<sub>3</sub>), 4.47 (m, 3H, CH<sub>2</sub> serine, CH serine), 7.09 - 7.23 (m, 4H, Ibu-CH aromatic). <sup>13</sup>C NMR (75 MHz, methanol-*d*<sub>4</sub>) δ ppm 17.89, 19.33, 22.78, 28.17, 28.72, 31.51, 36.77, 46.07, 46.34, 54.16, 64.86, 81.18, 83.85, 128.38, 130.49, 138.99, 141.82, 169.35, 175.83. *u*<sub>max</sub> (thin film, cm<sup>-1</sup>): 2974, 1737.1650, 1447, 1392, 1160, 631, 497. MS: C<sub>29</sub>H<sub>44</sub>N<sub>2</sub>O<sub>7</sub>, *m/z* (ES<sup>+</sup>) 533.32 [M+H]<sup>+</sup>. HRMS: Calculated C<sub>29</sub>H<sub>45</sub>N<sub>2</sub>O<sub>7</sub> 533.3227, found 533.3230

(S)-2-(1-aminocyclopropanecarboxamido)-3-((R)-2-(4-isobutylphenyl)propanoyloxy)propanoic acid (**169**).

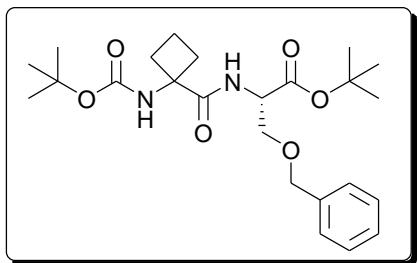


**168** (72 mg, 0.14 mM) was dissolved in 5 mL 97% formic acid and refluxed at 100°C for three hours. The reaction was cooled to room temperature and the formic acid removed *in vacuo*. The residue was taken up in 5 mL distilled water, filtered through a pipette plugged with glass wool and extracted with 2 mL Et<sub>2</sub>O. The aqueous layer was lyophilised to give 55 mg of **169** as a white solid in formate salt form (0.13 mM; 97%).

<sup>1</sup>H NMR (300 MHz, methanol-*d*<sub>4</sub>) δ ppm 0.91 (d, *J*=6.4, 6H, Ibu-CH(CH<sub>3</sub>)<sub>2</sub>), 1.04-1.36 (m, 4H, CH<sub>2</sub> cyclopropane), 1.46 (d, 3H, *J*=4.1, Ibu-CH<sub>3</sub>), 1.85 (m, 1H, Ibu-CH(CH<sub>3</sub>)<sub>2</sub>), 2.46 (d, *J*=7 Hz, 2H, Ibu-CH<sub>2</sub>CH), 3.78 (m, 1H, Ibu-CHCH<sub>3</sub>), 4.30-4.60 (m, 3H, CH<sub>2</sub> serine, CH serine), 6.98 - 7.32 (m, 4H, Ibu-CH<sub>ar</sub>), 8.11 (br. s, 1H, NH serine). <sup>13</sup>C NMR (75 MHz, methanol-*d*<sub>4</sub>) δ ppm 17.71, 18.73, 22.72, 31.50, 35.66, 46.03, 46.06, 54.06, 65.32, 128.32, 129.03, 139.06, 141.78, 175.30. *ν*<sub>max</sub> (thin film, cm<sup>-1</sup>): 2955, 1682, 1532, 1395, 1150, 1069, 525. MS: C<sub>20</sub>H<sub>28</sub>N<sub>2</sub>O<sub>5</sub>, *m/z* (ES<sup>+</sup>) 377.21 [M+H]<sup>+</sup>. HRMS: Calculated C<sub>20</sub>H<sub>29</sub>N<sub>2</sub>O<sub>5</sub> 377.2077, found 377.2081.

6.6.4. Cyclobutane carrier (section 3.1).

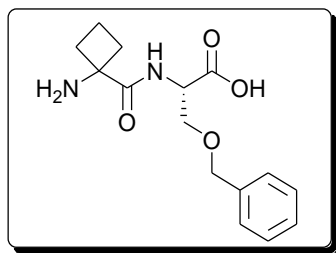
**(S)-tert-butyl 3-(benzyloxy)-2-(1-(tert-butoxycarbonyl)cyclobutanecarboxamido)propanoate (171).**



1-(*tert*-butoxycarbonyl)cyclobutanecarboxylic acid (**170**) (532 mg; 2.47 mM) and **50** (565 mg; 2.25 mM) were dissolved in 5 mL anhydrous DMF under nitrogen atmosphere at 0°C. DIPEA (783  $\mu$ L; 4.49 mM) was added dropwise and the reaction stirred for 10 minutes prior to the dropwise addition of DPPA (533  $\mu$ L; 2.47 mM). The solution was stirred at 0°C for 72 hours after which the solvent was removed *in vacuo*. The residue was dissolved in 20 mL EtOAc and washed with two 10 mL portions of  $\text{NH}_4\text{Cl}$ , two 10  $\text{Na}_2\text{CO}_3$  and one 20 mL portion of brine. The organic layer was dried over anhydrous  $\text{MgSO}_4$ , filtered and the solvent removed *in vacuo* to give 919 mg of **171** as a white solid (0.20 mM; 91%).

$R_f$ : 0.45 (EtOAc:Pet ether 4:6).  $^1\text{H}$  NMR (300 MHz, chloroform-*d*)  $\delta$  ppm 1.42 (s, 9H,  $\text{CH}_3$  Boc), 1.45 (s, 9H,  $\text{CH}_3$  *tert*-butyl), 2.01 (m,  $J=8.10$  Hz, 2H,  $\text{CH-CH}_2\text{-CH}$  cyclobutane), 2.09 - 2.21 (m, 2H,  $\text{CH-CH}_2\text{-CH}$  cyclobutane), 2.60 - 2.80 (m, 2H,  $\text{CH}_2\text{-CH}_2\text{-CH}_2$  cyclobutane), 3.66 (ABdd,  $J=9.23$ , 3.20 Hz, 1H,  $\text{CH}_2$  serine), 3.89 (ABdd,  $J=9.40$ , 3.20 Hz, 1H,  $\text{CH}_2$  serine), 4.41 - 4.60 (ABq, 2H,  $\text{CH}_2$  benzyl), 4.64 (dt,  $J=8.10$ , 3.11 Hz, 1H, CH serine), 7.26 - 7.35 (m, 5H, CH benzyl).  $^{13}\text{C}$  NMR (75 MHz, chloroform-*d*)  $\delta$  ppm 16.18, 28.32, 28.74, 31.75, 56.67, 60.12, 70.21, 73.35, 80.41, 83.15, 126.53, 128.62, 129.37, 139.20, 156.02, 170.43, 177.28.  $\nu_{\text{max}}$  (thin film,  $\text{cm}^{-1}$ ): 3436, 3308, 2979, 1728, 1495, 1634, 1392, 1290, 1253, 1155, 1084, 846.  $[\alpha]_D^{25}$  ( $\text{CHCl}_3$ ;  $c = 0.0097$ ): + 4.20. MS:  $\text{C}_{24}\text{H}_{36}\text{N}_2\text{O}_6$ ,  $m/z$  ( $\text{ES}^+$ ) 449.27  $[\text{M}+\text{H}]^+$ . HRMS: Calculated  $\text{C}_{24}\text{H}_{37}\text{N}_2\text{O}_6$  449.2652, found 449.2638. MP: 74.2°C

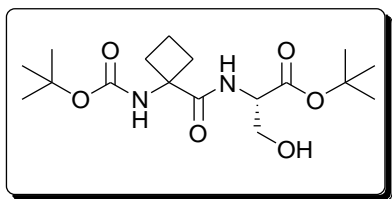
**(S)-2-(1-aminocyclobutanecarboxamido)-3-(benzyloxy)propanoic acid (**172**).**



**171** (143 mg, 0.32 mM) was dissolved in 5 mL 97% formic acid and refluxed at 100°C for three hours. The reaction was cooled to room temperature and the formic acid removed *in vacuo*. The residue was taken up in 5 mL distilled water, filtered through a pipette plugged with glass wool and extracted with 2 mL Et<sub>2</sub>O. The aqueous layer was lyophilised to give 99 mg of **172** as a white solid in formate salt form (0.29 mM; 92%).

<sup>1</sup>H NMR (300 MHz, methanol-*d*<sub>4</sub>) δ ppm 1.90 - 2.49 (m, 5H, CH<sub>2</sub>-CH<sub>2</sub>-CH<sub>2</sub> cyclobutane, CH<sub>2</sub>-CH-CH<sub>2</sub> cyclobutane), 2.55 - 2.74 (m, 1H, CH<sub>2</sub>-CH-CH<sub>2</sub> cyclobutane), 3.72 - 3.97 (m, 2H, CH<sub>2</sub> serine), 4.05 - 4.15 (m, 1H, CH serine), 4.46 - 4.66 (m, 2H, CH<sub>2</sub>-benzyl), 7.27 - 7.45 (m, 4H, CH benzyl), 8.34 - 8.46 (m, 1H, NH serine). <sup>13</sup>C NMR (75 MHz, methanol-*d*<sub>4</sub>) δ ppm 15.18, 16.51, 32.27, 54.48, 57.63, 74.08, 74.51, 128.95, 129.40, 129.56, 139.51, 165.03, 171.64.  $\nu_{\max}$  (thin film, cm<sup>-1</sup>): 2944, 1655, 1520, 1385, 1076, 695. MS: C<sub>15</sub>H<sub>20</sub>N<sub>2</sub>O<sub>4</sub>, *m/z* (ES<sup>+</sup>) 293.15 [M+H]<sup>+</sup>. HRMS: Calculated C<sub>15</sub>H<sub>21</sub>N<sub>2</sub>O<sub>4</sub> 293.1501, found 293.1508.

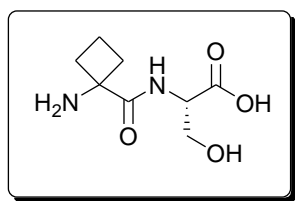
**(S)-tert-butyl 2-(1-(tert-butoxycarbonyl)cyclobutanecarboxamido)-3-hydroxypropanoate (**173**).**



**171** (700 mg, 1.56 mM) was dissolved in 5 mL MeOH. 10% Pd/C (100 mg) was added and the suspension stirred under a hydrogen atmosphere at room temperature for 24 hours. The reaction mixture was filtered through a Celite<sup>®</sup> bed and the organic solvent removed *in vacuo*. 554 mg of **173** was obtained as a white solid (1.54 mM, 99%).

R<sub>f</sub>: 0.19 (EtOAc:Pet ether 4:6). <sup>1</sup>H NMR (300 MHz, methanol-*d*<sub>4</sub>) δ ppm 1.46, (s, 9H, CH<sub>3</sub> Boc), 1.49 (s, 9H, CH<sub>3</sub> *tert*-butyl), 1.87 - 2.05 (m, 2H, CH-CH<sub>2</sub>-CH cyclobutane), 2.07 - 2.23 (m, 2H, CH-CH<sub>2</sub>-CH cyclobutane), 2.64 (m, 2H, CH-CH<sub>2</sub>-CH cyclobutane), 3.84 (m, *J*=3.58 Hz, 2H, ABq, 2H, CH<sub>2</sub> serine), 4.35 (br. s., 1H, CH serine). <sup>13</sup>C NMR (75 MHz, methanol-*d*<sub>4</sub>) δ ppm 16.21, 28.34, 28.79, 31.84, 32.75, 56.67, 60.14, 62.98, 80.92, 83.11, 175.03, 170.83, 176.34. *ν*<sub>max</sub> (thin film, cm<sup>-1</sup>): 3306, 2978, 1679, 1416, 1290, 1253, 1156, 1079, 845. [α]<sub>D</sub><sup>25</sup> (CHCl<sub>3</sub>; c = 0.0048): + 15.32. MS: C<sub>17</sub>H<sub>30</sub>N<sub>2</sub>O<sub>6</sub>, *m/z* (ES<sup>+</sup>) 359.22 [M+H]<sup>+</sup>. HRMS: Calculated C<sub>17</sub>H<sub>31</sub>N<sub>2</sub>O<sub>6</sub> 359.2182, found 359.2183. MP: 125.4°C

**(S)-2-(1-aminocyclobutanecarboxamido)-3-hydroxypropanoic acid (154).**

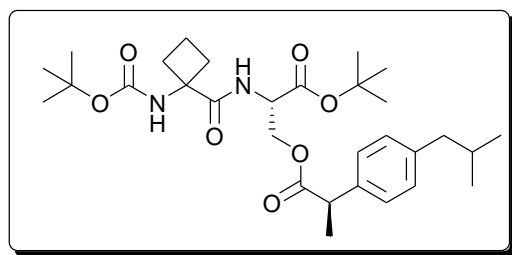


**173** (79 mg, 0.22 mM) was dissolved in 5 mL 97% formic acid and refluxed at 100°C for three hours. The reaction was cooled to room temperature and the formic acid removed *in vacuo*. The residue was taken up in 5 mL distilled water, filtered through a pipette plugged with glass wool and extracted with 2 mL Et<sub>2</sub>O. The aqueous layer was lyophilised to give 51 mg of **154** as a white solid in formate salt form (0.21 mM; 94%).

<sup>1</sup>H NMR (300 MHz, methanol-*d*<sub>4</sub>) δ ppm 1.92 - 2.51 (m, 4H, CH<sub>2</sub>-CH<sub>2</sub>-CH<sub>2</sub> cyclobutane), 2.58 - 2.72 (m, 1H, CH<sub>2</sub>-CH-CH<sub>2</sub> cyclobutane), 2.74 - 2.86 (m, 1H, CH<sub>2</sub>-CH-CH<sub>2</sub> cyclobutane), 3.71 - 3.99 (m, 2H, CH<sub>2</sub> serine), 4.55 (m, 1H, CH serine), 8.25 (br. s., 1H, NH serine). <sup>13</sup>C NMR (75 MHz, methanol-*d*<sub>4</sub>) δ ppm 15.15, 16.43, 28.28, 55.10, 56.69, 63.03, 163.87, 176.05.  $\nu_{\max}$  (thin film, cm<sup>-1</sup>): 3243, 2952, 1658, 1393, 759, 495. MS: C<sub>8</sub>H<sub>14</sub>N<sub>2</sub>O<sub>4</sub>, *m/z* (ES<sup>+</sup>) 203.10 [M+H<sup>+</sup>]. HRMS: Calculated C<sub>8</sub>H<sub>15</sub>N<sub>2</sub>O<sub>4</sub> 203.10, found 203.1032.



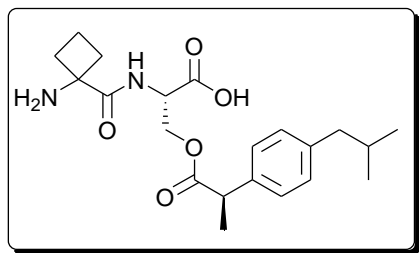
**(S)-2-(1-(*tert*-butoxycarbonylcyclobutanecarboxamido)-3-((R)-2-(4-isobutylphenyl)propanoyloxy)propanoic acid *tert*-butyl ester (174).**



Ibuprofen (**77**) (208 mg, 1.01 mM), DCC (229 mg, 1.11 mM) and DMAP (123 mg, 1.01 mM) were dissolved in 5 mL anhydrous DCM under a nitrogen atmosphere at 0°C and left to stir for 30 minutes. **173** (380 mg, 1.06 mM) in 2 mL anhydrous DCM was added and reaction mixture stirred at room temperature for 72 hours. The solution was filtered and the solvent removed *in vacuo*. The resultant white solid was purified by flash column chromatography (a gradient of 2:8 to 7:3 EtOAc: pet ether) to give 422 mg of **174** as a colourless oil (0.77 mM, 76%).

R<sub>f</sub>: 0.63 (EtOAc:Pet ether 4:6). <sup>1</sup>H NMR (300 MHz, methanol-*d*<sub>4</sub>) δ ppm 0.91 (d, *J*=6.6, 6H, Ibu-CH(CH<sub>3</sub>)<sub>2</sub>), 1.42 (s, 9H, CH<sub>3</sub>-Boc), 1.44 (Ibu-CH<sub>3</sub>), 1.46 (m, 9H, CH<sub>3</sub> *tert*-butyl), 1.78 - 2.02 (m, 3H, CH<sub>2</sub> cyclobutane, Ibu-CH(CH<sub>3</sub>)<sub>2</sub>), 2.03-2.19 (m, 2H, CH<sub>2</sub> cyclobutane), 2.47 (d, *J*=7.2 Hz, 2H, Ibu-CH<sub>2</sub>CH), 2.57 - 2.72 (m, 2H, CH<sub>2</sub> cyclobutane), 3.72 (q, *J*=7.16 Hz, 1H, Ibu-CHCH<sub>3</sub>) 4.38 - 4.55 (m, 3H, CH<sub>2</sub> serine, CH serine), 7.07 - 7.22 (m, 4H, Ibu-CH aromatic). <sup>13</sup>C NMR (75 MHz, methanol-*d*<sub>4</sub>) δ ppm 16.12, 19.20, 22.82, 28.21, 28.80, 31.52, 31.95, 46.05, 46.25, 54.13, 60.02, 64.78, 80.88, 83.68, 128.36, 130.52, 139.03, 141.81, 156.95, 169.40, 175.70. *u*<sub>max</sub> (thin film, cm<sup>-1</sup>): 3303, 2974, 1731, 1679, 1506, 1246, 1153, 845. MS: C<sub>30</sub>H<sub>46</sub>N<sub>2</sub>O<sub>7</sub>, *m/z* (ES<sup>+</sup>) 574.34 [M+H]<sup>+</sup>. HRMS: Calculated C<sub>30</sub>H<sub>47</sub>N<sub>2</sub>O<sub>7</sub> 547.3383, found 547.3385.

**(S)-2-(1-aminocyclobutanecarboxamido)-3-((R)-2-(4-isobutylphenyl)propanoyloxy)propanoic acid (175).**

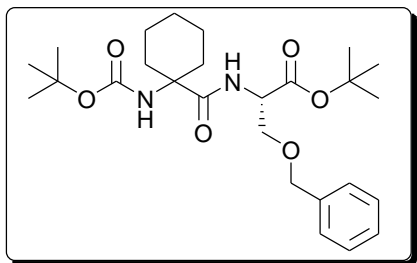


**174** (104 mg, 0.19 mM) was dissolved in 5 mL 97% formic acid and refluxed at 100°C for three hours. The reaction was cooled to room temperature and the formic acid removed *in vacuo*. The residue was taken up in 5 mL distilled water, filtered through a pipette plugged with glass wool and extracted with 2 mL Et<sub>2</sub>O. The aqueous layer was lyophilised to give 53 mg of **175** as a white solid in formate salt form (0.12 mM; 64%).

<sup>1</sup>H NMR (300 MHz, methanol-*d*<sub>4</sub>) δ ppm 0.90 (d, *J*=6.6, 6H, Ibu-CH(CH<sub>3</sub>)<sub>2</sub>), 1.44 (d, *J*=7, 3H, (Ibu-CH<sub>3</sub>), 1.84 (dt, *J*=13.61, 6.66 Hz, 1H, Ibu-CH(CH<sub>3</sub>)<sub>2</sub>), 1.93-2.16 (m, 2H, CH<sub>2</sub> cyclobutane), 2.19-2.32 (m, 2H, CH<sub>2</sub> cyclobutane), 2.44 (d, *J*=7 Hz, 2H, Ibu-CH<sub>2</sub>CH), 2.63 (m, 2H, CH<sub>2</sub> cyclobutane), 3.76 (q, *J*=6.84 Hz, 1H, Ibu-CHCH<sub>3</sub>), 4.40 - 4.62 (m, 3H, CH<sub>2</sub> serine, CH serine), 7.04 - 7.27 (m, 4H, Ibu-CH aromatic), 8.41 (br. s., 1H, NH serine). <sup>13</sup>C NMR (300 MHz, METHANOL-*d*<sub>4</sub>) δ ppm 15.22, 18.72, 22.77, 30.51, 31.49, 46.04, 46.08, 53.23, 59.46, 65.66, 128.34, 130.44, 139.26, 141.78, 176.37. *ν*<sub>max</sub> (thin film, cm<sup>-1</sup>): 2953, 1732, 1662, 1393, 1164, 738, 495. MS: C<sub>21</sub>H<sub>30</sub>N<sub>2</sub>O<sub>5</sub>, *m/z* (ES<sup>+</sup>) 391.22 [M+H]<sup>+</sup>. HRMS: Calculated C<sub>21</sub>H<sub>31</sub>N<sub>2</sub>O<sub>5</sub> 391.2233, found 391.2239.

6.6.5. Homocycloleucine carrier (section 3.1).

**(S)-tert-butyl 3-(benzyloxy)-2-(1-(tert-butoxycarbonyl)cyclohexanecarboxamido)propanoate (177).**



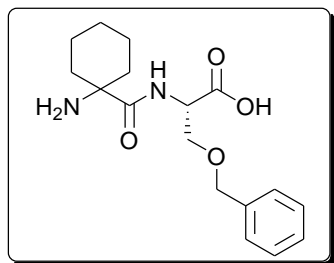
1-(*tert*-butoxycarbonyl)cyclohexanecarboxylic acid (**176**) (600 mg; 2.47 mM) and **50** (563 mg; 2.24 mM) were dissolved in 5 mL anhydrous DMF under nitrogen atmosphere at 0°C. DIPEA (781  $\mu$ L; 4.48 mM) was added dropwise and the reaction stirred for 10 minutes prior to the dropwise addition of DPPA (531  $\mu$ L; 2.47 mM). The solution was stirred at 0°C for 72 hours after which the solvent was removed *in vacuo*. The residue was dissolved in 20 mL EtOAc and washed with two 10 mL portions of  $\text{NH}_4\text{Cl}$ , two 10 mL portions of  $\text{Na}_2\text{CO}_3$  and one 20 mL portion of brine. The organic layer was dried over anhydrous  $\text{MgSO}_4$ , filtered and the solvent removed *in vacuo* to give 1.029 g of **177** as a white solid (0.97 mM; 97%).

$R_f$ : 0.55 (EtOAc:Pet ether 4:6).  $^1\text{H}$  NMR (300 MHz, methanol- $d_4$ )  $\delta$  ppm 1.22 - 1.37 (m, 2H,  $\text{CH}_2\text{-CH}_2\text{-CH}_2\text{-CH}_2\text{-CH}_2$  cyclohexane), 1.43 (s, 9H,  $\text{CH}_3$  Boc), 1.46 (s, 9H,  $\text{CH}_3$  *tert*-butyl), 1.59 (br. s., 4H,  $\text{CH}_2\text{-CH}_2\text{-CH}_2\text{-CH}_2\text{-CH}_2$  cyclohexane), 1.76 (m,  $J=3.77$  Hz, 2H,  $\text{CH-CH}_2\text{-CH}_2\text{-CH}_2\text{-CH}$  cyclohexane), 1.98 - 2.15 (m, 2H,  $\text{CH-CH}_2\text{-CH}_2\text{-CH}_2\text{-CH}$  cyclohexane), 3.66 (m,  $J=9.42$ , 1H,  $\text{CH}_2$  serine), 3.66 (m,  $J=9.42$ , 1H,  $\text{CH}_2$  serine), 4.42 - 4.59 (m, 3H,  $\text{CH}$  serine,  $\text{CH}_2$ -benzyl) 6.89 (s, 1H,  $\text{NH}$  homocycloleucine), 7.24 - 7.36 (m, 5H  $\text{CH}$  aromatic), 7.52 - 7.61 (m, 1H  $\text{NH}$  serine).  $^{13}\text{C}$  NMR (75 MHz, methanol- $d_4$ )  $\delta$  ppm 22.37, 26.50, 28.28, 28.80, 32.53, 33.53, 54.72, 60.57, 71.06, 74.38, 80.58, 83.21, 128.87, 129.39, 139.17, 156.67, 170.58, 177.70.  $\nu_{\text{max}}$  (thin film,  $\text{cm}^{-1}$ ): 3403-3294, 2975-2853, 1669, 1506, 1364, 1246, 1096, 754, 592.  $[\alpha]_D^{25}$  ( $\text{CHCl}_3$ ;  $c = 0.0062$ ): + 4.53. MS:

$C_{26}H_{40}N_2O_6$ ,  $m/z$  ( $ES^+$ ) 477.30 [ $M+H^+$ ]. HRMS: Calculated  $C_{26}H_{41}N_2O_6$  477.2965, found 477.2971.

MP: 75.6°C

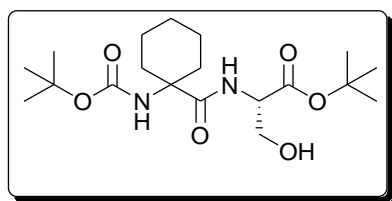
**(S)-2-(1-aminocyclohexanecarboxamido)-3-(benzyloxy)propanoic acid (**178**).**



**177** (155 mg, 0.33 mM) was dissolved in 5 mL 97% formic acid and refluxed at 100°C for three hours. The reaction was cooled to room temperature and the formic acid removed *in vacuo*. The residue was taken up in 5 mL distilled water, filtered through a pipette plugged with glass wool and extracted with 2 mL Et<sub>2</sub>O. The aqueous layer was lyophilised to give 117 mg of **178** as a white solid in formate salt form (0.32 mM; 98%).

<sup>1</sup>H NMR (300 MHz, methanol-*d*<sub>4</sub>)  $\delta$  ppm 1.43 - 1.91 (m, 8H, CH<sub>2</sub> cyclohexane), 2.06 - 2.28 (m, 2H, CH<sub>2</sub> cyclohexane), 3.74 - 3.97 (m, 2H, CH<sub>2</sub> serine), 4.52 - 4.58 (m, 3H, CH serine, CH<sub>2</sub> benzyl), 6.94 - 7.63 (m, 5H, CH aromatic), 8.37 - 8.47 (br. s., 1H, NH serine). <sup>13</sup>C NMR (75 MHz, methanol-*d*<sub>4</sub>)  $\delta$  ppm 22.02, 22.09, 25.28, 32.30, 33.22, 50.80, 61.17, 71.49, 74.02, 128.70, 128.95, 129.36, 139.54, 171.77.  $\nu_{max}$  (thin film, cm<sup>-1</sup>): 3294, 2926, 2857, 1516, 1361, 1100, 734, 667, 572. MS:  $C_{17}H_{24}N_2O_4$ ,  $m/z$  ( $ES^+$ ) 321.18 [ $M+H$ ]<sup>+</sup>. HRMS: Calculated  $C_{17}H_{25}N_2O_4$  321.1814, found 321.1817.

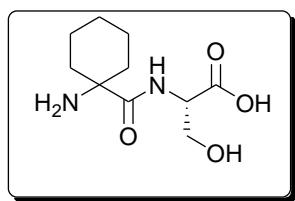
**(S)-tert-butyl 2-(1-(tert-butoxycarbonyl)cyclohexanecarboxamido)-3-hydroxypropanoate (179).**



**177** (732 mg, 1.54 mM) was dissolved in 5 mL MeOH. 10% Pd/C (100 mg) was added and the suspension stirred under a hydrogen atmosphere at room temperature for 24 hours. The reaction mixture was filtered through a Celite® bed and the organic solvent removed *in vacuo*. 587 mg of **179** was obtained as a white solid (1.52 mM, 99%).

R<sub>f</sub>: 0.41 (EtOAc:Pet ether 4:6). <sup>1</sup>H NMR (300 MHz, methanol-*d*<sub>4</sub>) δ ppm 1.21 - 1.40 (m, 2H, CH<sub>2</sub>-CH<sub>2</sub>-CH<sub>2</sub>-CH<sub>2</sub>-CH<sub>2</sub> cyclohexane), 1.43 - 1.47 (m, 9H, CH<sub>3</sub> Boc), 1.49 (s, 9H, CH<sub>3</sub> *tert*-butyl), 1.63 (m, 4H, CH<sub>2</sub>-CH<sub>2</sub>-CH<sub>2</sub>-CH<sub>2</sub>-CH<sub>2</sub> cyclohexane), 1.77 (m, *J*=13.37, 3.01 Hz, 2H, CH-CH<sub>2</sub>-CH<sub>2</sub>-CH<sub>2</sub>-CH cyclohexane), 2.00 (br. s., 2H, CH-CH<sub>2</sub>-CH<sub>2</sub>-CH<sub>2</sub>-CH cyclohexane), 3.83 (ABq, *J*=3.96 Hz, 2H, CH<sub>2</sub> serine), 4.28 - 4.39 (m, 1H, CH serine), 6.84 - 6.93 (m, 1H, NH homocycloleucine) 7.58 (d, *J*=7.54 Hz, 1H, NH serine). <sup>13</sup>C NMR (75 MHz, methanol-*d*<sub>4</sub>) δ ppm 22.40, 26.50, 28.27, 28.78, 32.78, 33.40, 56.60, 60.50, 62.94, 80.69, 83.11, 156.84, 170.87, 177.78. *u*<sub>max</sub> (thin film, cm<sup>-1</sup>): 3406, 3336, 2976-2898, 1684, 1507, 1157, 1073, 845, 568. [α]<sub>D</sub><sup>25</sup> (CHCl<sub>3</sub>; c = 0.0041): + 15.42. MS: C<sub>19</sub>H<sub>34</sub>N<sub>2</sub>O<sub>6</sub>, *m/z* (ES<sup>+</sup>) 387.25 [M+H]<sup>+</sup>. HRMS: Calculated C<sub>19</sub>H<sub>35</sub>N<sub>2</sub>O<sub>6</sub> 387.2495, found 387.2497. MP: 119.5°C

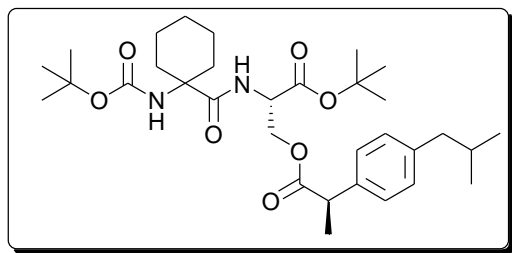
**(S)-2-(1-aminocyclohexanecarboxamido)-3-hydroxypropanoic acid (156).**



**179** (70 mg, 0.18 mM) was dissolved 5 mL 97% formic acid and refluxed at 100°C for three hours. The reaction was cooled to room temperature and the formic acid removed *in vacuo*. The residue was taken up in 5 mL distilled water, filtered through a pipette plugged with glass wool and extracted with 2 mL Et<sub>2</sub>O. The aqueous layer was lyophilised to give 49 mg of **156** as a white solid in formate salt form (0.18 mM; 98%).

<sup>1</sup>H NMR (300 MHz, methanol-*d*<sub>4</sub>) δ ppm 1.37 - 1.96 (m, 8H, CH<sub>2</sub> cyclohexane), 1.98 - 2.15 (m, 2H, CH<sub>2</sub> cyclohexane), 3.89 (d, *J*=4.90, 2H, CH<sub>2</sub> serine), 4.35 - 4.42 (m, 1H, CH serine). <sup>13</sup>C NMR (75 MHz, methanol-*d*<sub>4</sub>) δ ppm 21.95, 25.30, 32.51, 32.91, 51.14, 61.33, 63.34, 172.25.  $\nu_{\max}$  (thin film, cm<sup>-1</sup>): 2934, 1591, 1397, 719, 630, 533. MS: C<sub>10</sub>H<sub>18</sub>N<sub>2</sub>O<sub>4</sub>, *m/z* (ES<sup>+</sup>) 231.13 [M+H<sup>+</sup>]. HRMS: Calculated C<sub>10</sub>H<sub>19</sub>N<sub>2</sub>O<sub>4</sub> 231.1345, found 231.1351.

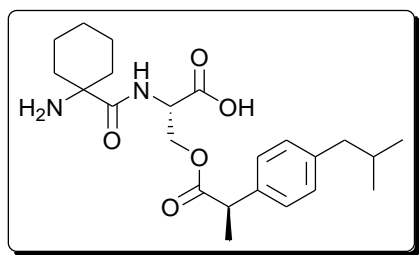
**(S)-2-(1-(*tert*-butoxycarbonylcyclohexanecarboxamido)-3-((R)-2-(4-isobutylphenyl)propanoyloxy)propanoic acid *tert*-butyl ester (180).**



Ibuprofen (**77**) (229 mg, 1.16 mM), DCC (252 mg, 1.22 mM) and DMAP (135 mg, 1.11 mM) were dissolved in 5 mL anhydrous DCM under a nitrogen atmosphere at 0°C and left to stir for 30 minutes. **179** (450 mg, 1.16 mM) in 2 mL anhydrous DCM was added and reaction mixture stirred at room temperature for 72 hours. The solution was filtered and the solvent removed *in vacuo*. The resultant white solid was purified by flash column chromatography (a gradient of 2:8 to 7:3 EtOAc: pet ether) to give 543 mg of **180** as a colourless oil (0.94 mM, 85%).

R<sub>f</sub>: 0.74 (EtOAc:Pet ether 4:6). <sup>1</sup>H NMR (300 MHz, methanol-*d*<sub>4</sub>) δ ppm 0.85 (d, *J*=6.6 Hz, 6H, Ibu-CH(CH<sub>3</sub>)<sub>2</sub>), 1.22 - 1.30 (m, 2H, CH<sub>2</sub>-CH<sub>2</sub>-CH<sub>2</sub>-CH<sub>2</sub>-CH<sub>2</sub> cyclohexane), 1.31-1.42 (m, 21H, CH<sub>3</sub> Boc, CH<sub>3</sub> *tert*-butyl, Ibu-CH<sub>3</sub>), 1.45-1.69 (m, 4H, CH<sub>2</sub> cyclohexane), 1.78 (dq, *J*=13.49, 6.81 Hz, 2H, CH-CH<sub>2</sub>-CH<sub>2</sub>-CH<sub>2</sub>-CH cyclohexane), 1.96 (d, *J*=10.7 Hz, 2H, CH-CH<sub>2</sub>-CH<sub>2</sub>-CH<sub>2</sub>-CH cyclohexane), 2.41 (d, *J*=7.2 Hz, 2H, Ibu-CH<sub>2</sub>CH), 3.66 (q, *J*=7.16 Hz, 1H, Ibu-CHCH<sub>3</sub>), 4.32 (m, 2H, CH<sub>2</sub> serine), 4.44 (m, 1H, CH serine), 7.02 - 7.17 (m, 4H, Ibu-CH aromatic), 7.55 (br. s., 1H, NH serine). <sup>13</sup>C NMR (75 MHz, methanol-*d*<sub>4</sub>) δ ppm 19.01, 22.36, 22.47, 22.78, 26.47, 28.21, 28.83, 31.54, 46.08, 46.19, 54.02, 61.18, 64.01, 80.66, 83.72, 128.41, 130.50, 138.99, 141.81, 169.54, 175.73. *ν*<sub>max</sub> (thin film, cm<sup>-1</sup>): 3419, 2931, 2867, 1736, 1367, 1151, 845, 668, 444. MS: C<sub>32</sub>H<sub>50</sub>N<sub>2</sub>O<sub>7</sub>, *m/z* (ES<sup>+</sup>) 575.37 [M+H]<sup>+</sup>. HRMS: Calculated C<sub>32</sub>H<sub>51</sub>N<sub>2</sub>O<sub>7</sub> 575.3696, found 575.3701.

**(S)-2-(1-aminocyclohexanecarboxamido)-3-((R)-2-(4-isobutylphenyl)propanoyloxy)propanoic acid (**181**).**



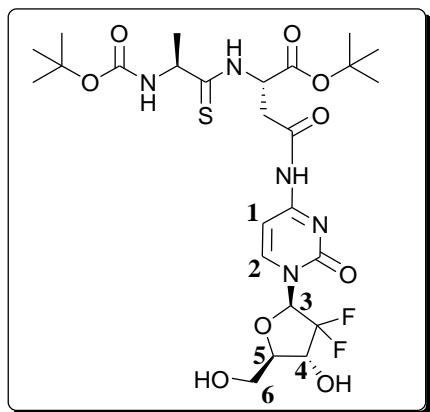
**180** (193 mg, 0.34 mM) was dissolved in 5 mL 97% formic acid and refluxed at 100°C for three hours. The reaction was cooled to room temperature and the formic acid removed *in vacuo*. The residue was taken up in 5 mL distilled water, filtered through a pipette plugged with glass wool and extracted with 2 mL Et<sub>2</sub>O. The aqueous layer was lyophilised to give 147 mg of **181** as a white solid in formate salt form (0.32 mM; 94%).

<sup>1</sup>H NMR (300 MHz, methanol-*d*<sub>4</sub>) δ ppm 0.91 (d, *J*=6.59 Hz, 6H, Ibu-CH(CH<sub>3</sub>)<sub>2</sub>), 1.32 - 1.92 (m, 11H, CH<sub>2</sub> cyclohexane, Ibu-CH<sub>3</sub>), 1.94 - 2.15 (m, 2H, CH-CH<sub>2</sub>-CH<sub>2</sub>-CH<sub>2</sub>-CH cyclohexane), 2.46 (d, *J*=7.16 Hz, 3H, Ibu-CH<sub>3</sub>), 3.65 - 3.80 (m, 1H, Ibu-CHCH<sub>3</sub>), 4.34 - 4.61 (m, 3H, CH<sub>2</sub> serine, CH serine), 6.94 - 7.35, (m, 4H, Ibu-CH aromatic). <sup>13</sup>C NMR (75 MHz, methanol-*d*<sub>4</sub>) δ ppm 19.27, 22.14, 26.29, 22.76, 31.52, 32.29, 33.87, 46.02, 46.10, 54.16, 60.43, 65.38, 128.39, 130.41, 138.83, 155.86, 170.71, 177.25. *u*<sub>max</sub> (thin film, cm<sup>-1</sup>): 3307, 2933, 2866, 1579, 1507, 1396, 1169, 578. MS: C<sub>23</sub>H<sub>34</sub>N<sub>2</sub>O<sub>5</sub>, *m/z* (ES<sup>+</sup>) 419.25 [M+H]<sup>+</sup>. HRMS: Calculated C<sub>23</sub>H<sub>35</sub>N<sub>2</sub>O<sub>5</sub> 419.2546, found 419.2547.



## 6.7 Synthesis of gemcitabine prodrugs (section 4.3.1)

**(S)-tert-butyl 2-((S)-2-(tert-butoxycarbonyl)propanethioamido)-4-(1-((2R,4R,5R)-3,3-difluoro-4-hydroxy-5-(hydroxymethyl)-tetrahydrofuran-2-yl)-2-oxo-1,2-dihydropyrimidin-4-ylamino)-4-oxobutanoate (195).**



Gemcitabine (**184**) (200 mg, 1.16 mM), **57** (286 mg; 0.76 mM), DCC (172 mg, 0.84 mM) and DMAP (93 mg, 0.76 mM) were dissolved in 5 mL anhydrous DCM under a nitrogen atmosphere at 0°C and stirred at room temperature for 72 hours. The solution was filtered and the solvent removed *in vacuo*. The resultant white solid was purified by flash column chromatography (a gradient of 3:7 to 4:1; EtOAc/pet ether) to give 338 mg of **195** as a cream solid (0.54 mM, 72%).

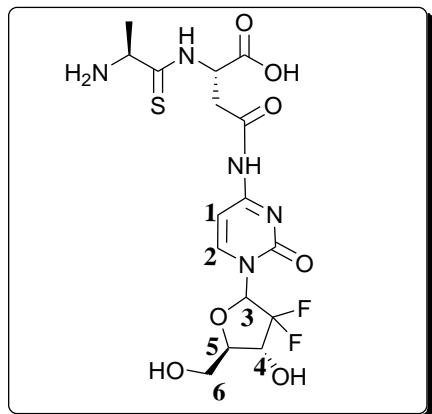
R<sub>f</sub>: 0.31 (EtOAc:Pet ether 6:4). <sup>1</sup>H NMR (300 MHz, methanol-*d*<sub>4</sub>) δ ppm 1.35 (s, 3H, CH<sub>3</sub> alanine), 1.39 (s, 9H, CH<sub>3</sub> Boc), 1.42 (s, 9H, CH<sub>3</sub> *tert*-butyl), 3.12 (t, *J*=4.71 Hz, 2H, CH<sub>2</sub> aspartate), 3.77 (m, 1H, CH<sub>2</sub>-tetrahydrofuran **6**), 3.87 - 3.98 (m, 2H, tetrahydrofuran **4**, CH<sub>2</sub>-tetrahydrofuran **6**), 4.26 (td, *J*=12.15, 8.48 Hz, 1H, tetrahydrofuran **5**), 4.34 - 4.45 (m, 1H, CH alanine), 5.31 (t, *J*=5.65 Hz, 1H, CH aspartate), 6.28 (m, *J*=7.16 Hz, 1H, tetrahydrofuran **3**), 7.48 (d, *J*=7.54 Hz, 1H, cytosine **2**), 8.38 (d, *J*=7.53 Hz, 1H, cytosine **1**). <sup>13</sup>C NMR (75 MHz, methanol-*d*<sub>4</sub>) δ ppm 20.30, 26.62, 27.19, 27.99, 29.18, 37.00, 53.30, 54.03, 56.25, 58.64, 68.22, 68.52, 68.83, 79.17, 81.25, 82.18, 82.25, 96.75, 118.93, 122.37, 144.53, 155.77, 156.03, 163.06, 168.53, 170.55, 206.16,

208.59.  $\nu_{\max}$  (thin film,  $\text{cm}^{-1}$ ): 3242, 2977, 2930, 1659, 1488, 1367, 1315, 1246, 1152, 1052, 785.

MS:  $\text{C}_{25}\text{H}_{37}\text{F}_2\text{N}_5\text{O}_9\text{S}$ ,  $m/z$  ( $\text{ES}^+$ ) 622.24  $[\text{M}+\text{H}]^+$ . HRMS: Calculated  $\text{C}_{25}\text{H}_{38}\text{F}_2\text{N}_5\text{O}_9\text{S}$  622.2358, found

622.2362. MP: 119.3°C

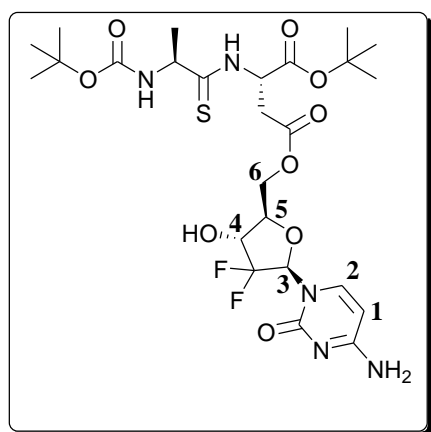
(S)-2-((S)-2-aminopropanethioamido)-4-(1-((2R,4R,5R)-3,3-difluoro-4-hydroxy-5-(hydroxymethyl)-tetrahydrofuran-2-yl)-2-oxo-1,2-dihydropyrimidin-4-ylamino)-4-oxobutanoic acid (**194**).



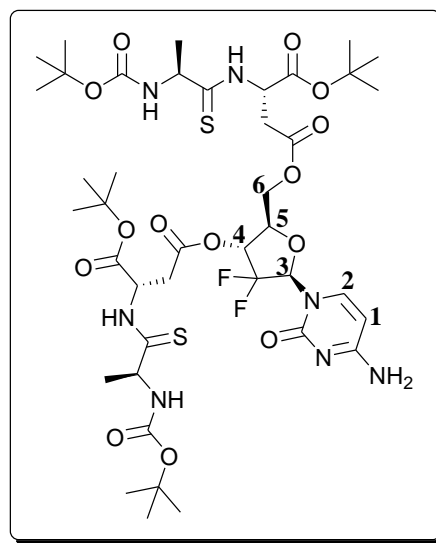
**195** (200 mg, 0.32 mM) was dissolved in 5 mL 97% formic acid and refluxed at 100°C for three hours. The reaction was cooled to room temperature and the formic acid removed *in vacuo*. The residue was taken up in 5 mL distilled water, filtered through a pipette plugged with glass wool and extracted with 2 mL Et<sub>2</sub>O. The aqueous layer was lyophilised to give 160 mg of **194** as a white solid in formate salt form (0.31 mM; 97%).

<sup>1</sup>H NMR (300 MHz, methanol-*d*<sub>4</sub>) δ ppm 1.42 (s, 3H, CH<sub>3</sub> alanine), 3.26 (m, 2H, CH<sub>2</sub> aspartate), 3.73 (dd, *J*=12.43, 3.01 Hz, 1H, CH<sub>2</sub>-tetrahydrofuran **6**), 3.81 - 3.93 (m, 2H, tetrahydrofuran **4**, CH<sub>2</sub>-tetrahydrofuran **6**), 4.03 - 4.10 (m, 1H, CH<sub>2</sub>-tetrahydrofuran **6**), 4.11 - 4.31 (m, 1H, tetrahydrofuran **5**), 4.38 - 4.50 (m, 1H, CH alanine), 5.20 - 5.36 (m, 1H, CH aspartate), 6.08 - 6.25 (m, 2H, tetrahydrofuran **3**), 7.56 (d, 1H, *J*=7.54 Hz, cytosine **2**), 8.43 (d, *J*=7.54 Hz, 1H, cytosine **1**). <sup>13</sup>C NMR (75 MHz, water-*d*<sub>2</sub>) δ ppm 59.21, 68.81, 69.11, 80.23, 93.13, 141.82, 157.86, 164.40. *ν*<sub>max</sub> (thin film, cm<sup>-1</sup>): 3195, 1727, 1651, 1614, 1378, 1198, 1072, 892, 609. MS: C<sub>16</sub>H<sub>21</sub>F<sub>2</sub>N<sub>5</sub>O<sub>7</sub>S, *m/z* (ES<sup>+</sup>) 466.12 [M+H]<sup>+</sup>. HRMS: Calculated C<sub>16</sub>H<sub>22</sub>F<sub>2</sub>N<sub>5</sub>O<sub>7</sub>S 466.1208, found 466.1204.

(S)-4-((2R,3R,5R)-5-(4-amino-2-oxopyrimidin-1(2H)-yl)-4,4-difluoro-3-hydroxy-tetrahydrofuran-2-yl)methyl-1-tert-butyl-2-((S)-2-tert-butoxycarbonylpropanethioamido)succinate (**196**).



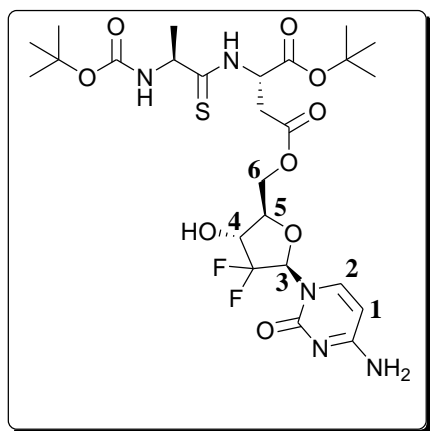
4-amino-1-((2R,4R,5R)-4-(1-tert-butyl-2-((S)-2-tert-butoxycarbonylpropanethioamido)succinate)-5-(methoxy)-(1-tert-butyl-2-((S)-2-tert-butoxycarbonylpropanethioamido)succinate)-3,3-difluoro-tetrahydrofuran-2-yl)pyrimidin-2(1H)-one (**197**).



And

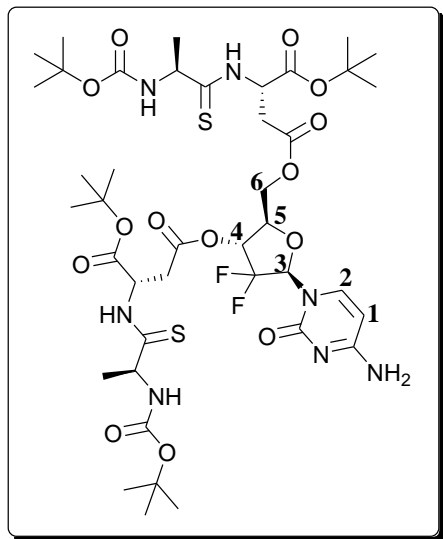
**57** (200 mg; 0.76 mM) and HATU (318 mg; 0.84 mM) were dissolved in 5 mL anhydrous DMF under a nitrogen atmosphere at 0°C. DIPEA (132  $\mu$ L; 0.76 mM) was added dropwise and the solution stirred for 1 hour. Gemcitabine (**184**) (286 mg; 0.76 mM) dissolved in 2 mL anhydrous DMF was added and the solution stirred at room temperature for three days. The solvent was removed *in vacuo* and the residue purified by flash column chromatography (a gradient of 2:8 to 7:3 EtOAc: pet ether) to give 16 mg of **196** as a cream solid (0.03 mM; 3%), 21 mg of **197** as a yellow oil (0.02 mM; 3%) and 245 mg of **195** as a cream solid (0.40 mM, 52%).

**(S)-4-((2R,3R,5R)-5-(4-amino-2-oxopyrimidin-1(2H)-yl)-4,4-difluoro-3-hydroxy-tetrahydrofuran-2-yl)methyl-1-tert-butyl-2-((S)-2-tert-butoxycarbonylpropanethioamido) succinate (196).**



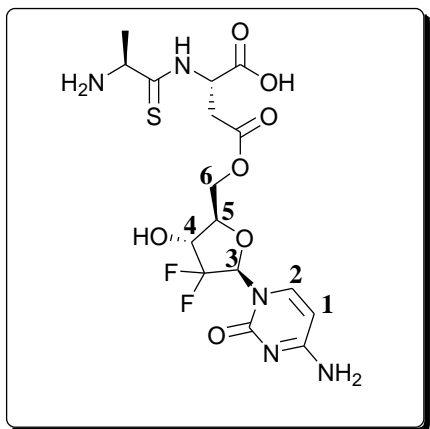
R<sub>f</sub>: 0.27 (EtOAc: pet ether 6:4). <sup>1</sup>H NMR (300 MHz, methanol-*d*<sub>4</sub>) δ ppm 1.34 (d, *J*=7.16 Hz, 2H, CH<sub>3</sub> alanine), 1.37 - 1.43 (m, 18H, CH<sub>3</sub> Boc, CH<sub>3</sub> *tert*-butyl), 3.01 (d, *J*=6.03 Hz, 2H, CH<sub>2</sub> aspartate), 4.08 (br. s., 1H, tetrahydrofuran **4**), 4.13 - 4.28 (m, 1H, tetrahydrofuran **5**), 4.33 - 4.52 (m, 3H, CH<sub>2</sub>-tetrahydrofuran **6**, CH alanine), 5.27 (t, *J*=6.03 Hz, 1H, CH aspartate), 5.94 (d, *J*=7.54 Hz, 2H, cytosine **1**), 6.21 (t, *J*=8.67 Hz, 2H, tetrahydrofuran **3**), 7.56 (d, *J*=7.54 Hz, 2H, cytosine **2**). <sup>13</sup>C NMR (75 MHz, methanol-*d*<sub>4</sub>) δ ppm 20.34, 26.61, 27.18, 34.44, 54.28, 56.28, 56.34, 62.18, 77.88, 79.24, 82.42, 95.34, 121.99, 141.12, 155.78, 156.14, 166.05, 168.37, 169.73, 206.59. *u*<sub>max</sub> (thin film, cm<sup>-1</sup>): 3337, 2978, 2933, 1731, 1065, 1504, 1368, 1153, 1038, 758, 629. MS: C<sub>25</sub>H<sub>37</sub>F<sub>2</sub>N<sub>5</sub>O<sub>9</sub>S, *m/z* (ES<sup>+</sup>) 622.24 [M+H]<sup>+</sup>. HRMS: Calculated C<sub>25</sub>H<sub>38</sub>F<sub>2</sub>N<sub>5</sub>O<sub>9</sub>S 622.2358, found 622.2357. MP: 123.5°C

**4-amino-1-((2R,4R,5R)-4-(1-tert-butyl-2-((S)-2-tert-butoxycarbonylpropanethioamido)succinate)-5-(methoxy)-(1-tert-butyl-2-((S)-2-tert-butoxycarbonylpropanethioamido)succinate)-3,3-difluoro-tetrahydrofuran-2-yl)pyrimidin-2(1H)-one (197).**



R<sub>f</sub>: 0.52 (EtOAc: pet ether 6:4). <sup>1</sup>H NMR (300 MHz, methanol-*d*<sub>4</sub>) δ ppm 1.34 (dd, *J*=6.78, 2.26 Hz, 6H, CH<sub>3</sub> alanine, CH<sub>3</sub> alanine), 1.37 - 1.45 (m, 36H, CH<sub>3</sub> Boc, CH<sub>3</sub> Boc, CH<sub>3</sub> *tert*-butyl, CH<sub>3</sub> *tert*-butyl), 3.00 (d, *J*=5.65 Hz, 2H, CH<sub>2</sub> aspartate), 3.02 - 3.24 (m, 2H, CH<sub>2</sub> aspartate), 4.33 - 4.48 (m, 6H, tetrahydrofuran **5**, CH<sub>2</sub>-tetrahydrofuran **6**, CH alanine, CH alanine), 5.27 (q, *J*=5.90 Hz, 2H, CH aspartate, CH aspartate), 5.33 - 5.45 (m, 1H, tetrahydrofuran **4**), 5.94 (d, *J*=7.54 Hz, 1H, cytosine **1**), 6.27 (t, *J*=8.10 Hz, 1H, tetrahydrofuran **3**), 7.58 (d, *J*=7.54 Hz, 1H, cytosine **2**). <sup>13</sup>C NMR (75 MHz, methanol-*d*<sub>4</sub>) δ ppm 20.41, 26.57, 26.64, 27.20, 33.96, 34.46, 53.95, 54.27, 56.32, 79.19, 82.43, 82.55, 95.46, 155.73, 155.90, 166.06, 168.11, 168.37, 168.81, 169.71. *ν*<sub>max</sub> (thin film, cm<sup>-1</sup>): 3339, 2977, 2933, 1731, 1650, 1504, 1393, 1367, 1152, 1085, 1050, 783. MS: C<sub>41</sub>H<sub>63</sub>F<sub>2</sub>N<sub>7</sub>O<sub>14</sub>S<sub>2</sub>, *m/z* (ES<sup>+</sup>) 980.39 [M+H]<sup>+</sup>. HRMS: Calculated C<sub>41</sub>H<sub>64</sub>F<sub>2</sub>N<sub>7</sub>O<sub>14</sub>S<sub>2</sub> 980.3921, found 980.3922.

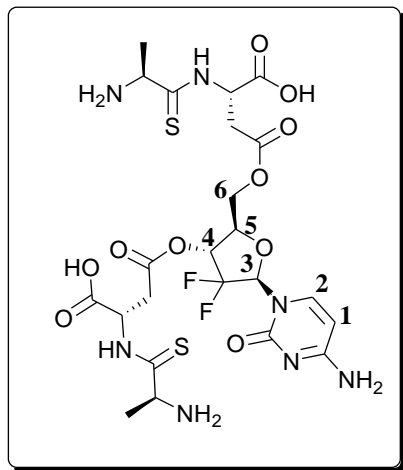
**(S)-4-(((2R,3R,5R)-5-(4-amino-2-oxopyrimidin-1(2H)-yl)-4,4-difluoro-3-hydroxy-tetrahydrofuran-2-yl)methoxy)-2-((S)-2-aminopropanethioamido)-4-oxobutanoic acid (**193**).**



**196** (13 mg, 0.02 mM) was dissolved in 5 mL 97% formic acid and refluxed at 100°C for three hours. The reaction was cooled to room temperature and the formic acid removed *in vacuo*. The residue was taken up in 5 mL distilled water, filtered through a pipette plugged with glass wool and extracted with 2 mL Et<sub>2</sub>O. The aqueous layer was lyophilised to give 10 mg of **193** as a white solid in formate salt form (0.02 mM; 96%).

<sup>1</sup>H NMR (300 MHz, methanol-*d*<sub>4</sub>) δ ppm 1.50 (d, *J*=6.78 Hz, 3H, CH<sub>3</sub> alanine), 3.04 (m, *J*=5.27 Hz, 2H, CH<sub>2</sub> aspartate), 4.03 (m, 1H, tetrahydrofuran **4**), 4.24 (m, 1H, tetrahydrofuran **5**), 4.32 - 4.45 (m, 3H, CH<sub>2</sub>-tetrahydrofuran **6**, CH alanine), 5.10 (m, *J*=7.16 Hz, 1H, CH aspartate), 5.92 (d, *J*=7.54 Hz, 1H, cytosine **1**), 6.18 (q, *J*=8.67 Hz, 2H, tetrahydrofuran **3**), 7.58 (d, *J*=7.91 Hz, 1H, cytosine **2**). <sup>13</sup>C NMR (75 MHz, water-*d*<sub>2</sub>) δ ppm 66.23, 68.84, 69.16, 69.33, 80.23, 84.13, 84.56, 96.21, 118.65, 123.16, 142.36, 154.31, 164.29. *u*<sub>max</sub> (thin film, cm<sup>-1</sup>): 3270, 2977, 2928, 1659, 1488, 1367, 1315, 1245, 1151, 1054, 785. MS: C<sub>16</sub>H<sub>21</sub>F<sub>2</sub>N<sub>5</sub>O<sub>7</sub>S, *m/z* (ES<sup>+</sup>) 466.12 [M+H]<sup>+</sup>. HRMS: Calculated C<sub>16</sub>H<sub>22</sub>F<sub>2</sub>N<sub>5</sub>O<sub>7</sub>S 466.1208, found 466.1215.

4-amino-1-((2R,4R,5R)-4-(2-((S)-2-aminopropanethioamido)-4-oxobutanoic acid)-5-(methoxy)-(2-((S)-2-aminopropanethioamido)-4-oxobutanoic acid)-3,3-difluoro-tetrahydrofuran-2-yl)pyrimidin-2(1H)-one (**198**).



**197** (17 mg, 0.02 mM) was dissolved in 5 mL 97% formic acid and refluxed at 100°C for three hours. The reaction was cooled to room temperature and the formic acid removed *in vacuo*. The residue was taken up in 5 mL distilled water, filtered through a pipette plugged with glass wool and extracted with 2 mL Et<sub>2</sub>O. The aqueous layer was lyophilised to give 12 mg of **198** as a white solid in formate salt form (0.02 mM; 97%).

<sup>1</sup>H NMR (300 MHz, water-*d*<sub>2</sub>) δ ppm 1.44 (dd, *J*=6.69, 2.54 Hz, 6H, CH<sub>3</sub> alanine, CH<sub>3</sub> alanine), 2.84 - 3.11 (m, 4H, CH<sub>2</sub> aspartate, CH<sub>2</sub> aspartate), 4.14 - 4.26 (m, 2H, CH<sub>2</sub>-tetrahydrofuran **6**) 4.28 - 4.47 (m, 4H, tetrahydrofuran **5**, CH alanine, CH alanine), 4.85 - 4.98 (m, 2H, CH aspartate, CH aspartate), 5.20 - 5.35 (m, 1H, tetrahydrofuran **4**), 5.97 (d, *J*=7.91 Hz, 1H, cytosine **1**), 6.14 (t, *J*=6.40 Hz, 1H, tetrahydrofuran **3**), 7.54 (d, *J*=7.16 Hz, 1H, cytosine **2**). <sup>13</sup>C NMR (75 MHz, water-*d*<sub>2</sub>) δ ppm 66.27, 68.51, 68.56, 68.72, 68.84, 69.16, 69.33, 80.17, 84.14, 84.62, 95.93, 118.42, 122.86, 142.29, 154.28, 154.37, 164.26, 164.31. *u*<sub>max</sub> (thin film, cm<sup>-1</sup>): 3340, 2977, 2931, 1645, 1494, 1366, 1282, 1246, 1149, 1047, 842. MS: C<sub>23</sub>H<sub>31</sub>F<sub>2</sub>N<sub>7</sub>O<sub>10</sub>S<sub>2</sub>, *m/z* (ES<sup>+</sup>) 668.16 [M+H]<sup>+</sup>. HRMS: Calculated C<sub>23</sub>H<sub>32</sub>F<sub>2</sub>N<sub>7</sub>O<sub>10</sub>S<sub>2</sub> 668.1620, found 168.1625.



## References

1. Gomez-Orellana, I.; *Expert Opin. Drug Deliv.* **2005**, 2(3), 419-433.
2. Lipinski, C. A.; Lombardo, F.; Dominy, B. W.; Feeney, P. J.; *Adv. Drug Deliv. Rev.* **2001**, 46, 3-26.
3. Estudante, M.; Morais, J. G.; Soveral, G.; Benet, L. Z.; *Adv. Drug Deliv. Rev.* **2013**, 65, 1340-1356.
4. Brandsch, M.; Knütter, I.; Bosse-Doenecke, E.; *J. Pharm Pharmacol.* **2008**, 60, 543-585.
5. Våbenø, J.; Nielsen, C. U.; Steffansen, B.; Lejon, T.; Sylte, I.; Jørgensen, F. S.; Luthman, K.; *Bio. Med. Chem.* **2005**, 13, 1977-1988.
6. Varma, V. M.; Ambler, C. M.; Ullah, M.; Rotter, C. J.; Sun, H.; Litchfield, J.; Fenner, K. S.; El-Kattan, A. F.; *Curr. Drug Metab.* **2010**, 11, 730-742.
7. Lu, H.; Klaassen, C.; *Peptides.* **2006**, 27, 850-857.
8. Agu, R.; Cowley, E.; Hhao, D.; MacDonald, C.; Kirkpatrick, D.; Renton, K.; Massoud, E.; *Mol. Pharm.* **2011**, 8, 664-672.
9. Meredith, D.; Boyd, C. A.; *Cell. Mol. Life Sci.* **2000**, 57, 754-778.
10. Mitsuoka, K.; Miyoshi, S.; Kato, Y.; Murakami, Y.; Utsumi, R.; Kubo, Y.; Noda, A.; Nakamura, Y.; Nishimura, S.; Tsuji, A.; *J. Nucl. Med.* **2008**, 49(4), 615-622.
11. Adibi, S. A.; *Gastroenterology.* **1997**, 113, 332-340.
12. Ganapathy, V.; Leibach, F. H.; *J. Biol. Chem.* **1983**, 258, 14189-14192.
13. Ganapathy, V.; Burckhardt, G.; Leibach, F. H.; *J. Biol. Chem.* **1984**, 259, 8954-8959.
14. Hoshi, T.; *Jpn. J. Physiol.* **1985**, 35, 179-191.
15. Ganapathy, V.; Miyamoto, Y.; Leibach, F. H.; *Beitr. Infusionther Klin. Ernähr.* **1987**, 17, 54-68.
16. Ganapathy, V.; Leibach, F. H.; *Curr. Opin. Cell. Biol.* **1991**, 3, 695-701.
17. Thwaites, D. T.; Kennedy, D. J.; Raldua, D.; Anderson, C. M.; Mendoza, M. E.; Bladen, C. L.; Simmons, N. L.; *Gastroenterology.* **2002**, 122, 1322-1333.
18. Matthews, D. M.; Addison, J. M.; Burston, D.; *Clin. Sci. Mol. Med.* **1974**, 46, 693-705.
19. Thwaites, D. T.; Brown, C. D. A.; Hirst, B. H.; Simmons, N. L.; *J. Biol. Chem.* **1993**; 268: 7640-7642.
20. Thwaites, D. T.; Hirst, B. H.; Simmons, N. L.; *Biochem. Biophys. Res. Commun.* **1993**, 19, 432-438.
21. Walter, E.; Kissel, T.; Amidon, G. L.; *Adv. Drug Delivery Rev.* **1996**, 20(1), 33-58.
22. Terada, T.; Saito, H.; Mukai, M.; Inui, K.-I.; *Am. J. Physiol. Renal Physiol.* **1997**, 273, F706-711.

23. Mackenzie, B.; Loo, D. D. F.; Fei, Y.-J.; Liu, W.; Ganapathy, V.; Leibach, F. H.; *J. Biol. Chem.* **1996**, 271, 5430-5437.
24. Amasheh, S.; Wenzel, U.; Boll, M.; Dorn, D.; Weber, E.-M.; Clauss, W.; Daniel, H.; *J. Membr. Biol.* **1996**, 155, 247-256.
25. Irie, M.; Terada, T.; Katsura, T.; Matsuoka, S.; Inui, K. I.; *J. Physiol.* **2005**, 565, 429-439.
26. Temple, C. S.; Bailey, P. D.; Bronk, J. R.; Boyd, C. A. R.; *J. Physiol.* **1996**, 494, 795-808.
27. Ganapathy, V.; Brandsch, M.; Leibach, F. H. In: *Physiology of the Gastrointestinal Tract*, 3rd ed.; Raven Press: New York, **1994**, 1773-1794.
28. Ganapathy, V.; Ganapathy, M. E., Leibach, F. H.; In: *Current topics in membranes*. San Diego: Academic Press. **2001**, 379–412.
29. Ganapathy, V.; Ganapathy, M. E.; Leibach, F. H.; In: Yamada T, ed. *Textbook of gastroenterology*. Philadelphia: Lippincott Williams & Wilkins. **2003**, 438–448.
30. Cheeseman, C.; *Am. J. Physiol.* **1992**, 263, R482–488.
31. Dyer, J.; Beechey, R. B.; Gorvel, J. P.; Smith, R. T.; Wootton, R.; Shirazi-Beechey, S. P.; *Biochem J.* **1990**, 269, 565–571.
32. Berthelsen, R; Nielson, C. U.; Brodin, B.; *J. Pharm. Pharma.* **2013**, 65, 970-979.
33. Terada, T.; Sawada, K.; Saito, H.; Hashimoto, Y.; Inui, K.; *Am. J. Physiol.* **1999**, 276, G1435–1441.
34. Irie, M.; Terada, T.; Okuda, M.; Inui, K. I.; *Pflugers Arch.* **2004**, 449, 186–194.
35. Saito, H.; Inui, K.; *Am. J. Physiol.* **1993**, 265, G2889-2894.
36. Shepherd, E. J.; Lister, N.; Affleck, J. A.; Bronk, J. R.; Kellett, G. L.; Collier, I. D.; Bailey, P. D.; Boyd, C. A.; *Biochem. Biophys. Res. Commun.* **2002**, 296(4), 918-922.
37. Smith, E. E.; Cléménçon, B.; Hediger, M. A.; *Mol. Asp. Med.* **2013**, 34, 323-336.
38. Spanier, B.; *J. Physiol.* **2014**, 592(5), 871-879.
39. Ziegler, T; Fernández-Estívariz, C.; Gu, L. H.; Bazargan, N.; Umeakunne, K.; Wallace, T. M.; Diaz, E. E.; Rosado, K. E.; Pascal, R. R.; Galloway, J. R.; Wilcox, J. N.; Leader, L. M; *Am. J. Clin. Nutr.* **2002**, 75, 922-930.
40. Merlin, D.; Si-Tahar, M.; Sitaraman, S. V.; Eastburn, K.; Williams, I.; Xia Liu, X.; Hediger, M. A.; Madara, J. L.; *Gastroenterology*. **2001**, 120, 1666–1679.
41. Bin Shi, B.; Song, D.; Xue, H.; Li, N.; Li, J.; *J. Surg. Res.* **2006**, 136, 38 – 44.
42. Dalmosso, G.; Nguyen, H.T.; Ingersoll, S. A.; Ayyadurai, S.; Laroui, H.; Charania, M. A.; Yan, Y.; Sitaraman S. V.; Merlin D.; *Gastroenterology*. **2011**, 141(4), 1334-1345.
43. Habold, C.; Reichardt, F.; Foltzer-Jourdainne, C.; Lignot, J. H.; *Pflugers Arch.* **2007**, 455, 323-332.
44. Ma, K.; Hu, Y.; Smith D.E.; *Pharm. Res.* **2012**, 29(2), 535-545.
45. Ferraris, R. P.; Diamond, J. M.; *Annu. Rev. Physiol.* **1989**, 51, 125–141.

46. Pan, X.; Terada, T.; Okuda, M.; Inui, K.; *J. Pharmacol. Exp. Ther.* **2003**, 307(2), 626-632.
47. Ashida, K.; Katsura, T.; Saito, H.; Inui, K.; *Pharm. Res.* **2004**, 21, 969-975.
48. Ashida, K.; Katsura, Motohashi, H.; Saito, H.; Inui, K.; *Am. J. Physiol. Gastrointest. Liver Physiol.* **2002**, 282, G617-623.
49. Thamotharan, M.; Bawani, S. Z.; Zhou, X.; Adibi, S. A.; *Am. J. Physiol.* **1999**, 276, C821-826.
50. Der-Boghossian, A. H.; Saad, S. R.; Perreault, C.; Provost, C.; Jacques, D.; Kadi, L. N.; Issa, N. G.; Sibai, A. M.; El-Majzoub, N. W.; Bikhazi, A. B.; *Can. J. Physiol. Pharmacol.* **2010**, 88, 753-759.
51. Miao, Q.; Liu, Q.; Wang, C.; Meng, Q.; Guo, X.; Peng, J.; Kau, T.; Liu, K.; *Drug Metab. Pharmacokinet.* **2011**, 26, 494-502.
52. Westphal, J.F.; Trouvin, J.H.; Deslandes, A.; Carbon, C.; *J. Pharmacol. Exp. Ther.* **1990**, 255(1), 312-317.
53. Westphal, J.F.; Jehl, F.; Brogard, J.M.; Carbon, C.; *Clin. Pharmacol. Ther.* **1995**, 57(3), 257-264.
54. Anderson, C.; Thwaites, D. T.; *Biochim. Biophys. Acta.* **2007**, 1768(7), 1822-1829.
55. Wenzel, U.; Kuntzs, S.; Daniel, H.; *J. Pharmacol. Exp. Ther.* **2001**, 299(1), 351-357.
56. Kimura, T.; Endo, H.; Yoshikawa, M.; Muranishi, S.; Sezaki, H.; *J. Pharmacobio-Dyn.* **1978**, 1, 262-267.
57. Hou, J. P.; Poole, J. W.; *J. Pharm. Sci.* **1969**, 58, 1510-1515.
58. Levine, R. R.; *Dig. Dis. Sci.* **1970**, 15, 171-188.
59. Dixon, C.; Mizen, L. W.; *J. Physiol.* **1976**, 269, 549-559.
60. Das, M.; Radhakrishnan, A. N.; *Biochem. J.* **1975**, 146, 133-139.
61. Fei, Y. J.; Kanai, Y.; Nussberger, S.; Ganapathy, V.; Leibach, F. H.; Romero, M. F.; Singh, S. K.; Boron, W. F.; Hediger, M. A.; *Nature.* **1994**, 368, 563-566.
62. Boll, M.; Markovich, D.; Weber, W. M.; Korte, H.; Daniel, H.; Murer, H.; *Pflugers Arch.* **1994**, 429, 146-149.
63. Liang, R.; Fei, Y. J.; Prasad, P. D.; Ramamoorthy, S.; Han, H.; Yang, F. T.; Hediger, M. A.; Ganapathy, V.; Leibach, F. H.; *J. Biol. Chem.* **1995**, 270, 6456-6463.
64. Covitz, K. M.; Amidon, G. L.; Sadee, W.; *Biochem.* **1998**, 37, 15214-15221.
65. Saito, H.; Okuda, M.; Terada, T.; Sasaki, S.; Inui, K.; *J. Pharmacol. Exp. Ther.* **1995**, 275, 1631-1637.
66. Bolger, M. B.; Haworth, I. S.; Yeung, A. K.; Ann, D.; von Grafenstein, H.; Hamm-Alvarez, S.; Okamoto, C. T.; Kim, K. J.; Basu, S. K.; Wu, S.; Lee, V. H.; *J. Pharm. Sci.* **1998**, 87, 1286-1291.

67. Yeung, A. K.; Basu, S. K.; Wu, S. K.; Chu, C.; Okamoto, C. T.; Hamm-Alvarez, S. F.; von Grafenstein, H.; Shen, W. C.; Kim, K. J.; Bolger, M. B.; Haworth, I. S.; Ann, D. K.; Lee, V. H.; *Biochem. Biophys. Res. Commun.* **1998**, 250, 103–107.
68. Fei, Y. J.; Liu, J. C.; Fujita, T.; Liang, R.; Ganapathy, V.; Leibach, F. H.; *Biochem. Biophys. Res. Commun.* **1998**, 246, 39–44.
69. Lee, V. H.; Chu, C.; Mahlin, E. D.; Basu, S. K.; Ann, D. K.; Bolger, M. B.; Haworth, I. S.; Yeung, A. K.; Wu, S. K.; Hamm-Alvarez, S.; Okamoto, C. T.; *J. Control. Release.* **1999**, 62, 129–140.
70. Pieri, M.; Gan, C.; Bailey, P.; Meredith, D.; *Int. J. Biochem. Cell Biol.* **2009**, 41(11), 2204–2213.
71. Kulkarni, A.; Davies, D.; Links, J.; Patel, L.; Lee, V.; Haworth, I.; *Pharm. Res.* **2007**, 24, 66–72.
72. Fei, Y. J.; Liu, W.; Prasad, P. D.; Kekuda, R.; Oblak, T. G.; Ganapathy, V.; Leibach, F. H.; *Biochem.* **1997**, 36, 452–460.
73. Chen, X. Z.; Steel, A.; Hediger, M. A.; *Biochem. Biophys. Res. Comm.* **2000**, 272, 726–730.
74. Links, J. L. S.; Kulkarni, A. A.; Davies, D. L.; Lee, V. H. L.; Haworth, I. S. J.; *J. Drug Target.* **2007**, 15, 218–225.
75. Kulkarni, A. A.; Haworth, I. S.; Lee, V. H. L.; *Biochem. Biophys. Res. Comm.* **2003**, 306, 177–185.
76. Kulkarni, A. A.; Haworth, I. S.; Uchiyama, T.; Lee, V. H. L.; *J. Biol. Chem.* **2003**, 278, 51833–51840.
77. Kramer, W.; *Biol. Chem.* **2011**, 392, 77–94.
78. Meredith, D.; *Philos. Trans. R. Soc. Lond. B. Biol. Sci.* **2009**, 364(1514), 203–207.
79. Terada, T.; Saito, H.; Sawada, K.; Hashimoto, Y.; Inui, K.-I.; *Pharm. Res.* **2000**, 17, 15–20.
80. Döring, F.; Will, J.; Amasheh, S.; Clauss, W.; Ahlbrecht, H.; Daniel, H.; *J. Biol. Chem.* **1998**, 273, 23211–23218.
81. Abramson, J.; Smirnova, I.; Kasho, V.; Verner, G.; Kaback, H.R.; Iwata, S.; **2003**, 301, 610–615.
82. Huang, Y.; Lemieux, M. J.; Song, J.; Auer, M.; Wang, D.N.; *Science.* **2003**, 301, 616–620.
83. Abramson, J.; Kaback, H. R.; Iwata, S.; *Curr. Opin. Struc. Biol.* **2004**, 14, 413–419.
84. Meredith, D.; Price, R. A.; **2006**, 213, 79–88.
85. Weitz, D.; Harder, D.; Casagrande, F.; Fotiadis, D.; Obrdlik, P.; Kelety, B.; Daniel, H.; *J. Biol. Chem.* **2007**, 282, 2832–2839.
86. Newstead, S.; Drew, D.; Cameron, A. D.; Postis, V. L. G.; Xia, X.; Fowler, P. W.; Ingran, J. C.; Carpenter, E. P.; Sansom, M. S. P.; McPherson, M. J.; Baldwin, S. A.; Iwata, S.; *EMBO J.* **2011**, 30, 417–426.

87. Solcan, N.; Kwok, J.; Fowler, P. W.; Cameron, A. D.; Drew, D.; Iwata, S.; Newstead, S.; *EMBO J.* **2012**, 31(16), 3411-3421.
88. Doki, S.; Kato, H. E.; Solcan, N.; Iwaki, M.; Koyama, M.; Hattori, M.; Iwase, N.; Tsukazaki, T.; Sugita, Y.; Kandori, H.; Newstead, S.; Ishitani, R.; Nureki, O.; *Proc. Natl. Acad. Sci. USA.* **2013**, 110(28), 11343-11348.
89. Guettou, F.; Quistgaard, E. M.; Trésaugues, L.; Moberg, P.; Jegerschöld, C.; Zhu, L.; Jong, A. J.; Nordlund, P.; Löw, C.; *EMBO Rep.* **2013**, 9, 804-810.
90. Newstead, S.; *Biochim. Biophys. Acta*, **2014**, 1850(3), 488-499.
91. Lyons, J. A.; Parker, J. L.; Solcan, N.; Brinith, A.; Li, D.; Shah, S. T. A.; Caffrey, M.; Newstead, S.; *EMBO Rep.* **2014**, 15(7), 731 – 815.
92. Foley, D. W.; Rajamanickam, J.; Bailey, P. D.; Meredith, D.; *Curr. Comput. Aided Drug Des.* **2010**, 6(1), 68-78.
93. Temple, C. S.; Stewart, A. K.; Meredith, D.; Lister, N. A.; Morgan, K. M.; Collier, I. D.; Vaughan-Jones, R. D.; Boyd, C. A. R.; Bailey, P. D.; Bronk, J. R.; *J. Biol. Chem.* **1998**, 273, 20–22.
94. Börner, V.; Fei, Y. J.; Hartrodt, B.; Ganapathy, V.; Leibach, F. H.; Neubert, K.; Brandsch, M.; *Eur. J. Biochem.* **1998**, 255, 698-702.
95. Meredith, D.; Temple, C. S.; Guha, N.; Sword, C. J.; Boyd, C. A. R.; Collier, I. D.; Morgan, K. M.; Bailey, P. D. *Eur. J. Biochem.* **2000**, 267, 3723-3728.
96. Vig, B. S.; Stouch, T. R.; Timoszyk, J. K.; Quan, Y.; Wall, D. A.; Smith, R. L.; Faria, T. N. *J. Med. Chem.* **2006**, 49, 3636-3644.
97. Bailey, P.; Boyd, C. A. R.; Collier, I. D.; Kellett, G. L.; Meredith, D.; Morgan, K. M.; Pettecrew, R.; Pritchard, R. G.; Price, R. A.; *Chem. Commun.* **2005**, 5352-5354.
98. Brandsch, M.; Thunecket, F.; Küllertz, G.; Schutkowski, M.; Fischer, G.; Neubert, K.; *J. Biol. Chem.* **1998**, 273: 3861-3864.
99. Bailey, P. D.; Boyd, C. A. R.; Collier, I. D.; Kellett, G. L.; Meredith, D.; Morgan, K. M.; Pettecrew, R.; Price, R. A. *Org. Biomol. Chem.* **2005**, 3, 4038-4039.
100. Niida, A.; Tomita, K.; Mizumoto, M.; Tanigaki, H.; Terada, T.; Oishi, S.; Otaka, A.; Inui, K.-I.; Fujii, N.; *Org. Lett.* **2006**, 8, 613-616.
101. Lister, N.; Sykes, A. P.; Bailey, P. D.; Boyd, C. A.; Bronk, J. R.; *J. Physiol. (London).* **1995**, 484, 173-182.
102. Bailey, P. D.; Boyd, C. A. R.; Bronk, J. R.; Collier, I. D.; Meredith, D.; Morgan, K. M.; Temple, C. S.; *Angew. Chem. Int. Edit.* **2000**, 39(3), 505-508.
103. Bailey, P. D.; Boyd, C. A.; Collier, I. D.; George, J. P.; Kellett, G. L.; Meredith, D.; Morgan, K. M.; Pettecrew, R.; Price, R. A.; *Chem. Commun. (Camb).* **2006**, 21(3), 323-325.

104. Gebauer, S.; Knütter, I.; Hartrodt, B.; Brandsch, M.; Neubert, K.; *J. Med. Chem.* **2003**, *46*, 5725-5734.
105. Tamai, I.; Nakanishi, T.; Nakahara, H.; Sai, Y.; Ganapathy, V.; Leibach, F. H.; Tsuji, A.; *J. Pharm. Sci.* **1998**, *87*, 1542-1546.
106. Cao, C.; Gao, Y.; Ping, Q.; *Asian J. Pharm. Sci.* **2012**, *7*(2), 110-112.
107. Cao, F.; Jia, J.; Yin, Z.; Gao, Y.; Sha, L.; Lai, Y.; Ping, Q.; Zhang, Y.; *Mol. Pharm.* **2012**, *9*(8), 2127-35.
108. Gupta, D.; Varghese Gupta, S.; Dahan, A.; Tsume, Y.; Hilfinger, J.; Lee, K. D.; Amidon, G. L.; *Mol. Pharm.* **2013**, *10*(2), 512-22.
109. Pierra, C.; Amador, A.; Benzaria, S.; Cretton-Scott, E.; D'Amours, M.; Mao, J.; Mathieu, S.; Moussa, A.; Bridges, E. G.; Standring, D. N.; Sommadossi, J. P.; Storer, R.; Gosselin, G.; *J. Med. Chem.* **2006**, *49*(22), 6614-20.
110. Shen, W.; Kim, J. S.; Kish, P. E.; Zhang, J.; Mitchell, S.; Gentry, B. G.; Breitenbach, J. M.; Drach, J. C.; Hilfinger, J.; *Bioorg. Med. Chem. Lett.* **2009**, *19*(3), 792-796.
111. Eriksson, U.; Peterson, L. W.; Kashemirov, B. A.; Hilfinger, J. M.; Drach, J. C.; Borysko, K. Z.; Breitenbach, J. M.; Kim, J. S.; Mitchell, S.; Kijek, P.; McKenna, C. E.; *Mol. Pharm.* **2008**, *5*(4), 598-609.
112. Steffansen, B.; Lepist, E. I.; Taub, M. E.; Larsen, B. D.; Frokjaer, S.; Lennernäs, H.; *Eur. J. Pharm. Sci.* **1999**, *8*, 67-73.
113. Lepist, E. I.; Kusk, T.; Larsen, D. H.; Anderson, D.; Frokjaer, S.; Taub, M. E.; Veski, P.; Lennernäs, H.; Friedrichsen, G.; Steffansen, B.; *Eur. J. Pharm. Sci.* **2000**, *11*, 43-49.
114. Friedrichsen, G.; Jakobsen, P.; Taub, M. E.; Begtrup, M.; *Bio. Med. Chem.* **2001**, *9*, 2625-2632.
115. Bailey, P. D.; (The University of Manchester, UK). *European Patent Office*, Int. Application No.: WO2005067978, **2005**.
116. Foley, D.; Bailey, P. D.; Pieri, M.; Meredith, D.; *Org. Bio. Chem.* **2009**, *7*, 1064-1067.
117. Foley, D.; Pieri, M.; Pettecrew, R.; Price, R.; Miles, S.; Lam, H. K.; Bailey, P. D.; Meredith, D.; *Org. Bio. Chem.* **2009**, *7*, 3652-3656.
118. Whomsley, Rhys. ; Franklin, R.; Golding, B. T.; Tyson, R. G.; U.S Patent No. 20110065798, **2011**.
119. Arndt, T.; Oost, T.; Lubisch, W.; Wernet, W.; Hornberger, W.; Unger, L.; Ruiz Caro, J.; *European Patent Office*, Int. Application No.: WO2008025736, **2008**.
120. Jain, S.; Patil, S. R.; Swarnakar, N. K.; Agrawal, A. K.; *Mol. Pharm.* **2012**, *9*(9), 2626-2635.
121. Cundy, K. C.; Gallop, M. A.; Sasikumar, V.; Woiwode, T. W.; Xu, F.; *European Patent Office*, Int. Application No.: WO2008157627, **2005**.
122. Takeshita, J.; *J. Clin. Psychiatry.* **2004**, *65*(1), 134-135.

123. Cafiero, T.; Razzino, S.; Mastronardi, P.; Cappabianca, P.; Alfieri, A.; *Minerva Anestesiol.* **1999**, 65(4), 169-174.
124. Canavero, S.; Bonicalzi, V.; *Clin. Neuropharmacol.* **2004**, 27(4), 182-186.
125. Canavero, S.; Bonicalzi, V.; *Pain.* **1998**, 74(2-3), 109-114.
126. Virsik, P. A.; *J.European Patent Office*, Int. Application No.: WO2009036322, **2009**.
127. Foley, D.; Doctoral thesis. University of Manchester. **2008**.
128. Moriarty, L. M.; Lally, M. N.; Carolan, C. G.; Jones, M.; Clancy, J. M.; Gilmer, J. F.; *J. Med. Chem.* **2008**, 51, 7991-7999.
129. Gilmer, J.F.; Murphy, M. A.; Shannon, J. A.; Breen, C. G.; Ryder, S. A.; Clancy, J. M.; *J. Pharm. Pharmacol.* **2003**, 55(10), 1351-1357.
130. Huynh, K-D.; Ibrahim, H.; Kolodziej, E.; Toffano, M.; Vo-Thanh, G.; *New J. Chem.* **2011**, 35(11), 2622 – 2631.
131. Enholm, E. J.; Cottone, J. S.; Allais, F.; *Org. Lett.* **2001**, 3(2), 145-7.
132. Jung, F. H.; Pasquet, G.; Lambert-van de Brempt, C.; Lohmann, J.-J. M.; Warin, N.; Renaud, R.; Germain, H.; De Savi, C.; Roberts, N.; Johnson, T.; Dousson, C.; Hill, G. B.; Mortlock, A. A.; Heron, N.; Wilkinson, R. W.; Wedge, S. R.; Heaton, S. P.; Odedra, R.; Keen, N. J.; Green, S.; Brown, E.; Thompson, K.; Brightwell, S.; *J. Med. Chem.* **2006**, 49, 955-970.
133. Bischoff, J. R.; Anderson, L.; Zhu, Y.; Mossie, K.; Ng, L.; Souza, B.; Schryver, B.; Flanagan, P.; Clairvoyant, F.; Ginther, C.; Chan, C. S.; Novotny, M.; Slamon, D. J.; Plowman, G. D.; *EMBO J.* **1998**, 17, 3052–3065.
134. Anaud, S.; Penrhyn-Lowe, S.; Venkitaraman, A. R.; *Cancer Cell.* **2003**, 3, 51-62.
135. Lin, B. W.; Wang, Y. C.; Chang-Liao, P. Y.; Lin, Y. J.; Yang, S. T.; Tsou, J. H.; Chang, K. C.; Liu, Y.W.; Tseng, J. T.; Lee, C. T.; Lee, J. C.; Hung, L. Y.; *Cell Death Dis.* **2014**, 5(3), E1106.
136. Manfredi, M. G.; Ecsedy, J. A.; Chakravarty, A.; Silverman, L.; Zhang, M.; Hoar, K. M.; Stroud, S. G.; Chen, W.; Shinde, V.; Huck, J. J.; Wysong, D. R.; Janowick, D. A.; Hyer, M. L.; Leroy, P. J.; Gershman, R. E.; Silva, M. D.; Germanos, M. S.; Bolen, J. B.; Claiborne, C. F.; Sells, T. B.; *Clin. Cancer Res.* **2011**, 17, 7614-7624.
137. Wilkinson, R. W.; Odedra, R.; Heaton, S.; Wedge, S. R.; Keen, N. J.; Crafter, C.; Foster, J. R.; Brady, M. C.; Bigley, A.; Brown, E.; Byth, K.; Barrass, N. C.; Mundt, K.; Foote, K. M.; Heron, N. M.; Jung, F.; Mortlock, A. A.; Boyle, F. T.; Green, S.; *Clin. Can. Res.* **2007**, 13, 3682-3688.
138. Osborne, N. F.; *J. Chem. Soc., Perkin Trans. 1*, **1980**, 150-155.
139. Schaffner, F.; Ray, A. M.; *Cancers.* **2013**, 5, 27-47.
140. Barkan, D.; Chambers, A. F.; *Clin. Cancer Res.* **2011**, 17(23), 7219-7223.
141. Marelli, U. K.; Rechenmacher, F.; Sobahi, T. R. A.; Mas-Moruno, C.; Kessler, H.; *Front. Oncol.* **2013**, 3, 1-12.

142. Nagae, M.; Re, S.; Mihara, E.; Nogi, T.; Sugita, Y.; Takagi, J.; *J. Cell. Biol.* **2012**, 197(1), 131-140.
143. Delouvrié, B.; Al-Kadhimi, K.; Arnould, J. C.; Barry, S. T.; Cross, D. A.; Didelot, M.; Gavine, P. R.; Germain, H.; Harris, C. S.; Hughes, A. M.; Jude, D. A.; Kendrew, J.; Lambert-van der Brempt, C.; Lohmann, J. J.; Ménard, M.; Mortlock, A. A.; Pass, M.; Rooney, C.; Vautier, M.; Vincent, J. L.; Warin, N.; *Bioorg. Med. Chem. Lett.* **2012**, 22(12), 4111-4116.
144. Delouvrié, B.; Al-Kadhimi, K.; Arnould, J. C.; Barry, S. T.; Cross, D. A.; Didelot, M.; Gavine, P. R.; Germain, H.; Harris, C. S.; Hughes, A. M.; Jude, D. A.; Kendrew, J.; Lambert-van der Brempt, C.; Lohmann, J. J.; Ménard, M.; Mortlock, A. A.; Pass, M.; Rooney, C.; Vautier, M.; Vincent, J. L.; Warin, N.; *Bioorg. Med. Chem. Lett.* **2012**, 22(12), 4117-4121.
145. Subiros-Funosas, R.; Prohens, R.; Barbas, R.; El-Faham, A.; Albericio, F.; *Chem. Eur. J.* **2009**, 15, 9394-9403.
146. El-Faham, A.; Subiros-Funosas, R.; Prohens, R.; Albericio, F.; *Chem. Eur. J.* **2009**, 15, 9404-9416.
147. El-Faham, A.; Carpino, L. A.; *J. Am. Chem. Soc.* **1995**, 117, 5401-5402.
148. Xia, C. Q.; Milton, M. N.; Gan, L. S.; *Curr. Drug. Metab.* **2007**, 8(4), 341-63.
149. Meredith, D.; Boyd, C. A. R.; Bronk, J. R.; Bailty, P. D.; Morgan, K. M.; Collier, I. D.; Temple, C. S.; *J. Physiol. (London)*. **1998**, 512(3), 629-634.
150. Pieri, M.; Hall, D.; Price, R.; Bailey, P.; Meredith, D.; *Int. J. Biochem. Cell Biol.* **2008**, 40(4), 721-730.
151. Artursson, P.; Karlsson, J.; *Biochem. Biophys. Res. Commun.* **1991**, 175, 880-890.
152. Omkvist, D. H.; Brodin, B.; Nielson, C. U.; *Br. J. Pharmacol.* **2010**, 161(8), 1793-1805.
153. Knütter, I.; Rubio-Aliaga, I.; Boll, M.; Hause, G.; Daniel, H.; Neubert, K.; Brandsch, M.; *Am. J. Physiol. Gastrointest. Liver Physiol.* **2002**, 283(1), G222-229.
154. Inoue, M.; Terada, T.; Okuda, M.; Inui, K.; *Cancer Lett.* **2005**, 230(1), 72-80.
155. Mitsuoka, K.; Miyoshi, S.; Kato, Y.; Murakami, Y.; Utsumi, R.; Kubo, Y.; Noda, A.; Nakamura, Y.; Nishimura, S.; Tsuji, A.; *J. Nucl. Med.* **2008**, 49(4), 615-22.
156. Nakanishi, T.; Tamai, I.; Takaki, A.; Tsuji, A.; *Int. J. Cancer.* **2000**, 88(2), 274-280.
157. Cancer research UK; Statistics and outlook for pancreatic cancer. Available <http://www.cancerresearchuk.org/cancer-help/type/pancreatic-cancer/treatment/statistics-and-outlook-for-pancreatic-cancer> [20/06/2014].
158. Li, X; Ma, Q; Xu, Q; Duan, W; Lei, J; Wu, E; *Curr. Pharm. Des.* **2012**, 18(17), 2404-2415.
159. Elinav, E.; Nowarski, R.; Thaïss, C. A.; Hu, B.; Jin, C.; Flavell, R. A.; *Nat. Rev. Cancer.* **2013**, 13(11), 759-771.
160. Arias, J. I.; Aller, M. A.; Arias, J.; *Mol. Cancer.* **2007**, 6, 29-34.
161. Rayburn, E. R.; Ezell, S. J.; Zhang, R.; *Mol. Cell Pharmacol.* **2009**, 1(1), 29-43.



162. Coussens, L. M.; Werb, Z.; *Nature*. **2002**, 420(6917), 860-867.
163. Grivennikov, S. I.; Greten, F. R.; Karin, M.; *Cell*. **2010**, 140(6), 883-99
164. Greenhough, A.; Smartt, H. J.; Moore, A. E.; Roberts, H. R.; Williams, A. C.; Paraskeva, C.; Kaidi, A.; *Carcinogenesis*. **2009**, 30(3), 377-386.
165. Ettarh, R.; Cullen, A.; Calamai, A.; *Pharmaceuticals*. **2010**, 3(7), 2007-2021.
166. Rodríguez-Burford, C.; Barnes, M. N.; Oelschlager, D. K.; Myers, R. B.; Talley, L. I.; Partridge, E. E.; Grizzle, W. E.; *Clin. Cancer Res.* **2002**, 8(1), 202-209.
167. Moody, T. W.; Switzer, C.; Santana-Flores, W.; Ridnour, L. A.; Berna, M.; Thill, M.; Jensen, R. T.; Sparatore, A.; Del Soldato, P.; Yeh, G. C.; Roberts, D. D.; Giaccone, G.; Wink, D. A.; *Lung Cancer*. **2010**, 68(2), 154-160.
168. Nagasawa, H.; Naito, T.; *Breast Cancer Res. Treat.* **1986**, 8, 249–255.
169. Mayorek, N.; Naftali-Shani, N.; Grunewald, M.; *PLoS One*. **2010**, 5(9), E12715.
170. Lichtenberger, L.; Waters, D.; Phan, T.; Dial, E *FASEB J.* **2014**, 28(1), S840.5
171. Hill, R.; Li, Y.; Tran, L. M.; Dry, S.; Calvopina, J. H.; Garcia, A.; Kim, C.; Wang, Y.; Donahue, T. R.; Herschman, H. R.; Wu, H.; *Mol. Cancer Ther.* **2012**, 11(10), 2127-2137.
172. Toschi, L.; Finocchiaro, G.; Bartolini, S.; Gioia, V.; Cappuzzo, F.; *Future Oncol.* **2005**; 1(1), 7-17.
173. Pancreatic cancer action; Chemotherapy Drugs Used to Treat Pancreatic Cancer. Available <http://pancreaticcanceraction.org/pancreatic-cancer/treatment/chemotherapy/chemotherapy-drugs-treat-cancer> [22/06/**2014**].
174. Pratt, S. E; Durland-Busbice, S.; Shepard, R. L.; Heinz-Taheny, K.; Iversen, P. W.; Dantzig, A. H.; *Clin. Cancer Res.* **2013**, 19(5), 1159-1168.
175. Slusarczyk, M.; Lopez, M. H.; Balzarini, J.; Mason, M.; Jiang, W. G.; Blagden, S.; Thompson, E.; Ghazaly, E.; McGuigan, C.; *J. Med. Chem.* **2014**, 57(4), 1531-1542.
176. Tsume, Y.; Incecayir, T.; Song, X.; Hilfinger, J. M.; Amidon, G. L.; *Eur. J. Pharm Biopharm.* **2014**, 86(3), 514-23.
177. Tsume, Y.; Borrás Bermejo, B.; Amidon, G. L.; *Pharmaceuticals*. **2014**, 7, 169-191.
178. Tsume, Y.; Amidon, G. L.; *Molecules*. **2012**, 17(4), 3672-3689.
179. Cross-cancer alteration summary for SLC15A1; Available <http://bit.ly/1t35p5Y> [23/09/**2014**]
180. Yamashita, M.; Cuevas Vicario, J. V.; Hartwing, J. F.; *J. Am. Chem. Soc.* **2003**, 125(52), 16347-16360.